Cardiovascular Magnetic Resonance of the Carotid Arterial Wall

Kathleen Anne Maricela Rose

Imperial College London
National Heart and Lung Institute

Thesis submitted for the degree of Doctor of Medicine (Res) of Imperial College, London,
2016

For Peter, Dominic and Benedict

DG

Declaration of Originality

The work in this thesis is my own except where otherwise stated or acknowledged.

Kathleen A.M. Rose

Copyright

The copyright of this thesis rests with the author and is made available under a Creative Commons Attribution-Non Commercial No Derivatives licence. Researchers are free to copy, distribute or transmit the thesis on the condition that they attribute it, that they do not use it for commercial purposes and that they do not alter, transform or build upon it. For any reuse or distribution, researchers must make clear to others the licence terms of this work.

Abstract

Background

Atherosclerosis is a leading cause of death [Lloyd-Jones 2009; Murray 1997] involving inflammatory processes throughout [Libby 2002]. Cardiovascular disease (CVD) incidence is increased in generalised inflammatory conditions [Esdaile 2001; Watson 2003; Rosenfeld 2011; Triant 2012]. However, the presence and burden of atherosclerosis in groups with such conditions but low traditional cardiovascular risk is unclear. The means to reduce cardiovascular risk in individuals without conventional modifiable risk factors remains unknown. Carotid arterial wall imaging allows assessment of atheroma burden and the effects of treatments to reduce it. Cardiovascular magnetic resonance (CMR) is non-invasive, radiation-free, and allows volumetric measures to be obtained.

Methods and Results

Using previously validated carotid CMR imaging techniques we undertook a series of studies in two conditions associated with inflammation and increased CVD: systemic lupus erythematosus (SLE) and HIV. We recruited SLE patients with LDL-cholesterol <3.4mmol/L into a 2-year placebo-controlled trial of rosuvastatin and evaluated vascular effects: no benefit from statin therapy on carotid arterial parameters was seen (Chapter 9). We combined baseline findings with results from a pilot study to further investigate the extent of CVD in SLE, demonstrating an excess of subclinical atherosclerosis (Chapter 8). In HIV, we investigated two cohorts using CMR: a group with adult-acquired HIV-infection that revealed evidence of early subclinical atherosclerosis (Chapter 10) and a group of perinatally infected young adults that revealed no apparent abnormalities suggesting early atherosclerosis (Chapter 11).

Conclusions

CMR allows quantification of atherosclerosis in different patient groups. Low traditional CVD risk SLE and adult HIV-infected patients exhibit subclinical atherosclerosis. It emerges that clearer assessment of CMR's limitations, the abnormalities seen in patient subgroups and of the different arterial wall pathophysiological changes in different inflammatory conditions is needed before employing carotid parameters as surrogates for assessing the effect of established or novel treatments on CVD risk.

Acknowledgements

The work for this thesis was carried out at the Cardiovascular Biomedical Research Unit, Royal Brompton Hospital and was supported by the National Institute of Health Research Cardiovascular Biomedical Research Unit at the Royal Brompton and Harefield NHS Foundation Trust, Imperial College London, and by a grant support from CORDA, the research charity.

Such studies are impossible to undertake unaided. I would like to extend my gratitude to all the staff of the Cardiovascular Biomedical Research Unit and Cardiac MR Department at the Royal Brompton Hospital as well as those at the recruitment centres for the SLE RCT trial – Rheumatology departments at the Hammersmith Hospital, Charing Cross Hospital, St Mary's Hospital and Northwick Park Hospital. I am grateful to my predecessors Dr Niall Keenan and Dr Cheuk Chan for their work in setting up the randomised trial of rosuvastatin in SLE, and to Dr Niall Keenan for carrying out the independent read of the CMR image data for the first eleven patients used in the cardiac and vascular findings in SLE study, as well as the historic healthy carotid cohort used in this thesis. I would like to thank Dr Alicia Maceira for providing the data for the historic healthy cardiac CMR cohort. I am especially grateful to Peter Drivas, Gill Smith and Ricardo Wage for their help and support scanning patients, particularly during my maternity leave and completing the young adult HIV study scans which took place after I had finished my time as a research fellow at the Brompton Hospital. The HIV studies in this thesis would not have been possible without Dr Jaime Vera Rojas, Dr Alan Winston, Dr Margaret Rhoads and Dr Gareth Tudor-Williams. I would like to thank Dr Jaime Vera Rojas and Dr Alan Winston for conceiving the study resulting in the CMR of carotid artery ageing in treated HIV-infected adults and for their advice writing up the findings, and Dr Jaime Vera Rojas for the recruitment of patients. I would like to thank Dr Gareth Tudor-Williams and Dr Margaret Rhoads for conceiving the study looking at perinatally infected young adults with HIV, and Dr Margaret Rhoads for recruiting the subjects, compiling the database (to which I remain blinded) and carrying out the statistical analysis. I would also like to thank Winston Banya for carrying out the statistical analyses in the SLE studies and the adult HIV study, as well as providing statistical advice and support throughout. I am grateful to my supervisors, Prof Dudley Pennell, Prof Richard Underwood and Prof Justin Mason, for their support and advice at various stages during my research and write-up. I also wish to thank the patients who participated in the studies, without whom none of this would have been possible.

Finally I would like to thank all my family for their love, patience and support. The greatest thanks of all I owe to my husband, Peter, without whom this would not have been possible.

Table of Contents

Declaration 3
Abstract 5
Acknowledgements 6
List of Figures and Tables 13

Chapter 1 Introduction 17

Chapter 2 Atherosclerosis 20
2.1 Introduction 20
2.2 Epidemiology of atherosclerosis and cardiovascular disease 20
2.3 Pathophysiology of atherosclerosis 22
2.3.1 Introduction 22
2.3.2 Initiation of atherosclerosis 23
2.3.3 Atheroma progression and complication 25
2.3.4 Calcification 26
2.3.5 Focal development of atheroma 26
2.3.6 Vulnerable plaques and vulnerable patients 27
2.4 Differences between the coronary and carotid arteries 29
2.5 Atherosclerosis imaging 29
2.5.1 Introduction 29
2.5.2 Angiography 30
2.5.3 Optical coherence tomography 30
2.5.4 Near infrared spectroscopy 31
2.5.5 Ultrasound 31
2.5.6 Multislice computed tomography 32
2.5.7 Nuclear imaging 33
2.5.8 High-resolution magnetic resonance imaging 33

Chapter 3 Lipids and the 3-hydroxy-3-methylglutaryl coenzyme A reductase inhibitors 35
3.1 Introduction 35
3.2 Cholesterol synthesis pathway 35
3.2.1 Introduction 35
3.2.2 Regulation of cholesterol synthesis 36
3.3 Lipoprotein classification 37

3.3.1 Introduction 37
3.3.2 The major lipoproteins 37
3.4 Lipids and atherosclerosis 38
3.4.1 Introduction 38
3.4.2 LDL 38
3.4.3 Lipoprotein (a) 39
3.4.4 IDL 40
3.4.5 VLDL and chylomicrons 40
3.4.6 HDL 40
3.5 3-hydroxy-3-methylglutaryl coenzyme A reductase inhibitors 41
3.5.1 Introduction 41
3.5.2 Mechanism of drug action - effect on lipids 41
3.5.3 Plaque regression and non-lipid related effects of the statins 42

Chapter 4 Basic Principles and Physics of Cardiovascular Magnetic Resonance 44
4.1 Introduction 44
4.2 Physics 44
4.2.1 Introduction 44
4.2.2 T1 relaxation 46
4.2.3 T2 relaxation 47
4.2.4 T2* relaxation 47
4.2.5 CMR sequences 48
4.3 Components of an MR scanner 51
4.3.1 MR scanner 51
4.3.2 Receiver coil 52
4.3.3 Construction of the MR image 52
4.4 CMR measurement of cardiac function and mass 55
4.4.1 Introduction 55
4.4.2 Ventricular volume and function 55
4.4.3 Ventricular mass 55
4.4.4 Myocardial scar 56
4.5 CMR imaging of atherosclerosis 56
4.5.1 Introduction 56
4.5.2 Multicontrast CMR 57
4.5.3 Contrast agents 58
4.5.4 1.5T versus 3.0T 60
4.5.5 Arterial wall CMR in clinical trials 60

4.5.6 The future 61

Chapter 5 Systemic Lupus Erythematosus 62

5.1 Introduction 62

5.2 Epidemiology 62

5.3 Aetiology and Pathogenesis 63

5.3.1 Introduction 63

5.3.2 Immunology 63

5.3.3 Genetics 65

5.3.4 Hormonal Factors 66

5.3.5 Environmental Factors 66

5.4 Diagnostic criteria 68

5.5 Cardiovascular disease in SLE 70

5.5.1 Introduction 70

5.5.2 Coronary artery disease 70

5.5.3 Carotid plaque 70

5.5.4 Carotid intima media thickness 71

5.5.5 Endothelial dysfunction and arterial stiffness 72

5.5.6 Myocardial mass and function 72

5.6 Aetiology of atherosclerosis in SLE 72

5.6.1 Introduction 72

5.6.2 Traditional risk factors 72

5.6.3 Autoantibodies 73

5.6.4 Inflammatory markers 74

5.6.5 Sex hormones, vitamin D and homocysteine 75

5.6.6 SLE treatment 75

5.6.7 Prevention of atherosclerosis in SLE 76

5.6.8 SLE as a risk factor 77

5.6.9 Summary 77

Chapter 6 Human Immunodeficiency Virus 78

6.1 Introduction 78

6.2 Epidemiology 78

6.3 The Human Immunodeficiency Virus 80

6.4 Immune dysfunction 80

6.4.1 Cell-mediated Immunity 80

6.4.2 Humoral Immunity 81

6.4.3 HIV controllers 81
6.4.4 Immune activation and Inflammation 81
6.5 Atherosclerosis in HIV 82
6.5.1 Introduction 82
6.5.2 Risk factors and cardiovascular risk in HIV 82
6.5.3 Chronic inflammation and immune activation 84
6.5.4 The role of antiretroviral drugs 85
6.6 HIV in children and young adults 85

Chapter 7 Methods 88
7.1 Assessment of the carotid artery 88
7.1.1 Imaging Hardware 88
7.1.2 Assessment of carotid artery wall volume 88
7.1.3 Assessment of carotid artery distensibility 91
7.2 Assessment of endothelial function 92
7.3 Assessment of cardiac ventricular volumes, function and mass 94

Chapter 8 Cardiac and vascular findings in systemic lupus erythematosus by CMR 97
8.1 Introduction 97
8.2 Methods 98
8.2.1 Patient Population 98
8.2.2 CMR protocol 98
8.2.3 Statistical methods 99
8.3 Results 100
8.3.1 Patient Characteristics 100
8.3.2 Carotid CMR 100
8.3.3 Cardiac CMR 101
8.3.4 Endothelial function 101
8.4 Discussion 109
8.4.1 Study limitations 111
8.5 Conclusion 112

Chapter 9 A randomised placebo controlled trial of rosuvastatin in systemic lupus erythematosus 113
9.1 Introduction 113
9.2 Methods 114
9.2.1 Patient population 114

9.2.2 Study design 115
9.2.3 CMR protocol 115
9.2.4 Outcome measures 116
9.2.5 Statistical methods 116
9.2.6 Power of study 117
9.2.7 Safety monitoring 117
9.2.8 Supplementary methods 117
9.3 Results 118
9.3.1 Patient characteristics 118
9.3.2 Adverse events 119
9.4 Discussion 130
9.4.1 Study limitations 131
9.4.2 Conclusion and clinical implications 134

Chapter 10 CMR of carotid artery ageing in treated HIV-infected subjects with low cardiovascular risk 135
10.1 Introduction 135
10.2 Methods 137
10.2.1 Patient population 137
10.2.2 CMR protocol 137
10.2.3 Sample Size and Statistical Analyses 138
10.3 Results 138
10.3.1 Patient Characteristics 138
10.3.2 Carotid CMR 139
10.3.3 Carotid artery ageing in HIV-infected individuals 139
10.4 Discussion 145
10.4.1 Study limitations 147
10.4.2 Conclusion 148

Chapter 11 Cardiovascular disease in young HIV-infected individuals 149
11.1 Introduction 149
11.2 Methods 150
11.2.1 Study population 150
11.2.2 CMR protocol 150
11.2.3 Sample size and statistical analysis 151
11.3 Results 151

11.3.1 Subject characteristics 151
11.3.2 Carotid CMR 152
11.4 Discussion 155
11.4.1 Study limitations 156
11.4.2 Conclusion 158

Chapter 12 General discussion, conclusions and future directions 159
12.1 Introduction 159
12.2 SLE studies 159
12.3 HIV studies 160
12.4 General limitations and conclusions 161
12.5 Future directions 163

Chapter 13 References 165

Appendix 214
Outputs arising from this thesis 215
Abbreviations 217

Supplemental data 220

List of Figures and Tables

Figures

Figure 2.1. World map showing the global distribution of CVD mortality rates.

Figure 2.2. The structure of the arterial wall.

Figure 2.3. Outward remodelling of the coronary left main stem artery in response to plaque formation.

Figure 2.4. Diagram showing different types of flow and shear stress at an arterial bifurcation.

Figure 2.5. Different types of vulnerable plaque as described by Naghavi 2003(a).

Figure 2.6. Intravascular coronary imaging showing a) coronary angiography b) OCT.

Figure 3.1. Cholesterol synthesis pathway.

Figure 3.2. Cholesterol synthesis regulation feedback mechanism.

Figure 4.1. Orientation of nuclear spins.

Figure 4.2. Net Magnetisation, RF pulses and flip angle.

Figure 4.3. Diagram showing the process of T1 relaxation.

Figure 4.4. Diagram showing the process of transverse relaxation.

Figure 4.5. Formation of a spin echo.

Figure 4.6. A pulse sequence diagram for gradient echo.

Figure 4.7. MR system components.

Figure 4.8. Image formation and slice selection.

Figure 4.9. Image formation - phase and frequency encoding.

Figure 4.10. Figure showing a molecular contrast agent.

Figure 6.1. Worldwide prevalence of HIV in adults at the end of 2013.

Figure 6.2. Estimated number[1] of people living with HIV (both diagnosed and undiagnosed) all ages: UK, 2014.

Figure 7.1. Stack of TOF images acquired perpendicular to the carotid artery long axis.

Figure 7.2. T1-weighted FSE images acquired perpendicularly to each other through the carotid bifurcation.

Figure 7.3. Stack of high-resolution T1-weighted FSE images, centred on the carotid bifurcation bilaterally, acquired in the same orientation as the TOF images.

Figure 7.4. Carotid artery image analysis using Atheroma Tools (CMRtools, Cardiovascular Imaging Solutions, London).

Figure 7.5. FMD analysis. The brachial artery lumen is contoured at baseline and at maximal dilatation.

Figure 7.6. Two-chamber (a) and four-chamber (b) images showing planning for short axis stack parallel to the atrioventricular groove (c).

Figure 7.7. LV and RV analysis using CMRtools showing semi-automated tracing of the epicardial and endocardial borders, and myocardial thresholding.

Figure 8.1. T1-weighted transaxial CMR images of the common carotid artery.

Figure 8.2. Mean carotid artery wall volume and W/OW ratio.

Figure 8.3. GE images from SLE patients.

Figure 9.1. Study consort diagram.

Figure 9.2. Carotid plaque in one individual, imaged at the same level at a) baseline, b) 1-year and c) 2-years. .

Figure 10.1. Graphs of carotid artery wall volume normalised to total vessel volume (W/OW ratio).

Tables

Table 4.1. Signal intensities of plaque components compared to adjacent muscle.

Table 5.1. Clinical and immunologic criteria used in the Systemic Lupus International Collaborating Clinics (SLICC) classification system.

Table 8.1. Baseline characteristics of patients studied.

Table 8.2. Carotid CMR measurements in SLE and control subjects.

Table 8.3. Multivariate regression analysis showing the strength of association between W/OW ratio and CVD risk factors in the SLE group.

Table 8.4. Left and right ventricular parameters for SLE patients and normal controls.

Table 8.5. Endothelium dependent and independent dilatation of the brachial artery.

Table 9.1. Baseline characteristics of the study patients by group.

Table 9.2. Change in lipids from baseline.

Table 9.3. Carotid artery measurements at a) baseline, b) 1-year and c) 2-years.

Table 9.4. Primary outcome (total wall volume) and other carotid artery measurements shown as a) change from baseline to year-1 and b) change from baseline to year-2.

Table 9.5. Results of linear mixed models (using all data points and including year as a covariate) – Coefficients of active treatment variable in comparison with placebo.

Table 9.6. Correlations of total carotid wall volume and carotid distensibility to ventricular ejection fraction and mass.

Table 10.1. Baseline characteristics including clinical and laboratory parameters.

Table 10.2. Carotid CMR measurements in HIV-infected and control subjects.

Table 10.3. Difference in W/OW between male and female HIV-infected subjects compared to male and female controls using the Z-score.

Table 10.4. Carotid artery parameters by age group showing mean and 95% confidence intervals.

Table 11.1 Demographic characteristics including clinical and laboratory parameters.

Table 11.2. HIV-infected group characteristics.

Table 11.3. Carotid CMR measurements in HIV-infected and control subjects.

Chapter 1
Introduction

Atherosclerosis is a multifactorial complex, active and progressive disorder involving inflammation at every stage [Libby 2002] and cardiovascular disease (CVD) will be the leading cause of death worldwide by 2020 [Lloyd-Jones 2009; Murray 1997]. The incidence of CVD is increased in generalised chronic inflammatory conditions be they autoimmune, such as rheumatoid arthritis and systemic lupus erythematosus, or infective in origin, such as the human immunodeficiency virus (HIV) or cytomegalovirus [Esdaile 2001; Watson 2003; Sackoff 2006; Rosenfeld 2011; Triant 2012]. In individuals with chronic inflammatory conditions, traditional modifiable cardiovascular risk factors are treated aggressively, but the means to reduce cardiovascular risk in those without modifiable conventional risk factors, remains unclear. Possibilities include more aggressive treatment of the underlying condition, attempting to shut down the chronic inflammatory process, or extending current atherosclerosis treatments to populations who currently do not fulfil criteria for their use.

Mediated by cytokines, a complex interaction between monocytes, smooth muscle cells (SMCs), lymphocytes and mast cells takes place in the arterial wall following endothelial injury [Libby 2002]. This results in intimal thickening and plaque formation (atherosclerosis) and repeated or continuous endothelial injury causes amplification of the inflammatory process and plaque enlargement [Ross 1976c; Libby 2012]. Acute plaque complications often arise from non-significant stenoses giving rise to the concept of the ‘vulnerable plaque’, the main features of which are a thin fibrous cap, a lipid-rich core and cap inflammation [Ambrose 1988; Naghavi 2003a; Finn 2010]. Despite the generalised nature of toxic and pro-inflammatory stimuli, atherosclerosis does not develop uniformly along arteries. Differences in flow dynamics and shear stresses, which reduce atheroprotective mechanisms, such as endothelial-derived nitric oxide (eNOS), make vessel branch points and the inner curves of arteries prone to atherosclerosis [Cheng 2006].

Arterial wall imaging allows assessment of atheroma burden and the effects of treatments to reduce atheroma to be ascertained. Increased carotid arterial wall thickness measured by ultrasound carotid intima media thickness (C-IMT), is used as a surrogate for early atherosclerosis and vascular remodelling and is related to the risk of CV events in the general population [Granér 2006; Chambless 1997; O’Leary 1999; Lorenz 2007; Belcaro 1996]. Cardiovascular magnetic resonance (CMR) imaging of the carotid artery is non-invasive, free from ionising radiation and can provide high-resolution images. Quantitative

measurement of vessel wall volumes, with image matching in sequential studies is possible; good interstudy reproducibility, allows for smaller sample sizes in clinical trials [Corti 2001; Varghese 2005a,b]. Carotid CMR has shown wall volumes increase with age in healthy individuals [Keenan 2009a]. Correlation of carotid wall thickness between B-mode ultrasound (CIMT) and CMR has been found to be high [Underhill 2006]. In inflammatory conditions such as Takayasu's arteritis [Keenan 2009b] and Behçets syndrome [Chan 2011] wall volumes are greater than those found in healthy controls.

In this thesis I explore the existence and extent of atherosclerosis in two conditions associated with chronic inflammation: SLE and HIV.

In SLE subclinical accelerated atherosclerosis is well documented [Manzi 1999; Bruce 2000; Roman 2003; Asanuma 2003; Sella 2003; Chung 2006; Kao 2013]. Previous work by our group using CMR has shown increased carotid wall volume and a high prevalence of carotid plaque in a small study of individuals with SLE, including in those with no known or clinically apparent evidence of CVD [Keenan 2010]. Statins are potent LDL-cholesterol lowering drugs, achieving a 10-60% reduction in levels [Law 2003] and are indicated for primary prevention in patients with an increased risk of CVD [Cleeman 2001]. Statins significantly reduce cardiovascular morbidity and mortality [Pedersen 1994; Shepherd 1995; Simes 1998; Ridker 2008; Gotto 2012], reduce hsCRP levels [Ridker 2008] and atheroma regression has been observed [Nicholls 2007b]. We therefore undertook to study a greater number of individuals with SLE to confirm the existence and extent of cardiovascular disease using CMR (Chapter 8). We also undertook a randomised placebo controlled trial of rosuvastatin (the most potent drug in its class) in SLE patients with LDL-cholesterol <3.4mmol/L using carotid CMR as a surrogate for coronary artery disease, to study the possible beneficial vascular effects of statins in this patient group (Chapter 9).

HIV is another condition involving chronic inflammation and immune activation that is associated with an excess of cardiovascular risk [Sackoff 2006; Triant 2012]. The relative contribution of traditional risk factors, the virus itself or the adverse metabolic effects caused by the antiretrovirals used in HIV treatment is debated. Numerous studies have used C-IMT to look for the presence and rate of progression of subclinical atherosclerosis in HIV-infected individuals and to try to tease out the relative contributions of HIV and the antiretrovirals on CVD [Ho 2009; Hanna 2015]. Findings have been conflicting due to study design variation including ultrasound methodology, and the presence of confounding factors, such traditional cardiovascular risk factors and antiretroviral therapy in the HIV-infected groups. This has made the effect of HIV-infection itself hard to ascertain. We therefore undertook what we

believe to be the first study using CMR to look at carotid wall volumes in a group of stable adult HIV-infected individuals with low traditional cardiovascular risk and compared findings with a historic healthy cohort (Chapter 11). We evaluated whether carotid CMR would be a useful modality to evaluate the effect of future treatments on cardiovascular health. In paediatric and young adult groups with HIV-infection, ultrasound studies evaluating accelerated atherosclerosis have found conflicting results [Bonnet 2004; Charakida 2005; McComsey 2007] and no CMR data is available. Unlike in the adult HIV population, where guidelines recommend aggressive management of traditional cardiovascular risk factors including dyslipidaemia, in the paediatric population, only conservative measures, such as dietary advice, are currently taken. Given this and the evidence of premature subclinical atherosclerosis in the adult HIV cohort in Chapter 11, we undertook to study a cohort of young adults with perinatally acquired HIV-infection (Chapter 12). These individuals were paired with healthy controls to look for the presence and extent of vascular abnormalities, and to evaluate the suitability of carotid CMR as an imaging modality for future studies in this population.

These studies add to the body of knowledge of cardiovascular pathology in chronic inflammatory conditions, assist in determining whether there is identifiable accelerated atheroma attributable to HIV and the potential usefulness of CMR in risk stratifying and evaluating new therapies in these populations.

Chapter 2
Atherosclerosis

2.1 Introduction

Cardiovascular disease is the leading cause of mortality and morbidity in developed countries, and its increasing prevalence in developing countries will make it the leading cause of death worldwide by 2020 [Lloyd-Jones 2009; Murray 1997].

Our understanding of the pathophysiology of atherosclerosis has evolved significantly over the last century. Although the importance of inflammation in atherogenesis was recognised in the 19th century [Virchow 1858], subsequent decades saw atherosclerosis viewed as a degenerative and passive process, where the gradual increase in plaque size resulted in luminal stenosis and symptoms due to ischaemia, thrombosis and infarction. The 'lipid hypothesis' regarded atherogenesis as a lipid storage problem with deposition of lipids in the arterial wall. This was supported by strong experimental evidence of hypercholesterolaemia in animal models [Ross 1976a], humans [Smith 1972] and epidemiological data [Kannel 1990; Castelli 1984], as well as a multitude of clinical trials of lipid-lowering therapy [Pedersen 1994; Shepherd 1995; Ridker 2008].

The advancement of cell biology in the second half of the 20th century shifted the focus of study to the role of smooth muscle cells (SMCs) in atherosclerotic plaques. These were found to migrate to and proliferate in the arterial intima in response to endothelial damage, forming the start of the atherosclerotic plaque [Ross 1976b; Ross 1976c]. Further study identified macrophages, lymphocytes and other cells of the immune system within plaque [Aquel 1985; Jonasson 1986]. The last 20-30 years has seen atherosclerosis recognised as a complex, active and progressive disease with inflammation involved at every stage from inception to the development of complications such as thrombosis, and has lead to the development of the concept of the vulnerable plaque [Naghavi 2003a; Finn 2010].

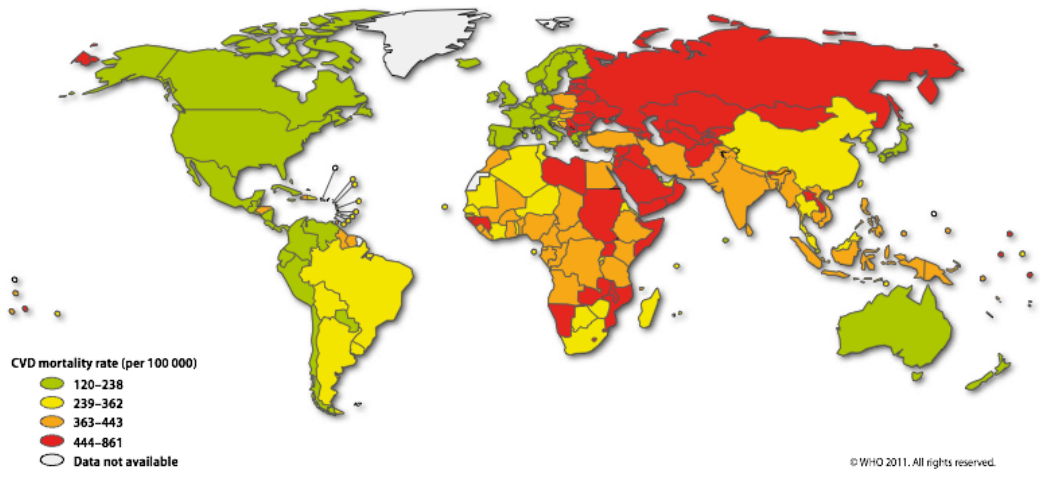
2.2 Epidemiology of atherosclerosis and cardiovascular disease

Cardiovascular disease (CVD) encompasses coronary heart disease (CHD) as well as cerebrovascular disease, peripheral vascular disease, cardiomyopathies, and congenital and rheumatic heart disease. CVD is the leading cause of death worldwide with over 80% of CVD deaths due to heart attack or stroke. An estimated 17.5 million people died from CVD in 2012, 7.4 million due to CHD and 6.7 million due to stroke. This is estimated to increase to 23.6 million by 2030 [WHO 2015].

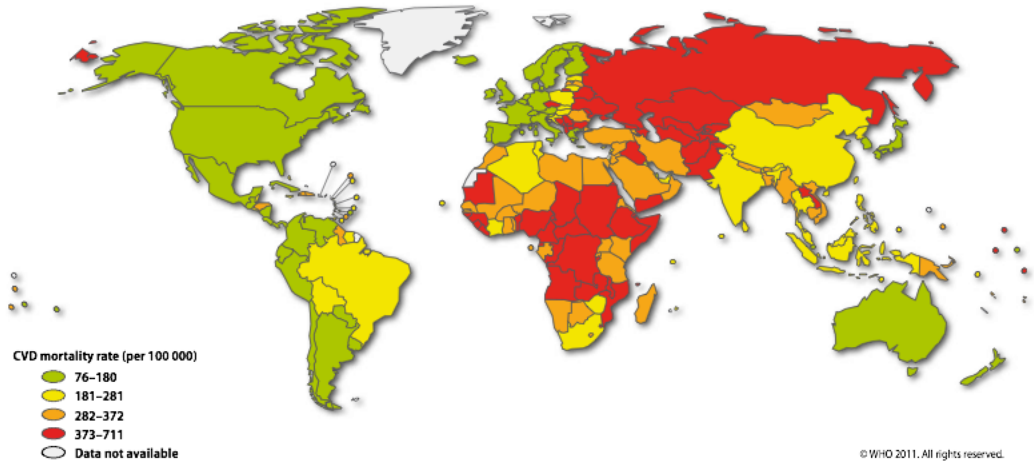
Although mortality rates are falling in most European countries, CVD remains the leading cause of death, accounting for approximately 50% (over 4 million) of all deaths [Nichols 2014]. CHD accounts for 1.8 million of these deaths. Mortality rates increase with age, but the great disparity in death rates and age at death between countries in the WHO European region exemplify differences in the stages of epidemiological transition countries find themselves in. Most Western and some Central and Eastern European countries are in the 'Fourth Proposition' when improved nutrition, sanitation and reduced environmental toxin exposure result in falling morbidity and mortality rates [McKeown 2009]. Many Central and Eastern European countries however are in the stage of 'Degenerative and man-made diseases' where improvements in CVD risk reduction and primary prevention are not widespread, and premature deaths from CVD remain high - (<65 years [McKeown 2009] and <75 years [Nichols 2014]). Figure 2.1 shows the age standardised CVD mortality rates for (a) males and (b) females around the world [Global Atlas on Cardiovascular Disease Prevention and Control 2011].

Figure 2.1. World map showing the global distribution of CVD mortality rates (age-standardised per 100,000) [from the Global Atlas on Cardiovascular Disease Prevention and Control. Mendis S, Puska P, Norrving B editors. World Health Organization, Geneva 2011].

a. Global distribution of age standardised CVD mortality rates for males.



b. Global distribution of age standardised CVD mortality rates for females.



In the United Kingdom, cancer has overtaken CVD as the leading cause of death – 29% versus 28% of all deaths in 2012 [Townsend 2014; Bhatnagar 2015]. CVD however was still the leading cause of death for women. 46% of all CVD deaths were due to CHD and CHD was the commonest cause of the 42,000 CVD premature deaths. Almost 2.3 million in the UK are living with CHD [Bhatnagar 2015].

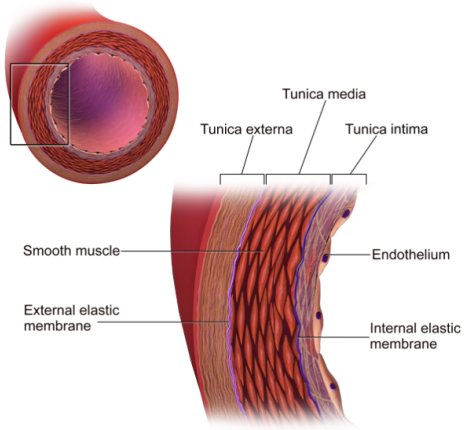
It is unclear whether improvements in CVD mortality will be maintained. In 2012 24.8% of UK adults were obese (BMI □30); in England 67% of men and 57% of women were overweight or obese (BMI □25) [Townsend 2014]. Amongst children aged 2 to 15 years, approximately 30% are overweight or obese [Townsend 2014]. A similar pattern has been observed in the United States, and the prevalence of diabetes mellitus has been increasing dramatically in parallel with this [Roger 2012].

2.3 Pathophysiology of atherosclerosis

2.3.1 Introduction

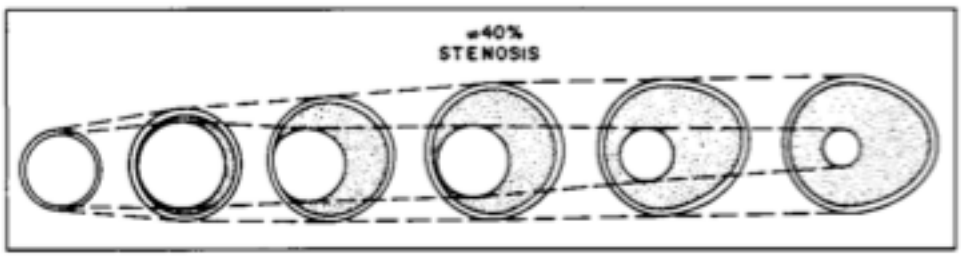
The arterial wall has three distinct layers (Figure 2.2). The innermost layer, the tunica intima, is bounded on the luminal side by a monolayer of endothelial cells resting on a basement membrane. Below this is an extracellular matrix of connective tissue and some SMCs. The intima is separated from the tunica media by the internal elastic lamina. The media is composed of SMCs and variable amounts of elastic tissue, collagen and proteoglycans. The outermost tunica adventitia, separated from the media by the external elastic lamina, is composed of connective tissue and fibroblasts.

Figure 2.2. The structure of the arterial wall [From Blausen.com staff. “Blausen gallery 2014”].



Atherosclerosis causes the arterial intima to thicken and a mature plaque gradually forms. In the initial stages, plaque formation leads to the outwards remodelling of the arterial wall so that the area of the lumen is preserved (Figure 2.3). Indeed, there is overcompensation of this process early on, so that lumen area actually increases. Eventually, however, this compensatory mechanism is insufficient and once the plaque occupies more than 40% of the internal elastic lamina area, the lumen narrows as the plaque encroaches inwards, resulting in reduced blood flow and eventually symptoms [Glagov 1987].

Figure 2.3. Outward remodelling of the coronary left main stem artery in response to plaque formation. Lumen area is preserved until the plaque occupies approximately 40% of the internal elastic lamina area, after which a sharp decline in lumen area becomes evident [Reproduced with permission from (Glagov 1987), Copyright Massachusetts Medical Society].



2.3.2 Initiation of atherosclerosis

The hallmark of the human atherosclerotic plaque has long been recognised as the lipid laden foam cell. Monoclonal antibodies have demonstrated that these are primarily derived from macrophages, although endothelial and SMCs can also become lipid-laden [Aqel 1985; Jonasson 1986].

Under normal circumstances, the intact endothelium, in contact with flowing blood, resists prolonged contact with and adhesion of, circulating lymphocytes. Endothelial injury, whether mechanical, haemodynamic [Helin 1971] (turbulence, hypertension), chemical [Harker 1974], immunologic [Hardin 1973], or toxic (e.g. smoking) [Pittilo 2000], causes expression of leucocyte adhesion molecules. Processes including oxidation and glycosylation modify lipoproteins accumulating in the sub-endothelial layer. Low-density lipoprotein (LDL) modification increases its uptake by macrophages and SMCs. LDL oxidation renders LDL particularly atherogenic. Plasma oxidised-LDL has been shown to be a strong predictor of coronary artery disease [Meisinger 2005].

The activated endothelium expresses adhesion molecules, including vascular adhesion molecule 1 (VCAM-1), intercellular adhesion molecule 1 (ICAM-1), E and P selectin, and cytokines including monocyte chemotactic protein 1 (MCP-1) and interleukin-8 (IL-8) [De Caterina 1995; De Caterina 2000]. Circulating monocytes adhere to the activated endothelium. Monocyte penetration into the tunica intima then occurs via a process of rolling and diapedesis along a cytokine chemotactic gradient [Libby 2006]. Within the intima, monocytes mature into macrophages under the influence of mediators such as macrophage colony-stimulating factor (M-CSF) [Libby 2002]. Scavenger receptors are expressed on their surface allowing modified lipoproteins to be bound and internalised. Thus, the lipid-laden foam cells characteristic of the early atherosclerotic plaque are formed. Macrophage replication within the intima is also promoted. Under the influence of their microenvironment, macrophages themselves secrete pro-inflammatory cytokines, matrix metalloproteinases (MMPs), reactive oxygen species (ROS) and tissue factor, amplifying the local inflammatory response [Libby 2002]. As atherosclerotic plaques mature, macrophage foam cells undergo apoptosis leading to the formation of the necrotic core [Libby 2012].

Other cells of the immune system also participate in atherosclerosis:

T-lymphocytes

T-lymphocytes are attracted to the inflamed arterial wall by chemokines (γ-IP-10, MIG and I-TAC), which interact with CXCR3 receptors expressed by the T-lymphocytes [Mach 1999]. Within the intima, T-lymphocytes encounter antigens (e.g. oxidised-LDL) and become activated. The cytokines they secrete, particularly CD154, which binds to macrophage CD40 ligand, cause macrophages to secrete MMPs, tissue factor and further cytokines [Libby 2002]. T-lymphocyte polarisation may also occur. TH1 cells (involved in cell-mediated immunity and mostly secreting pro-inflammatory mediators) tend to predominate over TH2 cells (involved in antibody-mediated immunity and mostly secreting anti- inflammatory

mediators) in the atheroma [Libby 2002]. Two further T-lymphocyte lineages may play a role in atherosclerosis. Regulatory T-cells may have a protective effect. An IL-17-producing T-helper lineage (TH17) is known to play an important role in autoimmune diseases [Taleb 2010]. The occurrence of accelerated atherosclerosis in patients with a variety of autoimmune diseases suggests involvement of autoimmune mechanisms in atherogenesis [Shoenfeld 2005]. Although TH17 cells have been shown variably to have both pro- and anti-inflammatory effects, current data suggest they may have a protective effect overall [Taleb 2010; Taleb 2009].

Mast cells

Small numbers of mast cells are found within atheromatous plaques. The chemokine eotaxin is over-expressed in atheroma. Its receptor, CCR3, is also over-expressed within plaques, localising primarily to macrophage rich areas, but also found on mast cells. Hence, eotaxin may mediate mast cell migration to and activation at sites of vascular inflammation [Haley 2000]. Once in the intima, mast cell degranulation with release of tumour necrosis factor-α (TNF-α), heparin and the proteinases tryptase and chymase may occur. Heparin may have inhibitory effects on SMCs whereas the proteinases may activate inactive forms of MMPs [Libby 2002].

Other

B-lymphocytes, killer cells and natural killer cells have also been identified in atherosclerotic plaques [Jonasson 1986]. Their exact role, however, remains to be defined. There is evidence that B1-lymphocytes may have atheroprotective properties whilst B2-lymphocytes are pro-atherogenic [Kyaw 2011].

2.3.3 Atheroma progression and complication

Following the onset of arterial wall inflammation, SMCs within the media migrate into the intima under the influence of chemotactic cytokines, particularly platelet-derived growth factor (PDGF), released by the activated endothelium and macrophages. Extracellular matrix degradation by MMP-9 and other proteinases facilitates this migration [Mason 1999]. The SMCs proliferate and, in response to growth factors such as transforming growth factor-β (TGF-β) and PDGF, secrete extracellular matrix proteins, including collagen. This mechanism forms the basis of the 'response to injury' hypothesis, part of the normal healing process. If the injury or inflammatory stimulus is removed early on, endothelial repair occurs and the lesion may regress. If the endothelial or arterial wall insult is repeated or continuous, the inflammatory process persists, amplifies and becomes maladaptive, resulting in further proliferation and enlargement of the lesion [Ross 1976c].

Collagen synthesis by SMCs helps to stabilise the plaque. The fibrous cap in contact with the lumen plays an important role in this. When extracellular matrix synthesis and breakdown is balanced, the fibrous cap is stable and the thrombogenic plaque contents are sequestered from the blood stream. T-lymphocyte derived interferon-γ (INF- γ) inhibits collagen production and reduces the effect of stimulatory growth factors and cytokines, including PDGF, on SMCs [Amento 1991]. MMPs degrade the extracellular matrix, and with ongoing inflammation collagen breakdown can exceed synthesis leading to thinning, destabilisation and rupture of the fibrous cap. Exposed plaque contents cause overlying thrombus to form resulting in vessel occlusion and/or distal embolisation. In many instances, small platelet thrombi may not lead to any clinically apparent sequelae but provide a stimulus for further up-regulation of the inflammatory response and sudden plaque expansion. Furthermore, plaque neovascularisation arising from the artery's vasa vasorum can occur. These vessels are fragile and can result in intraplaque haemorrhage, generating thrombin, which activates endothelial cells, macrophages, platelets and SMCs to secrete inflammatory mediators [Croce 2007], again causing further focal inflammation and a mechanism for sudden plaque growth.

2.3.4 Calcification

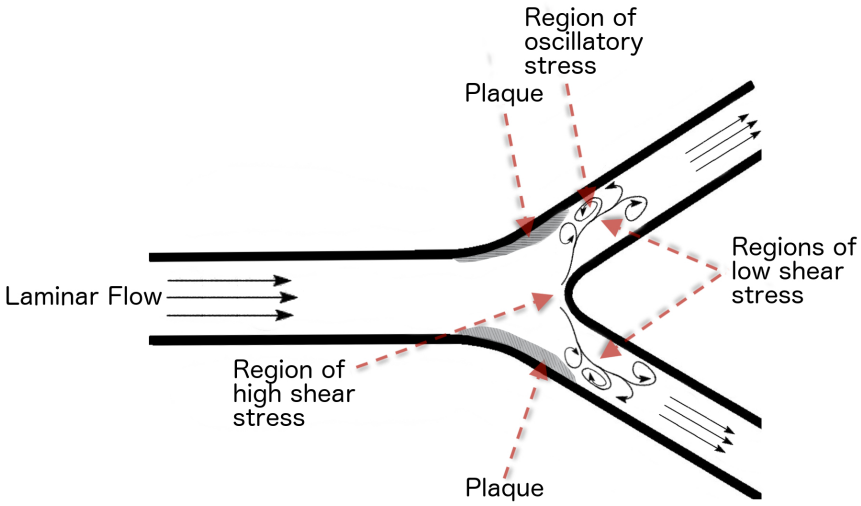
Calcification is often found in complex atherosclerotic plaques, although the process can begin early. Calcification is often found at sites of soft tissue chronic inflammation or injury and is believed to occur through passive deposition at sites of tissue degeneration or necrosis. Although inflammation and necrosis occur in the atherosclerotic plaque, and passive calcification may play a role, histopathological areas of bone-like calcification have also been found. Osteoblasts, osteoclasts and chondrocytes, all necessary for normal bone formation, have been identified within plaque, although the exact mechanisms by which this process is initiated and why only some plaques calcify are yet to be elucidated [Doherty 2003].

2.3.5 Focal development of atheroma

Despite the generalised nature of the stimuli leading to atherosclerosis, it has long been noted that atheroma does not develop uniformly along the arterial tree. Areas prone to atheroma include vessel branch points and the inner curves of arteries due to the type of blood flow they experience. Laminar blood flow generates shear stress. Areas of low shear stress are prone to atheroma whereas areas of normal or increased shear stress are protected (Figure 2.4). Oscillatory shear stress, which occurs at areas of arterial bifurcation and blood flow turbulence, predispose to atheroma formation [Cheng 2006]. Lowered shear stress or the occurrence of oscillatory shear stress reduces several atheroprotective

mechanisms such as lowering local endothelial-derived nitric oxide (eNOS), a vasodilator with anti-inflammatory properties [Cheng 2006]. This causes up-regulation of VCAM-1 and ICAM-1 expression [De Caterina 1995; Jongstra-Bilen 2006]. A reduction in the expression of the antioxidant enzyme superoxide dismutase, which reduces oxidative stress and hence pro-atherogenic LDL oxidation, also occurs [Fang 1998]. Differences in flow disturbance have also been shown to predispose to differences in plaque structure: atheromata in areas of lowered shear stress were larger containing fewer SMCs and collagen, but more lipids, and showed more outward remodelling than atheroma at sites of oscillatory shear stress. Hence, low shear stress produces atheroma with a vulnerable phenotype, whereas oscillatory shear stress results in stable plaques [Cheng 2006].

Figure 2.4. Diagram showing different types of flow and shear stress at an arterial bifurcation.



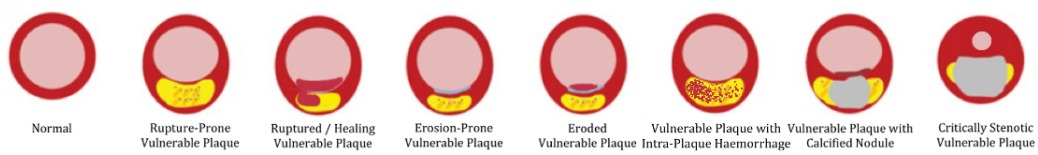
2.3.6 Vulnerable plaques and vulnerable patients

Acute coronary occlusion and the resultant acute coronary syndromes (myocardial infarction and unstable angina) frequently arise from mild to moderate stenoses, with many patients having never suffered prior symptoms. Ambrose *et al* demonstrated that only 22% of infarcts were associated with pre-existing coronary stenoses of >70%. Autopsy studies have shown plaque rupture to be the commonest plaque complication accounting for approximately 60-70% of acute myocardial infarctions [Naghavi 2003a; Finn 2010]. Plaque erosion accounts for 30-35% of myocardial infarctions with most of the rest due to thrombi associated with calcified nodules [Finn 2010]. These findings as well as studies demonstrating the involvement of active inflammatory processes within plaques prone to acute complications gave rise to the concept of the ‘vulnerable plaque’.

Vulnerable plaques contain one or more of a variety of features and have been classified into different types (see Figure 2.5). The main features are:

- a thin fibrous cap
- a lipid-rich core
- cap inflammation.

Figure 2.5. Different types of vulnerable plaque as described by Naghavi 2003a.



Stable plaques usually possess a thick fibrous cap of SMCs in a collagen-rich extracellular matrix [Finn 2010]. Activated macrophage and lymphocyte infiltration of the cap results in MMP secretion, matrix degradation and plaque instability. SMCs are also reduced, causing a further inability to replace collagen. This process is commonest at plaque shoulder regions (adjacent to normal intimal areas) resulting in thinning of the fibrous cap, which is most prone to mechanical failure from fluctuations in pressure and cyclic stretching and compression [Falk 1995].

An overall concept of the vulnerable patient has emerged [Naghavi 2003b]. This incorporates the presence of a vulnerable plaque phenotype with other features in the patients' blood and myocardium that increase their susceptibility to acute cardiovascular events. Factors increasing blood thrombogenicity include serological markers of atherosclerosis (e.g. abnormal lipoprotein profiles); markers associated with metabolic disorders (e.g. diabetes or the metabolic syndrome); markers of systemic inflammation (e.g. hsCRP, IL-6, ICAM-1, VCAM-1); markers of immune activation (e.g. anti-heat shock protein); and markers of apoptosis (e.g. Fas/Fas ligand). Serological markers indicating activation of the coagulation system may also occur in the vulnerable patient. These include increased markers of hypercoagulability (e.g. fibrinogen, D-dimer); increased platelet activation and aggregation; increased coagulation factors; decreased anticoagulation factors (e.g. protein C and S); decreased fibrinolysis; other thrombogenic factors (e.g. anticardiolipin antibodies, diabetes); and factors causing transient hypercoagulability (e.g. smoking, infection, adrenergic surge) [Naghavi 2003b].

2.4 Differences between the coronary and carotid arteries

The occurrence of and type of atherosclerotic plaque varies between arterial territories. Despite these differences, peripheral arteries such as the carotid arteries serve as surrogates for generalised CVD. They are used to study the effects of drugs on CVD due to their relative ease of imaging compared with coronary arteries.

An understanding of the differences between atheroma in the different territories is important:

- Atheroma pathology is broadly similar between the carotid and coronary circulations, although there is a predominance of foam cells in the carotid territory [Dalager 2007].
- Thrombus embolisation is more likely in the carotid circulation due to high blood flow [Golledge 2000]. Stroke due to thrombotic vessel occlusion is generally found with a severe (>95%) underlying carotid artery stenosis [Virmani 2006].
- Plaque ulceration is commoner in the carotid arteries. This is likely related to embolisation of thrombus overlying an area of plaque rupture, leaving an excavation in the plaque. Thrombus is more likely to remain adherent with lower flow rates in the coronary circulation [Virmani 2006].
- Intraplaque haemorrhage is commoner in carotid atheroma. This may be due to higher flow and increased pressure within the vessel lumen and vasa vasorum [Virmani 2006].
- Calcification occurs with similar frequency in coronary and carotid atheroma, but calcified nodules are seen more frequently in the carotids [Virmani 2006].

2.5 Atherosclerosis imaging

2.5.1 Introduction

Assessing atheroma burden and the effects of treatments to reduce it, requires arterial vessel wall imaging. The carotid artery is often used as a surrogate for the coronary arteries. Although an imperfect surrogate, the carotids are relatively large, superficial and immobile making them easily amenable to non-invasive imaging. The coronary arteries are much smaller and deeper making resolution harder, and cardiac and respiratory movement can create significant motion artefact.

When using the carotid artery as a surrogate it is important to recognise that wall thickening and plaque formation is much commoner and occurs earlier at the carotid bifurcation and the internal carotid artery (ICA), particularly the proximal outer wall of its sinus [Virmani 2006]. Plaque development in the carotid arteries (and indeed all arteries) is not uniform along the length or around the circumference of the vessel. Measurement of wall thickness at one point

is therefore a weaker measure than plaque area or volume in predicting future events or in assessing changes in plaque burden by clinical intervention. A modality that can image the carotid bifurcation and ICA, and assess wall and/or plaque volume, will allow for a significantly smaller sample size and shorter study duration than an imaging modality that can only assess the carotid in one dimension.

Numerous modalities to image the arterial wall exist and are currently used in trials to monitor atherosclerosis progression. All have advantages and disadvantages. The ideal modality should be safe, inexpensive, non-invasive (or minimally so), accurate, and reproducible, thus allowing serial studies in patients. Results should correlate with the extent of atherosclerosis and be able to predict clinical events.

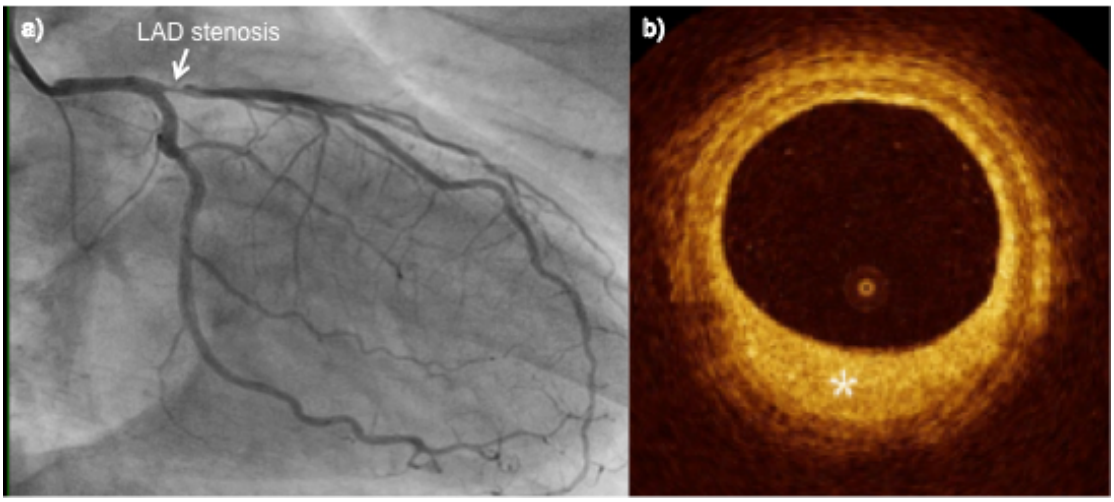
2.5.2 Angiography

Angiography remains the gold standard for assessing coronary disease. It obtains images of the lumen but gives no information of what is happening in the vessel wall (Figure 2.6). As we have seen, significant plaque burden may be present without any apparent stenosis being visible on angiography [Glagov 1987]. Angiography is also unable to give any information on plaque composition, although advances using invasive intravascular imaging modalities have been developed to overcome this limitation. Exposure to ionising radiation however remains, limiting it's use in clinical trials monitoring the progression or otherwise of atherosclerosis.

2.5.3 Optical coherence tomography (OCT)

OCT uses infrared light and has a higher resolution than intravascular ultrasound (IVUS - see below), but at the expense of poorer tissue penetration. It allows characterisation of superficial vessel wall structures including plaque fibrous caps, lipid pools and calcified nodules (see Figure 2.6), and can identify intraplaque microvessels, which are predictive of accelerated atherosclerosis progression [Zimarino 2016]. It is invasive, and an adjunct to coronary angiography, retaining the exposure to ionising radiation of that procedure.

Figure 2.6. Intravascular coronary imaging showing a) coronary angiography with a significant stenosis in the proximal left anterior descending (LAD), b) OCT showing a fibrous plaque [from Hasegawa 2015].



2.5.4 Near Infrared Spectroscopy (NIRS)

NIRS is a novel invasive catheter based imaging modality allowing assessment of the chemical composition of the atherosclerotic plaque. Changes in the reflection of emitted light form a chemogram where areas with a high probability of lipid are coloured yellow and areas with a low probability of lipid are coloured red [Zimarino 2016].

2.5.5 Ultrasound

Intravascular ultrasound (IVUS)

IVUS is an invasive, ultrasonic imaging modality performed during angiography with a catheter containing a high-frequency (20-45MHz) emitting transducer. It gives a grey-scale image of the vessel wall allowing imaging of the lumen and penetrating deep enough to provide information about the media-adventitial border. It allows visualisation of the severity and composition of plaques, which can be characterised as soft, fibrous, calcified or mixed plaques (the majority). Assessment is visually qualitative and therefore limits its use in assessing plaque morphology. Post-processing software allows virtual histology images to be generated. The amplitude and frequency of the reflected ultrasound beam generates colour-coded images classifying plaque components as necrotic (red), fibro-fatty (dark green), fibrous (light green) or calcified (white) [Zimarino 2016]. As with OCT and NIRS, it is invasive and an adjunct to coronary angiography, exposing the patient to ionising radiation.

Carotid ultrasound

Non-invasive B-mode ultrasound imaging can visualise the arterial wall with enough resolution to detect very early thickening of the intimal-medial layer [Uno 2010]. Although

carotid intimal-medial thickening (C-IMT) is not a pre-atherosclerotic stage (there is no evidence that plaque develops in regions of increased C-IMT), it appears to be a marker for the presence of atherosclerosis throughout the arterial tree [Uno 2010; Lorenz 2007; Poredos 2004]. Increasing C-IMT is associated with an increased prevalence of cardiovascular risk factors, the presence of atherosclerotic plaque and predicts risk of cardiovascular events in individuals with and without established CVD [Lloyd-Jones 2009; Uno 2010]. The use of C-IMT imaging in the evaluation of anti-atherosclerotic therapies is supported by previous studies, which have shown that drugs, such as the statins, which prevent cardiovascular events, cause regression of C-IMT [Smilde 2001]. Although non-invasive and free from ionising radiation, limitations include being highly dependent on the acquisition of quality images, lack of standardised imaging protocols, and a lack of consensus on what measures should be taken. Measuring both carotid walls would be more robust as would measures of the carotid bulb and ICA. These however are technically difficult to image with ultrasound. These factors mean that relatively large numbers of subjects, enrolled for a number of years, may be required for clinical studies.

2.5.6 Multislice computed tomography (MSCT)

MSCT is fast and easy to perform, with little difficulty in standardising imaging protocols. Its use in assessing and diagnosing CVD has increased significantly. It can detect and quantify the extent of coronary calcium. Improvements in resolution have improved its ability to detect lumen stenoses and atherosclerotic plaque within the artery wall [Uno 2010].

Coronary artery calcium score

Although the presence of calcium in the arteries is associated with underlying atheroma, absence of calcium does not equate to absence of atheroma. Intensive lipid lowering, which has shown beneficial effects on C-IMT, has little effect on coronary calcium scores [Nicholls 2007a]. This makes the use of non-contrast CT derived calcium scores unsuitable for clinical studies of anti-atherosclerotic treatments.

MSCT coronary angiography

Improved resolution allows the visualisation of atherosclerotic plaque using MSCT. It can distinguish normal areas of coronary artery from atherosclerotic areas and quantify atheroma burden. Coronary imaging with CT has been revolutionised by increased temporal and spatial resolutions (66-175ms; 240-600μm respectively), larger scan coverage, ECG-gating and a dramatic reduction in the radiation dose delivered - <1mSv possible for a full scan. Low-attenuation areas in plaque seem to accurately detect lipid-rich cores, whereas small high-attenuation areas represent calcification. Limited spatial resolution precludes

identification and measurement of fibrous caps, although a thin ring-like rim of contrast around plaques (termed 'napkin-ring sign') is believed to reflect neovascularisation and active inflammation [Zimarino 2016]. Despite improvements in resolution, exposure to ionising radiation, albeit significantly reduced doses, limits MSCT's use in longitudinal clinical studies of anti-atherosclerotic treatments.

2.5.7 Nuclear imaging

Nuclear imaging utilises tracer molecules, injected into the patient and detected by the scanner.

Single photon-emission computed tomography (SPECT)

Technetium-99 m-labelled (^{99m}Tc) radiotracers are used in myocardial perfusion imaging. ^{99m}Tc-labelled annexin A5, a novel SPECT tracer, has been proposed to detect apoptosis in plaques and hence, vulnerable plaques. Resolution however is limited and the tracer insufficiently specific to allow for regular use [Zimarino 2016].

Positron emission tomography (PET)

PET uses positron-emitting isotopes, most commonly fluorodeoxyglucose (FDG). FDG uptake is used to measure metabolic activity, and in plaques is taken up by macrophages. Hence plaques with significant FDG uptake have higher numbers of metabolically active macrophages and are more likely to be vulnerable [Zimarino 2016]. PET is limited by poor spatial resolution (5-7mm) and radiation exposure.

Co-registration with either CT or MRI is possible, yielding greater anatomical information e.g. whether FDG uptake is associated with plaque or with a closely associated lymph node. PET-CT has been used to investigate the relationship between circulating markers of inflammation and carotid plaque inflammation [Duivenvoorden 2013] and in statin studies, where reduction in arterial wall FDG-uptake was found in those randomised to statins [Tahara 2006] or to intensified statin therapy [Tawakol 2013].

2.5.8 High-resolution magnetic resonance imaging (MRI)

High-resolution MRI is the potential leading imaging modality for in vivo atherosclerotic plaque characterisation [Corti 2006]. It is non-invasive, does not involve ionising radiation, and can provide high-resolution images of various arterial territories. It enables the quantitative measurement of vessel wall volume. It is therefore ideal for use in longitudinal studies, with the matching of images possible.

The subject is placed in a strong magnetic field and the image is based on the radiofrequency signal given off following administration of a radiofrequency pulse. No contrast is needed. The emitted signal varies according to water concentration and relaxation times (see Chapter 4 Cardiovascular Magnetic Resonance). Multicontrast MRI uses a combination of T1-weighted (T1w), T2-weighted (T2w), and proton-density-weighted (PDW) images, and has enabled the characterisation of plaque anatomy and composition [Choudhury 2004] (see Chapter 4). Lipid lowering by statins in patients with hypercholesterolaemia and known atherosclerosis has been shown to cause atheroma regression in the carotid arteries and aorta after a minimum of 12 months [Corti 2001]. Limited temporal and spatial resolution, and issues related to cardiac and respiratory motion currently confines MRI studies to larger arteries such as the carotids and aorta; it cannot yet be used to routinely and reliably assess coronary disease.

Given these facts, MRI is the imaging modality used for the carotid research in this thesis. CMR imaging of atherosclerosis is discussed further in Chapter 4 Cardiovascular Magnetic Resonance.

Chapter 3
Lipids and the 3-hydroxy-3-methylglutaryl coenzyme A reductase inhibitors

3.1 Introduction

Coronary heart disease (CHD) is a multifactorial disorder influenced by genetic susceptibility as well as modifiable and non-modifiable risk factors, and their interactions. The potential association of cholesterol and atherosclerosis goes back to the start of the 20th century when the atherosclerotic plaques of human aortas were found to contain over twenty times the level of cholesterol as normal human aortas, and rabbits fed pure cholesterol developed hypercholesterolaemia and severe aortic atherosclerosis [Endo A 2010]. The identification of Familial Hypercholesterolaemia suggested a strong causal relationship between cholesterol and coronary heart disease - homozygotes with severely elevated cholesterol levels from birth manifest coronary heart disease in childhood, and heterozygotes develop premature atherosclerosis by early adulthood [Müller 1939]. Dyslipidaemias, particularly high levels of LDL-cholesterol, low levels of HDL-cholesterol and hypertriglyceridaemia are now known to be risk factors for CHD [Genest 1992; Prospective Studies Collaboration 2007].

3.2 Cholesterol synthesis pathway

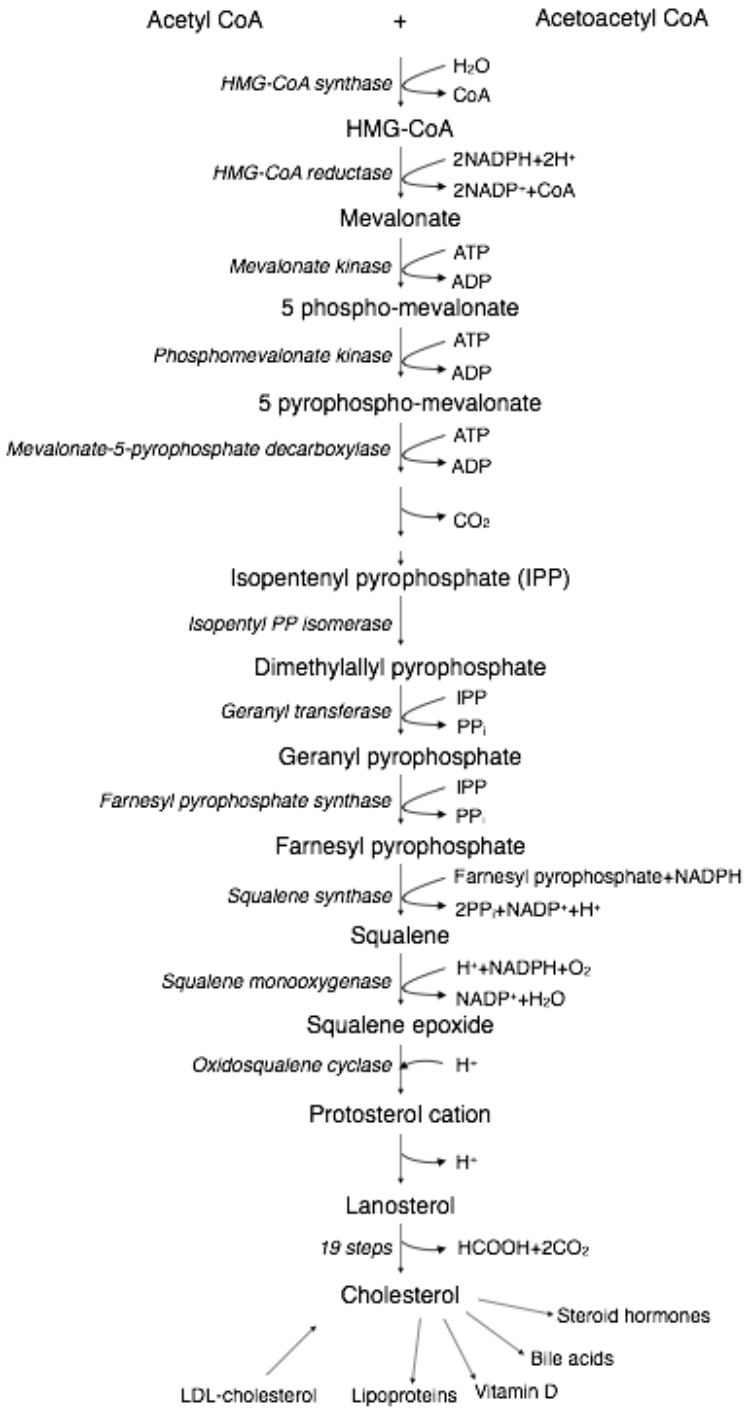
3.2.1 Introduction

Cholesterol is an essential component of animal cell plasma membranes, acting as a barrier between the cell and it's environment and maintaining membrane structural integrity and fluidity. Cholesterol insulates and plays a crucial role in the myelin sheath that surrounds neuronal axons, is involved in intracellular transport and cell signalling, and is the precursor of steroid hormones and bile acids.

Cholesterol can be obtained from the diet, but in humans, approximately 80% is synthesised. Production occurs mainly in the liver with the intestines also forming significant amounts. The synthesis of mevalonate is the committed step in the production of cholesterol (see Figure 3.1), which occurs in three steps:

Stage 1 – synthesis of isopentenyl pyrophosphate
Stage 2 – condensation of six molecules of isopentenyl pyrophosphate to form squalene
Stage 3 – cyclization of squalene to ultimately form cholesterol

Figure 3.1. Cholesterol synthesis pathway

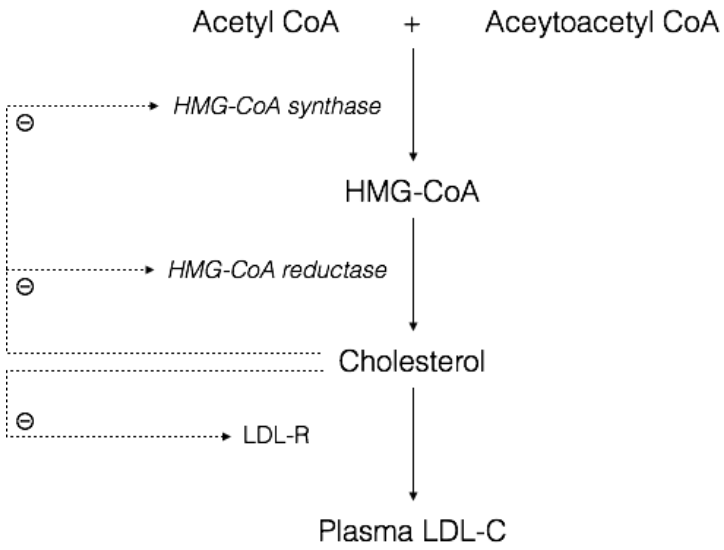


3.2.2 Regulation of cholesterol synthesis

The amount and rate of cholesterol synthesis responds to levels of cellular cholesterol. This feedback mechanism acts primarily at the level of HMG-CoA reductase as well as at the level of HMG-CoA synthase (Figure 3.2). Liver cells are influenced by dietary cholesterol as they take up cholesterol-rich chylomicron remnants. Cells elsewhere in the body respond to plasma cholesterol levels, primarily LDL-cholesterol, by up- or down-regulating plasma

membrane LDL-receptor production.

Figure 3.2. Cholesterol synthesis regulation feedback mechanism



3.3 Lipoprotein classification

3.3.1 Introduction

Lipids are insoluble and carried as lipoproteins in plasma. Lipoproteins consist of a hydrophobic lipid core surrounded by a shell of hydrophilic phospholipids, proteins and un-esterified cholesterol. Lipoproteins are associated with a variety of apolipoproteins, which have different functions and lend different physicochemical properties to the lipoprotein particles.

3.3.2 The major lipoproteins

Chylomicrons are formed in the intestine. These very large apoB-containing, triglyceride-rich particles carry dietary lipids (triglycerides (TGs), cholesterol) to tissues that utilise fatty acids as fuel and for fat synthesis. There, they are metabolised by lipoprotein lipase to release the TGs and cholesterol-rich chylomicron remnants are formed. Chylomicrons are associated with a variety of apolipoproteins including apoA-I, apoA-II, apoA-IV, apoC-I, apoC-II, apoC-III, and apoE.

Chylomicron remnants contain dietary cholesterol esters. They are transported to and taken up by the liver.

Very low-density lipoprotein (VLDL) particles are apoB-containing and TG-rich. They carry endogenous TGs and to a lesser extent cholesterol. They are produced by the liver, and like chylomicrons, their TGs are hydrolysed by lipoprotein lipase on blood vessel surfaces. They are associated with apolipoproteins including apoB-100, apoC-I, apoC-II, apoC-III and apoE.

Intermediate density lipoprotein (IDL) is the apoB-containing, cholesterol-rich VLDL remnant. Some are taken up by the liver for processing whilst others have more TGs removed to form low-density lipoprotein. They are associated with apolipoproteins including apoB-100, apoC-III and apoE.

Low-density lipoprotein (LDL) is the major cholesterol carrier in blood. They are apoB-containing cholesterol-rich particles transporting cholesterol to peripheral tissues and regulating *de novo* cholesterol synthesis at these sites (see above). They are associated with apolipoproteins including apoB-100 and apoC-III.

Lipoprotein (a) [Lp(a)] are apoB-containing, cholesterol-rich particles. They consist of LDL attached to an additional apolipoprotein called apo(a) and are generally denser and larger than LDL.

High-density lipoprotein (HDL) are apoA-I-containing, cholesterol-rich particles. They pick up cholesterol released into plasma by dying cells and from membrane turnover. The cholesterol is esterified and transported to the liver, to tissues synthesising steroid hormones or shuttled to VLDL or LDL. They are associated with apolipoproteins including apoA-I, apoA-II, apoC-I, apoC-II, apoC-III and apoE.

3.4 Lipids and atherosclerosis

3.4.1 Introduction

The 'lipid hypothesis' regarded atherogenesis as a lipid storage problem with deposition of lipids in the arterial wall. Although the association of hyperlipidaemia with atherosclerosis is well recognised, this does not reflect a simple problem of passive lipid storage. Rather, it is the abnormal handling of lipoprotein metabolism that is a major risk factor for atherosclerosis and dyslipidaemia has been found to be present in over 70% of patients with premature CHD [Genest 1992].

3.4.2 LDL

All LDL particles increase the risk of atherosclerosis and atherosclerotic cardiovascular events [Genest 1992; Prospective Studies Collaboration 2007; Parish 2012]. Apo B-100

containing lipoproteins interact with subendothelial extracellular matrix proteoglycans to initiate atherosclerosis [Olofsson 2005]. Macrophages can take up circulating LDL to form foam cells [Libby 2002; Libby 2012]. Oxidation of LDL can occur in arterial endothelial cells, smooth muscle cells and T-lymphocytes, as well as in macrophages, resulting in the promotion of inflammatory and immune changes through macrophage cytokine release and antibody production [Holvoet 1994; Libby 2002; Libby 2012]; disruption of the endothelial cell surface and impaired endothelial function resulting in the reduction of nitric oxide, a major mediator of endothelium-dependent vasodilatation [Chin 1992; Mathew 1997]; increased platelet aggregation, and thromboxane release (which contributes to vasoconstriction and thrombus formation) [Ardlie 1989; Magwenzi 2015]; and may play a role in plaque instability [Ehara 2001].

Small cholesterol-poor LDL particles penetrate the endothelial barrier more effectively than large LDL particles, and their retention allows longer for modification of surface phospholipids and un-esterified cholesterol by reactive oxygen species [Libby 2002; de Graaf 1991; Diffenderfer 2014]. Small LDL particles have apoB conformational changes that impair the efficiency of LDL receptor-mediated clearance, allowing these particles to circulate for longer where they become susceptible to oxidation, glycation, and glyco-oxidation [Lund-Katz 1998]. Most prospective studies have shown LDL particle concentration or apoB are stronger predictors of cardiovascular events than LDL cholesterol. In the Framingham Offspring Study LDL particle concentration was approximately twice as strongly related to CVD incidence compared to LDL-cholesterol [Cromwell 2007]. In individuals whose LDL-cholesterol and LDL particle concentration were discordant, (above-median LDL-cholesterol with below-median LDL particle concentration or vice versa), CVD event risk was more closely associated with LDL particle concentration than with LDL-cholesterol [Cromwell 2007].

3.4.3 Lipoprotein (a)

At least 40 subtypes of Lp(a) have been identified [Segrest 2002]. Increased levels have been positively associated with increased risk of CHD [Danesh 2000; Emerging Risk Factors Collaboration 2009] as have the smaller isoforms of Lp(a) [Simó 2001]. High Lp(a) levels have also been associated with premature CHD [Genest 1992].

Although LDL-cholesterol has a causal role and is accepted as a major risk factor in the initiation and progression of atherosclerosis, atherosclerosis has also been associated with other lipoprotein particles.

3.4.4 IDL

An increased incidence of CHD and acute CVD events have been seen in patients with elevated IDL levels [Masuoka 2000; Segrest 2002] and has been associated with the progression of C-IMT [Hodis 1997]. IDL can be taken up by macrophages to form foam cells [Ellsworth 1987] and can impair endothelial function [Kugiyama 1998].

3.4.5 VLDL and chylomicrons

The increased risk of atherosclerosis with VLDL, chylomicrons and other atherogenic lipoprotein particles may be due to that associated with their major components – TGs and apoC-III. TG-rich lipoprotein particles are associated with cholesteryl ester transfer protein-mediated lipid exchange resulting in lower levels of HDL-cholesterol. Smaller TG-rich HDL particles have reduced macrophage cholesterol efflux capacity reducing the efficiency of reverse cholesterol transport and hence HDL's cardioprotective effect (see below) [Kannel 2009]. Increased apoC-III levels are associated with increased TGs as well as increased atherosclerosis risk. The ability of lipoproteins to bind to vascular proteoglycans has been shown to be positively associated with the levels of apoC-III [Olin-Lewis 2002]. High levels of apoC-III have also been shown to inhibit lipoprotein and hepatic lipase (resulting in increased TG levels) and augment arterial inflammation (stimulating monocytes to adhere to endothelial cells) [Bobik 2008].

3.4.6 HDL

HDL particles, in contrast to other lipoproteins, are atheroprotective [Prospective Studies Collaboration 2007] and low levels of HDL are associated with premature atherosclerosis [Genest 1992]. Much of the anti-atherogenic effect of HDL is believed to be mediated by cholesterol efflux, the removal of excess cholesterol from macrophage cells. This is the initial step in HDL's reverse cholesterol transport from the periphery to the liver and has been shown to correlate inversely with the incidence of cardiovascular events [Rohatgi 2014].

HDL may have antioxidant and anti-inflammatory properties. Associated enzymes such as paraoxonase, platelet-activating factor acetylhydrolase, and lecithin-cholesterol acyltransferase can inhibit LDL oxidation, and associated apolipoproteins such as apoA-I, apoA-II, and apoE, can delay or prevent the formation of oxidised LDL [Kontush 2003]. It increases eNOS production thereby improving endothelial function [Bisoendial 2003] and inhibits VCAM-1, ICAM-1 and E-selectin expression [McGrath 2009]. HDL may also have an antithrombotic role by interfering with von Willebrand Factor self-association [Chung 2016], and by affecting fibrinolytic activity and reducing platelet aggregation [Pajkrt D 1997] among other mechanisms.

3.5 3-hydroxy-3-methylglutaryl coenzyme A reductase inhibitors

3.5.1 Introduction

There are several classes of lipid-reducing agents including 3-hydroxy-3-methylglutaryl coenzyme A reductase inhibitors (statins), fibric acid derivatives, bile acid sequestrants, cholesterol absorption inhibitors, nicotinic acid and the novel PCSK9 inhibitors. They differ in terms of their mechanisms of action, and the type and degree of lipid lowering. Lipid lowering, at least with the statins, has been shown to have beneficial effects in both primary and secondary prevention of CHD.

3.5.2 Mechanism of drug action - effect on lipids

An important control point in cholesterol biosynthesis is the formation of mevalonate, catalysed by 3-hydroxy-3-methylglutaryl coenzyme A reductase **(**HMG-CoA reductase) in an irreversible step (Figure 3.1). In 1973, the 3-hydroxy-3-methylglutaryl coenzyme A reductase inhibitor, mevastatin (compactin) was discovered by Akira Endo. It was one of three active metabolites derived from the mold Penicillium citrinum shown to potently inhibit cholesterol synthesis both in vitro and in vivo [Endo 2010].

Statins competitively inhibit HMG-CoA reductase, resulting in a reduction in the synthesis of cholesterol by the liver. Up-regulation of LDL receptor expression occurs causing increased uptake of plasma LDL, and consequent decrease in plasma LDL-cholesterol concentration [Goldstein 2009]. Statins are the most potent drugs for lowering LDL-cholesterol, with reductions in the range of 10-60% and their effect is dose dependent [Law 2003]. They are not, however, selective in reducing LDL-cholesterol subclasses, reducing the predominant subclass the most, although this is of course beneficial in those with an atherogenic dyslipidaemia profile [Rosenson 2009; Otvos 2002].

Statins alter HDL-cholesterol levels, typically raising them, although the effect is usually modest and can vary by statin type and dose [Jones 3003; Barter 2010]. HDL-cholesterol increase does not correlate with the observed reduction in LDL-cholesterol and may decline at higher statin doses, a phenomenon observed with atorvastatin [Jones 2003; Law 2003; Barter 2010].

Statins also reduce TG concentration by up to 46% and this effect is generally dose-dependent [Jones 2003; Bakker-Arkema 1996]. The mechanism of action may occur via LDL-receptor binding of apoB and apoE containing TG-rich VLDL and remnant particles, thereby reducing TG levels and the synthesis of these particles [Bakker-Arkema 1996].

Statin therapy is indicated for secondary prevention in patients with CHD, and for primary prevention in patients with an increased risk of CVD, with the target LDL varying according to risk profile: LDL <160mg/dL (<4.1mmol/l) for 0-1 risk factors; LDL <130mg/dL (<3.4mmol/l) for 2+ risk factors; LDL <100mg/dL (<2.6mmol/l) for known CHD or CHD risk equivalent [Cleeman 2001].

3.5.3 Plaque regression and non-lipid related effects of the statins

Significant reductions in cardiovascular morbidity and mortality have been demonstrated with statin therapy and associated reductions in LDL-cholesterol in many clinical trials [Pedersen 1994; Shepherd 1995; Ridker 2008; Simes 1998; Gotto 2012]. Regression of atherosclerotic plaque on statin therapy has been associated with reductions in LDL-cholesterol and with increases in HDL-cholesterol [Nicholls 2007b]. Plaque regression has been observed in studies using imaging by angiography [Blankenhorn 1993], IVUS [Nissen 2006], C-IMT [Hodis 1996] and MRI [Corti 2001; Migrino 2011, Corti 2005]. Although the potent reduction in LDL-cholesterol, and the consequent reduction in intimal lipoprotein accumulation and oxidation, could be expected to be the mechanism by which statins improve cardiovascular morbidity and mortality, the involvement of HMG-CoA reductase in the formation of compounds other than cholesterol and the possible involvement of statins in other immunomodulatory processes has led to a hypothesis that statins may exert additional (pleiotropic) effects.

The benefits on CHD observed with the statins are incompletely understood. Although the maximal hypolipidaemic effect with statins can be achieved by 6 weeks [Corti 2005] significant plaque regression is not seen before 6 months and often takes a minimum of 12-24 months to become apparent [Migrino 2011; Corti 2005; Corti 2001; Nissen 2006]. The clinical benefits of lipid lowering however are frequently seen as early as six months [Shepherd 1995; Ridker 2008], often before significant regression occurs. Other factors are therefore postulated to contribute. These include reduced leucocyte migration, inflammatory mediators and smooth muscle proliferation; plaque stabilisation; reversal of endothelial dysfunction; and decreased thrombogenicity.

Intermediate products of the cholesterol synthesis pathway are used in various other cell-signalling pathways, and one of the principle effects of statins appears to be inhibition of leukocyte/endothelial interaction. The isoprenoids geranylgeranyl pyrophosphate and farnesyl pyrophosphate, activate the small GTPase family of signaling molecules (e.g. RhoA), which are thought to control cellular functions such as cytoskeleton rearrangement, neutrophil migration, and reactive oxygen species (ROS) generation [Maher 2009]. Statins have been shown to reduce the trans-endothelial migration of neutrophils, important in the

early stages of atherosclerosis, by inhibiting RhoA [Maher 2009]. Statins have been shown to decrease levels of ICAM-1, [Rezaie-Majd 2003; Blanco-Colio 2007; Raza 2012] P-selectin, [Lefer 2001] TNF-□,[Raza 2012] and MCP-1 [Blanco-Colio 2007]. Clinically, statins have been observed to reduce circulating markers of inflammation such as hs-CRP [Ridker 2008], CRP and nuclear factor-k B [Mihos 2012]. This, together with inhibition of and reduction of the secretion of metalloproteases, such as MMP-9, from macrophages may contribute to plaque stabilisation by statins [Bellosta 1998]. A role in attenuating smooth muscle cell proliferation has been observed which may be important in reducing atherosclerosis [Lefer 2001].

Statins have been demonstrated to reduce macrophage superoxide formation and endothelial superoxide anion formation by preventing the prenylation of proteins belonging to the Rac family [Bellosta 2000], hence reducing ROS. Endothelial dysfunction occurs early on in atherosclerosis and up-regulation of eNOS by statins and resultant increase in NO improves endothelial function and protects against atherosclerosis [Laufs 1998]. This has been shown to occur in normocholesterolaemic as well as hypercholesterolaemic cells [Lefer 2001].

Statins have also been implicated in increasing fibrinolytic activity by increasing tissue plasminogen activator activity and decreasing plasminogen activator inhibitor-1 levels [Lefer 2001]. Decreased tissue factor expression by macrophages reduces activation of the coagulation cascade [Lefer 2001; Bellosta 2000].

Chapter 4
Basic Principles and Physics of Cardiovascular Magnetic Resonance

4.1 Introduction

Cardiovascular magnetic resonance (CMR) is a non-invasive imaging modality free from ionising radiation. It is able to image the arterial vessel wall as well as the lumen and is the gold standard for measuring cardiac ventricular mass and function [Hundley 2010], allowing a comprehensive cardiovascular assessment to be carried out. It is not limited by anatomical constraints (e.g. acoustic windows,) and imaging can occur in any plane. Vessel wall imaging is important, enabling the detection of subclinical disease, and allowing for appropriate primary prevention prior to the onset of symptoms or complications. It can help to identify individuals at risk from acute vascular events from plaque rupture by diagnosing atherosclerosis were other imaging modalities may fail – e.g. those with outward remodelling associated with plaque which would be interpreted as normal on imaging techniques relying on luminography. Information on plaque composition can also be obtained, potentially identifying vulnerable plaques at a higher risk of an acute cardiovascular event, something which occurs predominantly in mildly to moderately sized plaques [Ambrose 1988].

4.2 Physics

4.2.1 Introduction

Nuclear magnetic resonance (NMR) is a phenomenon in which nuclei in a magnetic field absorb and re-emit electromagnetic radiation. This energy is at a specific resonance frequency, which depends on the strength of the magnetic field and the magnetic properties of the atoms used. The human body is composed mainly of water and fat, which contain many hydrogen atoms. The hydrogen atom consists of a single nuclear proton (^{1}H) and an electron. CMR depends on the detection of the intrinsic angular momentum (spin) of the hydrogen protons as they interact with magnetic fields.

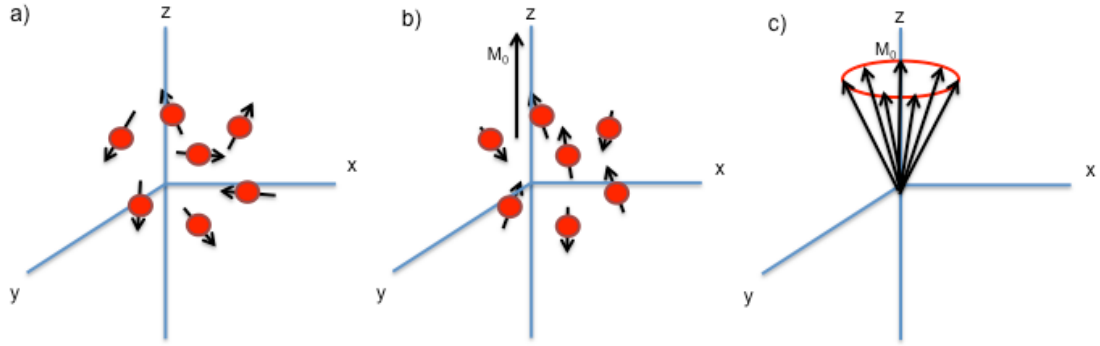
In the absence of a magnetic field, the spin of the hydrogen protons is randomly orientated (Figure 4.1). When placed in a large magnetic field ($\square_0$), such as that in the bore of a CMR scanner, the ^{1}H spins align themselves around the $\square_0$ field - a small excess align in parallel to the direction of the field (a low energy state), and the rest align in the anti-parallel direction (a high energy state). The protons aligned in parallel produce a net magnetisation vector (M_0) in the field direction (Figure 4.1).

The spin of ^{1}H protons around the direction of the B_0 field is known as precession. The frequency of precession is defined by the Larmor equation:

$\omega = (\gamma/2\pi) B_0$

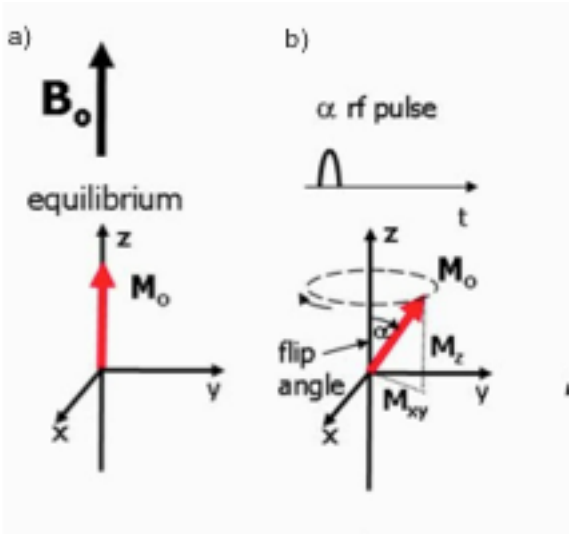
where ω is the precessional (or Larmor) frequency in Hertz (Hz); γ is the gyromagnetic ratio in Hz/Tesla, and related to the mass and charge of the atom used – for ^{1}H $\gamma/2\pi$ is 42.58 MHz/Tesla; B_0 is the magnetic field strength in Tesla (T).

Figure 4.1. Orientation of nuclear spins. B_0 field is in the z-axis. a) no magnetic field, b) and c) with magnetic field B_0 rotation occurs randomly around z-axis with no net magnetisation in xy.



The direction of the main magnetic field B_0 defines the z-axis (also known as the longitudinal direction), and M_0 lies along this axis. There is however, no net magnetisation in the xy-axis (transverse plane). To create an image (which is detected in the xy-axis by a receiver coil) the ^{1}H spins must be made to precess temporarily in the xy plane. This is achieved by applying a second, less powerful, magnetic field (B_1) perpendicular to B_0. This radiofrequency (RF) excitation pulse causes the ^{1}H protons to 'flip' through an angle (0-180^o) depending on the strength and the duration of the RF pulse. B_1 is transient, lasting milliseconds and is applied at the Larmor frequency of ^{1}H protons. ^{1}H protons absorb this energy and precess around the direction of the B_1 field, in the direction of the xy plane (Figure 4.2). When B_1 is switched off, ^{1}H protons precess around the B_0 field axis and return to align themselves with the B_0 field direction. In doing so an oscillating magnetic field can be detected by the receiver coils in the xy plane. The signal decays in amplitude over time, and the decay is known as relaxation. Two types of relaxation occur, T1 (longitudinal) and T2 (transverse or dephasing). Both types of relaxation occur at the same time, but T2 relaxation is typically much faster.

Figure 4.2. a) At equilibrium, the net magnetisation, M_o is at equilibrium, aligned along the z axis. b). When an rf pulse is applied, M_o makes an angle with the z-axis, known as the flip angle, and rotates around the axis in the direction of the curved arrow. At any instant the magnetisation can be split into two components, M_z and M_{xy}. The rotating Mxy component generates the detectable MR signal. [Adapted from Ridgway 2010].



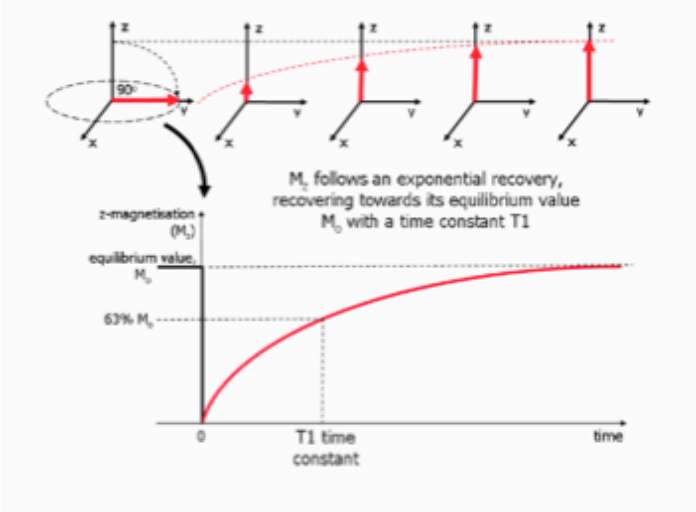
4.2.2 T1 relaxation

T1 relaxation, also known as spin-lattice relaxation, is a time constant characterised by the rate at which the longitudinal component of magnetisation, the M_z vector, recovers towards its state of equilibrium. It occurs due to energy release to the environment (lattice) and the net magnetisation vector increases (recovers) exponentially in the z-axis. It is also referred to as T1 recovery and derived from the equation:

$M_z(t)=M_0(1- e^{-t/T1})$

where t=time after RF pulse. Following a 90^o RF pulse, Mz is initially 0, but increases to its equilibrium value. T1 is defined as the time it takes for 63% of the longitudinal magnetisation to recover (Figure 4.3). Each tissue has a unique T1, which is utilised in CMR to create images. Myocardial T1 is 1100ms and blood 1600ms at 1.5T.

Figure 4.3. Diagram showing the process of T1 relaxation after a 90° RF pulse is applied. [Reproduced from Ridgway 2010].



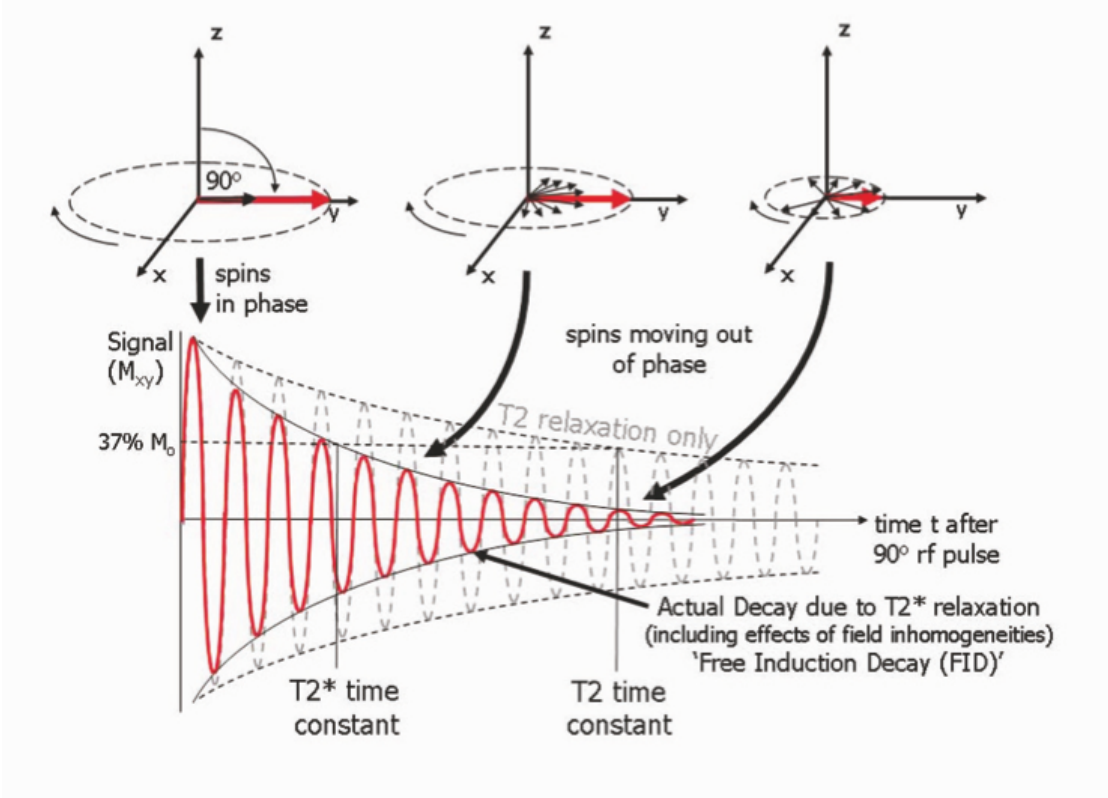
4.2.3 T2 relaxation

T2 relaxation, also known as spin-spin relaxation, is a time constant characterising the exponential decay of the transverse component of the magnetisation vector (M_{xy}) towards its equilibrium value as it rotates about the z axis. T2 is defined as the time for the transverse magnetisation to fall to 37% (1/e) of its initial value. T2 relaxation occurs as the precessing protons move out of phase with each other (Figure 4.4). A protons precession rate depends on the magnetic field it is in. $\square_0$ is constant, but the magnetic moment of each proton causes a slight variation in the magnetic field experienced by an adjacent proton. As protons move rapidly and randomly, the net effect is for the frequency of any given proton to fluctuate randomly resulting in a loss of coherence in the tissue being sampled. This is unavoidable and irreversible.

4.2.4 T2* relaxation

The observed rate of dephasing is greater than that expected from T2 relaxation (Figure 4.4). $\square_0$ field inhomogeneities are a second cause for dephasing. As $\square_0$ is inhomogeneous, the frequency of the spins in different regions varies. This causes randomisation of the spin phases and a decrease in the net transverse magnetisation. T2* relaxation includes this as well as T2 (spin-spin) relaxation and is therefore always shorter than T2. T2* is an exponential process.

Figure 4.4. Diagram showing the process of transverse relaxation after a 90° RF pulse is applied. [From Ridgway 2010].



4.2.5 CMR sequences

An imaging sequence is the combination of a set of RF pulses and applied gradients leading to image generation. In CMR, the signal is measured in the form of an echo. The two commonest types of echo used are spin echo (SE) and gradient echo (GE). In general, blood is black and fat white in SE sequences, and is therefore also known as black-blood imaging. GE sequences result in images where both blood and fat are white, termed white-blood imaging.

Spin echo

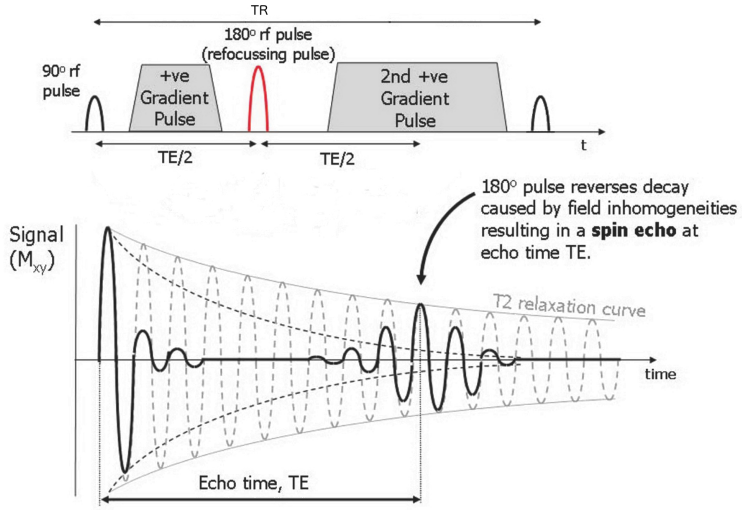
Spin echoes are created by the application of a 90° excitation RF pulse followed by a refocusing 180° RF pulse (Figure 4.5), which eliminates field inhomogeneities and therefore T2* relaxation. They are more robust than GE sequences and less affected by field inhomogeneities caused by metallic artefacts. SE sequences are used to acquire static images and are used for anatomical imaging. In CMR, image acquisition is timed to the ECG (ECG-gated) to minimize cardiac motion artefact.

The contrast obtained in the CMR image is dependent on the T1 and T2 relaxation. The time the spins remain in the transverse plane determines the amount of T2 relaxation that occurs.

This is called the time to echo (TE) and is the time taken between the centre of the 90° RF pulse and the centre of the echo; this is twice the duration between the 90° and 180° RF pulses. In general, the longer the TE, the greater the T2 contrast or weighting.

The repetition time (TR) of the sequence is based on T1 relaxation. It is the time between successive 90° RF pulses, and is the time needed to allow sufficient longitudinal signal recovery before another pulse series can be applied. A change in TR will alter the T1 contrast, or weighting, of the image. A long TR reduces the influence of T1 relaxation time differences in the image and vice versa.

Figure 4.5. Formation of a spin echo [Adapted from Ridgway 2010].



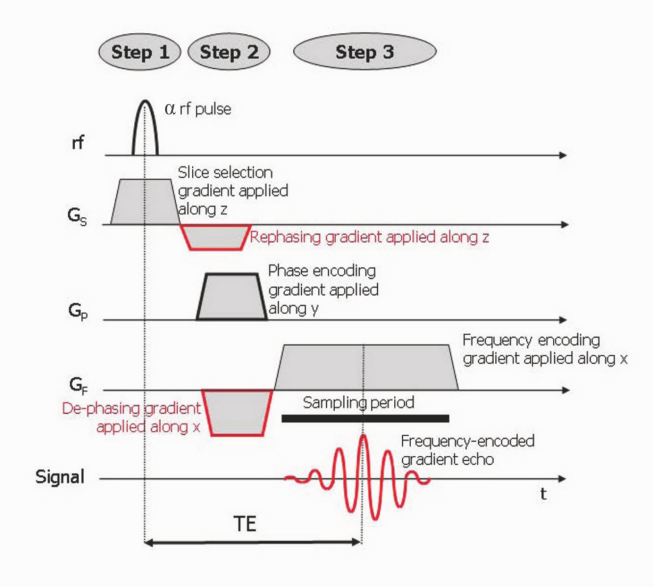
Images are built up by adding data acquired across a number of acquisitions, increasing the SNR. Fast spin echo (FSE) sequences are a variation that allows more lines of k-space to be acquired with each TR, reducing the imaging time. Multiple 180° refocusing RF pulses are applied with a varying phase encoding gradient applied within each 180° pulse. This allows many echoes, typically 16-64 in CMR, to be collected for each slice excitation (90°) pulse. Signal acquisition is usually carried out in diastole when the heart or vascular structure is relatively still.

Gradient echo

Gradient echoes are used to image moving objects, such as the heart. Rapid sequence repetition allows a sequence of images to be acquired during the cardiac cycle that are put together to form a cine loop. They are used for functional imaging in CMR. A short TR is needed, hence a low flip angle (8-35°) is used, as a 90° pulse would require a long TR for

longitudinal recovery. The short TR means the refocusing 180° RF pulse is not needed (Figure 4.6). T2* relaxation is therefore measured. As TR is shortened, the flip angle must also be reduced to maintain SNR. The low flip angle RF pulse (□) can be rapidly repeated. A rewinding gradient, equal and opposite to the phase encoding gradient is applies after each echo signal acquisition. A spoiler gradient, which dephases any remaining transverse magnetisation, is also applied at the end of each TR, just before the next □ RF pulse. These ensure no residual transverse magnetisation from the previous phase encode step contributes to the next signal. As an 180° RF pulse is not used, GE sequences are susceptible to field inhomogeneities such as metallic artefact.

Figure 4.6. A pulse sequence diagram for gradient echo. Steps 1, 2 and 3 refer to slice selection, phase and frequency encoding (see section 4.3.3) allowing spatial encoding along the z, x and y axes respectively. [Adapted from Ridgway 2010].



Balanced steady state free precession (SSFP) is the sequence most used for cardiac functional assessment. No spoiler gradient is needed and the spins on all orthogonal axes are rephased to zero after each TR. As the spins are kept in phase, transverse magnetisation is reused and superimposed with that generated by the RF pulse in the next TR. A larger flip angle, typically 60°, is used. As the transverse magnetisation of several TRs is superimposed, the signal amplitude and hence SNR is high. SSFP is sensitive to field inhomogeneities, therefore “shimming” is carried out to keep the magnetic field as uniform as possible over the area being imaged and reduce the likelihood of artefacts. Respiratory motion artefacts are minimised by breath holding in end expiration.

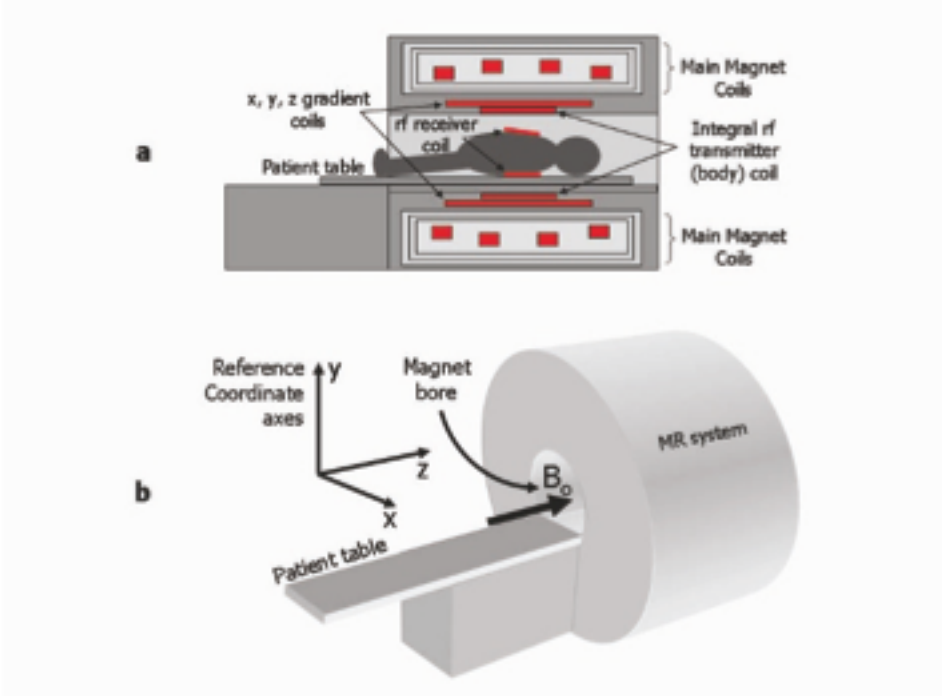
4.3 Components of an MR scanner

A magnetic resonance imaging (MRI) system is made up of a number of components: the MR scanner itself, receiver coils and a processing system to construct the image.

4.3.1 MR scanner

The primary component of the MR scanner is a superconducting magnet. These are ring magnets, made of a niobium-titanium alloy, which are super-cooled with liquid helium to <4.2 Kelvin, at which temperature there is almost no resistance. Very low electricity levels are therefore needed to generate high field strengths. The magnetic fields have a high degree of stability. Three main types of coils create the magnetic fields in the scanner bore (Figure 4.7).

Figure 4.7. MR system components. a) Diagram showing the relative locations of the main magnet coils, x, y, and z gradient coils, integral RF transmitter body coil and RF receiver coils. b) Typical arrangement for a cylindrical bore MR system showing the magnet bore and the reference coordinate axes with the static B_o field direction along the horizontal z-axis. [Reproduced from Ridgway 2010].



Main coils

These generate the strong, constant magnetic field ($\square_0$), in which the patient is placed. Its strength defines the operating field strength of the magnet in Tesla (T). $\square_0$ is usually between 1.0 to 7.0 T, and in CMR 1.5T and 3.0T scanners are used. Higher field strengths increase the signal-to-noise ratio (SNR), increasing image resolution and decreasing the time taken to acquire the image, but at the expense of increased artefact.

Gradient coils

Three orthogonal gradient coils are located inside the main magnet. They are resistant type electromagnets. Each generates a magnetic field in the same direction as B_o. They allow rapid adjustments to field strength with changes along the x, y or z axis depending on which coil is used. The gradient field strength increases or decreases along its applied direction and is superimposed onto the B_0 field. It is measured in millitesla per metre. Stronger gradients and faster switching reduce scan time but are limited by peripheral nerve stimulation.

Radiofrequency transmitter coil

This is mounted within the gradient coils. It generates a weaker field in the radiofrequency range (MHz) defined as B_1, which is perpendicular to B_0 (see below).

4.3.2 Receiver coil

These are radiofrequency (RF) coils, but are used to detect the MR signal. Modern scanners use an array of at least four coils, each with separate receivers, and are known as a phased array system, which can be used in parallel imaging. Coils are essentially small antennae in which the magnetic field induces an electric current, which is amplified, digitised, and filtered to extract frequency and phase information. They are placed on the patient, over the area to be imaged. Tissues adjacent to the surface coil have a good SNR and the coils limit the region from which the MR signal is received. The signal strength received decreases with distance from the coil.

4.3.3 Construction of the MR image

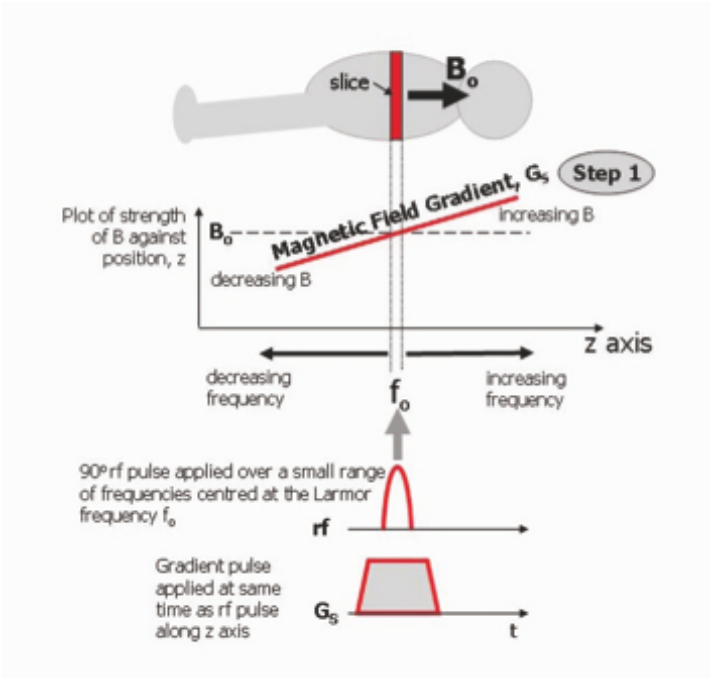
The static magnetic and RF fields combine to generate magnetic resonance signals. These MR signals contain spatial and magnitude information that is decoded to create an MR image. A two-dimensional cross-sectional image is built up using a combination of gradient magnetic fields and RF pulses.

Slice selection

A two-dimensional plane of a given thickness (a slice) is acquired in MRI. A linear slice selection magnetic field gradient (G_S) is applied perpendicular to the imaging plane to be acquired, resulting in a gradient in the precessional frequencies of the protons along its axis (Figure 4.8). A RF pulse transmitted perpendicularly to G_S consists of a small range of frequencies (the transmit bandwidth) and corresponds to the frequencies at a chosen point along G_S. Only tissue in this plane is therefore excited, and the thickness of the slice is

determined by the transmit bandwidth and the strength of G_S. Slice selection acquires data in the z axis, but does not encode data along the x and y axes. Phase and frequency encoding achieve these.

Figure 4.8. Selecting a slice. For step 1 of image formation process, a slice of tissue is selected by applying a magnetic field gradient G_S at the same time as the RF excitation pulse. The position along the gradient (in this example along the z axis) determines the Larmor frequency and resonance only occurs where this matches the frequency of the RF pulse, f_0, defining a plane (slice) of tissue perpendicular to the z-axis. In practice the RF pulse is applied over a small range of frequencies, thus defining the thickness of the slice. [Reproduced from Ridgway 2010].



Phase encoding

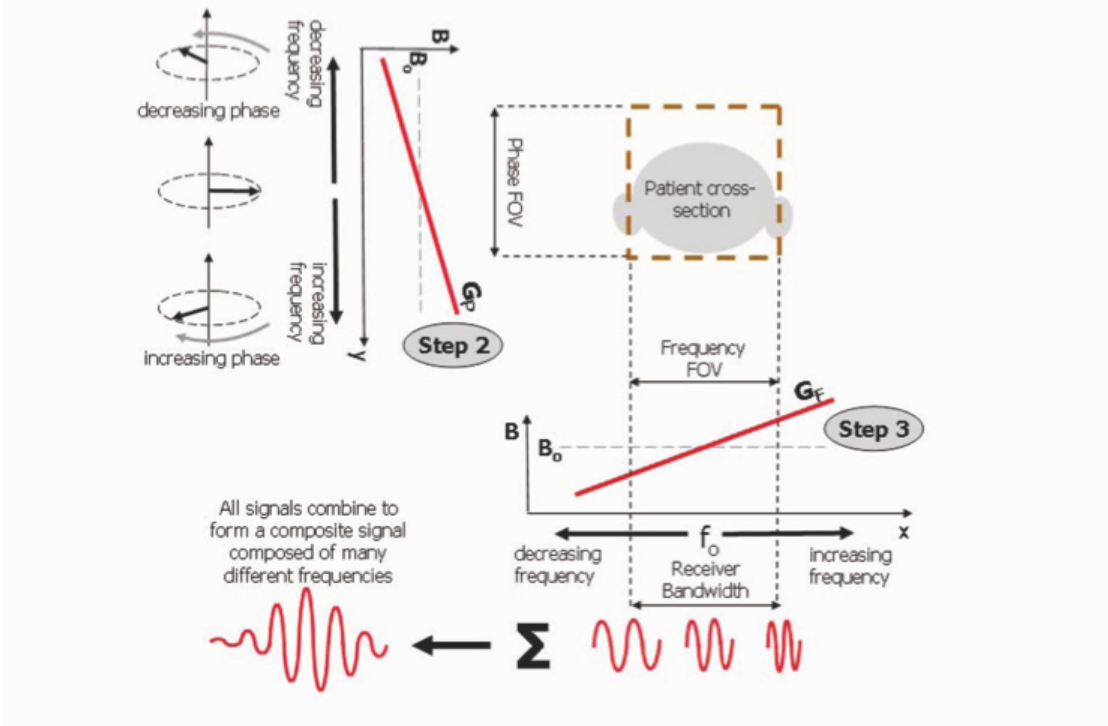
Phase encoding is carried out in one of the transverse axes (Figure 4.9). A phase encoding gradient (G_P) is applied with protons in the strongest part of the magnetic field having a higher frequency of precession and changing their relative phase depending on their position along the gradient. The direction of G_P is known as the phase encoding direction. The phase of a signal in the readout indicates its position in the phase encode direction. Many phase encoding gradients of increasing strength are required to localise the signal. The same slice selection and frequency encoding gradients are repeated with each step, but the phase encoding gradient strength is increased incrementally. The time interval between repetitions (TR) can be set by the operator to increase spatial resolution in the phase encode direction, but will increase scan duration.

Frequency encoding

The frequency-encoding gradient (G_F) is applied in the other transverse axis, perpendicular to G_S, allowing spatial encoding along this axis (Figure 4.9). Protons rotate at different frequencies according to their relative position along G_F. The signal is measured during the time G_F is applied and the direction of the frequency-encoding gradient defines the frequency encoding direction.

Slice selection, phase encoding and frequency encoding are described above as occurring in the z, x and y axes respectively. However, one strength of MRI is the ability to define any slice orientation. This is achieved by combining gradients along two or more axes to perform each of the localisation tasks.

Figure 4.9. Step 2, a phase encoding gradient, G_P, is applied in a direction along the selected image plane (in this case the phase encoding direction is along the y direction). This causes a range of phase shifts of the proton magnetic moments dependent on their position along the gradient as well as the slope and duration of the gradient. For step 3, following the phase encoding gradient, the frequency encoding gradient, G_F, is applied also in the plane of the selected slice but perpendicular to the phase encoding direction. The MR signal echo is measured during this period. The frequency encoding gradient determines the Larmor frequency according to position along its direction (in this case, the x direction). The detected MR signal from the slice of tissue is therefore comprised of many different frequencies. The field of view is predefined and matched to a specific range of frequencies, referred to as the receiver bandwidth. [Reproduced from Ridgway 2010].



K-space and the Fourier transform

K-space is an abstract concept and refers to a mathematical data matrix into which the raw MRI data is collected. Each point in k-space contains specific frequency and phase information (x,y coordinates) as well as signal intensity information. Each frequency encoding acquires a line of k-space (kx). Each phase encoding step moves up the ky axis to acquire another frequency encoding line. Once all the data is collected, a two-dimensional fast Fourier transform is applied to convert the data into an image. In general central regions of k-space encode contrast information and peripheral regions spatial resolution.

4.4 CMR measurement of cardiac function and mass

4.4.1 Introduction

CMR is considered the gold standard non-invasive imaging modality for the assessment of cardiac function and mass [Hundley 2010]. Images can be obtained in any plane irrespective of body habitus and there is no ionising radiation. Geometric assumptions are not made and mathematical calculations are not needed to account for missing data. CMR also allows for the assessment of a number of cardiac anatomical and functional parameters in one comprehensive study. Spatial and temporal resolutions have improved greatly and frame rates of 20-40ms are usual in breath-hold cine sequences [Hundley 2010].

4.4.2 Ventricular volume and function

CMR accurately measures both left and right ventricular volumes, stroke volume (SV) and hence, ejection fraction [Hundley 2010]. Correlation is excellent between the volume of water displaced by ventricular casts and volumes measured by CMR [Longmore 1985; Rehr 1985]. In normal hearts, SV, measured by subtracting the end systolic from the end diastolic volumes, should be equal for the left and right ventricle. SV ratios of 0.97±0.06 were demonstrated by Sechtem *et al*. confirming the accuracy of volume measurement by CMR. Measurements of SV, and therefore cardiac output, by invasive thermodilution techniques in animal studies [Culham 1988] and left ventriculography at cardiac angiography in humans [Utz 1987] have also correlated well with CMR measurements. Interstudy, interobserver and intraobserver reproducibility is excellent for both LV and RV measurements of volume and function by CMR, and has been confirmed in diseased hearts (LV hypertrophy, ischaemic and dilated cardiomyopathy) as well as in normal hearts [Sechtem 1987; Grothues 2002; Grothues 2004].

4.4.3 Ventricular mass

CMR measurement of myocardial mass has been validated against human cadaveric hearts

for LV mass [Katz 1988] and animal cadaveric hearts for LV and RV mass [Katz 1993]. Reproducibility is good with low variability between studies and in interobserver and intraobserver measurements [Katz 1988; Katz 1993; Grothues 2002; Grothues 2004].

4.4.4 Myocardial scar

The presence of myocardial scarring or fibrosis can be identified with CMR by the use of extracellular paramagnetic contrast agents. These are gadolinium chelates, which shorten T1 and appear bright (white) on a T1-weighted (T1W) GE inversion recovery sequence - late gadolinium enhancement (LGE). Injected intravenously, gadolinium distributes into the abnormal myocardial interstitium caused by an acute infarct or acute myocarditis, or by scarring due to previous infarction, healed inflammation or extracellular expansion in cardiomyopathies.

4.5 CMR imaging of atherosclerosis

4.5.1 Introduction

Atherosclerosis is an inflammatory-mediated disease of medium to large arteries with a predilection for certain arterial beds, especially the carotid, aorta, coronary and peripheral arteries. It causes a large global burden of morbidity and mortality. Atherosclerosis imaging is clinically important for symptom management as well as primary and secondary prevention. Plaque imaging can also be used to discriminate between unstable (vulnerable) plaques, which may be relatively small, asymptomatic, but highly likely to cause a CV event, and stable plaques, allowing aggressive disease modifying therapy to be targeted to those most at risk. In clinical research, the effect of treatment on atherosclerosis stability, or the arrest and possible regression of plaque growth can be evaluated.

The carotid arteries and aorta provide large, relatively motion-free and accessible structures for imaging. The carotid arteries are less challenging due to their superficial location. Aortic and carotid artery atherosclerosis has been associated with increased Framingham coronary risk score [Jaffer 2002], and the presence of coronary artery disease [Taniguchi 2004]. Aortic wall thickness as a measure of subclinical atherosclerosis has been associated with age, being male and black [Jaffer 2002; Li 2004]. The aorta and carotid arteries are therefore used as surrogates for coronary artery atherosclerosis in imaging studies. CMR allows visualisation of the entire arterial wall without geometric or imaging window constraints. Its lack of ionising radiation and high degree of reproducibility make it safe and suitable for use in longitudinal studies.

4.5.2 Multicontrast CMR

Plaque morphology

The different components of plaque can be identified by CMR due to their different relaxation properties. Multicontrast CMR involves the use of T1W, T2W, and proton weighted (PDW) FSE sequences, with the blood nulled by a preparatory RF pulse. Time of flight (TOF) sequences can also be used. Variations between the signal intensities allow the different plaque components to be identified (Table 4.1).

Table 4.1. Signal intensities of plaque components compared to adjacent muscle.
+ = hyperintense; - = hypointense; ± = isointense. [Adapted from Fuster 2005].

	CMR sequence and signal intensity			
Plaque component	**T1W**	**T2W**	**PDW**	**TOF**
Recent thrombus	+ to ±	- to ±	- to ±	+
Lipid	+	-	+	±
Fibrous tissue	±	± to +	+	± to -
Calcium	-	-	-	-

CMR is also able to identify carotid plaque rupture in patients with a recent stroke or transient ischemic attack [Yuan 2002a] as well as intraplaque haemorrhage [Chu 2004].

Validation and reproducibility

Carotid plaque area and volume measured by CMR has been validated in patients undergoing endarterectomy [Yuan 1998]. In vivo and ex vivo CMR plaque area showed strong agreement; interobserver and intraobserver variability was low with intraclass correlation coefficients ranging from 0.90 to 0.98. Carotid CMR has been shown to have good inter-study reproducibility with a coefficient of variation of 4.6% [Varghese 2005a]. A study by Corti *et al* demonstrated an error of 2.6% for aortic and 3.5% for carotid plaques on repeat imaging [Corti 2001].

Validation of plaque components identified on CMR has also been undertaken [Toussaint 1996; Yuan 2001a; Yuan 2001b]. Yuan *et al* demonstrated a sensitivity of 85% and specificity of 92% in identifying lipid-rich necrotic core. Thoracic aortic plaque CMR has been validated against transoesophageal echocardiography with strong correlations shown for plaque composition and plaque thickness [Fayad 2000]. CMR has also been compared against histological classification according to American Heart Association guidelines and

found to have good agreement, being able to discriminate advanced lesions from early and intermediate lesions [Cai 2002].

4.5.3 Contrast agents

Use of contrast agents can improve the sensitivity of detecting plaque components. They reduce the need for very high spatial resolution for the assessment of plaque morphology by multicontrast CMR alone, and if targeted to receptors or plaque components, reduce the need for image interpretation.

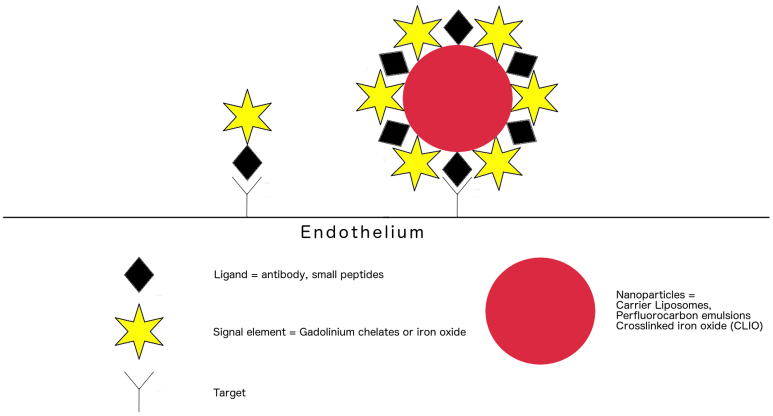
Gadolinium

Gadolinium is a paramagnetic contrast agent routinely used in CMR for perfusion imaging, identification of intracardiac thrombus and myocardial scar tissue. Gadolinium chelates increase the intraluminal signal after injection and are able to detect neovascularisation in plaques [Yuan 2002b; Kerwin 2003]. Gadolinium chelates are not specific for neovascularisation. As extracellular agents they have been shown to accumulate in areas of inflammation (due to increased vascular wall permeability) [Cai 2005] and fibrotic tissue (due to an increased volume of distribution) [Yuan 2002b; Cai 2005]. Kinetic models of their biodistribution may therefore be required to accurately identify plaque components, particularly in smaller vessels such as the coronary arteries where current levels of resolution make it difficult to differentiate between plaque components. Gadolinium uptake was seen to occur more in calcified plaques compared to non-calcified plaques when evaluated against MSCT [Yeon 2007]. It has also been used post myocardial infarction and appears to measure local inflammation [Ibrahim 2009].

Molecular imaging

Molecular imaging unites CMR with biological processes occurring in the arterial wall. In CVD these include angiogenesis, inflammation and thrombosis. Probes have been constructed to target markers including fibrins, selectins and integrins. A ligand is attached to a signal element and targeted to a specific receptor involved in the biological process under investigation. Signal elements used in CMR include gadolinium and iron oxides. Increased signal intensity and affinity to the target can be achieved by using a nanoparticle carrying large numbers of ligands and signal elements (Figure 4.10). They are used for research, not in routine clinical practice.

Figure 4.10. Figure showing a molecular contrast agent. The ligand and signal element can be directly linked or attached to a nanoparticle carrier.



Angiogenesis

To clearly identify areas of neovascularisation, CMR agents that remain, or remain longer in the intravascular space are needed. Integrin $\alpha_v\beta_3$, over-expressed on the endothelium of new vessels has been targeted to identify areas of neovascularisation [Winter 2003].

Inflammation

Inflammation in the fibrous cap results in its thinning and ultimately rupture. This is mediated by MMPs secreted by macrophages. Ultrasmall paramagnetic particles of iron oxide (USPIOs) are taken up by plaque macrophages and can be detected as areas of signal loss on CMR [Kooi 2003; Trivedi 2004]. Optimum imaging time is 24-36 hours after injection [Trivedi 2004]. USPIO uptake by plaque macrophages has been validated histologically and increased uptake in ruptured or vulnerable plaques demonstrated [Kooi 2003; Hyafil 2006].

Gadolinium loaded nanoparticles have also been targeted to areas of endothelial activation and vascular inflammation, targeting adhesion molecules such as ICAM-1, VCAM-1, E-selectin and P-selectin [Kim 2010], as well as MMPs [Lancelot 2008].

Thrombosis

Fibrin-targeted contrast agents are able to identify thrombus, a vulnerable plaque complication. Small thrombi overlying a ruptured plaque indicate those plaques at highest risk of further rupture and vessel occlusion. Gadolinium-loaded nanoparticles linked to a fibrin antibody have been used to increase thrombus signal compared to non-contrast images [Sirol 2005a] and ascertain the age of thrombus [Sirol 2005b]. Sensitivity and

specificity of 100% for thrombus detection has been demonstrated [Sirol 2005a; Sirol 2005b; Botnar 2004].

4.5.4 1.5T versus 3.0T

Carotid vessel wall imaging by CMR can overcome many of the limitations of C-IMT, including one-dimensionality, measurement site variability, and near field artefacts. It can be performed with constant resolution along the artery and combined into a three-dimensional model generating the wall volume for the length of artery studied. CMR measurements of wall area and thickness correlate well with measurements of C-IMT [Mani 2006]. Reproducibility is good with interstudy coefficients of variation of 4.6% [Varghese 2005a], allowing for a greatly reduced sample size in clinical studies. Inter-rater variability is low, with interobserver intraclass correlation coefficient of 0.96 at 1.5T field strength [Yuan 1998], and 0.90-0.99 at 3T [van Wijk 2014]. Higher field strengths increase the SNR, increasing image resolution and decreasing the time taken to acquire the image, but at the expense of increased artefact. USPIO plaque targeting should be more sensitive at higher field strengths. Measures of carotid wall volume have been compared at 1.5T and 3.0T field strengths with no significant differences reported, allowing comparison between scans acquired at the different field strengths to be made [Yarnykh 2006].

Studies defining normal CMR values for cardiac volumes, function and mass at 3.0T have not been published. Reproducibility studies at 1.5T and 3.0T have shown no significant differences in LV and RV volume, mass or function and a high degree of reproducibility between both field strengths [Hudsmith 2006; Ligabue 2008].

4.5.5 Arterial wall CMR in clinical trials

Carotid and aortic wall and plaque thickness, area and volumes have been used in clinical trials to look at the effect of standard and aggressive lipid-lowering regimes [Corti 2001; Corti 2002; Corti 2005; Migrino 2011]. Inward remodelling with plaque regression [Corti 2002] and reduction in the size of the lipid-rich core [Underhill 2008] have also been demonstrated, indicating that plaque stabilisation may be occurring. Carotid CMR has also been used to look at the effect of disease modifying treatment on the arterial wall in inflammatory conditions, e.g. Behcet's disease [Chan 2011]. The ability of in vivo CMR to quantify plaque volume and plaque composition with low inter-scan variability allows for relatively small numbers of patients to be recruited into clinical trials compared to those needed in studies using ultrasound [Saam 2005].

4.5.6 The future

The ability to identify targets indicating plaque vulnerability will allow drugs aimed at stabilising plaque as well as reducing plaque volume to be evaluated longitudinally. This will provide for a more refined assessment of drug effects in large groups of patients with CVD rather than the more blunt approaches now used. In diseases associated with increased CV risk, such as SLE and HIV, where the disease process may vary from that seen in the general population, the effect of drugs targeting specific inflammatory mechanisms within the arterial wall may be able to be assessed.

Chapter 5
Systemic Lupus Erythematosus

5.1 Introduction

Systemic lupus erythematosus (SLE) is a chronic autoimmune disease of unknown aetiology that can affect any organ system. It manifests a broad range of clinical presentations, and can run a varied clinical course, from a relatively benign disease to a rapidly progressive disease with organ failure and death. Gender remains the greatest risk for SLE with a female ratio of 9:1 typical in most studies [D'Cruz 2007].

5.2 Epidemiology

Epidemiological studies have shown large variations in the incidence and prevalence of SLE, according to geography and ethnicity which may reflect true population differences or differences in diagnosis and study methodology [Danchenko 2006; Pons-Estel 2010; Rees 2014]. Those with African, Afro-Caribbean or Asian ancestry are at a significantly greater risk of developing SLE, often with a more severe clinical manifestation. In the UK, overall estimated incidence rates are 3.8 to 4.91 per 100,000 - 21.9 to 31.46 per 100,000 in the Afro-Caribbean population versus 3.0 to 6.73 per 100,000 in the white population [Danchenko 2006; Rees 2014]. Similarly, prevalence in the Afro-Caribbean population is 159.4 to 517.51 per 100,000 compared with 20.5 to 134.53 per 100,000 for the white population [Danchenko 2006; Rees 2014]. This racial variation is consistent in worldwide epidemiological studies with incidence and prevalence of SLE being highest in non-Caucasian populations [Danchenko 2006; Pons-Estel 2010; Somers 2014].

SLE is often described as a disease of women in their reproductive years, although it can occur at any age. Early studies showed peak incidence rates in women aged 15-44 years with peak prevalence occurring at 45-64 years [Siegel 1973]. This pattern is still seen in black women in the United States [Pons-Estel 2010; Somers 2014]. In other populations, however, a different pattern has emerged, with the highest age-specific incidence rates occurring after 40 years of age. In the United Kingdom the highest age-specific incidence rate has been found to be between 40-49 years [Rees 2014] and 50-54 years [Somers 2007]. Other Northern European studies have found even later age-specific peak incidence rates - 50-59 years (Iceland) [Gudmundsson 1990]; 65-74 years (Sweden) [Ståhl-Hallengren 2000]. In males, small numbers make age-specific incidence rates difficult to interpret although peak incidence appears to be later than in women. In the UK incidence has been shown to peak in men between 60-69 years [Rees 2014] and 70-74years [Somers 2007;

Jiménez 2003]; these findings are echoed in other studies around the world [Somers 2014; Ståhl-Hallengren 2000]. Prevalence is significantly higher in women than in men at all ages, with an increasing trend seen in both sexes, which is more marked in women [Rees 2014; Somers 2014]. The peak age in prevalence has been found to be 60-69 years for women and 80–89 years for men in the UK [Rees 2014] compared with 40-49 years for women in the US [Somers 2014].

Temporal increases in worldwide incidence and prevalence have been noted. Between 1955 and 1974, the SLE incidence in the USA increased from 1.0 to 7.6 per 100,000 [Siegel 1970; Fessel 1974]. In Rochester, USA, the age-adjusted incidence of SLE more than tripled from 1·51 per 100,000 in 1950-79 to 5·56 per 100,000 in 1980-1992 [Uramoto 1999]. Similar increases were seen in Europe [Gudmundsson 1990; Voss 1998]. Although some of this increase may reflect an increase in disease occurrence, greater awareness of SLE, wider availability, sensitivity and use of antinuclear antibody (ANA) testing, more accurate diagnosis and the diagnosis of milder cases, are also likely to have contributed. The increased incidence observed over the last few decades may however, now be stabilising [Somers 2007; Ståhl-Hallengren 2000] or even falling [Rees 2014]. Prevalence, however, continues to increase largely due to improved survival – 5-year survival 50% in 1950 compared with 90% in the 1990s [Gladman 1996a], which continues to improve [Uramoto 1999; Urowitz 2008].

5.3 Aetiology and Pathogenesis

5.3.1 Introduction

The aetiology and pathogenesis of SLE remains unclear, but is clearly multi-factorial. Varied penetrance and lack of concordance amongst genetically identical twins [Deapen 1992] suggests that a variety of triggers as well as a susceptible genetic profile are likely key in inducing SLE onset and flares [Liu 2012]. Studies suggest a role for immunological, genetic, hormonal and environmental factors.

5.3.2 Immunology

Numerous immune defects occur in SLE, some episodic, some corresponding to disease activity and some contributing to the pathological changes seen in SLE. Abnormalities are predominantly involved in immune regulation and cause a loss of ‘self tolerance’ [Munoz 2005; Liu 2012].

The main immunological characteristics are high ANA titres, high levels of circulating immune complexes and increased complement consumption [Munoz 2005]. Autoantibodies are

present years before the onset of clinical features. A study looking at the stored serum samples of US military personnel showed that ANAs were present in 78% (at a dilution of 1:120 or more), anti-double stranded DNA (anti-dsDNA) antibodies in 55%, anti-Ro antibodies in 47%, anti-La antibodies in 34%, anti-Sm antibodies in 32%, anti-nuclear ribonucleoprotein (anti-nRNP) antibodies in 26%, and antiphospholipid (aPL) antibodies in 18%, often years before symptom onset and clinical diagnosis. Antibodies appear in a predictable course with a peak in their numbers prior to the appearance of clinical illness. The presence of antibodies alone, however, does not indicate disease, as evidenced by the occurrence of the same antibodies in some normal individuals, albeit in smaller quantities [Arbuckle 2003]. Other factors (e.g. variability in immune response, environmental triggers) may be needed to produce clinical illness [Liu 2012].

The autoantibodies associated with SLE are primarily directed against intracellular antigens [Liu 2012]. Apoptosis is an active, programmed and genetically conserved process that occurs in all tissues under both physiological and pathological conditions. If apoptotic cells are not cleared promptly, membrane integrity may be lost and intracellular material released, compromising the maintenance of self-tolerance [Liu 2012]. Necrosis occurs when external factors such as infection, mechanical injury and ischaemia affect cells resulting in disruption of the cell membrane [Munoz 2005].

Under normal conditions, apoptotic material is cleared by macrophages, which produce anti-inflammatory cytokines and/or sequester nuclear autoantigens, down-regulating the antigen presentation function of dendritic cells. Consequently, there is no inflammation and T- and B-cell tolerance is induced. In SLE, phagocytosis is significantly impaired [Landry 1977], allowing self-antigens to activate proinflammatory receptors (e.g. Fc receptors) [Liu 2012]. Apoptotic cells accumulate, become necrotic and accessible to tissue and follicular dendritic cells. The adaptive immune system is activated. Tissue dendritic cells produce inflammatory cytokines and present autoantigens to autoreactive T-cells. Follicular dendritic cells may sequester autoantigens and present them to autoreactive B-cells [Munoz 2005].

The innate immune system is also activated. Complement components C1q, C3 and C4 are involved in the clearance of dying cells [Munoz 2005, Taylor 2000, Gaipl 2001]. Complement binding has been found to be an early feature of necrosis and a late feature of apoptotic cell death, possibly acting as a backup mechanism to clear apoptotic cells [Gaipl 2001]. Complement deficiencies and reduced complement activity found in SLE patients impair this clearance mechanism, [Munoz 2005; Sturfelt 2005] further promoting inflammation.

There is also growing evidence for the role played by cytokines such as B-lymphocyte stimulators (BLys), interleukin-6, interleukin-17, interleukin-18, type I interferons and TNF-□, in the pathogenesis of SLE. These cytokines have roles in the differentiation, maturation and activation of various immune cells, mediating local inflammation and tissue injury [Yap 2013].

The pentraxins such as C-reactive protein (CRP) are highly conserved glycoproteins and acute-phase reactants involved in the regulation of inflammation. CRP acts as an opsonin by interacting with the Fc receptor on phagocytic cells, enhancing the phagocytosis of cells undergoing apoptosis. CRP also induces complement activation via the classical pathway [Munoz 2005]. CRP levels are inappropriately low in SLE patients, [Pereira da Silva 1980] and this may contribute to the impaired phagocytosis of apoptotic cells. CRP can also bind to the nuclear constituents of necrotic cells, such as histones and small nuclear ribonucleoproteins, and human-derived CRP has been shown to suppress renal inflammation in a murine model of human SLE. This suggests a major immunomodulatory role of CRP is to limit acute inflammation and tissue damage [Rodriguez 2005; Ogden 2005].

5.3.3 Genetics

Over 40 gene loci conferring susceptibility to SLE have been identified [Rullo 2013; Boackle 2013; Altorok 2013; Ghodke-Puranik 2015]. Familial and monozygotic twin studies support the idea of a genetic predisposition to SLE. However, even amongst monozygotic twins, concordance rates are only 24% [Deapen 1992] and SLE occurrence rarely follows a classical Mendelian inheritance pattern. It is assumed that the inheritance of multiple genes with varying effects, as well as epigenetic factors, combine to give an overall genetic risk for developing SLE [Boackle 2013; Ghodke-Puranik 2015].

Genes influencing the innate and adaptive immune pathways have been identified. These include the HLA genes involved in the major histocompatibility complex; genes involved with DNA degradation, cellular apoptosis and phagocytosis (e.g. TREX1, DNASE1, FAS, FASL, FCGR, C1q, C2, C4); genes involved in macrophage, natural-killer cell and dendritic cell signalling (e.g. Toll-like receptor [TLR-3, TLR-7, TLR-8, TLR-9], Type-I interferon pathway [IRF3, IRF 5, IRF7], STAT4, TNFAIP3, TNIP1); genes involved in B-cell function and signalling (e.g. BLK, BANK1, PRDM1); and genes involved in T-cell function and signalling (e.g. PTPN22, TNFSF4) [Rullo 2013; Ghodke-Puranik 2015].

The X-chromosome may also be important. Several predisposing gene variants, e.g. TLR7 and IRAK1, are located on the X-chromosome [Rullo 2013]. Men with Klinefelter's syndrome (XXY) have a risk of SLE similar to that of ethnically matched women whereas Turner's

syndrome (XO) is underrepresented amongst SLE patients, suggesting a gene-dose effect [Scofield 2008; Cooney 2009]. Other possibilities for SLE susceptibility and female predisposition include epigenetic mechanisms such as demethylation of the CD40LG promoter and the enhancer on the inactive X-chromosome [Lu 2007].

5.3.4 Hormonal Factors

Sex hormone involvement, particularly oestrogen, in the aetiology of SLE might be inferred from the 'average' SLE patient (female, with onset after puberty). Oestrogen can impair B-cell tolerance in mice [Grimaldi 2006; Petri 2008]. In human cohort studies a slightly increased risk of developing SLE has been found in those taking the oral contraceptive pill or hormone replacement therapy [Sanchez-Guerrero 1997; Costenbader 2007]. The existence of childhood, post-menopausal and the often more clinically severe male SLE, goes against this 'oestrogen hypothesis', although higher oestrogen levels have been reported in men with SLE [Petri 2008]. Conflicting evidence also exists on the risk of SLE flares when using oral contraceptives, hormone replacement therapy or during pregnancy [D'Cruz 2007; Petri 2008].

Other hormones have been implicated in SLE. Increased prolactin levels can promote the activation and survival of autoreactive B-cells, impairing B-cell immunological tolerance [Grimaldi 2006; Petri 2008]. High prolactin levels in SLE have been associated with increased disease activity levels [Petri 2008]. Reduced levels of the androgens testosterone and dehydroepiandrosterone (DHEA) have been reported with SLE in both sexes [Petri 2008]. Hence, the gender bias in SLE is not easily explained by simple hormonal influences. A complex interaction of sex hormones, the possible involvement of sex-linked genes and other factors is probably involved.

5.3.5 Environmental Factors

Environmental factors, such as ultraviolet light, infection, vitamin D deficiency, cigarette smoke, and chemicals have been implicated in the induction of SLE and disease flares. Epigenetic changes are believed to mediate many of the environmental factor effects via oxidative stress and modification of CD4+ T-cell gene expression [Somers 2014].

Ultraviolet Light

Ultraviolet (UV) light can induce SLE flares and may contribute to disease onset [Bijl 2006; Barbhaiya 2014]. Both UV-A and UV-B can induce keratinocyte apoptosis, releasing nuclear antigens and triggering an autoimmune inflammatory response [Bijl 2006; Barbhaiya 2014]. This appears to be dose dependent [Caricchio 2003]. Keratinocytes may also up-regulate

MHC-II, stimulate autoreactive B-cells by releasing autoantigens and proinflammatory cytokines, and present antigens to the immune system [Caricchio 2003].

Infections

Infections may trigger SLE by disturbing immunoregulation and causing tissue damage, resulting in antigen release [Danchenko 2006]. Bacterial and viral infections (e.g. Epstein-Barr, herpes zoster, cytomegalovirus, endogenous retroviruses) may contribute to the development of autoimmunity via molecular mimicry. An increased prevalence of these infections has been found in some SLE cohorts [James 2012; Cooper 2002; Adelman 2002; Nelson 2014].

Vitamin D Deficiency

Photosensitivity in SLE and consequent avoidance of sunlight exposure increases the risk of vitamin D deficiency. The protective immunomodulatory role of vitamin D is increasingly recognised and deficiency has been associated with higher SLE disease activity in some studies [Petri 2013]. Vitamin D level correction has been associated with reduced proteinuria and disease activity scores but no significant change in serological markers [Petri 2013].

Smoking

The importance of cigarette smoking in SLE onset is uncertain. Current evidence suggests a weak association (odds ratio 1.5, 95% confidence interval: 1.09–2.08) for developing SLE in current smokers versus never smokers. The mechanisms are unclear but could include tissue hypoxia, toxin-mediated cellular necrosis, interference in sex hormone metabolism and immunomodulatory effects [Costenbader 2004; Takvorian 2014].

Chemicals

Population-based studies have shown a consistent association between silica exposure and SLE onset [Parks 2006; Parks 2014]. In animals silica effects include increased pro-inflammatory cytokine production (TNF and IL-1) and macrophage toxicity resulting in cellular apoptosis and increased intracellular self-antigen exposure [Parks 2006].

Pesticides have been implicated in increasing the risk of SLE, but the specific type(s) of pesticide are unknown and data based on only a few case-control studies [Parks 2006]. Few studies have investigated the association of solvents and other hydrocarbons with SLE, and no definitive evidence has been found [Parks 2014].

5.4 Diagnostic criteria

Classification of SLE is done according to the consensus criteria of the American College of Rheumatology (formerly the American Rheumatism Association) first defined in 1971 [Cohen 1971] and subsequently revised in 1982 [Tan 1982], 1997 [Hochberg 1997] and 2012 [Petri 2012]. It was developed for use in clinical research as a tool for the identification and characterisation of SLE, and may fail to identify some patients particularly early on in the disease [Pons-Estel 2014]. A patient is classified as having SLE if 4 or more of the Systemic Lupus International Collaborating Clinics (SLICC) 2012 classification criteria (see Table 5.1) are met (this must include at least one clinical and one immunological criterion), or if there is biopsy-proven nephritis compatible with SLE in the presence of ANAs or anti-dsDNA antibodies. Symptoms and laboratory findings are cumulative and need not be present concurrently [Petri 2012].

Table 5.1. Clinical and immunologic criteria used in the Systemic Lupus International Collaborating Clinics (SLICC) classification system (adapted from Petri *et al*, 2012).

Clinical criteria	
1. Acute cutaneous lupus, including:	Lupus malar rash Bullous lupus Toxic epidermal necrolysis variant of SLE Maculopapular lupus rash Photosensitive lupus rash *in the absence of dermatomyositis* Subacute cutaneous lupus (non-indurated psoriaform &/or annular polycyclic lesions)
2. Chronic cutaneous lupus, including	Classic discoid rash Localised (above the neck) Generalised (above & below the neck) Hypertrophic (verrucous) lupus Lupus panniculitis (profundus) Mucosal lupus Lupus erythematous tumidus Chilblains lupus Discoid lupus/lichen planus overlap
3. Oral ulcers	Palate Buccal Tongue OR nasal *in the absence of other causes, e.g. vasculitis, Behcet's disease, infection (herpesvirus), inflammatory bowel disease, reactive arthritis, & acidic foods*
4. Non-scarring alopecia	Diffuse thinning or hair fragility with visible broken hairs *in the absence of other causes e.g. alopecia areata, drugs, iron deficiency, & androgenic alopecia*
5. Synovitis	Involving ≥2 joints, characterized by swelling or effusion OR tenderness in 2 or more joints and at least 30 minutes of morning stiffness
6. Serositis	Typical pleurisy for more than 1 day OR pleural effusions OR pleural rub Typical pericardial pain for more than 1 day OR pericardial effusion OR pericardial rub OR pericarditis by electrocardiography *in the absence of other causes, e.g. infection, uremia, & Dressler's pericarditis*
7. Renal	Urine protein–to-creatinine ratio (or 24-h urine protein) of 500 mg /24-h OR red blood cell casts
8. Neurologic	Seizures Psychosis Mononeuritis multiplex *in the absence of other known causes e.g. primary vasculitis* Myelitis Peripheral or cranial neuropathy *in the absence of other causes e.g. vasculitis, infection, & diabetes* Acute confusional state *in the absence of other causes, including toxic/metabolic, uremia, drugs*
9. Haemolytic anaemia	
10. Leukopenia (<4,000/mm^3 at least once) *in the absence of other known causes such as Felty's syndrome, drugs, and portal hypertension* OR lymphopenia (<1,000/mm^3 at least once) *in the absence of other known causes e.g. corticosteroids, drugs, & infection*	
11. Thrombocytopenia (<100,000/mm3) at least once *in the absence of other causes e.g. drugs, portal hypertension & thrombotic thrombocytopenic purpura*	
Immunologic criteria	
1. ANA level above laboratory reference range	
2. Anti-dsDNA antibody level above laboratory reference range (or >2-fold the reference range if tested by ELISA)	
3. Anti-Sm: presence of antibody to Sm nuclear antigen	
4. Antiphospholipid antibody positivity as determined by any of: Positive test result for lupus anticoagulant False-positive test result for rapid plasma reagin Medium- or high-titer anticardiolipin antibody level (IgA, IgG, or IgM) Positive test result for anti–'2-glycoprotein I (IgA, IgG, or IgM)	
5. Low complement: Low C3 Low C4 Low CH50	
6. Direct Coombs' test *in the absence of hemolytic anemia*	

ELISA = enzyme-linked immunosorbent assay

5.5 Cardiovascular disease in SLE

5.5.1 Introduction

The range of CVD in SLE includes Raynaud's phenomenon, vasculitis, endothelial dysfunction, a procoagulant tendency associated with antiphospholipid antibodies, atherosclerosis and myocardial dysfunction (particularly, increased left ventricular ejection fraction and mass due to left ventricular hypertrophy) [El-Magadmi 2004; Lima 2002; Pieretti 2007; Chow 2007]. The 5-year survival rate has increased [Gladman 1996a], partly due to a decrease in deaths from SLE disease activity and infections [Gustafsson 2014], but the mortality rate still exceeds that seen in the general population (SMR 2.4) [Bernatsky 2006; Gustafsson 2012]. Deaths from CVD have not decreased and accounted for 48% of all deaths in a recent Swedish SLE cohort study [Gustafsson 2012]. Studies of CVD in SLE include those looking at hard clinical outcomes (myocardial infarction, angina, stroke, transient ischaemic attack, claudication, peripheral arterial thrombosis) and those looking for the presence of atherosclerosis, either as definite disease (plaques and to a lesser extent arterial calcification) or for the presence of surrogate markers of atherosclerosis, particularly C-IMT.

5.5.2 Coronary artery disease

SLE is a recognised independent risk factor for atherosclerosis and coronary artery disease (CAD), with an incidence of myocardial infarction for women with SLE aged 35-44 years, greater than 50 times that in the Framingham dataset [Manzi 1997; El-Magadmi 2004]. Even after matching for traditional cardiovascular risk factors, CAD risk in SLE is 7-fold higher than that of healthy controls [Esdaile 2001].

Subclinical coronary atherosclerosis has been investigated in SLE. Coronary artery calcification has been shown to be significantly increased in SLE patients compared with age- and sex-matched controls by electron beam-CT (EBCT) - 31% versus 9% [Asanuma 2003]; 19.4% versus 6.2% [Chung 2006]; 47.6% versus 35.2% [Kao 2008]. Approximately one-third of women with SLE and no history of coronary artery disease have been shown to have abnormalities of myocardial perfusion on SPECT [Bruce 2000; Sella 2003].

5.5.3 Carotid plaque

The presence and extent of atherosclerotic plaque in the carotid arteries can be determined using non-invasive imaging techniques such as ultrasound and cardiovascular magnetic resonance (CMR). A plethora of carotid ultrasound studies looking at the presence and progression of plaque have been undertaken in healthy populations, populations with known CVD as well as in SLE [Belcaro 1996; Crouse 2006; Roman 2003; Eder 2014; Frerix 2014].

Atherosclerosis is a systemic disease [Rothwell 2001; Frerix 2014], and assessment of carotid plaque by ultrasound is used as a measure of systemic atherosclerosis and as a surrogate for the presence and possible effect of treatments on the coronary arteries.

The presence of carotid plaque has been found to predict future cardiovascular events in healthy populations [Roman 2006; Belcaro 1996]. In SLE patients, the prevalence of carotid plaque has found to be significantly greater than in healthy controls. In a cohort study by Roman *et al*. 37.1% of SLE patients versus 15.2% of controls had carotid plaque, independent of traditional cardiovascular risk factors [Roman 2003]. Further studies have observed the frequency of carotid plaques in SLE patients as between 30-43%, compared to 20-30% in controls [Manzi 1999; Thompson 2008; Anania 2010; Kao 2013]. As in controls, the presence of carotid plaques has been found to be predictive of future cardiovascular events [Kao 2013].

5.5.4 Carotid intima media thickness

Mean and maximum C-IMT values have been shown to correlate significantly with coronary artery disease and atheroma burden [Granér 2006], although less so than carotid plaque [Eder 2014]. C-IMT has also been found to be predictive of future cardiovascular events in healthy populations, although less so than carotid plaque [Chambless 1997; O'Leary 1999; Lorenz 2007; Belcaro 1996]. Although increased C-IMT is often thought of as an early manifestation of atherosclerosis, increased C-IMT and carotid plaques do not always co-exist, suggesting that they may be expressions of different atherosclerosis phenotypes [Eder 2014] or that C-IMT may reflect a non-atherosclerotic remodelling response to arterial wall injury [Stein 2011; Frerix 2014]. Indeed, increased C-IMT can be found at a younger age than the development of plaques and the presence of the former does not necessarily precede the latter [Frerix 2014].

In SLE, C-IMT has not been found to be consistently raised: C-IMT has been found to be increased in SLE patients with known CVD but was similar between SLE patients without CVD and controls [Svenungsson 2001] and reduced compared to controls in other studies [Roman 2003]. Atheromatous plaques can frequently be found without increased C-IMT in SLE [Frerix 2014]. Other studies have however found increased C-IMT in SLE patients with no overt CVD [Shang 2008]. Increased C-IMT in SLE patients has been associated with an increased risk for cardiovascular events (HR 1.35, 95% CI 1.15 to 1.59, $p < 0.01$), albeit lower than that for the presence of carotid plaque (HR 4.67, 95% CI 1.41 to 15.53, $p=0.01$) [Kao 2013].

5.5.5 Endothelial dysfunction and arterial stiffness

Endothelial dysfunction is a systemic process and one of the earliest stages of atherosclerosis, predating the development of focal plaque [Celermajer 1992; Flammer 2012]. It is assessed primarily by the measurement of flow-mediated dilatation (FMD) of the brachial artery and has been associated with all traditional cardiovascular risk factors [Celermajer 1992; Mason 2003] and with an increase in cardiovascular events [Suwaidi 2000]. Endothelial function is impaired in SLE, even in individuals without traditional cardiovascular risk factors [Lima 2002; El-Magadmi 2004; Wang 2014]. FMD has been shown to correlate negatively with C-IMT i.e. increasing C-IMT correlates with a greater degree of endothelial dysfunction [El-Magadmi 2004]. Endothelial dysfunction can be reversible, and has been shown to improve in SLE with reduced inflammation [Parker 2014] and with statin treatment [Ferreira 2007; Vera-Lastra 2016].

Arterial stiffness is also an early marker of vascular disease and is increased in the setting of traditional cardiovascular risk factors [Roman 2005]. Arterial stiffness is increased in SLE [Roman 2005; Shang 2008] and may be correlated with disease activity [Chow 2007; Shang 2008].

5.5.6 Myocardial mass and function

SLE is associated with myocardial dysfunction. Increased left ventricular ejection fraction and mass due to left ventricular hypertrophy has been found [Pieretti 2007; Chow 2007]. Echocardiography techniques looking at diastolic function and regional systolic and diastolic myocardial velocities can give an earlier indication of myocardial dysfunction, before global ejection fraction is affected. There is evidence that these measures are impaired in SLE patients with no CVD compared with controls [Buss 2010].

5.6 Aetiology of atherosclerosis in SLE

5.6.1 Introduction

Atherosclerosis in SLE may be mediated by SLE specific causes such as coronary vasculitis, immune-complex mediated endothelial damage and therapies to control SLE disease activity.

5.6.2 Traditional risk factors

Traditional CVD risk factor prevalence is increased in SLE [Svengusson 2001; Esdaile 2001; Asanuma 2003; Bruce 2003] and has been associated with the occurrence of CAD [Petri 1992; Asanuma 2003].

Smoking

Smoking increases CVD risk in the general population as well as in those with autoimmune disease. The odds ratio for developing SLE is 1.5 in smokers [Costenbader 2004] and SLE patients who smoke have greater disease activity and ds-DNA positivity [Benvenuti 2015].

Hypertension, insulin resistance, dyslipidaemia and the metabolic syndrome

Hypertension is a risk factor for CVD in all populations and is more prevalent amongst patients with SLE [Petri 1992; Bruce 2003; Asanuma 2003], affecting up to 33% of SLE patients without known CVD compared with 13% of controls [Bruce 2003]. Insulin resistance, as well as frank diabetes, is also more prevalent amongst SLE patients, in those both with and without known CVD, compared with controls [Svengusson 2001; Bruce 2003]. Dyslipidaemia is frequently seen amongst SLE patients. Increased LDL- and VLDL-cholesterol, increased TGs, and decreased HDL-cholesterol are seen, and a "lupus lipid pattern" has been observed, characterised by elevated VLDL-cholesterol and TGs with normal or low levels of LDL- and HDL-cholesterol [Benvenuti 2015]. Anti-lipoprotein lipase, anti-HDL and anti-apolipoprotein A1 antibodies, as well as lipid peroxidation and anti-ox-LDL antibodies, both of which increase the levels of pro-atherogenic oxLDL are also seen in SLE [Benvenuti 2015].

The metabolic syndrome is defined by a clustering of CVD risk factors including hypertension, dyslipidaemia (elevated TGs and LDL-cholesterol; low total and HDL-cholesterol), insulin resistance, central obesity, elevated CRP and elevated homocysteine. The metabolic syndrome is more prevalent among SLE patients [Bruce 2003; Asanuma 2003; Sabio 2008] compared with controls, occurs in younger patients and is associated with more hypertension, hypertriglyceridaemia, raised inflammatory markers, disease damage and corticosteroid use [Sabio 2008; Parker 2013]. The presence of the metabolic syndrome in SLE patients is associated with a 2-fold increase in CVD [Bruce 2003; Parker 2013].

5.6.3 Autoantibodies

Autoantibodies play a key role in SLE as well as in atherosclerosis. Anti-dsDNA is a marker of SLE and associated with disease activity. Association of anti-dsDNA and CVD is conflicting in SLE – some studies have shown an association with CVD event rates [Magder 2012] whereas others have shown no significant difference between anti-dsDNA and the presence of carotid artery plaque or clinical coronary or cerebrovascular disease [Roman 2003].

Antiphospholipid antibodies are common in SLE. In the Hopkins' Lupus Cohort 47% were anti-cardiolipin, 32.5% anti-□2-glycoprotein-1 and 26% lupus anticoagulant positive [Petri 2010]. Lupus anticoagulant was the most strongly associated with arterial and venous thrombosis, and the only antiphospholipid antibody associated with myocardial infarction. There was however no association between antiphospholipid antibodies and atherosclerosis, despite their ability to increase endothelial cell adhesion molecules and the movement of leucocytes into the vascular intima. This confirms the findings by Roman in 2003 where none of the antiphospholipid antibodies were associated with carotid plaque, or with clinical coronary or cerebrovascular disease [Roman 2003]. Other studies however have demonstrated an association of antiphospholipid antibodies with increased risk of CVD, with their presence predicting a first CVD event [Gustafsson 2009].

5.6.4 Inflammatory markers

Inflammatory mediators such as CRP and ICAM-1 may act as biomarkers for CVD in the general population [Ridker 2000; Ridker 2001; Blake 2002; Roman 2003; Ridker 2003]. Markers of systemic inflammation such as TNF-□, MCP-1, IL-6, fibrinogen, □- antitrypsin, serum amyloid A and CRP are increased in SLE patients with CVD [Gustafsson 2009; Gustafsson 2014]. Using a high-sensitivity assay, CRP levels predict cardiovascular events in the general population [Ridker 2000]. In SLE, CRP is not a good marker of disease activity and its role in CVD is conflicting. Some studies have shown an association between higher levels of CRP and CVD [Manzi 1999; Gustafsson 2009] whereas others have found no independent ability of CRP to predict CVD [Doria 2003; Kiani 2008]. In a study of carotid plaque in SLE although inflammatory mediators including CRP were elevated, the difference was not significant between those with and without plaque. The authors suggest that inflammatory markers may lose their discriminatory power with respect to CVD in conditions with elevated levels of inflammation, unlike the general population, where most inflammatory markers fall within normal ranges [Roman 2003].

The cytokine interferon-□ (IFN-□) may increase CVD risk in SLE by resulting in endothelial damage and vascular repair inhibition [Skaggs 2012]. IFN-□ secretion may cause endothelial cell apoptosis, resulting in vascular damage, and may prevent differentiation of endothelial progenitor and circulating angiogenic cells into endothelial cells, impairing vascular repair [Skaggs 2012; Gustafsson 2014]. IFN-□ levels correlate with disease activity and severity, and are associated with vascular disease including venous thrombosis [Gustafsson 2014].

5.6.5 Sex hormones, vitamin D and homocysteine

Oestrogen, prolactin, testosterone and DHEA have all been implicated in SLE development and flare frequency [Petri 2008]. High oestrogen and prolactin levels can cause B-cell tolerance breakdown [Grimaldi 2006; Petri 2008], however, hormonal interactions are complex and upregulation of other, mainly T-cell protective mechanisms occur. Menopausal onset has been found to occur earlier in SLE thus removing the atheroprotective effect found in women at an earlier age in those with SLE [Bruce 2003].

Low vitamin D has been implicated in a wide range of diseases including CVD, cancer and autoimmune diseases [Petri 2013]. Low vitamin D is frequently found in SLE patients possibly exacerbated by avoidance to sun exposure. Raising levels to 40ng/ml has been associated with a significant but clinically modest reduction in SLE disease activity score [Petri 2013], but the long-term beneficial effects on disease activity/severity and possible reduction in hard end-points such as CVD have yet to be elucidated and will require large trials.

Elevated homocysteine has been associated with CVD in the general population [Ridker 2000], and SLE patients have been found to have higher levels of homocysteine compared with controls [Bruce 2003]. In SLE, conflicting results have been found between homocysteine and CVD - some studies show no difference between homocysteine levels in SLE patients with or without a CVD event [Gustafsson 2009], whilst in others, raised homocysteine levels have been predictive of CVD [McMahon 2014]. Homocysteine levels were found to be higher in SLE patients with carotid plaques compared with those without plaque, but statistical significance was not reached, and the homocysteine levels were within the normal range and not significantly different to the control group [Roman 2003].

5.6.6 SLE treatment

SLE treatment is aimed at reducing disease activity and inflammation. This is achieved primarily by the use of corticosteroids, usually prednisolone, and hydroxychloroquine, although other agents such as mycophenolate, azathioprine, methotrexate and the anti-CD20 monoclonal antibody rituximab are also employed.

Steroids are known to increase lipids, particularly LDL-cholesterol and TGs and cause glucose intolerance therefore increasing the risk of atherosclerosis. Duration and cumulative steroid dose has been associated with increased CVD in SLE [Petri 1992; Svengusson 2001; Roman 2003], however, no association with average daily dose, ever use or pulsed treatment has been seen [Petri 1992; Roman 2003]. This suggests that increased CVD may

actually reflect disease activity and/or severity, with steroid use being a marker of this. Steroids reduce inflammation, another risk factor for CVD, and may therefore actually have atheroprotective effects particularly during disease flares. In a study by Roman *et al*, SLE patients with carotid plaque had received lower daily prednisolone doses compared with patients with no plaque [Roman 2003]. Acute CVD events have been associated with current corticosteroid use even after adjustment for disease activity, but not with previous use, suggesting that corticosteroids may only have a short-term effect on CVD risk [Magder 2012].

Hydroxychloroquine is an antimalarial that reduces disease flares and organ damage in SLE [Benvenuti 2015]. Its use has been found to be lower in SLE patients with carotid plaque compared to those without plaque [Roman 2003]. Hydroxychloroquine has been shown to improve the lipid profile in SLE by reducing LDL and VLDL-cholesterol and increasing HDL-cholesterol. It also reduces vascular inflammation and hyperglycaemia [Benvenuti 2015].

Other SLE therapies include monoclonal antibodies (rituximab and belimumab), which may improve the lipid profile in SLE whilst reducing disease activity; methotrexate, which has been shown to reduce the risk of CVD in other inflammatory arthropathies, and may have a similar effect in SLE; mycophenolate, which has not shown any change in CVD risk in preliminary studies in SLE but has been associated with reduced atherosclerosis in murine models of SLE; and azathioprine for which data is limited and conflicting with regards to CVD risk [Benvenuti 2015].

5.6.7 Prevention of atherosclerosis in SLE

The risk of CVD in SLE is not fully explained by traditional CV risk factors and risk is underestimated by the Framingham Risk Score [Esadile 2001; Bruce 2003]. The current strategy in reducing CVD risk in SLE involves treatment to reduce SLE disease activity as well as aggressive treatment of disease flares; use of steroid-sparing agents; and addressing modifiable risk factors such as hypertension, diabetes and smoking. Dyslipidaemia is currently treated with statins according to NCEP targets, although the increased risk of CAD in the SLE population and the ability of statins to reduce inflammatory markers such as CRP have resulted in statins becoming widely prescribed, even in those with no known CVD and normolipidaemia, and despite the lack of evidence that statins can effect a beneficial effect on surrogate markers of CVD or CVD events in these lower-risk SLE patients [Petri 2011].

5.6.8 SLE as a risk factor

SLE itself is an independent risk factor for CVD with a relative risk of 10.1 for nonfatal MI, 17.0 for death due to CHD, 7.5 for overall CHD and 7.9 for stroke after controlling for conventional risk factors [Esdaile 2001]. SLE may increase CVD risk due to disease activity, which is an independent risk factor for increased CVD events [Benvenuti 2015]. Other factors associated with SLE, such as a more sedentary lifestyle due to poor health, may enhance the effects of both traditional and SLE-related CVD risk factors.

5.6.9 Summary

The increased risk of CVD in SLE therefore represents a complex interplay of traditional CVD risk factors, SLE specific factors such as disease activity and severity, SLE treatments which can exert both atheroprotective as well as atherogenic effects, and the effects of sex hormones, an earlier menopause and the number and type of autoantibodies present.

Chapter 6
Human Immunodeficiency Virus (HIV)

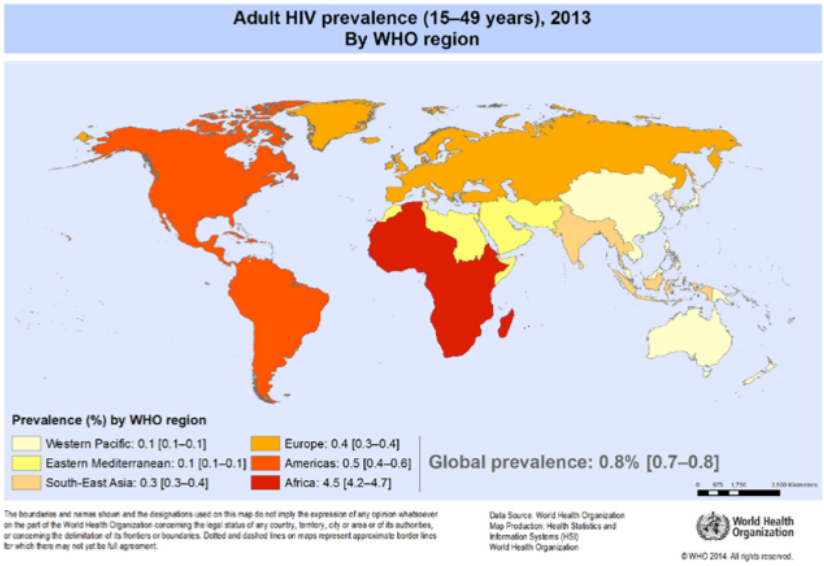
6.1 Introduction

The acquired immunodeficiency syndrome (AIDS) was first described in 1981 among homosexual men in the United States who presented with *Pneumocystis carinii* pneumonia and Kaposi's sarcoma [Centers for Disease Control 1981a; Centers for Disease Control 1981b]. HIV was later identified as the cause. Invariably fatal at the time, infection with HIV has become chronic and lifelong due to the introduction of effective combination anti-retroviral treatment (cART) in the mid-1990s [WHO Global Health Observatory Data Repository]. Despite this, mortality rates in HIV-infected individuals are still higher than in the general population and non-AIDS related morbidity and mortality is increasing [Sackoff 2006; Lohse 2007]. Cardiovascular disease, especially ischaemic heart disease, is an important cause of morbidity and mortality among HIV-infected individuals [Sackoff 2006;Triant 2012].

6.2 Epidemiology

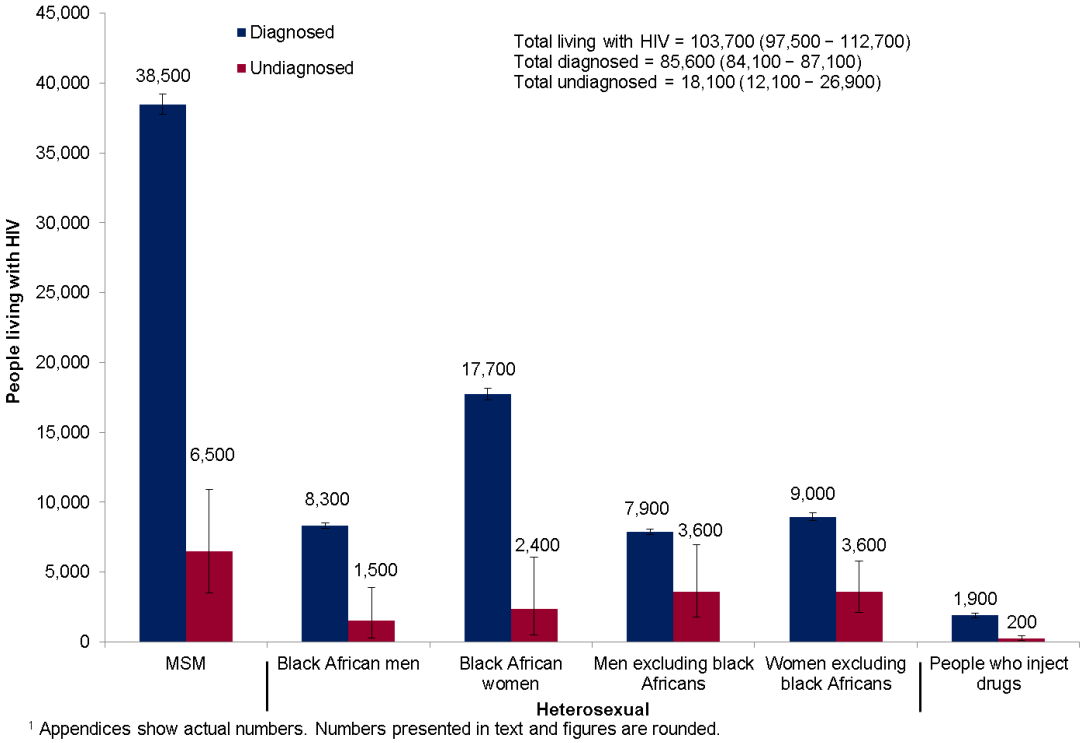
An estimated 35.0 million people worldwide were living with HIV at the end of 2013 [WHO Global Health Observatory Data Repository]. This equates to approximately 0.8% of adults aged 15-49 years worldwide. Prevalence, however, varies considerably between regions and countries (Figure 1). Sub-Saharan Africa remains the most severely affected region, with nearly 1 in 20 adults affected and containing almost 71% of the people living with HIV worldwide.

Figure 6.1. Worldwide prevalence of HIV in adults at the end of 2013 [from WHO Global Health Observatory Data Repository, Data on the size of the epidemic: Number of people (all ages) living with HIV. Accessed online 28/02/16].



In the UK an estimated 103,700 people were living with HIV in 2014, with one in four aged 50 years and over [Skingsley 2015]. The overall HIV prevalence was 1.9 per 1,000 people aged 15 and over. An estimated 18,100 (17%) of people were unaware of their infection. HIV in the UK remains largely concentrated among men who have sex with men (MSM) and men and women of black African ethnicity (Figure 2). In the UK, as in the US, the numbers of new HIV diagnoses have plateaued or decreased slightly in recent years, but the number of people living with HIV has increased as deaths have reduced dramatically with the widespread use of cART [Skingsley 2015; CDC HIV Surveillance Report 2014]. A falling rate of new infections is also being seen in some of the most severely affected regions in the world, such as sub-Saharan Africa, as cART and education programmes become increasingly available [WHO Global Health Observatory Data Repository]. Transmission rates however continue to be high in certain groups. In the UK and US transmission remains high in MSM as well as Black Africans (UK) and African-Americans, Latinos and mixed race individuals (US) [CDC HIV Surveillance Report 2014]. In Eastern Europe and parts of Asia, intravenous drug use and heterosexual sex are major modes of transmission. In sub-Saharan Africa, heterosexual transmission is the mode of transmission [WHO Global Health Observatory Data Repository; HIV/AIDS surveillance in Europe 2014].

Figure 6.2. Estimated number[1] of people living with HIV (both diagnosed and undiagnosed) all ages: UK, 2014 (From: HIV in the UK – Situation Report 2015: data to end 2014. November 2015. Public Health England, London).



[1] Appendices show actual numbers. Numbers presented in text and figures are rounded.

6.3 The Human Immunodeficiency Virus

HIV is a lentivirus, a retroviral family member. It infects cells of the human immune system including T-lymphocytes, macrophages and dendritic cells, causing immunosuppression. Untreated, it eventually causes AIDS. There are two types of HIV: HIV-1 and HIV-2. Molecular studies suggest that HIV-1 evolved from a strain of ape simian immunodeficiency virus (SIV), and HIV-2 evolved from a mangabey monkey SIV strain [Gao 1999; Keele 2006; Hirsch 1989]. Zoonotic transmission to humans, is believed to have occurred due to similarities between the SIV and HIV viral genomes, their geographical association in Africa and the practice of consuming primate meat in West Africa, providing a possible transmission route [Gao 1999].

HIV-1 is the most prevalent type and is further divided into groups and subtypes. There are four distinct viral groups, each believed to have evolved from different episodes of zoonotic transmission: groups M, N and O are derived from chimpanzees and group P from gorillas [Plantier 2009]. The pandemic strain causing most HIV infection is group M ("Main"). Other groups have more limited geographical distributions [Gao 1999]. The group M virus comprises 9 subtypes, of which subtype C accounts for almost half of global HIV-1 infections and is predominantly found in southern Africa and India. Subtype B is found predominantly in western and central Europe, North America, the Caribbean and South America [Hemelaar 2011]. Group O is limited to West Africa and group P, only discovered in 2009, to Cameroon [Gao 1999; Plantier 2009; Hemelaar 2011].

HIV-2 accounts for about 5% of worldwide HIV infections [WHO Global Health Observatory Data Repository]. It predominates in West Africa, Portugal, Spain and India, but is found worldwide. HIV-2 infection appears to follow a more indolent course and is intrinsically resistant to certain antiretroviral agents [Panel on Antiretroviral Guidelines for Adults and Adolescents].

The occurrence of multiple HIV strains as well as their differing rates of transmission, disease progression and mutation causing viral immune escape have and continue to pose challenges for the development of safe and effective vaccines and treatments.

6.4 Immune dysfunction

6.4.1 Cell-mediated Immunity

Early HIV infection is characterised by rapid viral replication, high viral load (>100,000 copies/mL) and CD4+ T cell count reduction, the hallmark of HIV infection, which may be

transient. In the acute stages (i.e. 1-2 weeks) an illness characterised by fever, lymphadenopathy, arthralgia/myalgia, sore throat, rash and headache may occur, although some will be asymptomatic. After about six months, viral levels stabilise. Untreated, HIV replication remains high and CD4+ cell destruction continues [Ho 1995]. However, rates of destruction and replacement are usually almost balanced, and the CD4+ cell count decline is slow [Ho 1995]. CD4+ cells in the gastrointestinal tract are massively depleted early in infection with minimum recovery after cART [Maartens 2014]. There is also a loss in T-helper-17 cells and mucosal-associated T-cells, which act as a front-line defence against bacteria. This, together with increased gastrointestinal tract permeability allows increased concentrations of bacterial products, such as lipopolysaccharide (LPS), in the blood [Maartens 2014].

6.4.2 Humoral Immunity

HIV also activates the humoral immune system. B cells are activated and, in advanced HIV infection, undergo terminal differentiation with increased antibody secretion. Many of these antibodies however are non-specific. As with cellular immunity, humoral immunity declines with time [Chong 2004].

6.4.3 HIV controllers

A substantial minority of HIV-infected individuals are termed '*long-term non-progressors'*. These individuals maintain a stable CD4+ cell count (>500 cells/microL), low viraemia levels (<10,000 copies/mL) and show no clinical progression, despite not receiving cART [Madec 2009]. A very small minority of HIV-infected individuals are termed '*elite controllers*'. These individuals are able to maintain undetectable viral loads (on current commercial assays) and maintain high CD4+ cell counts for long periods without cART [Pereyra 2009]. Viral load suppression in elite controllers is comparable to that seen in patients taking cART [Dinoso 2008]. Despite this, compared to non-HIV infected individuals, elite controllers remain at increased risk of the non-infectious complications of HIV including CVD due to very low levels of viral replication and chronic inflammation [Pereyra 2009; Pereyra 2012].

6.4.4 Immune activation and Inflammation

HIV infection is characterised by marked immune activation, involving both the adaptive and innate immune systems, and abnormalities in coagulation [So-Armah 2016]. There is chronic inflammation with persistently elevated inflammatory markers [Lo 2012]. Inflammatory markers increase with increasing viraemia [Floris-Moore 2009; Calmy 2009] and predict mortality [Tien 2010; So-Armah 2016]. HIV acts as a ligand for the Toll-like receptors (TLR7, TLR8) on dendritic cells, resulting in the production of interferon-□. LPS, from increased

gastrointestinal bacterial translocation, activates TLR4 resulting in the production of pro-inflammatory cytokines such as interleukin-6 (IL-6) and tumour necrosis factor-α (TNF-α) [Maartens 2014]. Direct correlations between plasma LPS levels in HIV-infected individuals, residual viraemia, cellular activation (including CD38+HLA-DR+CD8+T cells and monocytes), interferon responsive genes and pro-inflammatory cytokines such as interferon-α (IFN-α), IL-6 and TNF-α have been observed [Zevin 2016]. A reduction in bacteria beneficial to health and an increase of potentially inflammatory bacteria is also associated with HIV-infection [Zevin 2016]. HIV is associated with raised markers of endothelial activation including VCAM-1, P-selectin and MCP-1, which decrease with antiretroviral treatment [Calmy 2009]. Markers of inflammation in HIV-infection have been associated with increased mortality [So-Armah 2016; Kuller 2008], CVD [Duprez 2012], as well as cancer and neurological disease [Maartens 2014].

6.5 Atherosclerosis in HIV

6.5.1 Introduction

The development of increasingly potent antiretroviral drugs, effective drug combinations and once-a-day preparations, which have aided compliance and are increasingly accessible to HIV-infected individuals worldwide, has improved survival and resulted in concomitant increases in morbidity and mortality due to non-infectious complications of HIV. The increased incidence of CVD has become of concern due to the high prevalence of CVD risk factors amongst HIV-infected individuals, anti-retroviral-induced metabolic changes and the persistent inflammation and immune dysfunction associated with HIV-infection, which are known to promote the development and progression of atherosclerosis [Triant 2013; Hemkens 2014]. It is likely that both traditional and HIV-specific risk factors may act synergistically resulting in an increased CVD risk.

6.5.2 Risk factors and cardiovascular risk in HIV

Traditional cardiovascular risk factors, such as dyslipidaemia, impaired glucose tolerance, diabetes, central obesity, smoking and hypertension, are increased in HIV cohorts [Triant 2007; Saves 2003]. Control studies have shown an excess risk of CVD in HIV-infected individuals compared with HIV-uninfected controls even after adjustment for traditional cardiovascular risk factors, with adjusted relative risks of up to 2.12 [Triant 2007; Obel 2007]. Meta-analyses have found this to be true for both treated and untreated HIV-infected individuals [Hemkens 2014], and even elite controllers remain at increased risk of CVD [Hsue 2009; Pereyra 2012]. Post-mortem studies in young HIV-positive patients have shown significant atherosclerosis with a pattern described as being between typical atherosclerosis

and the accelerated atherosclerosis of cardiac transplant rejection (diffuse, circumferential) [Tabib 2000]. HIV has been found to be associated with endothelial dysfunction (as assessed by flow-mediated dilatation - FMD) [Arildsen 2013], coronary atherosclerosis on CT [Lo 2012], increased C-IMT and carotid plaques on ultrasound [Kaplan 2011; Hsue 2012] and aortic plaques on MRI [Floris-Moore 2009].

Dyslipidaemia

A fall in mean total cholesterol, LDL-cholesterol (including small LDL particles) and HDL-cholesterol occurs after HIV-infection [Riddler 2003; Riddler 2008]. cART initiation results in large increases in total and LDL-cholesterol, but levels return approximately to pre-HIV-infection levels, and are not greater than that associated with aging [Riddler 2003]. The LDL-cholesterol profile, however, changes with cART to include a greater proportion of small, dense LDL-lipoprotein particles as well as VLDL lipoprotein particles [Riddler 2008], both of which are associated with greater atherogenic potential. Elevated levels of these small dense LDL particles as well as apolipoprotein B, have been independently associated with coronary events in HIV-infected individuals receiving cART [Bucher 2012]. The reduction in HDL-cholesterol by HIV-infection may increase CVD risk by reducing the atheroprotective effects mediated by HDL-cholesterol, including reverse cholesterol transport and it's purported anti-inflammatory and anti-oxidant effects [Rohatgi 2014; Kontush 2003; McGrath 2009]. Significant increases in TGs are also seen in HIV-infected individuals receiving cART, increasing the risk of CVD, although the independent effect is small [Worm 2011].

Lipodystrophy

Alterations in body fat composition and distribution are seen in almost 50% of HIV-infected individuals on cART [Hemkens 2014; Stanley 2012]. Loss of subcutaneous fat from the face and limbs (lipoatrophy), increased central fat gain with visceral, breast, cervical and/or dorsocervical fat deposition (lipohypertrophy) or a combination of both is seen. Both lipoatrophy and lipohypertrophy have been associated with increased TGs, decreased HDL-cholesterol and insulin resistance [Hemkens 2014; Stanley 2012]. Inflammatory markers including hs-CRP, IL-6, and TNF-□ have been shown to be similar in HIV-infected men with lipodystrophy to obese non-HIV infected men, despite the HIV cohort having significantly lower body fat [Samara 2009]. HIV-infected individuals with lipodystrophy have increased Framingham risk scores and are at an increased risk of CVD [Lake 2011].

Impaired glucose tolerance and diabetes

Impaired glucose tolerance and overt diabetes has been found to be similar to or possibly modestly increased in cART-naïve, HIV-infected individuals compared to non-HIV infected

individuals [Stanley 2012]. cART treatment however is associated with an increased prevalence of diabetes. The D:A:D study showed that all cART regimens were associated with an increased risk of diabetes [Friis-Møller 2003]. Inflammatory markers, particularly TNF-□, have been associated with an increased risk of diabetes [Brown 2010]. TNF-□ is released by lymphocytes, macrophages and endothelial cells and is highly expressed in HIV-infected individuals. It is also produced by adipose tissue and interacts with the insulin receptor attenuating the effect of insulin binding and causing insulin resistance [Brown 2010]. Population studies examining the association of TNF-□ and diabetes, as well as the effect of TNF-□ blockers on insulin resistance, however have been conflicting [Brown 2010].

6.5.3 Chronic inflammation and immune activation

A growing body of evidence suggests that HIV-associated inflammation and immune dysfunction may contribute to the increased risk for CVD seen in HIV-infected individuals. Relative risk of ischaemic heart disease among those with a CD4+ cell count ≤200 cells/ml was found to be greater than in those with a cell count >200 cells/ml at cART initiation [Obel 2007]. Activated T-lymphocytes in HIV-infected individuals have been found to be associated with subclinical carotid artery disease (C-IMT) [Kaplan 2011].

In the SMART trial, individuals were assigned to either continuous cART (viral suppression) or interruption of cART until CD4+ counts <250cells/μL (drug conservation), in an attempt to reduce the adverse cardiovascular and metabolic effects of cART. However, an increased risk of CVD events in the drug conservation group compared to the viral suppression group was seen [El-Sadr 2006]. Increased levels of the inflammatory markers IL-6, hs-CRP and D-dimer were observed in the drug conservation group and predicted CVD [Duprez 2012]. The initiation of the atherosclerotic process as a result of injury or inflammation to the vascular endothelium results in the release of cytokines and adhesion molecules such as VCAM-1. These allow macrophages and lymphocytes to enter the vascular wall setting up an inflammatory cascade. VCAM-1 is raised with HIV infection and cART has been shown to reduce its levels [Calmy 2009]. Despite the significant declines in pro-inflammatory mediators (e.g. s-VCAM-1, P-selectin, leptin and D-dimer), increases in anti-inflammatory mediators (e.g. adiponectin, IL-10), and viral suppression in patients receiving cART [Calmy 2009], aortic arterial inflammation has been found to be similar in HIV-infected individuals with low Framingham risk scores to that in HIV-negative individuals with atherosclerosis [Subramanian 2012]. Arterial inflammation was associated with sCD163, a marker of macrophage activation.

6.5.4 The role of antiretroviral drugs

Protease inhibitors (PIs) and nucleoside reverse transcriptase inhibitors (NRTIs) are used in the treatment of HIV. Their role in increasing CVD risk remains controversial. PIs have been associated with increased rates of myocardial infarction (MI) [Friis-Møller 2007], possibly in part (but not entirely) attributable to dyslipidaemia. The evidence for NRTIs is conflicting. The D:A:D study has shown an increase in the risk of MI with increased duration of cART exposure, independently associated with PI use, although an effect of NRTIs could not be ruled out [Friis-Møller 2007]. A further analysis of the D:A:D study data demonstrated that the NRTIs abacavir and didanosine increased the risk of MI [D:A:D Study Group 2008]. Meta-analyses however have produced conflicting data with one recent study confirming the increased MI risk associated with abacavir and another finding no increased risk [Hemkens 2014]. In the PI group exposure to the first generation of drugs such as indinavir has been associated with an increased risk of MI, but the data for the newer drugs in this class remains limited [Hemkens 2014].

Anti-retroviral drugs may of course increase the risk of CVD by adverse metabolic effects. The PIs have been associated with increased diabetes and insulin resistance, particularly the first generation of drugs. NRTIs, especially the thymidine analogues zidovudine and stavudine, are also associated with a drug-induced risk of diabetes, possibly due to their mitochondrial toxicity [Hemkens 2014]. Dyslipidaemia, commonly seen in HIV-infected individuals, is also associated with cART. Increases in total cholesterol, LDL-cholesterol, and TGs are seen with PIs, a more marked effect occurring with the first-generation of drugs compared to newer ones (e.g. indinavir, lopinavir versus atazanavir, and darunavir). The NRTIs also increase LDL-cholesterol and TGs to varying degrees, and the non-nucleoside reverse transcriptase inhibitors (NNRTIs) such as efavirenz, can lead to higher increases in total and LDL-cholesterol than the newer PIs [Hemkens 2014].

6.6 HIV in children and young adults

HIV-infection acquired in utero or perinatally, untreated, caused death from AIDS by the age of 5 years. Twenty years of effective cART means the first generation of HIV-infected children have reached adulthood.

As in adults, cART results in adverse metabolic effects. They are known to cause the same pattern of dyslipidaemia in children [Rhoads 2006]. HIV-infection causes falls in LDL-cholesterol and HDL-cholesterol as in adults. Children newly exposed to cART experience a significant rise in LDL-cholesterol over the first year [Rhoads 2011; Sztam 2011]. In a United

Kingdom cohort of 449 children, PIs caused greater rises in total cholesterol than NNRTIs [Rhoads 2011]. 10.5% had LDL-cholesterol over the 95% percentile for LDL (3.33mmol/L), with 17 children having persistently raised LDL-cholesterol above the threshold (>4.1mmol/L) for pharmacological intervention. Unlike what has been observed to date in adults, NNRTIs also caused an increase in HDL-cholesterol in this paediatric population.

Lipodystrophy is also seen in a majority of HIV-infected children and adolescents with both peripheral atrophy and central lipohypertrophy occurring [Lipshultz 2013]. Both the PIs and the NNRTIs have been associated with fat redistribution [Lipshultz 2013; Sims 2011], although some studies have shown some beneficial effects with increased growth and lean body mass [Lipshultz 2013]. Other adverse metabolic effects seen in up to a third of HIV-infected children exposed to cART include impaired glucose tolerance and insulin resistance [Sims 2011]. Microalbuminuria, a marker of vascular disease or injury, has been observed in up to 15% of HIV-infected children and is inversely related to CD4+ cell count [Sims 2011].

As in adults, chronic inflammation and immune dysfunction caused by HIV occurs. HIV-infected children have higher circulating levels of inflammatory biomarkers (e.g. hsCRP, IL-6, monocyte chemoattractant protein-1 [MCP-1]) and vascular dysfunction (e.g. intercellular adhesion molecule [ICAM], VCAM), when compared to healthy children, and cART duration has been associated with increased VCAM-1 [Sims 2011].

Although no reports of MI in children with HIV-infection exist, subclinical premature atherosclerosis is more likely to be present than in healthy children. Non-invasive surrogates of CVD risk have been widely used in both adults and children with HIV-infection as CVD events are of low prevalence. Ultrasound, used to look for the presence of early atherosclerosis (abnormal FMD and C-IMT) in paediatric HIV populations, has led to conflicting results, possibly due to lack of sensitivity resulting in poor reproducibility of findings as well as lack of information on the natural history of C-IMT in children and the likelihood that C-IMT may change very little over time in this group [Bonnet 2004; Charakida 2005; McComsey 2007]. Charakida *et al.* showed that HIV-infected children had impaired vascular function (assessed by FMD) and increased C-IMT compared to healthy children, with those exposed to PIs having a greater C-IMT. High levels of hsCRP have been found to be associated with higher C-IMT in HIV-infected children [Sims 2011]. Bonnet *et al.* found HIV-infected children to have increased arterial stiffness and impaired vascular function compared with healthy controls, but C-IMT was not increased. A longitudinal study of C-IMT in children with HIV-infection showed a reduction in C-IMT with time, but as the natural history of C-IMT in children is not known, whether this was due to treatment effects,

increased CD4+ counts or other factors is unknown [Barlow-Mosha 2013]. Arterial stiffness and vascular dysfunction have been correlated with increasing age and duration of exposure to cART [Sims 2011].

High rates of coronary artery abnormalities with CMR have been found in children and young adults with HIV-infection, with more than 50% exhibiting luminal narrowing and irregularity of the coronary vessel wall [Mikhail 2011]. No control group was included in this study but the findings suggest the presence of premature atherosclerosis in HIV-infected children and young adults.

All these findings indicate that HIV-infection and long-term cART use may substantially increase the CVD risk for children and young adults with HIV-infection. Unlike in the adult HIV population, where guidelines recommend aggressive management of traditional cardiovascular risk factors including dyslipidaemia, in the paediatric population, more conservative measures, such as dietary advice and exercise, are currently taken, although for those with persistent and significant elevations, lipid-lowering treatment with HMG-CoA reductase inhibitors (statins) is recommended.

Chapter 7
Methods

In the four clinical studies described in this thesis (Chapters 8-11), the main focus was cardiovascular magnetic resonance (CMR) derived carotid artery parameters. The methods used are described in sections 7.1. A CMR assessment of endothelial function was also performed in some participants (section 7.2). In the Systemic Lupus Erythematosus (SLE) studies (Chapters 8 and 9) a cardiac CMR study with gadolinium contrast was also performed (section 7.3).

7.1 Assessment of the carotid artery

7.1.1 Imaging Hardware

Scanner

The scans for the SLE studies were performed using a 1.5 Tesla scanner (Siemens Avanto, Erlangen, Germany). The studies in HIV-infected individuals were performed using a 3.0 Tesla scanner (Siemens Skyra). All studies were electrocardiogram gated.

Coils

For all scans in the four studies, a purpose-built bilateral four-channel phased-array carotid surface coil (Machnet BV, Eelde, the Netherlands) was used. The head and neck were immobilised using a specially designed vacuum head and neck cushion. All subjects were positioned so that the region of the carotid bifurcation was in the isocentre of the magnet. To protect their hearing, all subjects were given in-the-ear earplugs.

7.1.2 Assessment of carotid artery wall volume

Imaging Protocol

Bright blood gradient echo localisers were acquired in all three orthogonal planes to locate the subjects' head and neck within the scanner. The carotid arteries were identified on the localisers and a stack of time-of-flight (TOF) images was acquired perpendicular to their long axis (Figure 7.1). A saturation band was placed cranially to the region being imaged so that a high signal would be obtained only from blood flowing in the caudo-cranial direction. The carotid bifurcation on each side was identified from the TOF images. Using a plane running through three points taken from the TOF images, one in the common carotid artery, one in the internal carotid artery and one in the external carotid artery, a low resolution T1-weighted fast spin echo (FSE) image was acquired through the bifurcation on each side. A second image was acquired perpendicular to this in the common carotid artery (Figure 7.2). These

T1-weighted FSE images were used to assess for the presence of any obvious carotid plaque, to determine the location and orientation of the carotid artery for further imaging, and to verify optimal coil position. Optimal coil position was defined as the carotid artery bifurcation being in the middle of the area of high signal underlying the coil. If the coil position was suboptimal, it was repositioned, and imaging recommenced.

Figure 7.1 Stack of TOF images acquired perpendicular to the carotid artery long axis.

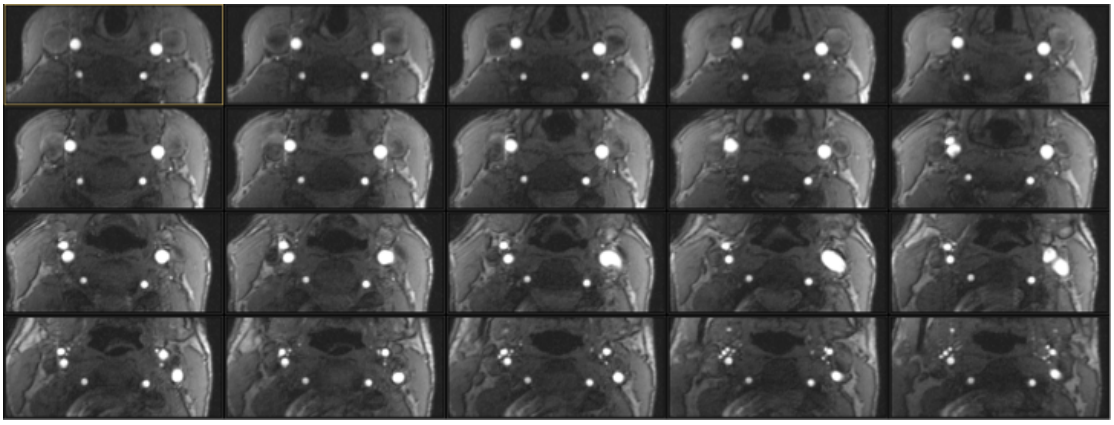
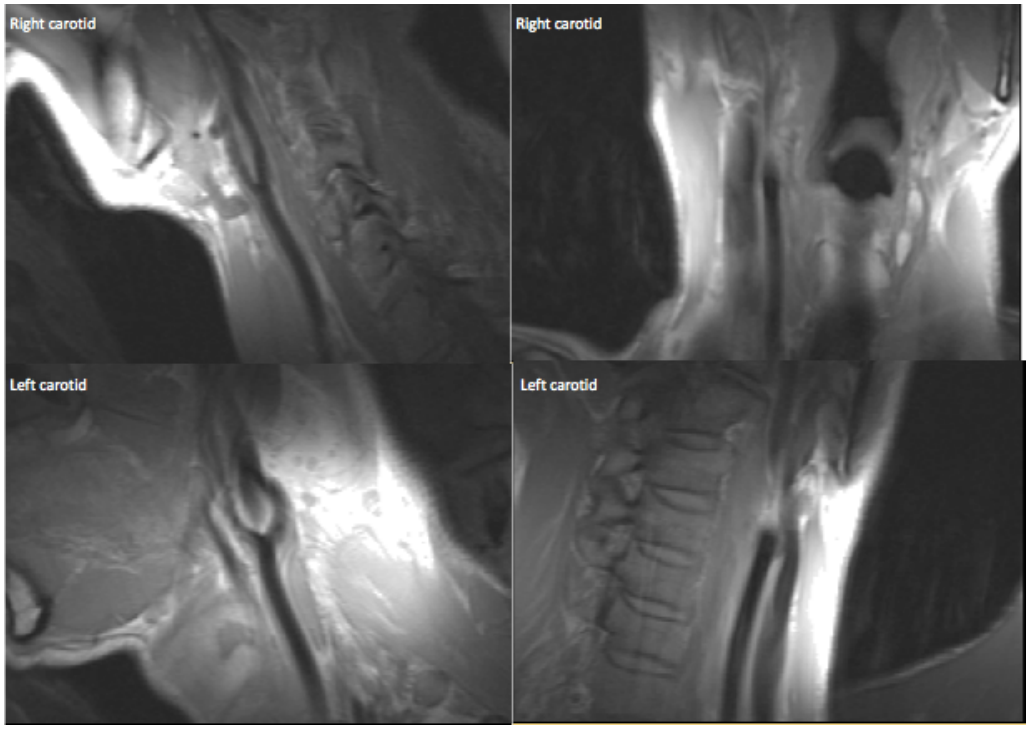


Figure 7.2 T1-weighted FSE images acquired perpendicularly to each other through the carotid bifurcation on the right (top) and left (bottom).



Using the localising images, described above, high-resolution images were then acquired. A contiguous stack of 20 high-resolution T1-weighted FSE images, centred on the carotid bifurcation bilaterally, was acquired approximately perpendicular to the longitudinal axis of both common carotid arteries, in the same orientation as the TOF images (Figure 7.3). 40 mm of longitudinal coverage per artery was acquired. Slice thickness was 2 mm. For the SLE studies (Chapters 8 and 9) performed on the 1.5 Tesla scanner, typical sequence parameters were: field of view (FOV) read 110mm and 60mm phase, imaging matrix 256x150, TE 10ms, TR 550ms, echo train length 9, bandwidth 230 Hz/pixel, 4 averages, pixel size 0.43mmx0.43mm (interpolated to 0.21mmx0.21mm). For the HIV studies (Chapters 10 and 11) performed on the 3.0 Tesla scanner, typical sequence parameters were: field of view (FOV) read 110 mm, FOV phase 100%, TE 11ms, echo train length 9, readout time 90ms, bandwidth 230 Hz/pixel, 3 averages, pixel size 0.43mmx0.43mm (interpolated to 0.21mmx0.21mm). In all cases, image acquisition was ECG-gated to each cardiac cycle with end-diastolic triggering. Dark blood preparation was used with the inversion time (TI) determined by average R-R interval. Saturation bands were placed anteriorly and posteriorly to the region imaged to reduce artefact from swallowing and CSF pulsation, and improve the image in the region of interest i.e. the carotid arteries. Phase oversampling was used as needed to eliminate “wrap artefact” from the carotid artery images.

Figure 7.3 Stack of high-resolution T1-weighted FSE images, centred on the carotid bifurcation bilaterally, acquired in the same orientation as the TOF images.

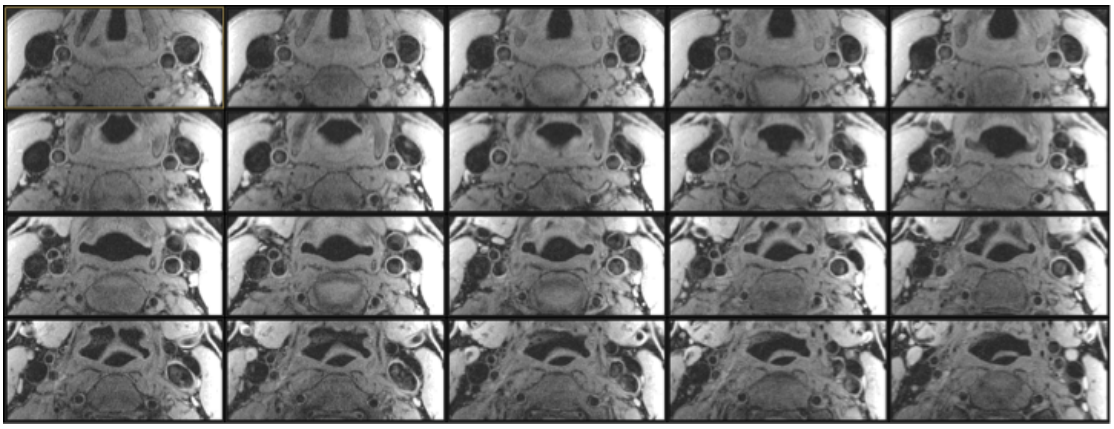
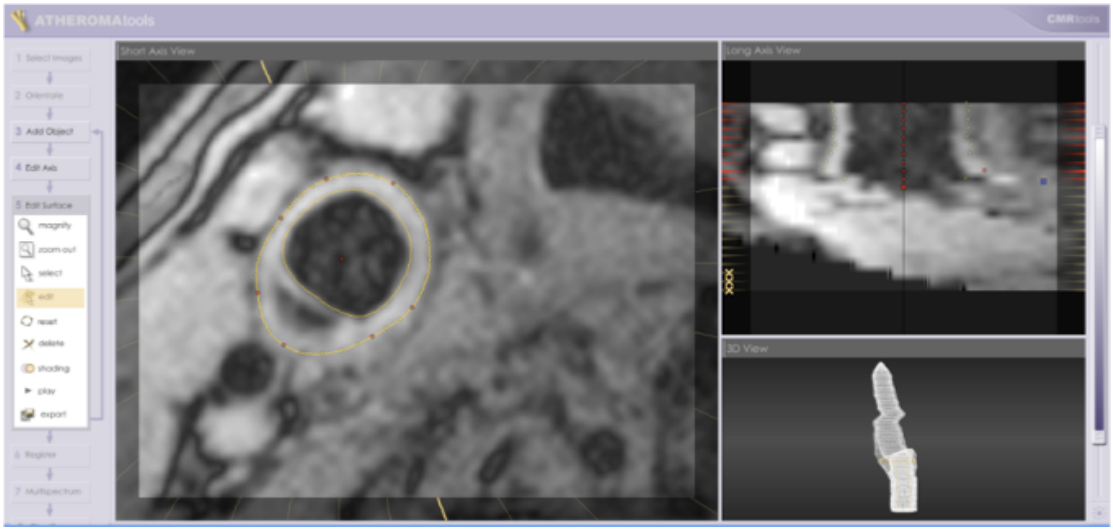


Image Analysis

Carotid artery image analysis was performed using Atheroma Tools (a plug-in of CMRtools, Cardiovascular Imaging Solutions, London), dedicated software developed at and validated by the Royal Brompton Hospital CMR Unit [Varghese 2006]. The internal and external surfaces of the common and internal carotid arteries were contoured manually for each slice to give luminal and total vessel (adventitial) areas. A three dimensional model was generated

to give the lumen volume, wall volume and total vessel volume for the standardised 40mm length (Figure 7.4). The total wall volume is expressed as a percentage of the total vessel volume, the wall/outer wall ratio (W/OW ratio). The W/OW ratio is an index of arterial thickening [Saam 2005]. A visual assessment was made for the presence of atheroma.

Figure 7.4 Carotid artery image analysis using Atheroma Tools (CMRtools, Cardiovascular Imaging Solutions, London), showing contouring of the luminal and adventitial carotid artery borders (left), and 3D model of the carotid artery (bottom right).



7.1.3 Assessment of carotid artery distensibility

Arterial stiffness is one of the earliest manifestations of adverse structural and functional changes in the blood vessel wall that can be detected. It is a measure of vascular health [Cavalcante 2011]. Arterial distensibility, a measure of arterial stiffness, is the relative change in blood vessel area during each cardiac cycle and reflects the ability of the artery to expand and contract. Decreased arterial distensibility (increased arterial stiffness) occurs with aging due to degenerative processes in the media of the arterial wall, where changes in elastin organisation and increases in collagen occur in the extracellular matrix [Palombo 2016]. Many studies have shown a link between arterial distensibility/stiffness and atherosclerotic burden and CVD events. Distensibility of the carotid arteries using ultrasound has been used as a novel risk factor for CVD in studies including the Rotterdam Study [van Popele 2001] and the Multi-Ethnic Study of Atherosclerosis [Bild 2002]. Whereas ultrasound has been used previously in the assessment of arterial distensibility, the improvement in temporal resolution of CMR has led to this technique being used increasingly, with both the aorta and carotids being suitable. CMR imaging allows the acquisition of a two-dimensional image for use in distensibility analysis versus the one-dimensional image obtained with ultrasound. Other advantages of CMR over ultrasound include the ability to image in a plane

perpendicular to the artery and an increased reproducibility in imaging position between sequential scans.

Imaging Protocol

Using the two longitudinal, perpendicular low-resolution T1-weighted FSE images described in section 7.1.2, a cine image perpendicular to the common carotid artery just below the carotid bulb was acquired on each side. The imaging sequence used was a steady state free precession (SSFP) sequence. Sequence parameters were FOV 105mm x 52mm, flip angle 60 degrees, bandwidth 977 Hz/pixel, voxel size of 0.66 x 0.82 x 6mm. Prospective ECG-gating was used.

Image Analysis

A cine image perpendicular to the common carotid artery was manually contoured using Atheroma Tools at end diastole and end systole for each side, and the percentage distensibility calculated.

7.2 Assessment of endothelial function

Endothelial dysfunction is a pathological state where an imbalance between substances causing vasodilatation and vasoconstriction occurs [Flammer 2012]. Nitric oxide (NO) is one of the most important vasodilators and is also involved in inhibiting platelet adhesion and aggregation, leucocyte migration and smooth muscle proliferation – key steps in the development of atherosclerosis. Most, if not all, CVD risk factors are associated with endothelial dysfunction, and endothelial dysfunction can be seen as an index of the overall CVD risk burden and vasculoprotective factors in an individual [Bonetti 2003]. It is an early marker of atherosclerosis preceding the development of morphological vascular change [Flammer 2012] and is therefore used as a surrogate for the assessment of vascular health. Measured response to pharmacological agents or haemodynamic provocation tests are used to assess it.

Flow-mediated vasodilatation (FMD) of the brachial artery using vascular ultrasound is the most widely used technique to assess endothelial function. It measures the ability of the brachial artery to respond to endothelial NO release during reactive hyperaemia (flow-mediated) after occlusion of the artery for 5-minutes. A blood pressure cuff placed distally to the brachial artery is inflated to 20-50mmHg above systolic pressure (protocols vary between laboratories [Bonetti 2003]) rendering the forearm ischaemic. When the cuff is released the increased flow and shear stress results in the release of NO, which leads to dilatation of the brachial artery. The diameter of the brachial artery is measured before cuff inflation and after

cuff deflation until maximal dilatation has occurred. Endothelial independent vasodilatation measuring the change in brachial artery diameter in response to sublingual glyceryl trinitrate (GTN) spray is also conventionally assessed. CMR allows the assessment of brachial artery FMD using the same technique [Sorenson 2002] and has been used in clinical trials as an end-point to look for improvement in overall vascular health [Tanner 2007; Chan 2011].

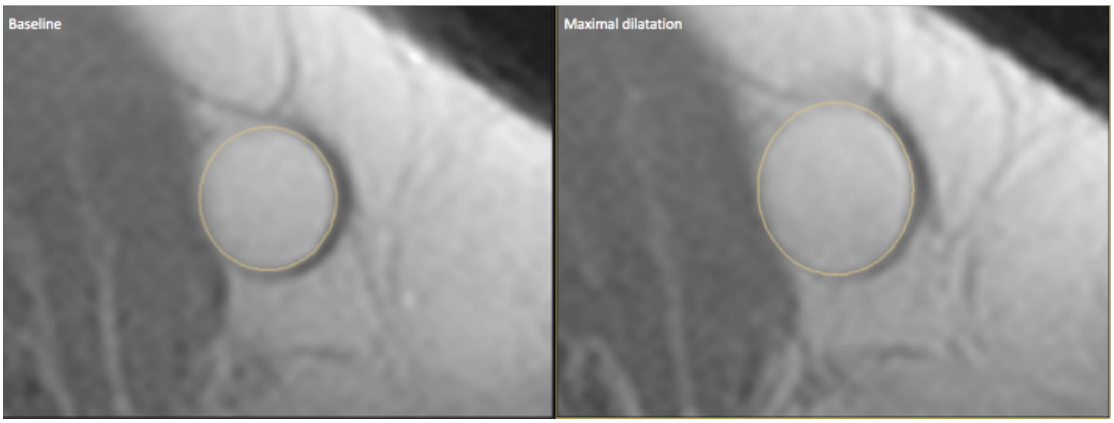
Imaging Protocol

Brachial artery reactivity (BAR), to assess FMD, was carried out using a previously validated CMR protocol [Sorenson 2002]. A small loop surface coil was placed over the right brachial artery. To measure endothelium dependent reactivity, the artery was occluded at the forearm distal to the coil, by inflating a blood pressure cuff to 20mmHg above systolic pressure. The artery was scanned immediately and at one-minute intervals for five minutes on cuff deflation. A single slice TruFISP sequence was used. Sequence parameters were: FoV 70mm read and 70mm phase, TE 4.2ms, TR 246ms, bandwidth 268 Hz/pixel, slice thickness 5mm, 1 average. Non-endothelium dependent reactivity was then measured - 400μg sublingual GTN was given and the artery scanned immediately and at 1-minute intervals until maximal dilatation had taken place.

Image Analysis

Analysis of the brachial images was carried out by contouring around the internal lumen at baseline and maximal dilatation for both endothelium-dependent and independent dilatation (Figure 7.5). The CMRtools program automatically calculated the area and the FMD was expressed as the percentage change in area.

Figure 7.5 FMD analysis. The brachial artery lumen is contoured at baseline and at maximal dilatation.



7.3 Assessment of cardiac ventricular volumes, function and mass

CMR is the gold-standard technique for assessing ventricular volume, function and mass. A full three-dimensional dataset can be acquired, and image acquisition is not limited by anatomical features, cardiac orientation or imaging 'windows' as occurs with echocardiography. No geometrical assumptions are made as there is no need to extrapolate from one and two-dimensional data, reducing the possibility and magnitude of measurement errors.

Imaging Protocol

A standard CMR protocol was performed for the cardiac study using an eight-element phased array receiver coil with the heart in the isocentre of the magnet. Initial rapid pilot scans, to optimise subject position in the magnetic field, were obtained using a breath-hold in the standard orthogonal planes (axial, sagittal, coronal). HASTE (half-Fourier acquisition turbo spin-echo) images were then acquired in the orthogonal axial, sagittal and coronal planes. These free-breathing, sequences result in single-frame, black blood images which are useful for rapid morphological assessment of the heart and surrounding structures. Using these low-resolution FSE images a two-chamber pilot view was obtained, followed by four perpendicular short-axis pilot views. The mitral valve and left ventricular apex were identified from the pilot images allowing balanced steady-state free precession cine images to be acquired in the vertical long axis (two-chamber), horizontal long axis (four-chamber), left ventricular outflow tract and right ventricular outflow tract planes during expiratory breath-hold using ECG-gating. A contiguous short-axis stack was obtained from the ventricular base to the apex, imaging parallel to the atrioventricular groove [Kramer 2008]. Cine images were acquired every 1cm and sequence parameters were: in-plane resolution 1.4 x 1.8mm, slice thickness 8mm, and temporal resolution 50ms (Figure 7.6).

At the baseline study, late gadolinium enhancement images (long-axis planes and short-axis stack) were obtained approximately 10 minutes after an intravenous injection of gadolinium contrast (Gadovist, Bayer-Schering, Berlin, Germany, 0.1mmol/kg) was given. An ECG-gated expiratory breath-hold inversion recovery prepared segmented turbo-fast low angle shot gradient echo sequence was used. These images were repeated in an orthogonal phase encoding direction to exclude artefacts. The inversion time was optimised in all cases to null the normal myocardium (typically 320-440ms).

Figure 7.6 Two-chamber (a) and four-chamber (b) images showing planning for short axis stack parallel to the atrioventricular groove (c).

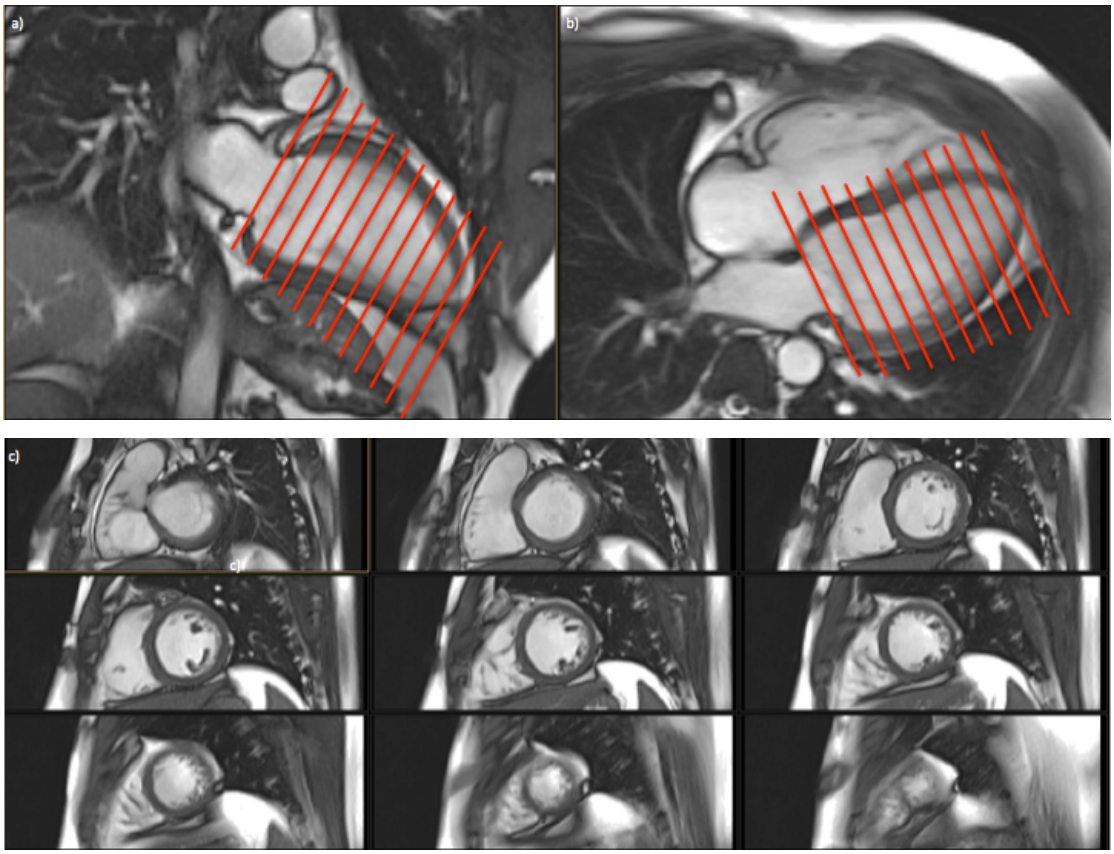


Image Analysis

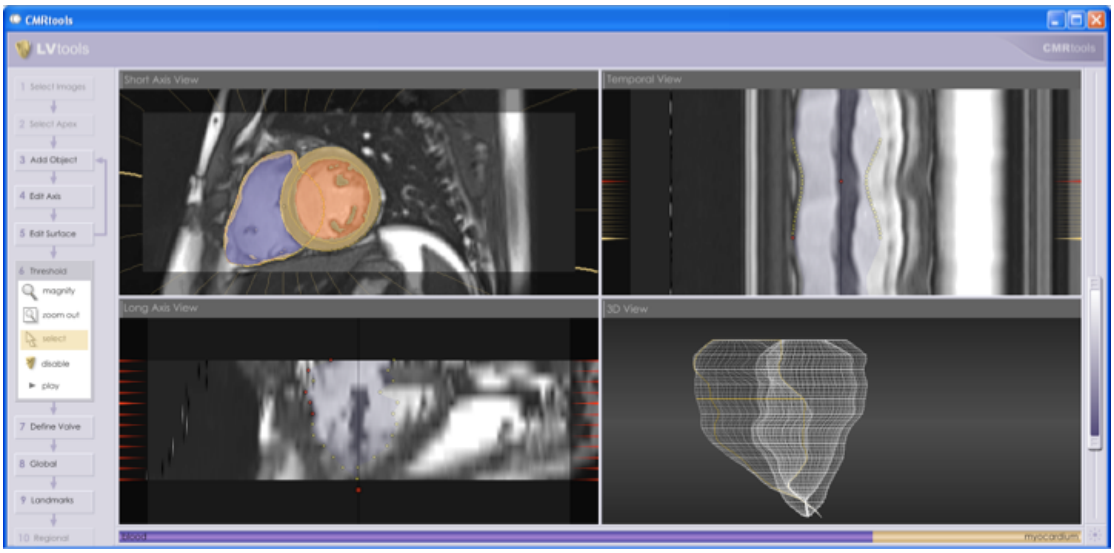
Cardiac image analysis was performed using LVtools (a plug-in of CMRtools, Cardiovascular Imaging Solutions, London). Left and right ventricular volumes (end-diastolic volume, end-systolic volume, stroke volume, and ejection fraction) and LV mass were determined after contouring of the epicardial and endocardial borders. The LVtools software allows for a semi-automated tracing of the epicardial and endocardial borders by placing points at anatomical boundaries within the images.

Intensity-based thresholding is then used to define the blood pool. Signal intensity is used to define individual voxels as blood or myocardium and the threshold altered until appearances correlate with visual assessment. Papillary muscles and trabeculations are included in the myocardial volume rather than in the blood pool volume. Using the long-axis views, the mitral and aortic valve planes can be defined and tracked throughout the cardiac cycle, so long-axis motion of the heart is taken into account in the calculation of the ventricular indices.

Semi-automated tracing of the epicardial and endocardial borders and myocardial thresholding were carried out for each short-axis image slice (Figure 7.7), and the slices

summated to give total blood and heart volumes at end-diastole and end-systole. Subtraction of the total blood volume from the total heart volume gave the total myocardial tissue volume. Myocardial mass was determined using the density of myocardium (1.05g/cm^3) at end-diastole. Ventricular volumes and mass were then indexed to body surface area. Visual assessment was made of the presence and pattern of late gadolinium enhancement.

Figure 7.7 LV and RV analysis using CMRtools showing semi-automated tracing of the epicardial and endocardial borders, and myocardial thresholding (top left).



Chapter 8
Cardiac and vascular findings in systemic lupus erythematosus by CMR

8.1 Introduction

Systemic lupus erythematosus (SLE) is a chronic multisystem inflammatory autoimmune disease, with a significant excess of CVD [Manzi 1997; El-Magadmi 2004; D'Cruz 2007]. It is associated with premature atherosclerosis. There is an increased prevalence of impaired vascular function (endothelial dysfunction and arterial stiffness) [El-Magadmi 2004; Lima 2002] as well as carotid plaque and increased C-IMT on ultrasound studies [Manzi 1999; Roman 2003; Kao 2013]. It has also been found to be associated with increased left ventricular ejection fraction and mass due to left ventricular hypertrophy on echocardiography [Pieretti 2007].

Atherosclerotic plaque and changes in C-IMT are both associated with increased CVD event risk and are used as surrogates for CVD [Chambless 1997; Roman 2006; Belcaro 1996; Kao 2013]. However, they do not necessarily co-exist and one does not precede the other, indicating that different mechanisms are involved in their development. Plaque and increased C-IMT can be focal or diffuse, and they are typically assessed using ultrasound to obtain a one-dimensional measure, with different centres examining varying segments of the carotid artery. This may result in diseased regions of the carotid being missed. CMR overcomes these limitations by allowing a long three-dimensional segment of the carotid artery to be imaged and measured. This increases the likelihood that focal plaque or localised increased C-IMT will not be missed. CMR also allows endothelial function (by FMD) and vascular stiffness to be assessed. Cardiac CMR provides an accurate measurement of ventricular volume, function and mass, and uniquely enables assessment of the myocardium for the presence of fibrosis or scarring due to previous inflammation or infarction. Cardiac CMR studies have focused predominantly on the presence of myocardial fibrosis in SLE patients with myocarditis [Mavrogeni 2013] and with a history of typical and atypical cardiac symptoms [Mavrogeni 2016], while also looking at a non-selected cohort [Seneviratne 2016]. These studies have shown a significant prevalence of myocardial fibrosis, predominantly mid-wall, associated with increased age but not necessarily SLE duration and consistent with possible previous myocardial inflammation. Subendocardial fibrosis consistent with myocardial infarction was also seen, as expected, in patients with known CAD as well as a proportion of SLE patients with cardiac symptoms but no known CVD.

Although there is a lower threshold for investigating CVD in SLE patients due to the magnitude of increased risk and physician awareness, the routine investigation of asymptomatic patients is not undertaken. CMR is unique in enabling assessment of cardiac and vascular health in one comprehensive study, and as far as we are aware, this is the first such CMR study in an asymptomatic and predominantly low CVD risk SLE group.

8.2 Methods

8.2.1 Patient Population

Forty-one female patients, aged 18 to 80 years inclusive, with a diagnosis of SLE by American College of Rheumatology (ACR) criteria [Tan 1982], were recruited from four London centres - Imperial College Healthcare NHS Trust (Hammersmith, Charing Cross and St Mary's Hospitals), and London Northwest Healthcare NHS Trust (Northwick Park Hospital). Eleven patients were initially recruited and scanned by Dr Niall Keenan in a pilot study as part of his MD thesis, and a further thirty patients were subsequently recruited, scanned and analysed by me and the data pooled. Patient history was taken and physical examination and ECG performed. Disease activity and damage were assessed using the Systemic Lupus Erythematosus Disease Activity Index SELENA Modification (SLEDAI) [Bombardier 1992] and the Systemic Lupus International Collaborating Clinics/ACR Damage Index (SLICC/ACR) respectively [Gladman 1996b]. The SLE group was compared against two populations of normal female volunteers recruited in previous studies by members of our research group. Both these populations had been recruited through an advertising campaign and screened with a health questionnaire, physical examination, blood tests and ECG. Any volunteers with an elevated cardiac risk score or CVD risk factors, including hypertension, hypercholesterolaemia, or diabetes, or who had an abnormal ECG, were excluded from the studies. Fifty normal volunteers underwent CMR carotid artery wall imaging [Keenan 2009a], and sixty normal volunteers underwent CMR for LV and RV structure and function (without gadolinium contrast) [Maceira 2006a; Maceira 2006b]. All patients gave informed written consent. The hospital research ethics committee approved the study.

8.2.2 CMR protocol

All carotid artery studies were performed on dedicated 1.5 Tesla scanners (Siemens Avanto or Sonata, Erlangen, Germany) as described in Sections 7.1.2 Imaging Protocol and 7.1.3, Imaging Protocol. In summary, a contiguous stack of 20 high-resolution T1-weighted FSE images, centred on the carotid bifurcation bilaterally, was acquired approximately perpendicular to the longitudinal axis of both common carotid arteries giving a 40 mm of longitudinal coverage per artery. All images were analysed off-line using Atheroma Tools, a plug-in of CMRtools software (Cardiovascular Imaging Solutions, London), as described in

Sections 7.1.2 Image Analysis and 7.1.3 Image Analysis. A visual assessment was made for the presence or absence of atherosclerotic plaque.

Cardiac studies were performed using a standard CMR protocol (see Section 7.3, Imaging Protocol). In summary, a contiguous short-axis stack of cine images was acquired every 1cm from the ventricular base to the apex, imaging parallel to the atrioventricular groove [Kramer 2008]. Late gadolinium enhancement (LGE) images (long-axis planes and short-axis stack) were obtained approximately 10 minutes after an intravenous injection of gadolinium contrast (Gadovist, Bayer-Schering, Berlin, Germany, 0.1mmol/kg) was given. Cardiac image analysis was performed using LVtools (a plug-in of CMRtools, Cardiovascular Imaging Solutions, London) as described in Section 7.3, Image Analysis. Left and right ventricular volumes (end-diastolic volume, end-systolic volume, stroke volume, and ejection fraction) and LV mass were obtained by contouring of the epicardial and endocardial borders. Cardiac parameters were indexed to body surface area (BSA). Visual assessment was made of the presence and pattern of LGE.

Assessment of endothelial function was carried out by brachial artery reactivity (to assess FMD) as described in Section 7.2. The internal brachial artery lumen at baseline and maximal dilatation were contoured for both endothelium dependent and independent dilatation. CMRtools automatically calculated the area and FMD was expressed as the percentage change in area. Post-menopausal females and females menstruating at the time of their scan underwent the BAR scan. Pre-menopausal females not menstruating at the time of the scan did not undergo the BAR scan, as significant fluctuations occur with hormonal changes during the menstrual cycle [Hashimoto 1995] and most were part of the SLE RCT (Chapter 9) which required serial FMD assessments. FMD changes in the menstrual phase are comparable to changes seen in male subjects [Hashimoto 1995], allowing comparisons to be made. Results were compared to a historical normal control cohort [Wiesmann 2004].

8.2.3 Statistical methods

Descriptive statistics were performed on baseline population data and the populations compared. Unpaired t-tests were performed to compare data between the patient groups. A multivariate regression analysis was performed to assess for the strength of association between the carotid artery wall/outer wall (W/OW) ratio in SLE and CVD risk factors. A Univariate analysis was performed to assess for predictors of SLE. For carotid artery wall volume and W/OW, age-adjusted Z-scores and 95% reference ranges were derived for the normal and SLE populations and the results compared. A Z-score is a statistical measurement of a score's relationship to the mean of a normally distributed group of scores.

A Z-score of 0 indicates the score is the same as the mean, and Z-scores of +1 or -1 indicate one standard deviation above or below the mean. Descriptive statistics were derived for the presence of plaque and LGE.

8.3 Results

8.3.1 Patient Characteristics

Baseline characteristics for SLE patients and both groups of normal controls are shown in Table 8.1. There was no significant difference in age between the groups. The SLE group had had a diagnosis of SLE made on average 15.5 years previously. Three patients (7%) had known cerebrovascular disease and one (2%) had known coronary artery disease. Sixteen (39%) were known or found to be hypertensive, six (15%) had hypercholesterolaemia, one (2%) was diabetic and eight (19%) were current smokers. Seven (17%) were on lipid-lowering treatment with a statin and eleven (27%) were on an antihypertensive. The SLE group was significantly heavier with a higher body mass index (BMI) than the control groups, and had a significantly higher heart rate. Blood pressure was also increased compared to the controls although this was only significant for systolic blood pressure when compared to the normal carotid group and for diastolic blood pressure when compared to the normal cardiac group; diastolic blood pressure was also elevated compared to the normal carotid group but did not reach significance. Twenty-eight (68%) of the SLE patients were on corticosteroids, which may account for the increased BMI in this group. Thirty-two patients were taking an additional disease-modifying drug: 66% hydroxychloroquine, 17% azathioprine, 15% mycophenolate and 5% methotrexate. The average SLEDAI score was 3.2 indicating low disease activity; no patients were suffering a disease flare at the time of participation in the study. All patients completed the full carotid and cardiac CMR protocol except for two who declined gadolinium contrast and in whom no LGE images were acquired. Twenty-four (59%) of the SLE patients underwent endothelial function assessment by FMD of the brachial artery – the rest either declined due to discomfort having already undergone carotid and cardiac scanning, or were not in a suitable phase of their menstrual cycle to allow for meaningful repeat assessment as part of the SLE RCT (see Chapter 9) [Hashimoto 1995].

8.3.2 Carotid CMR

Atherosclerotic plaque (Figure 8.1) was identified in 18 (44%) of SLE patients with a further 9 (21%) having areas of focal carotid vessel wall thickening, giving a total of 29 (71%) with evidence of subclinical atherosclerosis. Multicontrast CMR of the plaques identified that 7 (39%) were predominantly calcified, 5 (28%) were predominantly fibrous of which 1 had a very small lipid core, and none comprised predominantly a large lipid core; plaque

composition was not available for 6 of the SLE patients identified as having atherosclerotic plaque.

Volumetric analysis of the 40mm longitudinal sections of the carotid arteries scanned showed that the carotid artery was significantly thicker in SLE patients compared to normal controls (Table 8.2) – wall volume was 12% greater than in normal (p=0.006), and W/OW was 5% greater (p=0.02). In 6 (15%) of SLE patients, W/OW ratio was greater than the normal range (Figure 8.2). The SLE patients' regression lines for the wall volume and W/OW ratio were above those for the normal control group, although only slightly so. There were no significant differences in either total vessel or lumen volumes compared to normal controls. There was also no significant difference in carotid artery distensibility although values were lower, as would be expected in the presence of arterial wall thickening and atherosclerosis, in the SLE patient group. Multivariate regression analysis showed that hypertension and diabetes were significantly associated with increased W/OW, but corticosteroid use and current smoking was not (Table 8.3).

8.3.3 Cardiac CMR

Ventricular parameters

Ventricular parameters are shown in Table 8.4. Left and right ventricular volumes were significantly smaller in SLE patients, particularly end systolic volumes, and this is reflected in the significantly higher ejection fraction seen in the SLE group. Ventricular volumes indexed to BSA were also significantly smaller in the SLE patients. There was no significant difference in left ventricular mass.

LGE

LGE, indicating myocardial fibrosis, was seen in seven (17%) of the SLE patients. In three patients (7% of the SLE patient cohort) the pattern seen suggested previous, unrecognised, myocardial infarction – LGE was transmural with associated thrombus in one; the other two were subendocardial (Figure 8.3). None was know to have coronary artery disease. Three patients had midwall and one patient subepicardial fibrosis, patterns consistent with previous myocarditis (10% of the SLE patient cohort). Gadolinium was not administered to the historic normal cohort, so the presence or otherwise of myocardial fibrosis in that cohort is unknown.

8.3.4 Endothelial function

Mean endothelium-dependent dilatation (FMD) of the brachial artery was significantly reduced in SLE patients compared to normal historical controls (6.3% vs. 15.5%, p=0.02),

indicating significant endothelial dysfunction. Endothelium-independent vasodilatation in response to GTN was similar between the two groups (Table 8.5).

Table 8.1. Baseline characteristics of patients studied. Results are shown as mean (95% confidence interval) for continuous variables or numbers (%) for categorical variables.

		SLE (n=41)	Normals - carotids (n=50)	p	Normals - cardiac (n=60)	p
Age (years)		48.6 (44.5, 52.7)	44.3 (40.2, 48.4)	0.14	49.1 (44.9, 53.3)	0.87
Race	White	21 (51)	48 (96)	**<0.001**		
	Afrocaribbean/Black	10 (24)	1 (2)	**0.001**		
	Asian	5 (12)	1 (2)	0.05		
	Mixed	1 (2)	0 (0)	0.27		
	Not recorded	4 (10)	0 (0)	0.02	60	
Heart rate (bpm)		74.1 (70.3, 77.9)	67.2 (64.4, 70.0)	**0.003**	66.1 (63.5, 66.7)	**0.0006**
Systolic blood pressure (mmHg)		126.9 (121.6, 132.2)	117.4 (114.1, 120.6)	**0.003**	122.3 (118.4, 126.3)	0.16
Diastolic blood pressure (mmHg)		76.8 (72.8, 80.8)	72.8 (71.0, 74.7)	0.08	71.8 (69.7, 74.0)	**0.03**
Body mass index (kg/m^2)		26.2 (24.3, 28.1)	22.9 (22.3, 23.5)	**0.006**	23.9 (22.7, 25.1)	**0.03**
Body surface area (m^2)		1.71 (1.66, 1.76)	1.71 (1.67, 1.75)	0.98	1.71 (1.68, 1.75)	0.92
Years since SLE diagnosis		15.5 (12.41, 18.6)	N/A		N/A	
SLEDAI		3.2 (2.43, 4.02)	N/A		N/A	
SLICC		0.77 (0.46, 1.08)	N/A		N/A	
Cerebrovascular disease		3 (7)	None		None	
Coronary artery disease		1 (2)	None		None	
Hypertension		16 (39)	None		None	
Diabetes mellitus		1 (2)	None		None	
Hypercholesterolaemia		6 (15)	None		None	
Current smoker		8 (19)	None		None	
Current treatment						
Corticosteroids		28 (68)	N/A		N/A	
Azathioprine		7 (17)	N/A		N/A	
Methotrexate		2 (5)	N/A		N/A	
Hydroxychloroquine		27 (66)	N/A		N/A	
Mycophenolate mofetil		6 (15)	N/A		N/A	
Statins		7 (17)	None		None	
Antihypertensive		11 (27)	None		None	

SLE disease duration not recorded for 2 patients.

Figure 8.1. T1-weighted transaxial CMR images of the common carotid artery showing (a) a normal volunteer with a thin and smooth vessel wall; (b) an SLE patient with arterial wall thickening (white arrow); (c) an SLE patient with atherosclerotic plaque – images are (from left-to-right) T1-weighted, T2-weighted and proton density weighted. A fibrous cap (red arrow) and underlying calcification (star) is seen.

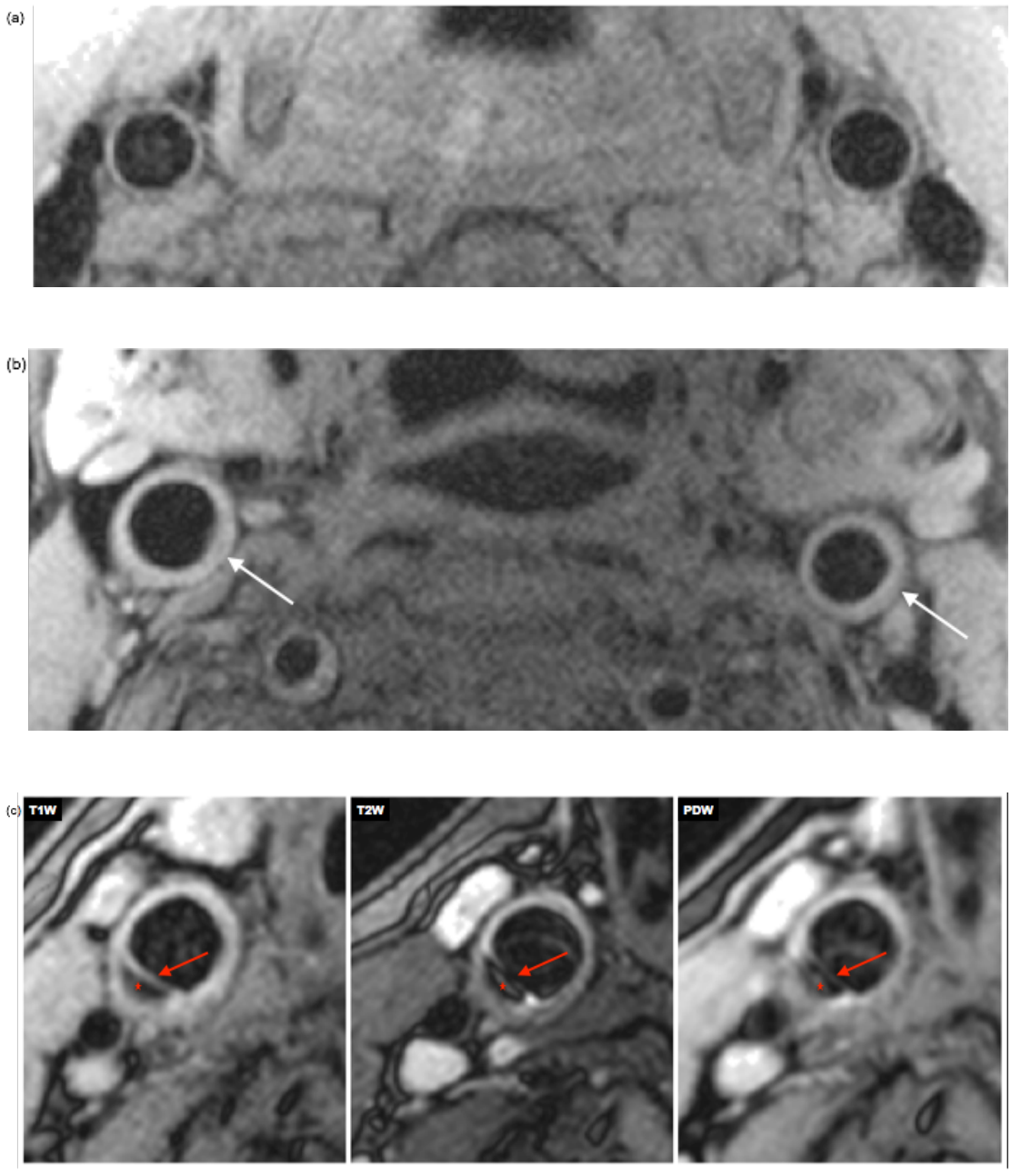


Table 8.2. Carotid CMR measurements in SLE and control subjects.

	SLE (n=41)	**Normals - carotids (n=50)**	**p**
Lumen Volume (mm^3)	1456.8 (1361.1, 1552.5)	1397.6 (1324.0, 1471.3)	0.32
Wall Volume (mm^3)	716.3 (666.7, 765.8)	639.8 (611.2, 668.4)	**0.006**
Total Vessel Volume (mm^3)	2173.1 (2040.9, 2305.3)	2037.5 (1938.8, 2136.2)	0.095
W/OW Ratio (%)	33.0 (31.8, 34.2)	31.5 (30.9, 32.1)	**0.02**
Distensibility (%)	21.8 (19.4, 24.3)	22.8 (21.0, 24.6)	0.49

Values are mean (95% confidence interval). Significant values are shown in bold text.

Figure 8.2. Mean carotid artery wall volume and W/OW ratio. (a) The regression lines (red and blue) represent the mean and 95% confidence intervals respectively for the normal control group; the black regression line represents the mean for the study population. (b) Box plots of age- and sex-matched Z-scores derived from the normal control group.

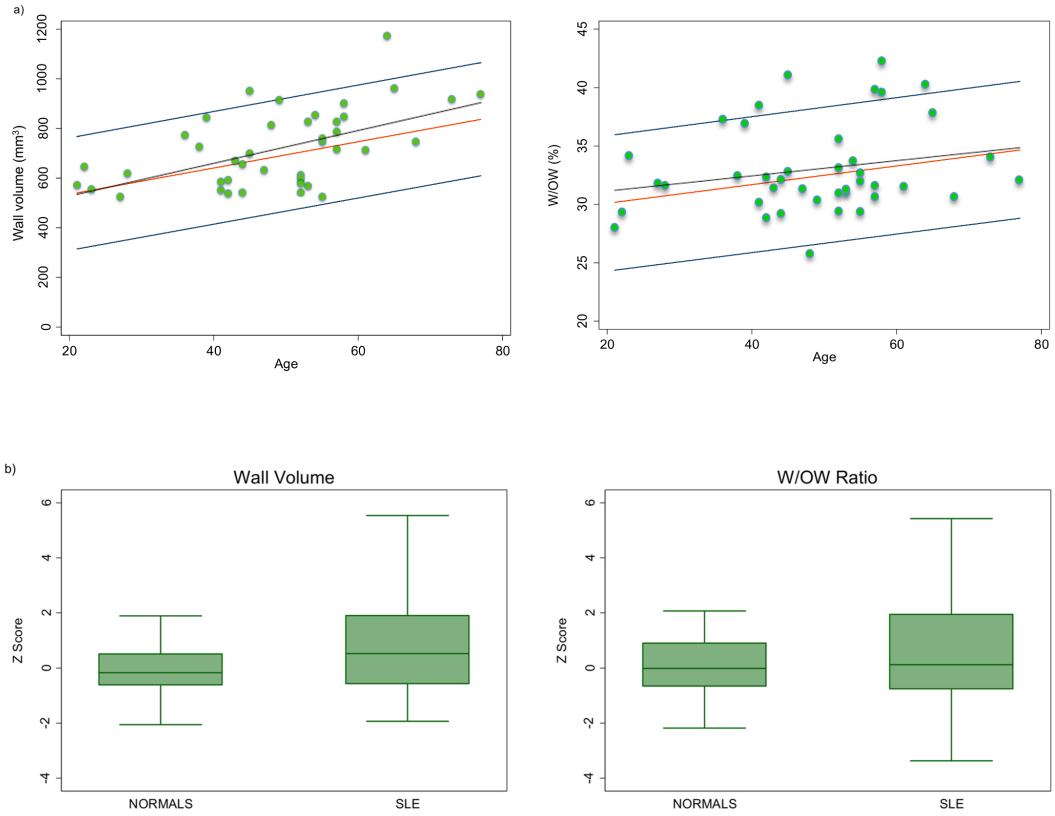


Table 8.3. Multivariate regression analysis showing the strength of association between W/OW ratio and CVD risk factors in the SLE group.

Variable	**Coefficient (95% CI)**	**p**	**Adjusted Coefficient (95% CI)**	**p**
Hypertension	3.18 (0.85, 5.50)	0.009	3.50 (1.24, 5.77)	**0.004**
Diabetes	9.59 (2.50, 16.68)	0.009	10.79 (4.08, 17.50)	**0.003**
Current smoker	0.26 (-2.70, 3.23)	0.86	0.24 (-2.43, 2.90)	0.86
Steroid use	1.09 (-1.62, 3.80)	0.42	-0.23 (-2.63, 2.16)	0.85

Table 8.4. Left and right ventricular parameters for SLE patients and normal controls. Absolute values are given; measures of ventricular volume and left ventricular mass are also given indexed to body surface area (BSA).

	SLE (n=41)	**Normals - cardiac (n=60)**	**p**
LVEDV (ml)	112.2 (115.2, 119.2)	123.8 (118.3, 129.3)	**0.01**
LVESV (ml)	31.8 (28.5, 35.0)	37.8 (35.3, 40.2)	**0.003**
LVSV (ml)	80.4 (75.4, 85.4)	86.1 (82.3, 89.8)	0.07
LVEF (%)	71.9 (69.9, 73.9)	69.7 (68.5, 70.8)	**0.04**
LV mass (g)	104.7 (97.2, 112.1)	107.7 (103.0, 112.4)	0.47
LVEDV/BSA (ml/m^2)	65.8 (61.9, 69.6)	72.2 (69.6, 74.8)	**0.005**
LVESV/BSA (ml/m^2)	18.8 (16.8, 20.7)	22.0 (20.7, 23.3)	**0.005**
LV mass/BSA (g/m^2)	61.1 (57.4, 64.8)	62.7 (60.7, 64.6)	0.41
RVEDV (ml)	112.9 (105.2, 120.6)	124.9 (118.8, 130.9)	**0.02**
RVESV (ml)	33.0 (29.1, 36.9)	42.2 (38.7, 45.6)	**0.002**
RVSV (ml)	79.9 (75.1, 84.7)	82.7 (79.1, 86.3)	0.37
RVEF (%)	71.3 (69.3, 73.2)	66.7 (65.0, 68.3)	**0.0008**
RVEDV/BSA (ml/m^2)	65.5 (60.6, 70.3)	72.8 (69.9, 75.7)	**0.007**
RVESV/BSA (ml/m^2)	20.6 (17.8, 23.8)	24.6 (22.7, 26.4)	**0.02**

Values are mean (95%confidence interval). LV = left ventricle; RV = right ventricle; EDV = end diastolic volume; ESV = end systolic volume; SV = stroke volume; EF = ejection fraction.

Figure 8.3. GE images from SLE patients – (a) and (b) show early gadolinium enhancement; all other images are LGE. (a) and (b) Mural thrombus at the cardiac apex. (c) and (d) Transmural fibrosis indicating a full thickness myocardial infarction. (e) and (f) subendocardial fibrosis indication a subendocardial infarction [Keenan 2010].

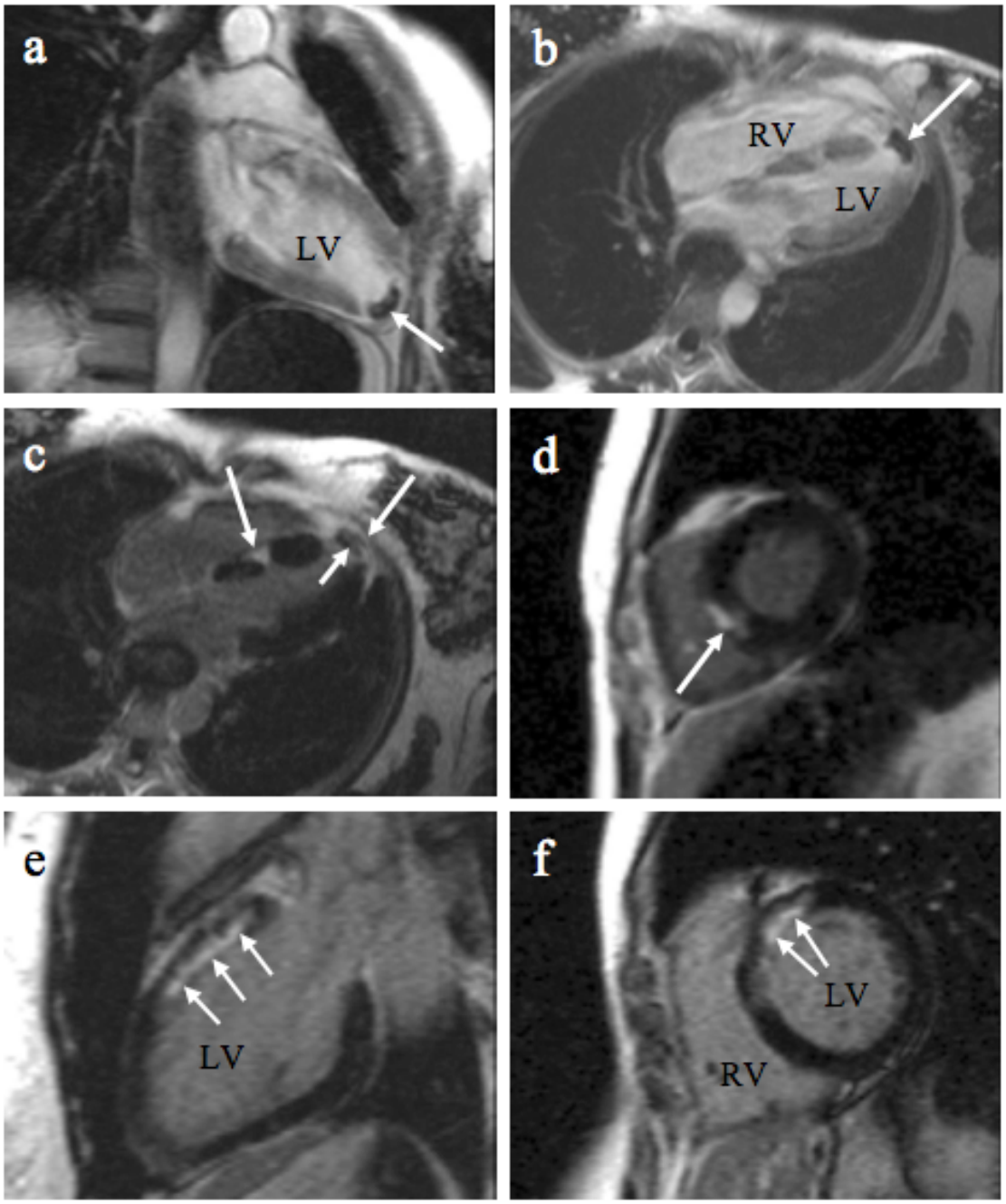


Table 8.5. Endothelium dependent and independent dilatation of the brachial artery - % change in area.

	SLE (n=24)	**Normal controls (n=12)**	**p**
Endothelium-dependent dilatation (%) [FMD]	6.3 (1.31, 11.3)	15.5 (11.6, 19.4)	**0.02**
Endothelium-independent dilatation (%) [GTN]	48.2 (36.8, 59.5)	57.0 (42.4, 71.6)	0.34

8.4 Discussion

Despite the reduced mortality from CVD seen recently in the general population [Mozaffarian 2015], deaths from CVD have not decreased amongst SLE patients and account for up to 48% of all deaths [Gustafsson 2012]. Previous studies have reported a high frequency of vascular dysfunction and premature atherosclerosis and this study confirms this, identifying carotid arterial wall thickening, a high prevalence of carotid plaque and endothelial dysfunction, as well as the presence of previously unrecognised cardiac pathology, in one single attendance at a CMR unit.

The carotid artery wall volume and W/OW ratio are increased in SLE patients without a decrease in lumen size. This is consistent with the outward remodelling seen in the early stages of atherosclerosis [Glagov 1987] and can only therefore be visualised with imaging of the whole vessel, not just the lumen as occurs in angiography. To our knowledge, this is the first study looking at arterial wall assessment in SLE patients. Previous studies of C-IMT by ultrasound have shown conflicting results on whether arterial wall is thickened in SLE. C-IMT was increased in SLE patients with known CVD, but not in those without known CVD [Svenungsson 2001]; increased in SLE patients with no overt CVD compared to controls [Shang 2008]; but decreased compared to controls in another study [Roman 2003]. Increased C-IMT in SLE patients, however, has been associated with an increased risk for cardiovascular events (HR 1.35) [Kao 2013]. We have found a 49% prevalence rate of carotid plaque which is consistent with previous ultrasound studies in which carotid plaques have been found in 30-43% amongst SLE cohorts [Manzi 1999; Roman 2003; Thompson 2008; Anania 2010; Kao 2013], despite a significant proportion of our cohort having low CVD risk by traditional risk scoring. Only three patients with carotid plaque were known to have CVD. Of those with known low CVD risk, 5/38 (13%) had carotid plaque present. None of our normal control group, who were selected to have no history of CVD, no CVD risk factors and a low CVD risk score, had carotid plaque. In SLE, as in the general population, carotid plaque has been found to be strongly predictive of cardiovascular events [Roman 2006; Belcaro 1996; Kao 2013].

CMR arterial wall assessment is a different technique to ultrasound (US) and measures arterial adventitia as well as the endothelial and medial layers. The adventitia cannot usually be distinguished clearly on CMR, but it has been shown that measurements correlate well with measurements of C-IMT [Mani 2006]. It can overcome many of the limitations of C-IMT: variability of measurement site, near field artifacts, and problems related to ‘imaging windows’. CMR is also a three-dimensional technique and the vast majority of C-IMT studies to date have been one-dimensional. The absolute values, and techniques cannot therefore

be directly compared between studies, but principles and findings can be applied. In our cohort, consisting predominantly of young SLE patients with a low CVD risk, the carotid arterial wall is significantly thickened compared to the normal age- and sex- matched control group.

The earliest changes associated with impaired vascular function and atherosclerosis include endothelial function assessed by FMD and measures of arterial stiffness, both of which are associated with risk factors for atherosclerosis and with an increase in cardiovascular events [Celermajer 1992; Suwaidi 2000; Roman 2005]. We have found that CMR is able to identify significantly impaired endothelial function in SLE patients; arterial stiffness was increased compared to normal controls, but not significantly so. This is another way in which increased cardiovascular risk can be identified, used to risk stratify and assess treatment efficacy in SLE patients, as endothelial dysfunction and arterial stiffness can be reversible [Parker 2014]. The results are consistent with those obtained by ultrasound studies where both endothelial function and arterial distensibility have been found to be abnormal in SLE cohorts even in patients with low CVD risk [Lima 2002; El-Magadmi 2004; Roman 2005; Shang 2008; Wang 2014].

The presence of hypertension and diabetes, both known CVD risk factors, were independently associated with increased W/OW ratio in our SLE cohort. Interestingly, current steroid use was not, despite being taken by 68% of the SLE patients. Corticosteroid use is a surrogate for disease activity and therefore inflammation in SLE, which itself can increase the risk of atherosclerosis. Corticosteroids increase the risk of hypertension, dyslipidaemia and diabetes, all of which are CVD risk factors. Corticosteroids also lead to weight gain, as seen in our cohort, which may reduce physical activity beyond that due to SLE symptoms, further compounding the risk of hypertension, impaired glucose tolerance and dyslipidaemia. They are however atheroprotective by reducing inflammation. Our findings are consistent with previous studies where the risk of atherosclerosis has been seen with increased duration of steroid use, but not with current treatment, average daily dose or the use of pulsed corticosteroid therapy [Petri 1992; Roman 2003]. Acute CVD events have been associated with current corticosteroid use, even after adjustment for disease activity, suggesting that corticosteroids may only have a short-term effect on CVD risk [Magder 2012], possibly in those with established atherosclerosis, but not necessarily increasing the risk of developing atherosclerosis when used short-term. We did not have information on corticosteroid therapy duration in our SLE cohort.

Similar to previous echocardiography studies of SLE patients [Pieretti 2007; Chow 2007], we found a significantly higher ejection fraction in the SLE cohort. There was however no increase in left ventricular mass as has been observed previously. This may reflect the greater accuracy of CMR in measuring LV myocardial mass from a stack of slices covering the entire ventricle compared with echocardiography were only one-dimensional measures of the basal septum and posterior wall are taken and the mass calculated using certain geometric assumptions, ignoring wall thickness at other sites, and the longitudinal dimension of the ventricle.

Myocardial fibrosis was seen in 17% of our SLE cohort. In three the pattern seen suggested previous myocardial infarction, despite there being no known history of coronary artery disease. A recent CMR study of an unselected cohort of adult SLE patients identified myocardial fibrosis in 37% of patients [Seneviratne 2016], however, only one of these was consistent with myocardial infarction and occurred in a patient with known CVD who had previously undergone coronary artery bypass grafting and coronary stenting. The other patterns of myocardial fibrosis were consistent with previous myocardial inflammation and 24% of patients in that study were known to have had a clinical history of pericarditis. This contrasts with our current study where only 10% had findings consistent with previous myocarditis.

The current study includes two groups of SLE patients, the first un-selected for CVD risk (recruited and investigated by Dr Niall Keenan), and a second larger group of low CVD-risk SLE patients recruited as part of a randomised control trial (see Chapter 9). If this second group is excluded, the prevalence of 'silent' coronary artery disease in the unselected group is 18%, suggesting a possible significant undetected burden of coronary artery disease amongst SLE patients. This echoes findings using other imaging techniques such as electron beam-CT (EBCT) where a high prevalence of coronary artery calcification in SLE patients compared with controls has been found [Asanuma 2003; Chung 2006; Kao 2008], and single photon emission computed tomography (SPECT) where approximately one-third of women with SLE and no history of coronary artery disease have been shown to have abnormalities of myocardial perfusion [Bruce 2000; Sella 2003].

8.4.1 Study limitations

This is a relatively small cross-sectional study involving two phases of recruitment with slightly different criteria – the first eleven patients were an 'all-comer' SLE cohort ranging from those with known atherosclerosis to a few low-risk individuals, whereas the second phase comprised a mainly low traditional CVD risk SLE group, where none had known

atherosclerosis. The presence and magnitude of CVD may therefore be lower than that which may be present in the SLE population at large. The study does not include male patients, who may have a different CVD risk profile, and the study may therefore not be applicable to male SLE patients.

There was a mean age difference between the normal historic cohort and the SLE cohort, with the latter being 4.3 years older. This did not reach statistical significance, but as carotid wall volume and W/OW is known to increase with age [Keenan 2009a], age differences may have influenced the observed results and be of clinical significance. It would have been useful to include age in the multivariate analysis to estimate its contribution to the increased W/OW in the SLE cohort and to compare this with the contribution of aging to increased W/OW the normal historic cohort.

Systolic blood pressure was also significantly increased in the SLE cohort compared to the normal cohort. As C-IMT has been shown to increase with systolic blood pressure [Tavil 2007], possibly as a result of increased mechanical stress, wall volume by CMR would therefore be expected to increase as well. Indeed, hypertension was positively associated with W/OW in our study, which may at least in part account for the higher wall volume and W/OW seen in the SLE cohort.

8.5 Conclusion

Our CMR study confirms the presence of early atherosclerosis in SLE assessed by a combination of endothelial dysfunction, increased arterial stiffness as well as increased carotid arterial plaque and wall thickness. It also demonstrates the existence of significant 'silent' cardiac disease in those with no history of cardiac symptoms. In many of these patients, the only evidence of atherosclerosis was the presence of an abnormal carotid CMR, suggesting that CMR offers a way of detecting asymptomatic premature atherosclerosis in patients with SLE, improving risk stratification, and allowing targeted secondary prevention in those who have few if any traditional CVD risk factors. CMR also provides a number of reproducible end-points, such as arterial wall volume and W/OW, which can be used as surrogate end-points for CVD in clinical trials looking at the ability of therapies to reduce CVD risk in SLE populations. We therefore undertook a randomised controlled trial looking at the effect of rosuvastatin, a potent lipid-lowering agent, on carotid arterial wall parameters in SLE patients with no current indication for statin therapy (Chapter 9).

Chapter 9
A randomised placebo controlled trial of rosuvastatin in systemic lupus erythematosus

9.1 Introduction

Systemic lupus erythematosus (SLE) is a recognised independent risk factor for atherosclerosis and coronary artery disease (CAD). It is one of the strongest known risk factors for CAD with an incidence of myocardial infarction greater than 50 times that in the Framingham dataset, for women with SLE aged 35-44 years [Manzi 1997; El-Magadmi 2004]. A bimodal pattern of death in SLE was noted in 1976 with an early peak related to nephritis and sepsis and a second peak reflecting deaths related to premature myocardial infarction [Urowitz 1976]. Even after matching traditional cardiovascular risk factors, the risk of CAD in SLE is 7-fold higher than that of healthy controls [Esdaile 2001]. The relative risk of death from myocardial infarction of 17 [Esdaile 2001], suggests that SLE-specific risk factors and inflammation play a role [Svenungsson 2001; Ridker 2000]. The duration and severity of SLE disease activity correlates positively with CAD risk, consistent with the paradigm of atherosclerosis as a disease of vascular inflammation [Manzi 1997; Karp 2008; Ross 1999]. SLE has been associated with increased coronary-artery calcification on CT [Asanuma 2003], increased carotid intimal media thickness (C-IMT) on B-mode ultrasound [Svenungsson 2001], and carotid plaques [Roman 2003].

C-IMT is a surrogate for the presence of atherosclerosis throughout the arterial tree and has been shown to be predictive of cardiovascular events in populations with and without established cardiovascular disease [Lorenz 2007]. Cardiovascular magnetic resonance (CMR) of the carotid vessel wall can overcome many of the limitations of C-IMT, such as one-dimensionality, measurement site variability, and near field artefacts, and has been shown to correlate well with measurements of C-IMT [Mani 2006]. Constant resolution along the length of the artery can be achieved with CMR and 2D images combined into a three-dimensional model giving the wall volume for the length of artery studied. Reproducibility is good with interstudy coefficients of variation of 4.4% [Varghese 2005b], allowing for smaller sample size in clinical studies.

Statins significantly reduce cardiovascular morbidity and mortality in patients with hyperlipidaemia, diabetes or established CAD [Pedersen 1994; Shepherd 1995]. Importantly, in the JUPITER study rosuvastatin significantly reduced the incidence of major cardiovascular events in healthy individuals without hyperlipidaemia (LDL-C<3.4mmol/L) but

with elevated levels of C reactive protein measured by a high-sensitivity assay (hs-CRP) [Ridker 2008]. Statins reduce progression and induce the regression of atherosclerotic plaque, as assessed by angiography [Blankenhorn 1993], intravascular ultrasound [Nissen 2006], C-IMT measurements by ultrasound [Hodis 1996] and CMR [Corti 2001; Corti 2005; Migrino 2011]. In addition to potent reduction of LDL-cholesterol [Pedersen 1994; Shepherd 1995; Ridker 2008], statins exert immunomodulatory and anti-inflammatory effects. These include anti-oxidant actions [Bellosta 1998], and reduction of hs-CRP [Ridker 2008], nuclear factor-κB activity [Mihos 2012], inflammatory cytokines (e.g. TNF-α [Raza 2012], MCP-1 [Blanco-Colio 2007]) and ultimately leukocyte trans-endothelial migration [Maher 2009]. Statins may also increase fibrinolytic activity [Lefer 2001] and decrease tissue factor, thus reducing activation of the coagulation cascade [Lefer 2001; Bellosta 2000].

While statin therapy modulates biomarkers of inflammation, including surrogates of vascular risk, in rheumatoid arthritis [McCarey 2004] and neurological models of inflammation [Malfitano 2014], there are scant and equivocal data with regards to clinical outcomes. Indeed a recent study using atorvastatin versus placebo in SLE failed to show any benefit on disease activity, measures of inflammation, C-IMT or carotid plaque in the treatment group [Petri 2011]. Furthermore, patients with SLE were specifically excluded from the JUPITER study [Ridker 2008]. Despite this, the increased risk of CAD in the SLE population has resulted in statins becoming widely prescribed, even in those with mild disease and normolipidaemia. We therefore sought to investigate whether treatment with rosuvastatin, in stable SLE subjects without hyperlipidaemia and no other current indication for the use of statins, can retard the development of atherosclerosis as measured by CMR.

9.2 Methods

9.2.1 Patient population

Subjects were aged 18 to 80 years inclusive, male or female, with a diagnosis of SLE by American College of Rheumatology (ACR) criteria [Tan 1982; Hochberg 1997], no current indication for statins and a fasting LDL-C<3.4mmol/L. Women with childbearing potential were required to have used effective contraception for at least one month prior to screening, and advised to continue the same contraceptive method during the study and for 30 days after completion. Patients with raised creatine kinase (CK) or liver function tests (LFTs) were allowed to enrol if, in the opinion of the responsible rheumatologist, the test abnormality was minor and not a contraindication to the use of a statin. Exclusion criteria were known atherosclerotic vascular disease (ischaemic heart disease, cerebrovascular disease, peripheral vascular disease); current or previous statin therapy; renal dysfunction (estimated creatinine clearance < 60/ml/1.73/m^2); hyperlipidaemia (fasting LDL-C >3.4mmol/L); active

myositis or CK >150IU/L with a pathological cause; liver disease with LFTs >1.5 times the upper limit of normal; contraindications to CMR; pregnancy; breastfeeding; and treatment with cyclosporin A.

9.2.2 Study design

The study was a 2-year randomised double-blind, placebo-controlled trial of rosuvastatin 20mg versus matching placebo. Recruitment took place in four London centres - Imperial College Healthcare NHS Trust (Hammersmith, Charing Cross and St Mary's Hospitals), and London Northwest Healthcare NHS Trust (Northwick Park Hospital). CMR was performed at the Royal Brompton Hospital at baseline, 1 year and 2 years. CMR studies consisted of 2 or 3 parts. All patients underwent carotid artery and cardiac studies with some also undergoing a brachial artery reactivity (BAR) scan to assess flow-mediated dilatation (FMD) – see supplementary methods below. The Clinical Trials and Evaluation Unit at Royal Brompton Hospital carried out randomisation to treatment with rosuvastatin or placebo after the baseline CMR study. Subjects were followed up every three months in their usual rheumatology clinic, with a clinical examination and standard blood tests (including markers of inflammation [CRP, ESR] and disease activity [dsDNA, complement levels]). Disease activity and damage were assessed at baseline and quarterly using the Systemic Lupus Erythematosus Disease Activity Index SELENA Modification (SLEDAI) [Bombardier 1992] and the Systemic Lupus International Collaborating Clinics/ACR Damage Index (SLICC/ACR) respectively [Gladman 1996b]. Lipid profile was checked annually. An electrocardiograph (ECG) was performed at baseline. All patients provided written informed consent.

9.2.3 CMR protocol

All studies were performed on a 1.5 Tesla scanner (Siemens Avanto, Erlangen, Germany). A purpose-built bilateral four-channel phased array carotid surface coil (Machnet, Eelde, The Netherlands) with a specially designed head and neck cushion was used for carotid imaging. The CMR protocol is described in Sections 7.1.2 and 7.1.3, Imaging Protocols. Briefly, a contiguous stack of 20 high-resolution T1-weighted fast spin echo (FSE) images, centred on the carotid bifurcation bilaterally, was acquired approximately perpendicular to the longitudinal axis of both common carotid arteries, giving 40 mm of longitudinal coverage per artery.

The cardiac study was performed using a standard CMR protocol as described in Section 7.3, Imaging Protocol. Briefly, a contiguous short-axis stack was obtained from ventricular base to apex imaging parallel to the atrioventricular groove. At the baseline study, late

gadolinium enhancement (LGE) images (long-axis plane and short-axis stack) were obtained approximately 10 minutes after giving an intravenous injection of gadolinium contrast (Gadovist, Bayer-Schering, Berlin, Germany, 0.1mmol/kg).

All images were analysed off-line by a blinded investigator using CMRtools software (Cardiovascular Imaging Solutions, London). Carotid images were analysed using Atheroma Tools (a plug-in of CMR tools) as described in Sections 7.1.2 and 7.1.3, Image Analyses. A visual assessment was made for the presence or absence of atherosclerotic plaque. Left and right ventricular volumes (end-diastolic volume, end-systolic volume, stroke volume, and ejection fraction) and LV mass were determined after manual contouring of the epicardial and endocardial borders (see Section 7.3, Image Analysis). Ventricular volumes and mass were indexed to body surface area. Visual assessment was made of the presence and pattern of late gadolinium enhancement. Two separate analyses were carried out. I carried out the initial analysis, and a second (results given below and which will be presented in a manuscript for publication) was done subsequently. This came about as staff shortages necessitated my heavy involvement in recruitment and patient follow up, as well as carrying out the scans and analysing them. I was therefore party to their clinical progress, symptoms, disease activity and blood test results (except the year-1 and year-2 lipid profiles to which I remained blinded), resulting in the introduction of potential bias, as I was not truly fully blinded to all patient parameters.

9.2.4 Outcome measures

The primary outcome measure was defined as the change from baseline in subclinical atherosclerosis as assessed by bilateral carotid artery wall volume. Measures of vessel volume, lumen volume and wall volume expressed as a percentage of the total vessel volume (wall/outer wall ratio) were also assessed. Secondary outcome measures included change from baseline in carotid artery distensibility, endothelial function assessed by brachial artery reactivity, and correlation of vascular findings to ventricular volumes and function.

9.2.5 Statistical methods

Categorical data were presented as number (%) and comparisons done using the chi squared or Fishers exact test. Normally distributed data were presented as mean (SD) and analysed using the unpaired or paired t test. Non-normally distributed data were presented as median (IQR) and comparisons done using the Mann-Whitney (Wilcoxon rank sum) test. To assess the differences between treatment groups from baseline, the difference in the variable values was obtained between the two time points and these differences compared using the unpaired t test. Linear mixed models were used to assess the predictors of the

primary outcome measure and some secondary outcomes. Where there was a significant imbalance in baseline variables, such as age, this variable was adjusted for in the linear mixed models analysis

9.2.6 Power of study

Using a previous CMR study that showed an interstudy SD of 4.4% [Varghese 2005b] the study was powered to detect 1 SD of change with a sample size of 60. This would yield >90% power at a p-value of 0.05 to detect a difference of 4.4% between the groups. This is considered to be an observable difference relative to changes in carotid atheroma over one year seen in other trials [Corti 2002]. The trial, however, under-recruited with 33 patients randomised instead of the target of 60. Therefore the actual study power achieved at a p-value of 0.05 was 68% at year-1 and 66% at year-2.

9.2.7 Safety monitoring

The Data Safety Monitoring Committee reviewed the study throughout the trial and was provided with all adverse event records. Safety monitoring of CK and LFTs were performed at one month and three months and then at the quarterly visits. Withdrawal from the study and discontinuation of trial therapy would be triggered by a CK >5 times or LFTs >3 times the upper limit of the reference range.

9.2.8 Supplementary methods

Males, post-menopausal females and females menstruating at the time of their first and subsequent scans also underwent a BAR scan to assess FMD. Pre-menopausal females not menstruating at the time of the first scan did not undergo the BAR scan, as significant fluctuations occur with hormonal changes during the menstrual cycle [Hashimoto 1995]. BAR was carried out using a previously validated CMR protocol [Sorenson 2002]. This is described in Section 7.2. Briefly, to measure endothelium dependent reactivity, the right brachial artery was occluded distally at the forearm by inflating a blood pressure cuff to 20mmHg above systolic pressure. The artery was scanned immediately and at one-minute intervals for five minutes on cuff deflation. Non-endothelium dependent reactivity was then measured after giving 400μg sublingual glyceryl trinitrate (GTN) and the artery scanned immediately and at 1-minute intervals until maximal dilatation had taken place. The arterial intimal border was contoured semi-automatically at baseline and maximal dilatation. The change was expressed as a percentage. Insufficient numbers had BAR performed to allow for statistical comparison.

9.3 Results

9.3.1 Patient characteristics

Thirty-nine patients who fulfilled the ACR diagnostic criteria [Tan 1982; Hochberg 1997] were consented and thirty-three were enrolled and randomised (Figure 9.1). The mean (SD) age was 48.1 (13.4) years (range 21-77), 94% were female, 55% Caucasian, 30% Afro-Caribbean, and 15% were of other ethnic origins. At recruitment 15% were positive for antiphospholipid antibodies, 23% were lupus anticoagulant positive, 91% were ANA positive (data for one person missing), and 60% were positive for extractable nuclear antigens. The mean (SD) eGFR was 90.8 (19.7) ml/min/1.73m^2, total cholesterol 4.5 (0.59) mmol/L, LDL-C 2.6 (0.47) mmol/L, HDL-C 1.4 (0.38) mmol/L, and TG 1.27 (0.62) mmol/L. With respect to SLE disease activity no differences were found between the groups for C3, C4, ESR and anti-dsDNA. The SLEDAI scores confirmed inactive disease in both groups and no difference in SLICC damage indices were apparent. The mean (SD) of C3, C4 and dsDNA were 1.17 (0.89) mg/dL, 0.58 (1.08) mg/dL and 43.4 (56.6) IU/ml respectively; normal ranges were C3 0.7-1.7 mg/dL, C4 0.15-0.54 mg/dL and dsDNA 0-30 IU/ml. 9% had albuminuria (1+ and 2+) on urine dip testing.

The rosuvastatin and placebo groups were similar with respect to the majority of baseline variables (Table 9.1). Although differences were apparent for the eGFR, leukocyte and neutrophil counts, these were minor and the values were within the respective normal ranges. Smoking was more prevalent in the rosuvastatin group but the difference did not reach statistical significance. SLE duration overall was not statistically different between the groups. Two patients were diagnosed with hypertension during the study period and commenced on appropriate therapy. No patients were diagnosed with diabetes mellitus during the study.

61% of patients were taking prednisolone at a mean dose of 6mg (range 1-20mg), 18% were prescribed azathioprine, 73% hydroxychloroquine, 15% mycophenolate, 3% methotrexate and 3% tacrolimus. There was no statistically significant difference between the groups with regards to drug treatment for SLE (Table 9.1).

Total cholesterol and LDL-cholesterol were significantly decreased at 1 year (p 0.0001 and p 0.0012 respectively, table 9.2). However, lipid-lowering did not reach statistical significance at 2 years compared to baseline (p=0.10 for both total cholesterol and LDL-cholesterol). Median (IQR) reported study drug compliance (calculated from patient returns of medication) was 94 (80.5, 97.5)% at year-1 and 98 (89,100)% at year-2 in those taking rosuvastatin and 91 (87, 100)% at year-1 and 91 (85, 98)% at year-2 in the placebo group. Thus lipid-lowering

at year-2 was not what would be expected from the calculated compliance i.e. significantly reduced in the rosuvastatin group.

At baseline, carotid plaque was identified in 39%: 44% in the rosuvastatin group and 35% in the placebo group (p=0.60). The plaques were small and eccentric with no clinically significant reduction in lumen volume. Two subjects had visually apparent worsening of their carotid plaques (1 each from the rosuvastatin and placebo groups); one subject in the rosuvastatin group developed a small plaque by the end of the study, where the area of carotid wall had appeared thickened at baseline. No other significant visual changes were observed during the study. A further 33% (38% rosuvastatin group, 29% placebo group, p=0.58) had some visually apparent thickening of the carotid wall at baseline. Figure 9.2 shows carotid plaque at the same level taken at baseline, year-1 and year-2.

Carotid artery wall volume was comparable in the placebo and rosuvastatin groups at baseline, year-1 and year-2 (Table 9.3). There was no significant difference between the groups with regards to the other carotid measurements. No difference in the change in wall volume or other carotid measurements between the groups was seen at either the year-1 or year-2 follow-up (Table 9.4). Carotid artery distensibility was similar between the study groups at baseline. After 2 years, distensibility had decreased significantly (p = 0.039) in the group receiving rosuvastatin (Table 9.5).

Cardiac parameters (left and right ventricular volume, mass and function) were not significantly different between the study groups at baseline, and there was no change during the 2-year study duration. One patient had a small area of subendocardial LGE; one patient did not consent to having gadolinium contrast. All other LGE studies were normal. There was no correlation between either total carotid wall volume or carotid distensibility and cardiac parameters including left ventricular ejection fraction and left ventricular mass (Table 9.6).

9.3.2 Adverse events

A total of 9 serious adverse events (SAEs) and 62 adverse events (AEs) occurred during the study period. Of the SAEs, 5 occurred in the placebo group (to 3 patients) and 4 in the rosuvastatin group (4 patients). The SAEs were all due to hospitalisation, none of which was considered related to the study drug. Causes were lupus-flare, costochondritis, polyarthritis, a planned cholecystectomy and pneumonia in the placebo group; and hip fracture due to a fall, post-elective surgery bleeding, pericarditis, and surgery for severe aortic stenosis (picked up incidentally on baseline CMR) in the rosuvastatin group. One SAE resulted in interruption of the study medication (rosuvastatin) for a few days whilst investigations were

carried out; this occurred at the end of the 2-year study period. One patient withdrew from the trial after aortic valve surgery for personal reasons.

Of the 62 AEs, 26 occurred in the placebo group (to 10 patients) and 36 in the rosuvastatin group (to 13 patients). Of these, 56 were classed as mild, 6 as moderate and none as severe. Of the AEs, 56 were definitely unrelated to the study drug. Known interruption of the study drug occurred in 1 patient, and study drug was restarted on review by the trial team 1 month later. Of the 6 AEs due to an uncertain cause, interruption of the study drug occurred in 3 cases; all 3 patients restarted the study drug and continued with the trial. Two other patients did not interrupt the study drug due to their AE, and 1 patient withdrew from the study shortly after their AE with blood tests and clinical review having been normal. Of the AEs definitely or possibly related to lupus (11 and 4 respectively), 60% occurred in the rosuvastatin group.

Figure 9.1. Study consort diagram.

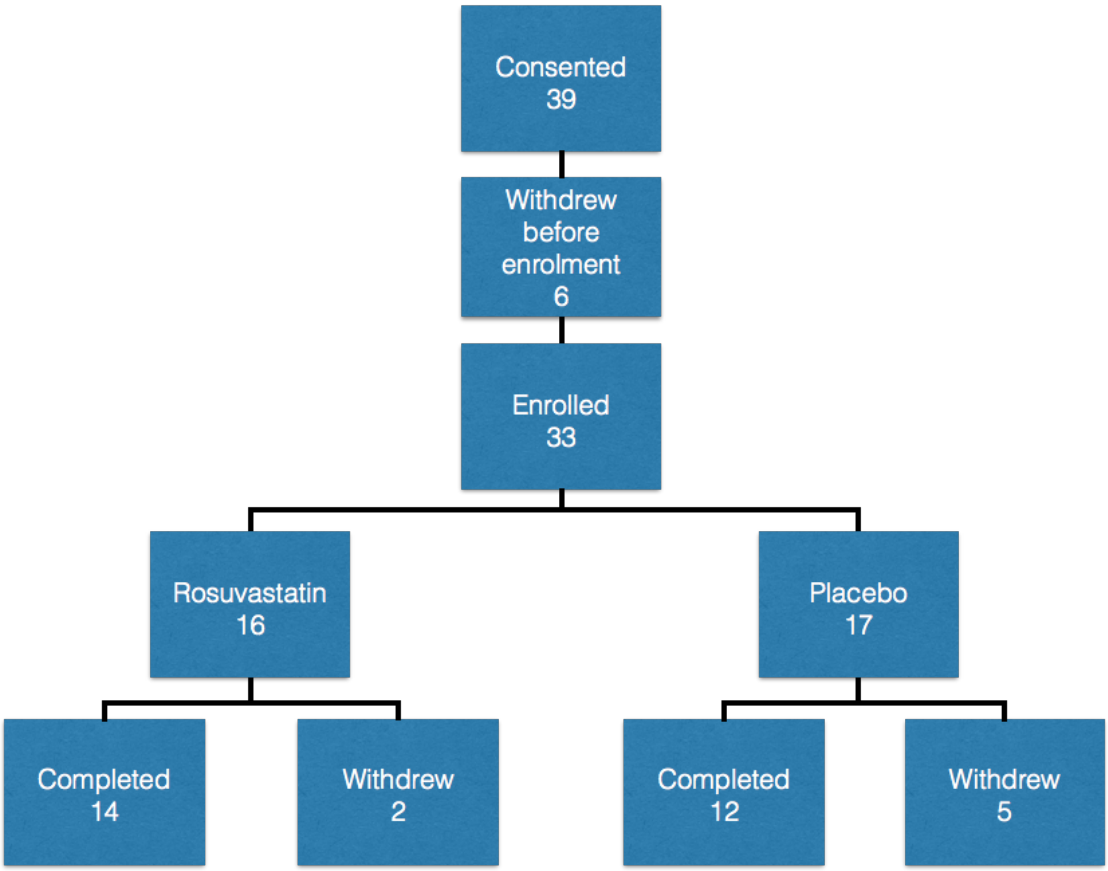


Figure 9.2. Carotid plaque in one individual, imaged at the same level at a) baseline, b) 1-year and c) 2-years. Images are T1-weighted and show a fibrous cap (white arrow) overlying an area of calcification (black arrow), which is of low signal, surrounded by fibrous tissue.

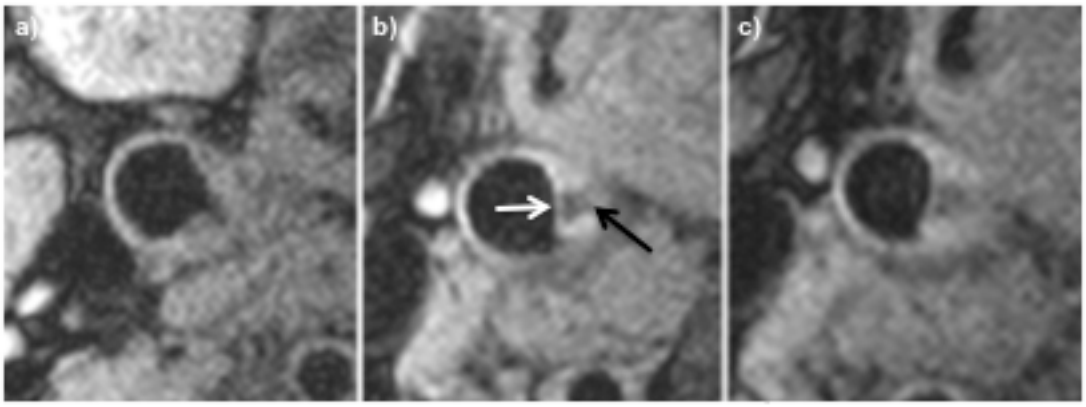


Table 9.1. Baseline characteristics of the study patients by group.

	Placebo (n=17)	Rosuvastatin (n=16)	p-value
Demographic and clinical characteristics			
Female	15 (100%)	14 (87.5%)	1.00
Race			
Caucasian	7 (47%)	10 (62.5%)	
Afro-Caribbean	6 (40%)	2 (12.5%)	0.28
Other	2 (13%)	4 (25%)	
Years since SLE diagnosis			
0-2	0 (0%)	1 (6%)	
2-5	2 (13%)	2 (12.5%)	0.43
5-10	5 (33%)	2 (12.5%)	
10+	7 (47%)	10 (62.5%)	
Hypertension	2 (13%)	3 (19%)	1.00
Diabetes mellitus	0 (0%)	0 (0%)	N/A
Smoker	1 (7%)	6 (37.5%)	0.08
Carotid plaque			
Yes	6 (35%)	7 (44%)	0.60
No	11 (65%)	9 (56%)	
Age (yrs)	44.3 (14.4)	50.8 (12.9)	0.20
BMI (kg/m^2)	25.2 (5.5)	26.5 (5.0)	0.51
BSA (m^2)	1.7 (0.15)	1.72 (0.18)	0.74
Blood pressure (mmHg)			
Systolic	124.9 (18.1)	123.4 (22.1)	0.84
Diastolic	73.7 (11.2)	71.9 (12.9)	0.67
Heart rate (bpm)	77.1 (9.1)	76.4 (13.5)	0.87
SLE drug treatment			
Prednisolone	11 (65%)	9 (56%)	0.62
Azathioprine	3 (18%)	3 (19%)	0.94
Hydroxychloroquine	12 (71%)	12 (75%)	0.78
Mycophenolate	3 (18%)	2 (12.5%)	0.68
Blood parameters			
Total cholesterol (mmol/L)	4.43 (0.47)	4.40 (0.51)	0.86
LDL cholesterol (mmol/L)	2.57 (0.41)	2.60 (0.56)	0.86
HDL cholesterol (mmol/L)	1.41 (0.38)	1.30 (0.24)	0.34
Sodium (mmol/L)	141.13 (2.26)	140.44 (2.22)	0.39
Potassium (mmol/L)	4.01 (0.37)	4.26 (0.31)	0.054
Urea (mmol/L)	4.18 (1.03)	5.23 (1.78)	0.059
Creatinine (µmol/L)	67.2 (8.9)	73.6 (14.5)	0.15
eGFR ($ml/min/1.73m^2$)	99.78 (20.91)	84.70 (13.78)	**0.024**
Creatine kinase (IU/L)	71 (53, 143)	80.5 (50.5, 125)	0.80
Albumin (g/L)	38 (35, 40)	39.5 (36, 41.5)	0.33
Bilirubin (µmol/L)	6 (4, 10)	7 (5, 10.5)	0.45
Alkaline phosphatase (IU/L)	62 (45, 74)	62 (49.5 71.5)	0.77
Alanine transaminase (IU/L)	18 (14, 25)	21 (16, 24)	0.38
Haemoglobin (g/dL)	12.47 (1.48)	12.66 (1.44)	0.71
Total white cell count ($x10^9/L$)	4.2 (3.9, 5.7)	5.7 (4.8, 7.1)	**0.04**
Lymphocytes	1.44 (1.10, 1.90)	1.33 (0.92, 1.85)	0.68
Neutrophils	2.7 (2.4, 3.1)	4.13 (2.75, 4.70)	**0.046**
CRP (mg/L)	5 (1, 6)	4 (1.25, 10.6)	0.69

ESR (mm/hr)	16 (8, 49)	25 (12.5, 46)	0.59
dsDNA (U/ml)	56.4 (10.0, 85.0)	13.0 (10.0, 25.0)	0.07
C3 (mg/dL)	0.99 (0.92, 1.15)	1.05 (0.85, 1.18)	0.90
C4 (mg/dL)	0.17 (0.14, 0.23)	0.20 (0.12, 0.25)	0.93
Anticardiolipin	1 (7.1)	3 (18.8)	0.60
Lupus anticoagulant	3 (20)	3 (21.4)	1.00
Disease activity score			
SLEDAI score	1 (0,1)	0 (0,1)	**0.05**
SLICC score	2 (1,4)	0 (0,2)	0.14

Data are mean (standard deviation) for normally distributed variables, median (interquartile range, IQR) for continuous variables with a skewed distribution or n (%) for categorical variables. BMI indicates body mass index; BSA, body surface area; HDL, high-density lipoprotein; LDL, low-density lipoprotein; eGFR, estimated glomerular filtration rate; CRP, C-reactive protein; ESR, erythrocyte sedimentation rate; C3, complement component 3; C4, complement component 4; dsDNA, double-stranded DNA. SLE disease duration not recorded for 1 patient in the placebo group and 1 patient in the rosuvastatin group.

Table 9.2. Change in lipids from baseline.

Treatment group	Mean LDL-C (mmol/L)				p-value for change
	At baseline	After 1 yr	After 2 yrs	Mean change	
Rosuvastatin	2.60 (0.56)	1.60 (0.79)	-	-1.00 (-1.40, -0.60)	0.001
Placebo	2.57 (0.41)	2.54 (0.53)	-	-0.08 (-0.38, 0.22)	
Rosuvastatin	2.60 (0.56)	-	1.99 (0.90)	-0.61 (-1.06, -0.16)	0.10
Placebo	2.57 (0.41)	-	2.55 (0.67)	-0.14 (-0.47, 0.20)	

Table 9.3. Carotid artery measurements at a) baseline, b) 1-year and c) 2-years. (Results are mean ±SD).

a) Baseline

Variable	**Placebo (n=15)**	**Rosuvastatin (n=16)**	**p**
Total Wall Volume (mm^3)	1328.24 ± 303.50	1378.83 ± 207.29	0.61
Total lumen Volume (mm^3)	3032.29 ± 819.25	3019.44 ± 497.92	0.96
Total Vessel Volume (mm^3)	4360.53 ± 1092.48	4398.27 ± 688.11	0.91
WOW (%)	30.77 ± 2.77	31.45 ± 1.60	0.43
Distensibility (%)	20.33 ± 6.86	21.03 ± 6.73	0.78

b) 1-year follow-up

Variable	**Placebo (n=12)**	**Rosuvastatin (n=15)**	**p**
Total Wall Volume (mm^3)	1244.59 ± 246.68	1325.49 ± 235.70	0.39
Total lumen Volume (mm^3)	2952.21 ± 821.74	2950.07 ± 589.21	0.99
Total Vessel Volume (mm^3)	4196.80 ± 1050.67	4275.56 ± 804.79	0.83
WOW (%)	30.06 ± 2.29	31.12 ± 2.10	0.22
Distensibility (%)	23.64 ± 9.78	18.33 ± 5.07	0.11*

c) 2-year follow-up

Variable	**Placebo (n=12)**	**Rosuvastatin (n=14)**	**p**
Total Wall Volume (mm^3)	1250.03 ± 214.63	1303.23 ± 171.75	0.49
Total lumen Volume (mm^3)	3006.03 ± 787.89	2915.60 ± 369.99	0.70
Total Vessel Volume (mm^3)	4256.06 ± 974.49	4218.83 ± 517.54	0.90
WOW (%)	29.80 ± 2.76	30.92 ± 1.84	0.23
Distensibility (%)	21.5 ± 8.02	18.36 ± 7.39	0.32

*t-test with unequal variance

Table 9.4. Primary outcome (total wall volume) and other carotid artery measurements shown as a) change from baseline to year-1 and b) change from baseline to year-2. Results are shown as mean (95%CI).

a) change from baseline to year-1

Variable	Placebo (n=12)	Rosuvastatin (n=15)	Treatment effect	p
Total Vessel Volume	-163.73	-122.71	41.02	0.77
(mm^3)	(-375.04, 45.58)	(-326.12, 80.71)	(-240.11, 322.16)	
Total Wall Volume	-83.65	-53.35	30.30	0.49
(mm^3)	(-159.41, -7.89)	(-111.86, 5.16)	(-58.90, 119.51)	
Total Lumen Volume	-80.08	-69.36	10.72	0.92
(mm^3)	(-246.14, 85.98)	(-226.86, 88.14)	(-208.24, 229.68)	
W/OW (%)	-0.71	-0.33	0.38	0.56
	(-2.02, 0.59)	(-1.09, 0.44)	(-0.98, 1.75)	

b) change from baseline to year-2

Variable	Placebo (n=12)	Rosuvastatin (n=14)	Treatment effect	p
Total Vessel Volume	-104.47	-113.15	- 8.86	0.95
(mm^3)	(-319.10, 110.16)	(-353.50, 127.20)	(-319.10, 301.73)	
Total Wall Volume	-78.20	-64.66	13.54	0.80
(mm^3)	(-169.89, 13.48)	(-136.86, 7.53)	(-95.43, 122.52)	
Total Lumen Volume	-26.26	-48.48	-22.22	0.84
(mm^3)	(-185.38, 132.85)	(-224.16, 127.17)	(-250.27, 205.82)	
W/OW (%)	-0.97	-0.71	0.26	0.71
	(-2.41, 0.48)	(-1.38, -0.03)	(-1.17, 1.69)	

Table 9.5. Results of linear mixed models (using all data points and including year as a covariate) – Coefficients of active treatment variable in comparison with placebo.

Variable	Active treatment coefficient (95%CI)	P value
CMR parameters		
Total vessel volume	47.17 (-561.82, 660.15)	0.88
Total wall volume	65.98 (-95.68, 227.65)	0.42
Total lumen volume	-16.92 (-481.56, 447.71)	0.94
W/OW	0.92 (-0.56, 2.39)	0.22
Carotid distensibility	-2.53 (-4.92, -0.13)	0.039
Lipid parameters		
Total cholesterol	-0.56 (-0.86, -0.26)	<0.0001
LDL- cholesterol	-0.46 (-0.73, -0.19)	0.001
HDL- cholesterol	-0.05 (-0.16, 0.06)	0.38

Table 9.6. Correlations of total carotid wall volume and carotid distensibility to ventricular ejection fraction and mass.

	Placebo			Rosuvastatin		
	Year	**Ro**	**p**	**Year**	**Ro**	**p**
Total wall volume						
LVEF	0	0.05	0.87	0	0.22	0.43
	1	-0.08	0.80	1	0.09	0.76
	2	0.39	0.24	2	0.18	0.53
LV mass	0	0.12	0.71	0	0.20	0.48
	1	-0.08	0.80	1	0.08	0.78
	2	0.04	0.91	2	-0.15	0.62
Distensibility						
LVEF	0	0.02	0.94	0	0.40	0.13
	1	0.21	0.51	1	-0.18	0.52
	2	-0.006	0.99	2	0.22	0.47

9.4 Discussion

Death rates in the general population due to cardiovascular disease (CVD) have decreased by up to 30.8% in the first ten years of this century [Mozaffarian 2015]. Approximately 47% of the decrease in deaths from CVD in the USA is due to the use of evidence based medical therapies such as the statins [Ford 2007]. Indeed, statins have been associated with a reduction in CVD in other at risk groups, such as diabetics with no additional CVD risk factors [Eldor 2009], and in those with a raised CRP in the presence of normal levels of LDL-cholesterol [Ridker 2008]. Unfortunately, despite advances in the treatment of SLE and a reduction of all-cause mortality, the risk of death from CVD has remained unchanged [Björnådal 2004]. In contrast, there is emerging data that in rheumatoid arthritis, aggressive management of disease activity combined with modification of traditional risk factors can significantly reduce the risk of CV events [Roubille 2015; Solomon 2015].

Although the use of statins in SLE patients without hypercholesterolaemia has appeared attractive due to their known effect on reducing cardiac events in patients with CVD, and also because of their anti-inflammatory, immunomodulatory and anti-thrombotic effects [Mihos 2012; Raza 2012; Blanco-Colio 2007] no clear evidence for their routine use has emerged. Concerns have also been raised that statins may induce lupus or cause a flare of known SLE [Moulis 2012], but again no clear evidence exists.

This 2-year interventional study of rosuvastatin in normolipidaemic SLE patients with mild disease has shown no benefit in improving the primary endpoint of total carotid wall volume, which is a marker of subclinical atherosclerosis. This echoes a recent study by Petri *et al.* where the administration of atorvastatin versus placebo showed no benefit in the primary endpoint, namely analysis of C-IMT by ultrasound [Petri 2011]. Moreover, our secondary endpoint of carotid artery distensibility worsened in the statin group. Arterial distensibility is a marker of vascular health and arterial stiffness has been associated with cardiovascular mortality and morbidity [Suwaidi 2000; Cavalcante 2011]. SLE patients at low risk for CVD have been found to exhibit increased arterial stiffness [Sacre 2014]. The lack of improvement in carotid artery distensibility in our study correlates with the failure to reduce carotid wall volume, both being markers of cardiovascular risk [Simons 1999]. Statins have been found to improve arterial stiffness (measured by pulse wave velocity) in a recent meta-analysis [Upala 2016]. Individual studies however have been conflicting in their results [Upala 2016; Rizos 2010], and the effects seen can vary depending on the arterial bed examined [Shige 2001]. Most studies have been carried out in patients with hyperlipidaemia and/or known CVD. It is possible that the conflicting results obtained in previous studies are due to one or a combination of the type of statin used, variation between PWV protocol used and the arterial

bed studied [Shige 2001; Ballard 2015]. The effect of statins on arterial stiffness on various conditions, particularly when not associated with hyperlipidaemia is unclear/unknown.

These combined data leave us with the question of when statins should be recommended to patients with SLE. An LDL-C target of <100 mg/dL (<2.6mmol/L) has been recommended [Stojan 2013]. Ideally disease-specific indices should be derived. The lipid environment in patients with inflammatory diseases *per se*, and SLE in particular is complex. A putative pro-inflammatory form of HDL (piHDL) is increased in patients with SLE [McMahon 2006] and may enhance LDL-oxidation and foam cell deposition. The total cholesterol to HDL-C ratio may be a more applicable measure of CV risk in SLE patients. Our findings add weight to the argument that statins should not be routinely prescribed to SLE patients who lack traditional cardiovascular risk factors, have stable disease and no clear indication for statin therapy [Robertson 2013].

9.4.1 Study limitations

This study had several significant limitations. One limitation is the low number of SLE patients recruited, which resulted in under-powering of the study for its endpoints. This reflects both the difficulties in recruiting predominantly young women of child-bearing age who are asymptomatic and otherwise well into a long-term demanding clinical trial and the number of SLE patients already prescribed statins by their care providers. Indeed during screening, 22% of potential SLE patients identified were already prescribed a statin. It would be interesting to ascertain whether these patients have the same CVD risk profile as our study group, or whether other risk factors such as a family history of premature CVD are present.

Another limitation is the apparent poor compliance with medication during year-2 of the trial. Statins produce significant reductions in total cholesterol and LDL-cholesterol levels which are maintained over time with continued administration. Similar statin lipid-lowering effects in SLE patients have been found in previous studies [Petri 2011]. The absence of a significant difference in total cholesterol and LDL-cholesterol at the end of the second year in our study suggests that the medication returned was not an accurate reflection of medication consumed. Thus, the lack of difference in the primary endpoint may be due to poor compliance rather than the inability of rosuvastatin to effect a change in the study endpoint. This highlights the pertinent issues surrounding compliance with medication by asymptomatic patients. Both SLE patients [Chambers 2007] and patients on prescribed statins [Maningat 2013] have demonstrated poor compliance with treatment which may result in adverse clinical outcomes. Hence our study likely reflects an important real-world problem in

managing this group of patients. Indeed non-adherence rates up to 76% have been reported [Costedoat-Chalumeau 2013].

Some differences in demographics existed between the groups. Although these did not reach statistical significance, the difference in age of 6.5 years, may have been clinically significant, particularly in a small, underpowered study. The placebo group had a mean age of 44.3 years (range 21-73 years) and the rosuvastatin group 50.9 years (range 28-77 years), so the baseline results, expected rate of progression and possibly response to the study drug, may have varied. Using values derived from the change in carotid wall volume with age in a healthy female population [Keenan 2009a], a mean difference of 10mm^3 (using the difference between mean wall volumes in the 40-49 year and 50-59 year cohorts in that study) to 19.7mm^3 (using the average increase in carotid wall volume per year across their entire cohort of 20-69 years) would have been expected between the groups in our study, with the higher values in the rosuvastatin group. The rosuvastatin group's wall volume was 50.6mm^3 higher at baseline than that of the placebo group, consistent with aging. However, the absolute volumes were higher than would be expected in a healthy population. In Keenan's study, the mean wall volume increase varies with age. Over the course of the current study, wall volume progression may have been different due to differences in the mean age of the groups. Wall volume would have been expected to increase, at least in the placebo group by between 2mm^3 and 6.06mm^3, a difference, which given the potential measurement errors inherent to the technique (6% [Kang 2000]), may be too small to be detected and the study duration may therefore have been too short to detect any real changes. The expected rate of change in the rosuvastatin group would have been between -2mm^3 and 6.06mm^3 over this period [Keenan 2009a]. However, over the study period, carotid wall volume values actually fell in both groups (Table 9.3). Possible reasons for the wall volume decrease in the placebo group include the younger age of this group not resulting in the expected rate of wall volume progression, although this seems unlikely, given the natural history of carotid wall volume is to increase over time [Keenan 2009a]. The fall in wall volume may have been due to concomitant drug effects, which may also have been at play in the rosuvastatin group, as both cohorts were on similar SLE treatment regimes. More likely, however, the explanation is again that the study was underpowered to detect real difference between the groups, and was further compounded by the much higher drop-out rate in the placebo group than in the rosuvastatin group (29% versus 12.5%).

It is possible that our power calculations were based on incorrect assumptions. Power calculations were based on previous studies showing coefficients of variation of 4.4-4.6% with predominantly males and a mean LDL-cholesterol of 3.5mmol/L, including patients

treated for hypercholesterolaemia [Varghese 2005a], or with known carotid atherosclerosis [Varghese 2005b; Saam 2005]. The vast majority of subjects in the current study were female, who have lower absolute carotid wall volumes and slower rates of progression with age [Keenan 2009a], had no known history of atherosclerosis and had LDL-cholesterol <3.4mmol/L. Hence, our power calculations may have been based on cohorts in which a study drug versus placebo would have been expected to generate greater differences in carotid wall volume, than could have occurred in our group of patients. Under-recruitment in our study would have compounded this problem. The coefficients of variation obtained by the observer analysing the data in this study were 15-19% for the wall volume (Table(a) Appendix), much higher than that seen in the studies from which the power calculations were derived. This would also have made those power calculations meaningless, magnifying the under-powering effect and resulting in a study, which would not be able to detect any possible drug effect using the measurement technique employed.

It is possible that the wrong arterial territory was looked at. SLE is associated with a significantly increased risk of coronary artery disease and myocardial infarction [Manzi 1997; El-Magadmi 2004], and although C-IMT is associated with an increase in cardiovascular risk in both healthy populations and populations with other cardiovascular risk factors [Lorenz 2007], it is possible that in SLE the atherosclerotic process varies between the different arterial territories and a study looking at the coronary arteries may have yielded a more relevant, and possibly different, result for this group of patients.

It is possible that the wrong measurement parameters were used and that a change in plaque volume and/or composition would have been a better surrogate measurement. In our study however, the carotid plaques seen were mostly calcified and other areas showed thickening of the carotid wall with no discrete plaque formation, which may not reflect the same pathophysiological mechanism as lipid-rich atherosclerosis. Therefore no significant statin effect would have been expected. Indeed, in a previous study by Corti *et al.* [Corti 2002], areas of normal vessel wall as assessed by wall thickness showed no change with statin therapy, and no decrease in coronary calcium score was observed in SLE patients treated with atorvastatin [Petri 2011]. A study looking at the presence and composition of atherosclerosis in the coronary arteries of a low traditional cardiovascular risk SLE cohort and how this responds to statin therapy may therefore be a better modality to employ.

The use of surrogate end points instead of actual cardiovascular events is another limitation. Given the low incidence of CV events, large patient numbers would need to be recruited and followed up over many years. Problems with compliance mean that even then the outcome

may be inconclusive. So far studies in both RA and SLE have failed to prospectively recruit enough patients to show any significant change in the incidence of cardiovascular events [Mason 2015]. There is also the possibility that a different statin may have exerted a different effect on this group of SLE patients, although this is unlikely given what is known about different statins in other patient groups.

9.4.2 Conclusion and clinical implications

The current study provides no evidence to suggest that the routine prescription of statins is justified in SLE patients with no current National Cholesterol Education Program (NCEP) indication for lipid lowering [Cleeman 2001]. However, SLE disease activity should be treated aggressively alongside management of traditional cardiovascular risk factors. SLE patients with hyperlipidaemia should continue to be treated with statins and other lipid-lowering medications to achieve the recommended NCEP targets. In parallel, other strategies to improve control of SLE disease activity need to be developed.

Chapter 10
CMR of carotid artery ageing in treated HIV-infected subjects with low cardiovascular risk

10.1 Introduction

Among people living with HIV-infection (estimated at 35.3 million worldwide [WHO Global Health Observatory Data Repository]; 107,800 in the UK in 2013, see section 6.2), the increase in non-infections complications of HIV and non-AIDS related morbidity and mortality [Sackoff 2006; Lohse 2007] can be attributed, in part, to the transformation of HIV-infection from an invariably fatal condition to a chronic and lifelong condition. One in four HIV-infected individuals in the UK is now ≥50 years of age [Yin 2014], a change brought about by the introduction of combination anti-retroviral treatment (cART) in the mid-1990s. However, mortality rates are still higher among HIV-infected individuals than among the general population [Sackoff 2006; Lohse 2007]. CVD, particularly ischaemic heart disease (IHD), constitutes an important cause of morbidity and mortality [Sackoff 2006; Triant 2012].

The roles played by long-term cART and HIV-infection itself remain controversial and hard to assess. Traditional cardiovascular risk factors such as dyslipidaemia, impaired glucose tolerance, diabetes, central obesity, smoking and hypertension are prevalent in this population, clearly contributing to increased CVD morbidity and mortality and acting as a confounding factor in our understanding of the effects of HIV-infection itself on CVD risk [Saves 2003; Triant 2007]. However, even after adjustment for these risk factors, HIV-infected individuals show an excess risk of CVD of up to 2.12 as compared with HIV-uninfected controls [Triant 2007; Obel 2007]. Other chronic inflammatory diseases, such as rheumatoid arthritis [Watson 2003], and infections, such as Chlamydia and cytomegalovirus [Rosenfeld 2011], have also been associated with increased CVD risk, and inflammation is implicated at every stage in the progression of atherosclerosis (see section 2.3).

Potential CVD risks associated with antiretroviral drugs and anti-retroviral-induced metabolic changes are discussed in section 6.5.4. However, it is worth noting that among long term non-progressors and HIV-controllers with low viral loads and maintained CD4+ cell counts (see section 6.4.3) higher C-IMT has been observed and there is still an excess risk of CVD [Hsue 2009; Pereyra 2009; Pereyra 2012].

HIV-associated immune dysfunction may contribute to the increased risk for CVD seen in HIV-infected individuals. The relative risk of IHD is greater for those with a CD4+ cell count

≤200 cells/ml than for those with a cell count >200 cells/ml at cART initiation [Obel 2007] and in HIV-infection, activated T-lymphocytes are associated with increased C-IMT indicating subclinical carotid artery disease [Kaplan 2011].

There is increasing evidence that HIV-associated chronic inflammation (see section 6.4.4) may also make a contribution to increased CVD risk. HIV infection is characterised by persistently elevated inflammatory markers [Lo 2012], which increase with increasing viraemia [Floris-Moore 2009; Calmy 2009]. Raised inflammatory markers in HIV-infection are associated with CVD [Duprez 2012] and increased mortality [So-Armah 2016; Kuller 2008]. HIV-associated elevated markers of endothelial activation fall but may not normalise with cART [Calmy 2009]. Despite viral load suppression in patients receiving cART [Calmy 2009], aortic arterial inflammation has been found to be similar in HIV-infected individuals with low Framingham risk scores to that in HIV-negative individuals with atherosclerosis [Subramanian 2012].

Increasing C-IMT is associated with increased prevalence of cardiovascular risk factors, the presence of atherosclerotic plaque and increased CVD event risk in non-HIV populations [Lloyd-Jones 2009; Uno 2010]. Many studies have used C-IMT to look for the presence and rate of progression of subclinical atherosclerosis in HIV-infected individuals [Ho 2009; Hanna 2015]. Findings have been conflicting due to variations in study design and ultrasound methodology, e.g. different centres examining varying segments of the carotid artery.

Imaging of the carotid artery wall by CMR can overcome many limitations of C-IMT: the one-dimensional nature of the measure, measurement site variability, susceptibility to near field artefacts and problems with ‘imaging windows’. Although CMR arterial wall assessment differs in some respects from C-IMT (the former including arterial adventitia as well as the intimal and medial layers), measurements of wall area and thickness have been shown to correlate well with measurements of C-IMT [Mani 2006].

To our knowledge, no carotid CMR studies have been carried out in HIV-infected individuals with low traditional cardiovascular risk and we therefore undertook to assess carotid wall volume and subclinical atherosclerosis by CMR in such a group compared to a low cardiovascular risk, HIV-uninfected cohort.

10.2 Methods

10.2.1 Patient population

Thirty-three HIV-infected patients were recruited from the outpatient HIV unit at St Mary's Hospital, Imperial Healthcare NHS trust, London, United Kingdom. Inclusion criteria were HIV-infection (known to be HIV antibody positive ≥2 years), male or female sex, 20 to 70 years old, stable on cART and plasma HIV RNA<50 copies/mL (Quantiplex assayTM, Bayer, Emeryville, CA, USA). Exclusion criteria were current or previous history of CVD, positive family history of premature vascular disease, current or previous history of modifiable risk factors for atherosclerosis (current or former smoking, hypertension, hyperlipidaemia, diabetes), Framingham risk score of greater than 10% or DAD risk score of greater than 5% [Friis-Møller 2010], the taking of any cardiovascular medication (e.g. anti-platelet, antihypertensive, lipid-lowering medications), alcohol abuse, recreational drug use within 6 months, and any contraindication to CMR. The Imperial College London NHS health care trust Ethics Committee approved the study. All subjects gave informed written consent. Clinical assessment was carried out at a screening visit (by Dr Jaime Vera) including age, height, weight, ethnicity, HIV-disease history, blood pressure, ECG, blood tests (CD4 lymphocyte count, plasma HIV RNA, fasting lipids, glucose, electrolytes, urea and creatinine), and assessment of cardiac risk factors. Subjects found to have elevated blood pressure (>140/90 mm Hg), elevated total cholesterol to HDL ratio (>5), elevated triglycerides, elevated glucose, or an abnormal ECG were excluded from the study and referred to their physician for further management. A historic cohort of thirty-five HIV-uninfected healthy subjects with no known CVD, no current or previous history of major modifiable risk factors for atherosclerosis and low cardiovascular risk scores (<10%), matched for age, sex and where possible, ethnicity was used as a control group [Keenan 2009a].

10.2.2 CMR protocol

CMR was performed using a 3.0T scanner (Siemens Skyra, Erlangen, Germany) and a purpose-built bilateral four-channel phased-array carotid surface coil (Machnet BV, Eelde, the Netherlands), with the head and neck immobilised, at the Cardiovascular Biomedical Research Unit, Royal Brompton Hospital, London, United Kingdom. The CMR protocol is described in Sections 7.1.2 and 7.1.3, Imaging protocols. Briefly, a contiguous stack of 20 high-resolution T1-weighted fast spin echo (FSE) images, centred on the carotid bifurcation bilaterally, was acquired approximately perpendicular to the longitudinal axis of both common carotid arteries, giving 40 mm of longitudinal coverage per artery. CMR image analysis, whilst blinded to all parameters other than HIV-status was performed off-line by me using

dedicated software (Atheroma Tools, a plug-in of CMR tools, Cardiovascular Imaging Solutions, London, UK) as described in Sections 7.1.2 and 7.1.3, Image analyses. A visual assessment was made for the presence or absence of atherosclerotic plaque.

The historic cohort had been scanned previously on a 1.5T scanner using similar protocols and the images had been analysed using the same methods employed for this study, in order to provide 'normative' data and to serve as a control group in future studies [Keenan 2009a]. Measures of carotid wall volume obtained at 1.5T and 3.0T field strengths have been compared previously and measurement differences did not reach significance; so it is legitimate to compare scans obtained at 1.5T and 3.0T field strengths [Yarnykh 2006].

10.2.3 Sample Size and Statistical Analyses

The calculated minimum sample size to detect a difference between the two groups (22 patients: 11 cases and 11 controls) was based on an assumed increase in wall volume of 25% amongst the HIV-infected cohort in the context of the findings of Keenan *et al.* [Keenan 2009a], a study in which the highest rate of increase in wall volume was observed in the 60 to 69 years old age group, showing a mean wall volume of 1083mm^3 (estimated standard deviation 189). Our aim was to recruit a sample of five subjects matched for age and sex in each age group (20 to 39 years, 40 to 49 years, 50+ years) per sex.

Categorical data are presented as number (%), with comparisons performed using the chi-squared or Fishers Exact test. Normally distributed numeric data are presented as a mean (SD) or 95% confidence interval and they were analysed using a 2-sample independent t-test. Non-normally distributed data (as assessed by visual inspection of graphical data and test for normality) are presented as median values and inter-quartile ranges (IQR). Comparisons were performed using the Mann-Whitney (Wilcoxon rank-sum) test. The strength of association between measured carotid artery variables (W/OW ratio, wall volume, lumen volume, vessel volume) and age was assessed by linear regression analysis. The strength of association of patient demographic and HIV-specific parameters with W/OW ratio was also assessed using linear regression analysis.

10.3 Results

10.3.1 Patient Characteristics

Table 10.1 shows HIV-infected and control group baseline characteristics (as enumerated in section 10.2.1). Age, sex-distribution, total cholesterol levels, blood pressure, BSA and 10-year coronary risk were similar between both groups. HIV-infected individuals had a mean age of 45.2±9.7 years. Mean duration of known HIV-infection was 8.8±4.4 years. All subjects

were stable on cART with median treatment duration of 7 years (2-21 years); 24 were on a non-nucleoside reverse transcriptase inhibitor (NNRTI) based regimen and 9 on a protease inhibitor (PI) based regimen. All subjects were receiving an NRTI backbone comprising of tenofovir, abacavir and zidovudine in 24, 6 and 3 subjects, respectively. Of those on a PI based regimen, 5 were on darunavir, 3 were on atazanavir and 1 was on lopinavir. All patients on PIs were on a boosted combination with ritonavir.

10.3.2 Carotid CMR

The mean carotid CMR measurements for HIV-infected patients and controls are shown in Table 10.2. The mean W/OW ratio in the HIV-infected group was significantly greater than that of the control group (36.7±3.7% versus 32.5±2.8% p<0.0001); HIV-infected females showed a greater difference from female controls than HIV-infected males did from male controls (Table 10.3). Carotid artery total lumen volumes, vessel volumes and wall volumes did not differ significantly between the study groups, though mean total wall volume was greater in the HIV-infected group than in the control group (1712±317mm^3 versus 1575±418mm^3). Mean carotid artery distensibility was lower in the HIV-infected group than in the control group (22.9% versus 24.2%), but not significantly so (p=0.35). Univariate regression analysis showed that HIV-infection is positively associated with W/OW ratio (coefficient 5.28, P=0.0001). No significant associations were revealed by multivariate regression analyses using demographic and HIV-specific parameters: age, ethnicity, CD4 cell count, nadir CD4 cell count, years since HIV diagnosis, years on cART and NRTI or PI usage, except a lower W/OW ratio on comparing the nucleoside reverse transcriptase inhibitor abacavir with zidovudine (W/OW 5.48, p=0.038)). In the multivariate analysis, W/OW was still significantly associated with HIV-status, independently of age, (r=4.37, p= 0.001).

10.3.3 Carotid artery ageing in HIV-infected individuals

Mean carotid artery lumen volume, wall volume, total vessel volume, W/OW ratio and distensibility for HIV-infected individuals are shown in Table 10.4, broken down by age group and sex. Figure 10.1 illustrates the increase with age observed in wall volume, total vessel volume and W/OW ratio in both the HIV-infected group and the control group. Carotid plaques were not detected in any individuals in this study.

Age and male sex were predictors of greater W/OW ratio, wall volume and total vessel volume in both groups. In HIV-infected males, wall volume and total vessel volume were positively associated with age. After the third decade, increase in the W/OW ratio (i.e. vessel wall thickening) is accelerated compared to male controls (Figure 10.1b). Compared to female controls, WO/W ratio was significantly greater in HIV-infected females (36.4% versus

31.3%, *P*=0.0002). The increase in W/OW ratio was greater among HIV-infected females compared to female controls than among HIV-infected males when compared to male controls (36.2% versus 33.4% p=0.0019). Elevated W/OW ratio in HIV-infected females was present in the third decade, with very little subsequent change (Figure 10.1c). This trend is different from the one observed in the female control group where W/OW ratio significantly increased with age.

Table 10.1. Baseline characteristics including clinical and laboratory parameters

	HIV-infected subjects (n=33)	Control Subjects (n=35)	*p*
Age (years)	45.2 (41.8, 48.7)	46.9 (42.9, 50.9)	0.52
Sex n (%)			
Male	19 (57)	19(55)	0.97
Female	14(43)	16(45)	0.89
Ethnicity n (%)			
White	16(48)	30(85)	**<0.0001**
Black	14(42)	2(5)	
Other	3(3)	3(8)	
Body surface area (m^2)	1.81 (1.76, 1.87)	1.88 (1.79,1.96)	0.22
Blood pressure (mmHg)			
Systolic	123.7 (120.0, 127.4)	121.3 (117.5, 125.2)	0.38
Diastolic	76.1 (73.3, 79.0)	76.2 (73.8, 78.6)	0.97
Total Cholesterol (mmol/L)	4.7 (4.5, 4.9)	4.9 (4.6, 5.2)	0.34
10-year coronary risk (%)	3.97 (2.58, 5.36)	3.72 (2.5, 4.9)	0.78
HIV disease related parameters			
Baseline CD4 cell count (cells/uL)	638.48 (556.72, 720.25)	N/A	
Nadir CD4 cell count (cells/uL)	276.36 (207.40, 345.33)	N/A	
Baseline plasma HIV RNA level copies/mL n(%)	33 (100)	N/A	
Years since HIV diagnosis	8.82 (7.27, 10.37)	N/A	
Years on cART	7.5 (6.0, 9.0)	N/A	
cART therapy at screening n(%)			
NNRTI based	24 (72)	N/A	
PI based	9 (28)	N/A	
NRTI therapy at screening n(%)			
Tenofovir based	24 (72)	N/A	
Abacavir based	6 (18)	N/A	
Zidovudine based	3 (9)	N/A	

Values are numbers for categorical variables or mean (95% confidence interval) for continuous variables. cART indicates combine antiretroviral therapy; NNRTI, non-nucleoside reverse transcriptase inhibitor; NRTI, nucleoside reverse transcriptase inhibitor; PI, protease inhibitor.

Table 10.2. Carotid CMR measurements in HIV-infected and control subjects.

	HIV-infected subjects (n=33)	Control subjects (n=35)	*p*
Total Lumen Volume (mm^3)	2966.6 (2763.5, 3169.7)	3277.5 (2988.4, 3566.7)	0.079
Total Wall Volume (mm^3)	1712.1 (1599.4, 1824.8)	1574.8 (1431.3, 1718.3)	0.13
Total Vessel Volume (mm^3)	4678.7 (4391.7, 4965.8)	4852.3 (4433.3, 5271.4)	0.49
W/OW Ratio (%)	36.7 (35.4, 38.0)	32.5 (31.5, 33.5)	**< 0.0001**
Distensibility (%)	22.9 (20.6, 25.1)	24.2 (22.4, 26.1)	0.35

Values are mean (95% confidence interval). Significant values are shown in bold text.

Table 10.3. Difference in W/OW between male and female HIV-infected subjects compared to male and female controls using the Z-score.

	HIV-infected subjects - median (IQR)	Control subjects - median (IQR)	*p*
Males	1.36 (0.21,2.75)	0.39 (-0.52, 0.91)	**0.024**
Females	1.77 (0.14, 2.39)	-0.50 (-1.00, 0.32)	**0.008**

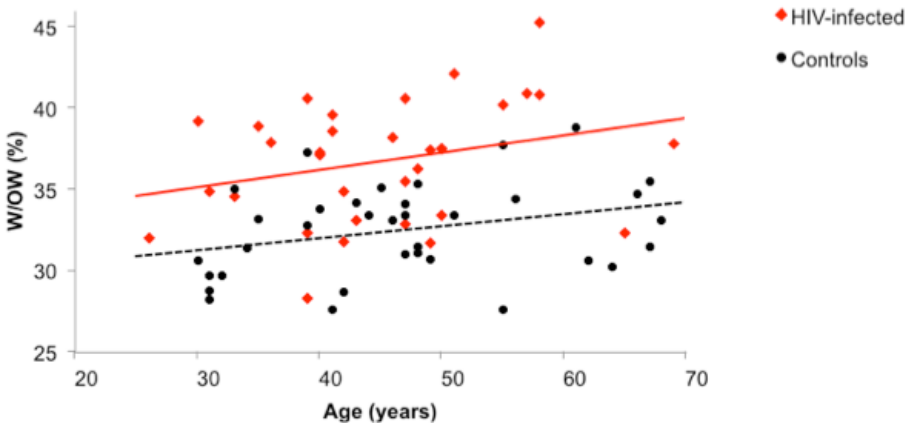
Significant values are shown in bold text.

Table 10.4. Carotid artery parameters by age group showing mean and 95% confidence intervals

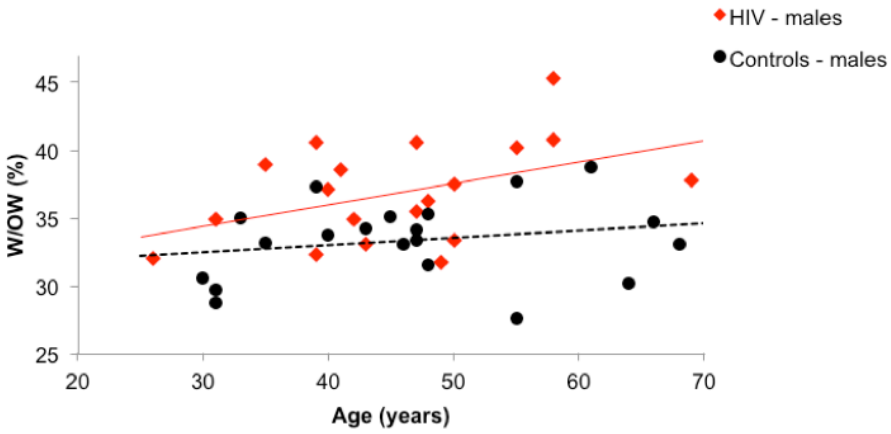
	20-39 years	**40-49 years**	**50-69 years**	***p***
HIV-Males	n= 6	n=8	n=5	
Total Lumen Volume (mm^3)	2786.8 (2371.0, 3202.6)	3443.6 (3015.8, 3871.4)	3372.5 (2786.2, 3958.9)	0.047
Total Wall Volume (mm^3)	1673.8 (1267.5, 2080.0)	1919.3 (1759.9, 2078.8)	2052.8 (1723.7, 2381.9)	0.11
Total Vessel Volume (mm^3)	4460.6 (3804.5, 5116.7)	5362.9 (4831.1, 5894.8)	5425.3 (4598.8, 6251.9)	0.032
Average Distensibility (%)	22.5 (17.5, 27.5)	24.8 (19.3, 30.4)	21.2 (15.0, 27.4)	0.52
W/OW Ratio (%)	37.3 (31.9, 42.8)	36.0 (33.6, 38.4)	37.9 (34.3, 41.6)	0.63
HIV-Females	n=4	n=5	n=5	
Total Lumen Volume (mm^3)	2733.0 (1501.7,	2571.0 (2313.7, 2828.2)	2601.9 (2046.3, 3157.6)	0.86
Total Wall Volume (mm^3)	1424.1 (1292.0, 1556.6)	1460.5 (1252.6, 1668.4)	1594.8 (1434.0, 1755.5)	0.27
Total Vessel Volume (mm^3)	4157.1 (2813.0, 5501.1)	4031.5 (3640.0, 4423.1)	4196.7 (3761.3, 4632.1)	0.87
Average Distensibility (%)	22.8 (17.8, 27.9)	23.1 (17.9, 28.2)	21.6 (-0.04, 43.1)	0.96
W/OW Ratio (%)	35.0 (27.3, 42.7)	36.2 (32.9, 39.5)	38.1 (31.2, 45.2)	0.54

Figure 10.1. Graphs of carotid artery wall volume normalized to total vessel volume (W/OW ratio) plotted against age with regression line.

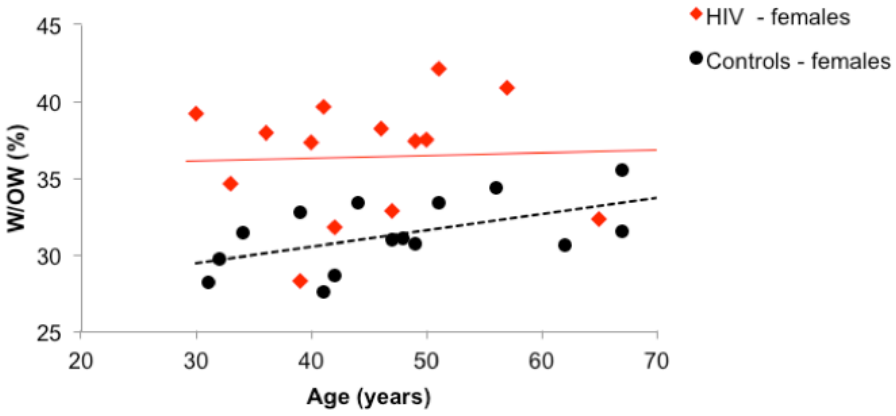
a) HIV-infected (red) and HIV-negative controls (black).



b) HIV-infected males (red) and HIV-negative control males (black).



c) HIV-infected females (red) and HIV-negative control females (black).



10.4 Discussion

This study demonstrates that HIV-infected individuals on cART with low CVD risk exhibit markers of early atherosclerosis at a younger age than controls. Increased carotid-artery intima and media thickness is an independent predictor of MI and stroke [Chambless 1997; O'leary 1999; Lorenz 2007].Therefore, the rate of vascular events in HIV-infected individuals is likely to remain raised in spite of aggressive management of modifiable traditional CVD risk factors.

The DAD study found an independent association between increased CVD risk and the antiretroviral agents indinavir, abacavir and lopinavir [Friis-Møller 2003]. Conflicting results have been found in other studies using carotid ultrasound with regards to the contribution to the observed increased arterial wall thickening made by HIV-infection itself, the type of antiretroviral therapy and traditional risk factors. In some studies PIs have been associated with increased carotid plaques [Maggi 2000] and C-IMT [Seminari 2002], but more recently in larger studies, no association with increased C-IMT could be established Mercie 2002; Hsue 2004]. Our study showed no association between antiretroviral regimens containing PIs and increased arterial wall thickness when compared to non PI-containing antiretroviral regimens. However, it was not powered to do so and only a few patients on PI-based therapy were enrolled. The NRTI abacavir is generally associated with increased CVD risk [Obel 2007], but contrary to this, in our study a lower W/OW ratio was observed on comparing abacavir with zidovudine. This is unlikely to be of real significance: the confidence interval is large (-10.63, -0.34), the sample size is low (6 abacavir, 3 zidovudine) and the model is a poor fit (R-squared=0.14). It is possible that this result is partly due to a channelling bias in our HIV-infected cohort with clinicians using abacavir only in subjects considered to have very low CVD risk.

The presence and progression of increased C-IMT over time are known to be associated with traditional CVD risk factors [Mercie 2002]. Our study cohorts comprised HIV-infected and HIV-uninfected individuals without traditional CVD risk factors. Being cross-sectional our study has not followed up any participants longitudinally, nevertheless the divergence with increasing age between the lines for patients and controls in Figure 10.1(a) suggests that HIV-infection and/or cART may be associated with the progression of arterial wall thickening beyond that which is normally seen with age [Keenan 2009a]. Furthermore, effective viral suppression among the patients in this study does not seem to abolish the risk. Of course, viral suppression does not constitute eradication and low-grade chronic inflammation and T-cell activation persists [Kaplan 2011;Neuhaus 2010; Hunt 2012]. Exposure to HIV-infection itself and/or the adverse metabolic effects of cART are putative causal factors in the

increased CVD risk seen with HIV-infection. If increased arterial wall thickening was historic, reflecting a period of untreated HIV-infection or less than optimal viral suppression, one might expect that the difference between patients and controls would not increase with increasing age. However, because this is a cross-sectional study, unmeasured differences may be present between younger and older HIV-infected individuals – e.g. immunosenescence with increasing age might allow the effect of HIV-infection and/or adverse metabolic effects of cART to be more pronounced in older subjects, resulting in the diverging lines between patients and controls observed with age (Figure 10.1a).

C-IMT has been found to be higher, progress more rapidly, and be associated with a nadir CD4+ count <200cells/μL suggesting that HIV-infection itself is a predictor of increased C-IMT [Hsue 2004]. More recently however, a B-mode ultrasound study following two large cohorts of HIV-infected patients and HIV-uninfected controls, found no association between increased carotid intima-media thickness over time and HIV-infection – the increases observed were consistent with those seen with age [Hanna 2015]. The development of carotid plaque however, was significantly increased in the HIV-infected cohort when the CD4+ count was <500cells/μL at baseline, with risk increasing the lower the CD4+ count. They however found no association between plaque formation and nadir CD4+ level [Hanna 2015]. The measurements of wall volume in our study include all the differing locations measured for C-IMT as well as areas of thickening, defined as plaques, in the various ultrasound studies. Multivariate analysis in our current study revealed a trend towards increased wall volume and increased W/OW ratio with baseline CD4+ counts <500cells/μL, but no such trend with nadir CD4+ counts. However, it is not possible to draw firm conclusions with regards to this, since our study was not powered to detect such changes, our overall numbers are small and only 8 individuals in our cohort exhibited baseline CD4+ counts <500cells/μL, and none had baseline CD4+ counts <200cells/μL.

A markedly increased W/OW ratio in HIV-infected females was observed in our study. It is possible that sex hormones are involved. Vascular tissue contains oestrogen and androgen receptors with androgens mediating a variety of actions on endothelial and smooth muscle cells [Karim 2013]. The cardioprotective effect of oestrogen is well established. Oestrogen is known to provide protection against HIV Tat protein-induced inflammatory reactions in human vascular endothelium [Lee 2004]. Conversely, progesterone, present in many hormonal contraceptives, has been shown to have an immunosuppressive effect, possibly resulting in susceptibility to HIV progression [Hel 2010]. It may therefore increase the risk of vascular damage. Premature ovarian failure and early menopause is associated with HIV-infection [Hunt 2012], which can also lead to reduced oestrogen levels. Therefore excess

atherosclerosis in the HIV-infected females in our cohort could be caused by alterations in sex hormones relative to controls, resulting from HIV-infection. Contraceptive information, sex hormone levels and the number of peri- or postmenopausal females in our study are not known.

Carotid arterial wall thickening and plaque quantification by CMR has been the subject of study in various patient groups. These have included groups at high risk of and with known CVD [Mani 2006; Yuan 1998], as well as cohorts with chronic inflammatory conditions associated with premature atherosclerosis. [Keenan 2009b] CMR has also been used longitudinally to assess the effect of drugs on carotid arterial disease progression or regression, e.g. statins [Corti 2005] (see also Chapters 8 and 9) and immunomodulatory drugs [Chan 2011]. Carotid CMR could therefore be used to study the effects of established cardiovascular or anti-retroviral therapies in HIV-infected cohorts with and without traditional modifiable cardiovascular risk factors, e.g. hypertension, hyperlipidaemia or smoking. It could also be used to assess the effect of novel HIV therapies on the development or otherwise of atherosclerosis. The results of our study may serve as a baseline from which the effects of risk factors and treatments can be assessed.

10.4.1 Study limitations

Although the study was adequately powered overall, the numbers recruited are small. In particular the comparatively low number of older HIV-infected females may be a reason for the less pronounced difference in W/OW ratio observed in this group when compared with controls. Furthermore, the only subject in the 60-70 year group was an outlier (Figure 10.1c). We cannot exclude the possibility that racial variation contributed to the observed variation in the W/OW ratio, as the HIV-infected cohort contained a higher proportion of individuals of black ethnicity than the control group (see Table 10.1). Studies have previously shown that C-IMT is higher at the common carotid among black adults than among white adults; this is not observed for the internal carotid arteries [Urbina 2002; Manolio 2008]. Differences in traditional CVD risk factor profiles between racial groups, although adjusted for statistically [Urbina 2002], could have affected results in those studies. The effects of ethnicity on our results should have been mitigated by the fact that the scans were centered on the carotid bifurcation, with the result that wall measurements of the internal as well as the common carotid arteries were taken into account. From this perspective, it seems unlikely that the increased W/OW ratio observed in HIV-infected individuals in our study is solely due to the difference in ethnic profile between the groups. We found no significant association between W/OW ratio and either abacavir or PIs. This may have been due to under-powering of the study to detect this or to the exclusion of patients susceptible to the adverse metabolic

effects of cART and/or manifesting such effects clinically, i.e. dyslipidaemia and hyperglycaemia. Since this is a cross-sectional cohort study, the observed carotid arterial wall thickening cannot be attributed to HIV-infection itself, since all patients were also on cART.

10.4.2 Conclusion

This carotid CMR study has shown evidence of premature subclinical atherosclerosis in an HIV-infected cohort with low measurable CVD risk factors. In spite of these individuals being stable on cART with effective viral load suppression, they nevertheless show earlier and greater carotid arterial wall thickening when compared to an HIV-uninfected control group. As increasing carotid intima-media thickness is independently predictive of stroke and MI in HIV-uninfected populations [Chambless 1997; O'leary 1999; Lorenz 2007], these findings suggest the rate of cardiovascular events is likely to remain high in HIV-infected individuals in spite of aggressive management of traditional CVD risk factors. The need for early detection and aggressive treatment of the early signs of CVD is therefore highlighted. Given the known association between HIV-infection and chronic low-grade inflammation and immune activation [Lo 2012], and the known adverse metabolic effects of current cART regimes [Friis-Møller 2003], the occurrence of premature subclinical atherosclerosis in the absence of traditional CVD risk factors underlines the importance of novel antiretroviral drug development.

Chapter 11

Cardiovascular Disease in young HIV-infected individuals

11.1 Introduction

In adult HIV infected individuals there is increasing evidence of early onset cardiovascular disease (CVD) and an increased risk of death from myocardial infarction [Sackoff 2006; Lohse 2007; Triant 2012]. New evidence suggests that HIV infection itself may play a large role in the aetiology of CVD [Hsue 2009]. Our study in Chapter 10 has shown evidence of premature subclinical atherosclerosis in an HIV-infected cohort with low measurable CVD risk factors where HIV and/or its treatment is likely to play a role. Antiretroviral therapy controls HIV-infection and may therefore act to reduce the risk of CVD, however there is strong evidence that antiretroviral therapy raises cholesterol levels in both adult and paediatric populations, which may reduce the potential CVD-risk benefits associated with control of the HIV infection [Rhoads 2006; Friis-Møller 2007]. Cardiovascular risk factors are aggressively managed in the adult HIV population, with patient education and medical intervention including anti-hypertensive and lipid-lowering medication. To date, however, only conservative measures, such as dietary advice, are taken in the paediatric population despite the same pattern of dyslipidaemia being seen in children as is seen in the adult HIV population [Rhoads 2006].

Research in HIV-infected children using ultrasound procedures such as flow-mediated dilatation (FMD), pulse wave velocity and C-IMT have shown conflicting, but mostly positive results suggesting accelerated atherosclerosis compared to normal controls [Bonnet 2004; Charakida 2005; McComsey 2007], although more recent studies have shown that highly active antiretroviral therapy (HAART) can reverse these abnormalities [Ross 2010; Kenny 2015]. C-IMT has the disadvantage of being one-dimensional and highly dependent on the acquisition of quality images, therefore requiring a relatively large number of study subjects. CMR overcomes many of the limitations of ultrasound by allowing a long three-dimensional segment of the carotid artery to be imaged and a measure of wall volume to be obtained. This increases the likelihood that focal plaque or localised increased C-IMT will not be missed. CMR measurements of wall area and thickness have been shown to correlate well with measurements of C-IMT [Mani 2006]. CMR also allows for endothelial function (by FMD) and vascular stiffness to be assessed [Sorenson 2002]. CMR carotid scanning has good reproducibility allowing for smaller sample sizes in clinical studies [Corti 2001; Saam 2005; Varghese 2005a].

To our knowledge, no studies using CMR assessment of carotids to document evidence of accelerated atherosclerosis in young adults with lifelong HIV infection has been carried out. We therefore undertook to assess the burden of atherosclerosis in young HIV-infected adults, and whether CMR would be a useful modality to monitor CVD status and interventional trial effectiveness in this patient group.

11.2 Methods

11.2.1 Study population

Fifty-one individuals, twenty-four HIV-infected individuals and twenty-seven HIV-uninfected controls, were recruited from the outpatient HIV unit at St Mary's Hospital, Imperial Healthcare NHS Trust, London, United Kingdom. Inclusion criteria for the HIV-infected group were being 18-24 years of age and infected with HIV from birth. Exclusion criteria were current poor health, neurocognitive impairment, current pregnancy or any contraindication to CMR. HIV-infected participants each referred an HIV-uninfected control matched by age, sex, race and smoking status. Exclusion criteria for the control group were as for the HIV-infected group plus discovery of HIV-positive status, history of cardiovascular disease, hypertension (BP>140/90), diabetes, hypercholesterolaemia (total cholesterol >5 mmol/L), or a family history of cardiovascular disease in a first degree relative (male <55years; female <65years).

All participants completed a questionnaire on their family history and underwent a clinical examination including blood pressure, weight (kg), height (cm), waist and hip circumferences (cm), ECG and blood tests. All participants had lipid levels measured and HIV-infected individuals also had glucose levels, full blood count, CD4+ count and viral load measured, as well as urinary protein/creatinine ratio. Control subjects, after consent was obtained, were counseled and a HIV test performed. Eight HIV-infected individuals were excluded due to not completing the CMR scan. Eleven controls were excluded: 1 underlying medical condition not known at enrolment, 3 raised cholesterol results, and 7 did not complete the CMR scan.

11.2.2 CMR protocol

CMR was performed using a 3.0T scanner (Siemens Skyra, Erlangen, Germany) and a purpose-built bilateral four-channel phased-array carotid surface coil (Machnet BV, Eelde, the Netherlands), with the head and neck immobilised, at the Cardiovascular Biomedical Research Unit, Royal Brompton Hospital, London, United Kingdom. The CMR protocol is described in Sections 7.1.2 and 7.1.3, Imaging protocols. Briefly, a contiguous stack of 20 high-resolution T1-weighted fast spin echo (FSE) images, centred on the carotid bifurcation bilaterally, was acquired approximately perpendicular to the longitudinal axis of both common

carotid arteries, giving 40 mm of longitudinal coverage per artery. Brachial artery reactivity (to assess FMD) was carried out using a previously validated CMR protocol [Sorenson 2002]. The CMR protocol is described in Section, 7.2 Imaging protocol. CMR image analysis, whilst blinded to all parameters, was performed off-line by me using dedicated software (Atheroma Tools, a plug-in of CMR tools, Cardiovascular Imaging Solutions, London, UK) as described in Sections 7.1.2, 7.1.3 and 7.2, Image analyses. A visual assessment was made for the presence or absence of atherosclerotic plaque.

11.2.3 Sample size and statistical analysis

Carotid CMR has been shown to have good inter-study reproducibility with a coefficient of variation of 4.6% [Varghese 2005a] and measurement error of 5.8% for wall volume and 3.2% for W/OW ratio [Saam 2005]. Power analysis based on these measurement errors shows that a study with fourteen subjects in each group could detect a 5% change in W/OW ratio and a 10% change in wall volume between the groups [Saam 2005]. Sixteen subjects were therefore recruited for each of our study groups.

Statistical analysis was done using SPSS version 22 by Dr Margaret Rhoads. Categorical data were presented as numbers and percentages, and comparisons made using the chi-squared or Fishers Exact test. Continuous variables were assessed for normal distribution by the Kolmogorov-Smirnov statistic. Normally distributed data were presented as a mean (standard deviation) and compared using a 2-sample independent t-test. Non-normally distributed data were presented as median values and inter-quartile ranges (IQR) and comparisons done using the Mann-Whitney test.

11.3 Results

11.3.1 Subject characteristics

Table 11.1 shows the demographic data for the HIV-infected and HIV-uninfected control groups. There was a small but significant difference in age between the groups, with a higher age in the control group (p=0.048), and in ethnicity, with all in the HIV-infected group being Black African as opposed to only 62.5% in the control group (p=0.007); the remaining control subjects were Black Caribbean. There were no significant differences between the groups with regards to smoking history, alcohol consumption or illicit drug use. Anthropometric measurements, heart rate and blood pressure were similar between the groups. ECGs were normal for axis and LVH criteria by the Sokolow-Lyon and Cornell Indices in all participants, with a difference only seen in the Cornell Index between the groups.

Lipid measurements were non-fasting. All HIV-uninfected controls had total cholesterol levels <5mmol/L; one HIV-infected subject had a total cholesterol level >5mmol/L. A low HDL-cholesterol (<1.2mmol/L) was seen in five controls and eight HIV-infected subjects (p=0.347). One subject in each group had an LDL-cholesterol level >3.0mmol/L; no subjects had a non-HDL level >4.0mmol/L, TC/HDL ratio >6.0mmol/L, or triglyceride levels >4.0mmol/L. No significant differences were found for lipid measurements between the groups. Triglycerides were excluded from analysis as results were non-fasting and their levels fluctuate widely with eating.

Characteristics specific to the HIV-infected group are shown in Table 11.2. Three (18.8%) of the HIV-infected individuals were long-term non-progressors (LTNPs) and therefore not on HAART. Eleven (68.8%) were currently on HAART of which 9 (56.25 %) were on a protease inhibitor (PI) and 1 (6.25%) was on Abacavir. Eleven (68.8%) participants had received a PI at some stage. Two (14.3%) participants had a clinical diagnosis of lipodystrophy and were also not currently on HAART, although they had been previously.

The median viral load (VL) was 106 copies/ml (IQR 50, 1074). The median CD4 count was 500 cells/μL (IQR 400, 679.5). There were two missing CD4 nadirs on patients who started antiretroviral therapy out of the UK and the median CD4 nadir of the remaining fourteen subjects was 270 cells/μL (IQR 142.5, 492.5). The median urinary protein/creatine ratio was 12.05 (IQR 11.03, 13.78).

11.3.2 Carotid CMR

Although there was a trend towards smaller vessels with a greater W/OW in the HIV-infected group, driven by the smaller lumen volume, the difference was not significant (Table 11.3). Wall volume was not increased in the HIV-infected group. When the three LTNPs, who had not been exposed to the effects of HAART, were removed from the analysis, the differences between the groups reduced even further – mean lumen volume p=0.170; mean wall volume p=0.682; mean vessel volume p=0.170; W/OW p=0.199.

Table 11.1 Demographic characteristics including clinical and laboratory parameters.

	HIV-infected subjects (n=16)	Control subjects (n=16)	*p*
Age (years)	20.29 (1.86)	21.60 (1.98)	**0.048**
Sex n (%)			
- Female	11 (68.8)	11 (68.8)	n/s
- Male	5 (31.3)	5 (31.3)	
Ethnicity n (%)			
- Black African	16 (100)	10 (62.5)	**0.007**
- Black Caribbean	0 (0)	6 (37.5)	
Smoking status			
- Current	3 (18.8)	3 (18.8)	
- Ex-smoker	1 (6.3)	1 (6.3)	n/s
- Never	12 (75.0)	12 (75.0)	
Alcohol consumption n (%)			
- Yes	12	14	n/s
- No	4	2	
Drug use n (%)			
- Cannabis	5 (31.3)	5 (31.3)	n/s
- Cocaine	0 (0)	0 (0)	n/s
Height (cm)	165.9 (11.4)	169.0 (7.56)	n/s
Weight (kg)	64.6 (9.16)	69.3 (11.44)	n/s
Body Mass Index	23.7 (4.36)	24.3 (4.32)	n/s
Waist Circumference (cm)	72.8 (70.50, 79.0)	73.9 (71.25, 85.38)	n/s
Hip Circumference (cm)	92.0 (87.25, 101.25)	102 (93.0, 107.88)	n/s
Waist/Hip Ratio	0.79 (0.74, 0.85)	0.77 (0.72, 0.80)	n/s
Heart rate (bpm)	70 (13.68)	70.9 (11.84)	n/s
Blood pressure (mmHg)			
- Mean arterial	82.4 (6.56)	83.4 (8.96)	
- Systolic	112.8 (9.24)	116.0 (12.84)	n/s
- Diastolic	66.9 (6.64)	66.6 (7.92)	
ECG axis (degree)	56.4 (29.72)	59.6 (15.48)	n/s
ECG LVH criteria			
- Sokolow-Lyon Index	27.9 (9.6)	28.5 (9.2)	n/s
- Cornell ECG Criteria	14.8 (7.84)	10.2 (5.72)	**0.027**
Total Cholesterol (mmol/L)	4.00 (0.62)	3.58 (0.76)	n/s
HDL Cholesterol (mmol/L)	1.27 (0.39)	1.25 (0.35)	n/s
LDL Cholesterol (mmol/L)	2.29 (0.58)	1.97 (0.74)	n/s
Non-HDL cholesterol (mmol/L)	2.67 (0.60)	2.33 (0.66)	n/s
TC/HDL ratio (mmol/L)	3.36 (0.91)	3.01 (0.83)	n/s

Values are numbers (percentages) for categorical variables, mean (standard deviation) for normally distributed continuous variables or median (interquartile range) for non-normally distributed continuous variables.

Table 11.2. HIV-infected group characteristics.

Parameter	
Glucose (mmol/L)	4.69 (0.16)
Urinary protein/creatinine ratio	3.67 (4.6)
Haemoglobin (g/dL)	12.3 (1.36)
Platelet count (x10^9/L)	239.1 (60.4)
HIV viral load (copies/ml)	106 (IQR 50.0, 1074.0)
CD4+ cell	
- Count (cells/μL)	513.4 (217.6)
- Nadir (cells/μL)	325.5 (236.8)
- Percentage (%)	26.4 (10.36)
Protease inhibitor use n (%)	
- Current	9 (56.3)
- Ever	11 (68.8)
Currently on HAART n (%)	11 (68.8)
Currently on abacavir n (%)	1 (6.3)
Long-term non-progressor n (%)	3 (18.8)
Lipodystrophy n (%)	2 (14.3)

Values are numbers (percentages) for categorical variables, mean (standard deviation) for normally distributed continuous variables or median (interquartile range) for non-normally distributed continuous variables.

Table 11.3. Carotid CMR measurements in HIV-infected and control subjects.

	HIV-infected subjects (n=16)	Control subjects (n=16)	*p*
Mean lumen volume (mm^3)	1155.22 (939.82, 1294.13)	1258.77 (1150.07, 1506.44)	0.055
Mean wall volume (mm^3)	735.91 (665.98, 840.36)	754.24 (722.73, 868.10)	0.498
Mean vessel volume (mm^3)	1891.72 (1617.36, 2124.85)	2031.09 (1904.08, 2329.50)	0.083
W/OW Ratio (%)	41.0 (37.8, 42.1)	38.7 (37.3, 39.7)	0.055
Distensibility (%)			
- Left carotid	30.1 (26.0, 44.8)	32.0 (28.6, 38.5)	0.96
- Right carotid	34.7 (28.3, 42.1)	32.9 (29.1, 40.1)	0.68

Values are median (interquartile range).

11.4 Discussion

The increased risk of CVD associated with HIV-infection in adults [Sackoff 2006; Lohse 2007; Triant 2012], as well as the increased risk seen in those with interruption of continuous HAART [El-Sadr 2006] and in LTNPs [Hsue 2009], suggests that HIV-infection itself plays a role in the increased CVD risk. This has implications for all those with HIV-infection, but is particularly pertinent in children and young adults living with HIV-infection whose CVD risk management has been mainly conservative up until now.

This carotid CMR study demonstrates that young adults with perinatally acquired HIV-infection do not demonstrate evidence of early CVD compared with age, sex and ethnically matched controls. This is reassuring, given the increased rates of CVD seen among HIV-infected adults who generally acquired HIV after childhood [Sackoff 2006; Lohse 2007; Triant 2012], and suggests that current treatment strategies with HAART in paediatric populations have not increased the risk of CVD as these patients enter adulthood. This is in keeping with recent studies that have demonstrated that abnormalities in the CVD surrogates of C-IMT and pulse wave velocity (a measure of vascular function) reverse with continuous HAART [Ross 2010; Kenny 2015]. This suggests that HIV-infected children and young adults may be at increased CVD risk, but that continuous HAART with good viral suppression can arrest and possibly normalise this risk.

The trend to an increased W/OW ratio in the current study disappeared when LTNPs were excluded from the analysis. Although only three in number, therefore making firm conclusions impossible, this is in keeping with previous ultrasound based studies that have shown C-IMT in HIV-controllers to be similar to that of HIV-infected individuals with detectable viraemia not on antiretrovirals, and higher than C-IMT in HIV-uninfected controls [Hsue 2009]. Despite maintaining CD4+ cell counts, ongoing chronic inflammation, immune activation and low-level viraemia has been shown to persist in LTNPs and HIV-controllers [Hsue 2009; Pereyra 2009; Pereyra 2012] and may account for the observed higher C-IMT in these groups.

The similar carotid wall thickness seen between HIV-infected and HIV-uninfected young adults in this study conflicts with that observed in studies in adult HIV-infected cohorts [Hsue 2004; Rose 2016], but is similar to that observed in other studies where no significant differences were found in C-IMT between HIV-infected and HIV-uninfected controls, although the development of focal carotid plaque was greater in the HIV-infected cohorts [Hanna 2015]. Possible mechanisms for these differences may include a change in physiology in older adults were the initial vascular insult mediated by HIV-infection is not fully reversed by

HAART, or differences in compliance and risk behaviour between younger and older cohorts which may result in HIV resistance or re-infection with resistant strains, necessitating 2nd and 3rd line antiretroviral regimens to be initiated. The development of immunosenescence in HIV-infected adults, which may increase susceptibility to the adverse metabolic effects of HAART or allow the deleterious vascular effects of HIV-infection to be more pronounced, may also play a role, and immune and cellular senescence has been found to be associated with atherosclerosis [Spyridopoulos 2009; Kaplan 2011; Wang 2012].

Both protease inhibitors (PIs) and non-nucleoside reverse transcriptase inhibitors (NNRTIs) have been associated with adverse metabolic effects including lipodystrophy, insulin resistance, and dyslipidaemia (including raised LDL-cholesterol), in paediatric populations [Rhoads 2006; Rhoads 2011, Barlow-Mosha 2013]. In adult HIV-infected cohorts, conflicting results have been found between the association of CVD risk and antiretrovirals - the DAD study [Friis-Møller 2003] found indinavir, abacavir and lopinavir to be independently associated with increased CVD risk, and PIs have been associated with increased C-IMT [Seminari 2002] and carotid plaques [Maggi 2000], but other studies have failed to find an association between PIs and increased C-IMT [Mercie 2002; Hsue 2004].

Hence, although HIV-infection may be associated with increased CVD risk in adult cohorts, via mechanisms which have yet to be fully elucidated, young adults who acquired their HIV infection perinatally and who receive HAART do not demonstrate abnormalities suggesting early atherosclerosis compared to matched controls. This is reassuring and supports the argument that early diagnosis and treatment of children with HIV is warranted in order to induce viral suppression and reduce immune activation. The selection of metabolically friendly HAART regimens should however be paramount, as should education about the increased CVD risk of HIV-infection in adulthood and the identification and management of traditional CVD risk factors.

11.4.1 Study limitations

Based on the magnitude of changes observed in previous studies of other disease populations (e.g. Takayasu's arteritis [Keenan 2009b] and studies which calculated the cohort size required to detect a given treatment effect in CMR carotid wall volume parameters [Saam 2005], this study was adequately powered. However, the numbers remain low at sixteen per group. As discussed in previous chapters in this thesis, the Saam et al. study [Saam 2005] was based on 20 patients, most displaying advanced carotid artery disease, who had a mean age of 68 years (range 52-78 years). It is therefore probable that this study may not provide an appropriate basis for the power calculation in a study of young

adults with few traditional CVD risk factors, to detect a difference or change in carotid wall volume parameters between the groups. It is possible that a larger cohort is actually required. Similarly, the study by Keenan *et al.* [Keenan 2009b], which found a significant difference between sixteen patients with Takayasu's arteritis and a normal control group, may not serve as a suitable model. Takayasu's arteritis is an inflammatory condition affecting large and medium-sized arteries, which causes a panarteritis with intimal proliferation. HIV-infection does not produce direct arterial inflammation as a major component of its disease process. The disease processes are very different and it is not clear that an adequately sized cohort to detect differences present in one disease population will serve to adequately find differences in another. The occurrence or rate of change of carotid wall volume parameters is unknown in teenagers and young adults, be they healthy or otherwise. Our study may therefore have actually been very underpowered.

Importantly, the HIV-infected group was a heterogeneous group who included three LTNPs who were HAART inexperienced, two individuals with lipodystrophy who had ceased HAART and the remainder had commenced HAART at various ages/points in their lives with HIV according to changing guidelines for HAART initiation and where in the world they were residing at the time. However, all had started HAART when the CD4 cell count had fallen to <350cells/μL. The study did not include enough LTNPs, to make substantive conclusions about them, and indeed we had not set out to look at this group specifically. The findings may therefore not apply to LTNPs or to elite controllers.

The ethnic composition and difference in ethnicity between the groups is another limitation, although this is likely to be small. This study includes only Black subjects and may therefore not be applicable to other racial groups. Studies of carotid wall thickness (C-IMT) in HIV-uninfected adults have shown a greater C-IMT in Black Americans compared with Caucasians. This however was limited to the level of the common carotid, but not the internal carotid arteries [Urbina 2002; Manolio 2008]. Comparisons between Black Africans and Black Caribbeans, many of whom have a broad range of ethnic ancestry, has not been undertaken to our knowledge, nor have the studies been carried out in young adults. The use of a length of the common and internal carotid arteries in our study should reduce the effect of small ethnic variations in carotid wall thickness (if any exist) in our results, and the fact that the 37.5% of the control group who were not Black African were all Black Caribbean should also minimise any racial variation.

Another limitation is the difference in age between the study groups. Although the absolute difference was small, it was significant, with the control subjects being older. Although the

changes in C-IMT with age in this age group are not documented, in healthy adult populations, increasing age is associated with increasing C-IMT [Keenan 2009a]. Therefore the HIV-infected group may be expected to have had a smaller wall volume and W/OW due to age alone and the lack of difference found between the groups could therefore be due to HIV-related factors. However, the difference in wall volume between groups due to age would be expected to be minimal.

11.4.2 Conclusion

This carotid CMR study in young adults with perinatally acquired HIV-infection, mostly HAART experienced and compliant, is reassuring in showing no apparent demonstrable abnormalities suggesting early atherosclerosis.

Chapter 12
General discussion, conclusions and future directions

12.1 Introduction

This thesis sought to study the presence and pattern of cardiovascular disease, particularly carotid vascular disease in two conditions with chronic inflammation and immune activation, SLE and HIV.

12.2 SLE studies

Chapter 8 sought to further define the presence and pattern of cardiovascular disease in the SLE population using CMR. It confirmed the presence of early atherosclerosis in SLE assessed by a combination of endothelial dysfunction, increased arterial stiffness as well as increased carotid arterial plaque and wall thickness. It also demonstrated the existence of significant 'silent' cardiac disease in those with no history of cardiac symptoms. In many of these patients, the only evidence of atherosclerosis was the presence of an abnormal carotid CMR, suggesting that CMR offers a way of detecting asymptomatic premature atherosclerosis in patients with SLE, improving risk stratification, and allowing targeted secondary prevention in those who have few if any traditional CVD risk factors.

In light of the cardiovascular findings by CMR in SLE patients, a randomised placebo controlled trial was undertaken, looking at the effect of rosuvastatin, a potent lipid-lowering agent, on carotid arterial wall parameters in SLE patients with no current National Cholesterol Education Program (NCEP) indication for lipid lowering. This is reported in Chapter 9. The results from this study were negative, but it is impossible to draw any robust conclusions from the outcome due to several study limitations (discussed in Chapter 9), particularly the significant under-recruitment. Despite these reservations, the study provides no evidence to suggest that the routine prescription of statins is justified in SLE patients with no current National Cholesterol Education Program (NCEP) indication for lipid lowering [Cleeman 2001].

Two sets of analyses of the CMR data obtained in Chapter 9 were carried out. The RCT study protocol had stated that the person analysing the CMR data (i.e. myself) was to coordinate and effectively run the study for the principal investigator, scan patients, but not otherwise play a direct role in patient identification, recruitment and follow-up. However, lack of adequate staffing and clinical commitments at the recruitment sites meant that there was no one available to routinely recruit and follow-up patients, resulting in my full involvement at

all stages in the trial throughout the 2-year period and my effective un-blinding. The result obtained by the observer blinded only to treatment allocation and lipid results (myself) yielded very different results (not presented), to the fully blinded observer, almost certainly caused by observer bias due to effective un-blinding, demostrating the importance of full blinding for data analysers in randomised trials. The large (for both observers) coefficients of variation seen for the carotid volume and distensibility parameters (Table(a) Appendix) were much higher than that reported previously [Corti 2001; Varghese 2005a; Varghese 2005b; Samm 2005], suggesting that our measurement modality/technique was not performing as well as expected. Intraclass correlation coefficients (Table(b) Appendix) were also lower than those previously described [Yuan 1998; Kang 2000; Saam 2005] suggesting the measurement error in our study was greater than in other studies.

These findings reinforce the use of a single observer to take measurements in a longitudinal clinical study in order to reduce the scan-to-scan error. Co-training of observers to make similar judgement calls and improvements in software to aid edge detection may minimise the interobserver variability and be of use for cohort studies where different observers may be involved, especially when using historical datasets to compare to a current cohort. The need for full blinding of observers in trials involving an element of subjectivity in image analysis is shown to be crucial. This is particularly so when any expected changes are likely to be small.

12.3 HIV studies

CMR studies of the carotid arteries in HIV are uncommon and to our knowledge the study reported in Chapter 10 is the first using CMR to assess carotid wall volume and determine the level of subclinical atherosclerosis in HIV-infected individuals with low cardiovascular risk. This has shown evidence of premature subclinical atherosclerosis despite subjects being stable on cART with good viral suppression compared with HIV-uninfected controls. As increasing C-IMT has been found to be independently predictive of future stroke and myocardial infarction in HIV-uninfected populations [Chambless 1997; O'Leary 1999; Lorenz 2007], the findings suggest that the rate of cardiovascular events is likely to remain elevated in HIV-patients despite aggressive treatment of cardiovascular risk factors. This highlights the need to detect and manage aggressively early signs of cardiovascular disease. Given the known low-grade inflammation and immune activation associated with HIV-infection [Lo 2010] and the known deleterious metabolic effects of existing cART regimens [Friis-Møller 2003], the presence of premature subclinical atherosclerosis despite the exclusion of all traditional cardiovascular risk factors highlights the need for the development of novel antiretroviral treatments.

The findings in Chapter 10 are of particular concern for perinatally infected children as both HIV-infection itself and the adverse metabolic effects of the various antiretroviral therapies have been postulated to result in the increased CVD risk seen in HIV. In Chapter 11, in the first (to our knowledge), carotid CMR study in perinatally infected young HIV adults, we undertook to assess the burden of atherosclerosis in this group and whether CMR would be a useful modality to monitor CVD status and interventional trial effectiveness. Reassuringly, in agreement with other recent studies [Ross 2010; Kenny 2015] no apparent demonstrable abnormalities suggesting early atherosclerosis were seen in a mostly HAART experienced and compliant patient group.

12.4 General limitations and conclusions

The limitations pertinent to each study are discussed in each relevant chapter, but some more generally applicable limitations were seen.

Sample size is obviously critical in any study and it is vital that the number recruited should be, at the minimum, the smallest number needed to achieve the power to detect the assumed difference between the groups being studied. In calculating the sample size, the correct patient group needs to be selected and the assumptions made for the cohort to be studied need to be correct and factored in if they are different to those seen in the groups from which the power calculations are derived. Hence, the SLE RCT in Chapter 9 was clearly under-recruited, but even at full recruitment it may have been underpowered to detect any change at 2-years, as the expected change would have been small and the higher CoVs and lower ICCs in our study may have masked any effect which may have occurred. The power calculations derived from cohorts with a different gender profile, greater traditional cardiovascular risk factors and known atherosclerosis [Varghese 2005a; Varghese 2005b; Saam 2005], would have magnified this effect. In the study of young adults infected perinatally with HIV, individuals were paired which helped to reduce the difference between the groups, however as the numbers recruited were based on the differences seen in other patient groups, including those where the presence of vascular inflammation is a common part of the disease process, our sample size may again have been too small, increasing the chances of a false negative result. The adult HIV cohort was again a small study, but the power calculation for it was derived from the changes in carotid volume changes seen with age in a healthy population [Keenan 2009a] and the numbers recruited met the ones required for the power calculation, except amongst older females. This study was small but confirmed the findings of a recent study using C-IMT by ultrasound where the C-IMT increase with age in the HIV cohort exceeded that seen in the HIV-uninfected controls [Fitch 2013].

The need to carefully train and co-train in the analysis of CMR images is exemplified by the high CoVs and low ICCs seen in this thesis. Failure to do so will result in the need for greater numbers of recruits into CMR studies to achieve adequate power, something that is undesirable as the ability to use small sample sizes is one of the advantages of CMR. Measurement differences can occur by changes in the level setting and windowing used to view and analyse images, which can be critical for visual edge detection, and these should be standardised as much as possible with environmental light factors and screen resolution kept constant. These measures should help to reduce both intra and inter-observer variation in studies performed at the same centre. Improvements in edge detection software may also help.

In comparing cohorts, either historical or contemporary, who are matched for sex and age, W/OW ratio is used to account for differences in absolute vessel volumes due to body size. It would be interesting to see if adjusting for BSA as is routinely done for cardiac parameters would provide a better measure.

Lastly the possibility that CMR of the carotid artery was not the correct modality to use, at least in the SLE RCT in Chapter 9 needs to be considered. Although we found that wall volume and W/OW were increased in individuals with SLE in Chapter 8, Figure 8.2 shows most individuals lay within 2SD of the mean of the healthy non-SLE cohort. As the SLE cohort in Chapter 8 included a few individuals with known CVD or with increased CVD risk, it may be that they are the ones producing the significant difference. It would be interesting to see what the difference between the SLE cohort and the controls is when these known CVD/high CVD risk SLE subjects are removed. It may also be necessary to take into account the difference between the pathophysiology of calcified plaques, carotid wall thickening (due to increased fibrous tissue without discrete plaque formation) and lipid-rich coronary plaques (which cause the increased coronary artery risk seen in the SLE and HIV cohorts). Any therapies aimed at reducing this risk may show no demonstrable change in the carotid artery despite have a clinical effect in the coronary territory. This limitation would also apply in other conditions with increased coronary risk, for example HIV, when the cardiovascular effects of drug therapy were being assessed and carotid CMR imaging was used.

In conclusion, CMR provides a valuable non-invasive and well-tolerated imaging modality to quantify the degree and nature of cardiovascular disease in different patient groups. It can serve as an accurate and reproducible test but a clear understanding of its limitations and the need for careful co-training of observers in and between study centres is required to produce low measurement errors and allow for the comparison of results. Understanding of the

various pathophysiological changes occurring in different disease processes and patient sub-groups within these diseases, and the effect on these processes on the carotid arterial wall in terms of plaque formation and remodelling, needs to be understood before employing carotid arterial parameters as cardiovascular surrogates for assessing the effect of established or novel treatments on CVD risk.

12.5 Future directions

It would be interesting to see whether an increased number of subjects recruited into a placebo controlled trial of statin therapy in SLE for a longer period of study duration would achieve any measureable changes in carotid wall parameters. This would require a larger multi-centre study to enable sufficient numbers of suitable patients to be enrolled and should use a core-lab to analyse the fully blinded CMR data with removal of all possible confounders including patient sex and scan date. The additional assessment of endothelial function by FMD as well as arterial stiffness should be included and a panel of disease specific biomarkers plus biomarkers associated with increased cardiovascular risk in other patient cohorts should be included in an attempt to define which could be used in SLE patients with a similar risk profile to improve risk stratification for SLE.

It would be interesting to see what improvement in carotid vessel volume reproducibility could be achieved by obtaining results from 2+ observers who have had some instruction and experience in analysing carotid wall images. The observers would then be co-trained to make the same assumptions with regards to edge detection and image windowing under standardised environmental conditions. The results before and after training could then be compared.

In the HIV cohorts studied, it would be interesting to see what changes do or do not develop in carotid artery parameters of the young perinatally infected cohort by restudying them and their controls in the future. Whether they come to resemble the adult cohort studied in this thesis and demonstrate increased wall volume as they age over and above that expected, or whether they continue to show no significant differences compared to controls might provide insights into how HIV-infection itself and the current HAART are affecting CVD risk in this group. This could provide a basis for the need to develop novel therapies and provide further intervention to modify CVD risk. The assessment of endothelial function in such a group and how it changes over time compared with controls would also be of interest.

In the adult HIV cohort, who were all low risk for CVD based on traditional risk factors, assessment of other parameters of vascular health such as endothelial function and

assessment of cardiac structure and function by CMR would be of interest. The increased prevalence of cardiac steatosis, fibrosis and dysfunction has been observed in HIV-infected subjects compared to controls [Holloway 2013]. The HIV cohort in that study was more heterogeneous and included individuals with a higher risk for CVD than in the study in this thesis and it would be interesting to see whether some of these findings are specific to HIV-infection and its treatment and occur in an otherwise low-risk cohort. It would also be of interest to assess the burden and character of coronary artery disease in an otherwise low risk HIV group as, from what we have seen in the SLE RCT in Chapter 9, the pathophysiology of atherosclerosis in HIV may vary between the carotid and coronary territories, and this would have implications for future studies looking at the modification of imaging parameters by interventional therapies. Coronary artery atherosclerosis would be better imaged by CT coronary angiography than CMR due to the better resolution achieved with the former, and if significant abnormalities were found which are more likely to undergo change with treatment than carotid parameters, the radiation exposure could be justified in longitudinal studies. Again, the development of a disease-specific biochemical panel that could be correlated to structural and functional changes in vascular parameters, and could be used to risk stratify CVD risk and measure treatment effect, would be of great benefit in the management of HIV-infected individuals.

Chapter 13
References

Adelman MK, Marchalonis JJ.Endogenous retroviruses in systemic lupus erythematosus: candidate lupus viruses. Clin Immunol. 2002; 102: 107-116.

Altorok N, Sawalha AH. Epigenetics in the pathogenesis of systemic lupus erythematosus. Curr Opin Rheumatol. 2013; 25: 569-576.

Ambrose JA, Tannenbaum MA, Alexopoulos D, Hjemdahl-Monsen CE, Leavy J, Weiss M, Borrico S, Gorlin R, Fuster V. Angiographic progression of coronary artery disease and the development of myocardial infarction. J Am Coll Cardiol. 1988; 12: 56-62.

Amento EP, Ehsani N, Palmer H, Libby P. Cytokines and growth factors positively and negatively regulate interstitial collagen gene expression in human vascular smooth muscle cells. Arterioscler Thromb. 1991; 11: 1223-1230.

Anania C, Gustafsson T, Hua X, Su J, Vikström M, de Faire U, Heimbürger M, Jogestrand T, Frostegård J. Increased prevalence of vulnerable atherosclerotic plaques and low levels of natural IgM antibodies against phosphorylcholine in patients with systemic lupus erythematosus. Arthritis Res Ther. 2010; 12: R214.

Aqel NM, Ball RY, Waldmann H, Mitchinson MJ. Identification of macrophages and smooth muscle cells in human atherosclerosis using monoclonal antibodies. J Pathol. 1985; 146: 197-204.

Arbuckle MR, McClain MT, Rubertone MV, Scofield RH, Dennis GJ, James JA, Harley JB. Development of autoantibodies before the clinical onset of systemic lupus erythematosus. N Engl J Med. 2003; 349:1526-1533.

Ardlie NG, Selley ML, Simons LA. Platelet activation by oxidatively modified low density lipoproteins. Atherosclerosis. 1989; 76: 117-24.

Arildsen H, Sørensen KE, Ingerslev JM, Østergaard LJ, Laursen AL. Endothelial dysfunction, increased inflammation, and activated coagulation in HIV-infected patients improve after initiation of highly active antiretroviral therapy. HIV Med. 2013; 14: 1-9.

Asanuma Y, Oeser A, Shintani AK, Turner E, Olsen N, Fazio S, Linton MF, Raggi P, Stein CM. Premature coronary-artery atherosclerosis in systemic lupus erythematosus. N Engl J Med. 2003; 349: 2407-2415.

Bakker-Arkema RG , Davidson MH, Goldstein RJ, Davignon J, Isaacsohn JL, Weiss SR, Keilson LM, Brown WV, Miller VT, Shurzinske LJ, Black,DM. Efficacy and Safety of a New HMG-CoA Reductase Inhibitor, Atorvastatin, in Patients With Hypertriglyceridemia. JAMA. 1996; 275: 128-133.

Ballard KD, Lorson L, White CM, Thompson PD, Taylor BA. Effect of Simvastatin on Arterial Stiffness in Patients with Statin Myalgia. Adv Prev Med. 2015; 2015: 351059.

Barbhaiya M, Costenbader KH. Ultraviolet radiation and systemic lupus erythematosus. Lupus. 2014; 23: 588-595.

Barlow-Mosha L, Eckard AR, McComsey GA, Musoke PM. Metabolic complications and treatment of perinatally HIV-infected children and adolescents. J Int AIDS Soc. 2013; 16: 18600.

Barter PJ, Brandrup-Wognsen G, Palmer MK, Nicholls SJ. Effect of statins on HDL-C: a complex process unrelated to changes in LDL-C: analysis of the VOYAGER Database. J Lipid Res. 2010; 51(6): 1546-1553.

Belcaro G, Nicolaides AN, Laurora G, Cesarone MR, De Sanctis M, Incandela L, Barsotti A. Ultrasound morphology classification of the arterial wall and cardiovascular events in a 6-year follow-up study. Arterioscler Thromb Vasc Biol. 1996; 16: 851-856.

Bellosta S, Via D, Canavesi M, Pfister P, Fumagalli R, Paoletti R, Bernini F. HMG-CoA Reductase Inhibitors Reduce MMP-9 Secretion by Macrophages. Arterioscler Thromb Vasc Biol. 1998; 18: 1671-1678.

Bellosta S, Ferri N, Bernini F, Paoletti R, Corsini A. Non-lipid-related effects of statins. Ann Med. 2000; 32: 164-176.

Benvenuti F, Gatto M, Larosa M, Iaccarino L, Punzi L, Doria A.Cardiovascular risk factors, burden of disease and preventive strategies in patients with systemic lupus erythematosus: a literature review. Expert Opin Drug Saf. 2015; 14: 1373-1385.

Bernatsky S, Boivin JF, Joseph L, Manzi S, Ginzler E, Gladman DD, Urowitz M, Fortin PR, Petri M, Barr S, Gordon C, Bae SC, Isenberg D, Zoma A, Aranow C, Dooley MA, Nived O, Sturfelt G, Steinsson K, Alarcón G, Senécal JL, Zummer M, Hanly J, Ensworth S, Pope J, Edworthy S, Rahman A, Sibley J, El-Gabalawy H, McCarthy T, St Pierre Y, Clarke A, Ramsey-Goldman R. Mortality in systemic lupus erythematosus. Arthritis Rheum. 2006; 54: 2550-2557.

Bhatnagar P, Wickramasinghe K, Williams J, Rayner M, Townsend N. The epidemiology of cardiovascular disease in the UK 2014. Heart. 2015; 101(15): 1182-1189.

Bijl M, Kallenberg CG. Ultraviolet light and cutaneous lupus. Lupus. 2006; 15: 724-727.

Bild DE, Bluemke DA, Burke GL, Detrano R, Diez Roux AV, Folsom AR, Greenland P, Jacob DR Jr, Kronmal R, Liu K, Nelson JC, O'Leary D, Saad MF, Shea S, Szklo M, Tracy RP. Multi-Ethnic Study of Atherosclerosis: objectives and design. Am J Epidemiol. 2002; 156: 871-881.

Bisoendial RJ, Hovingh GK, Levels JHM, Radjesh J. Bisoendial, MD; G. Kees Hovingh, MD; Johannes H.M. Levels, PhD; Lerch PG, Andresen I, Hayden MR, Kastelein JJP, Stroes ESG. Restoration of endothelial function by increasing high-density lipoprotein in subjects with isolated low high-density lipoprotein. Circulation. 2003; 107: 2944-2948.

Björnådal L, Yin L, Granath F, Klareskog L, Ekbom A. Cardiovascular disease a hazard despite improved prognosis in patients with systemic lupus erythematosus: results from a Swedish population based study 1964-95. J Rheumatol. 2004; 31: 713-719.

Blake GJ, Ridker PM. Inflammatory bio-markers and cardiovascular risk prediction. J Intern Med. 2002; 252: 283-294.

Blanco-Colio LM, Martin-Ventura JL, de Teresa E, Farsang C, Gaw A, Gensini G, Leiter LA, Langer A, Martineau P, Egido J, on behalf of the ACTFAST investigators. Elevated ICAM-1 and MCP-1 plasma levels in subjects at high cardiovascular risk are diminished by atorvastatin treatment. Atorvastatin on Inflammatory Markers study: A substudy of Achieve

Cholesterol Targets Fast with Atorvastatin Stratified Titration. Am Heart J. 2007; 153: 881-888.

Blankenhorn DH, Azen SP, Kramsch DM, Mack WJ, Cashin-Hemphill L, Hodis HN, DeBoer LWV, Mahrer PR, Masteller MJ, Vailas LI, Alaupovic P, Hirsch LJ and the MARS Research Group. Coronary angiographic changes with lovastatin therapy. The Monitored Atherosclerosis Regression Study (MARS). Ann Intern Med. 1993; 119: 969-976.

Blausen.com staff. "Blausen gallery 2014". Wikiversity Journal of Medicine. DOI:10.15347/wjm/2014.010. ISSN 20018762.

Boackle SA. Advances in lupus genetics. Curr Opin Rheumatol. 2013; 25: 561-568.

Bobik A. Apolipoprotein CIII and atherosclerosis: beyond effects on lipid metabolism. Circulation. 2008; 118:702-704.

Bombardier C, Gladman DD, Urowitz MB, Caron D, Chang CH. Derivation of the SLEDAI. A disease activity index for lupus patients. The Committee on Prognosis Studies in SLE. Arthritis Rheum. 1992; 35: 630-640.

Bonetti PO, Lerman LO, Lerman A. Endothelial dysfunction: a marker of atherosclerotic risk. Arterioscler Thromb Vasc Biol. 2003; 23: 168-175.

Bonnet D, Aggoun Y, Szezepanski I, Bellal N, Blanche S. Arterial stiffness and endothelial dysfunction in HIV-infected children. AIDS. 2004; 18: 1037-1041.

Botnar RM, Perez AS, Witte S, Wiethoff AJ, Laredo J, Hamilton J, Quist W, Parsons EC Jr, Vaidya A, Kolodziej A, Barrett JA, Graham PB, Weisskoff RM, Manning WJ, Johnstone MT. In vivo molecular imaging of acute and subacute thrombosis using a fibrin-binding magnetic resonance imaging contrast agent. Circulation. 2004; 109: 2023-2029.

Brown TT, Tassiopoulos K, Bosch RJ, Shikuma C, McComsey GA. Association between systemic inflammation and incident diabetes in HIV-infected patients after initiation of antiretroviral therapy. Diabetes Care. 2010; 33: 2244-2249.

Bruce IN, Burns RJ, Gladman DD, Urowitz MB. Single photon emission computed tomography dual isotope myocardial perfusion imaging in women with systemic lupus

erythematosus. I. Prevalence and distribution of abnormalities. J Rheumatol. 2000; 27: 2372-2377.

Bruce IN, Urowitz MB, Gladman DD, Ibañez D, Steiner G. Risk factors for coronary heart disease in women with systemic lupus erythematosus: the Toronto Risk Factor Study. Arthritis Rheum. 2003; 48: 3159-3167.

Bucher HC, Richter W, Glass TR, Magenta L, Wang Q, Cavassini M, Vernazza P, Hirschel B, Weber R, Furrer H, Battegay M, Bernasconi E. Small dense lipoproteins, apolipoprotein B, and risk of coronary events in HIV-infected patients on antiretroviral therapy: the Swiss HIV Cohort Study. J Acquir Immune Defic Syndr. 2012;60:135-142.

Buss SJ, Wolf D, Korosoglou G, Max R, Weiss CS, Fischer C, Schellberg D, Zugck C, Kuecherer HF, Lorenz HM, Katus HA, Hardt SE, Hansen A. Myocardial left ventricular dysfunction in patients with systemic lupus erythematosus: new insights from tissue Doppler and strain imaging. J Rheumatol. 2010; 37: 79-86.

Cai JM, Hatsukami TS, Ferguson MS, Small R, Polissar NL, Yuan C. Classification of human carotid atherosclerotic lesions with in vivo multicontrast magnetic resonance imaging. Circulation. 2002; 106: 1368-1373.

Cai J, Hatsukami TS, Ferguson MS, Kerwin WS, Saam T, Chu B, Takaya N, Polissar NL, Yuan C. In vivo quantitative measurement of intact fibrous cap and lipid-rich necrotic core size in atherosclerotic carotid plaque: comparison of high-resolution, contrast-enhanced magnetic resonance imaging and histology. Circulation. 2005; 112: 3437-3444.

Calmy A, Gayet-Ageron A, Montecucco F, Nguyen A, Mach F, Burger F, Ubolyam S, Carr A, Ruxungtham K, Hirschel B, Ananworanich J, on behalf of the STACCATO Study Group. HIV increases markers of cardiovascular risk: results from a randomized, treatment interruption trial. AIDS. 2009; 23: 929-939.

Caricchio R, McPhie L, Cohen PL. Ultraviolet B radiation-induced cell death: critical role of ultraviolet dose in inflammation and lupus autoantigen redistribution. J Immunol. 2003; 171: 5778-5786.

Castelli WP. Epidemiology of coronary heart disease: the Framingham study. Am J Med. 1984; 76: 4-12.

Catalano O, Antonaci S, Opasich C, Moro G, Mussida M, Perotti M, Calsamiglia G, Frascaroli M, Baldi M, Cobelli F. Intra-observer and interobserver reproducibility of right ventricle volumes, function and mass by cardiac magnetic resonance. J Cardiovasc Med (Hagerstown). 2007; 8: 807-814.

Cavalcante JL, Lima JA, Redheuil A, Al-Mallah MH. Aortic stiffness: current understanding and future directions. J Am Coll Cardiol. 2011; 57: 1511-1522.

Celermajer DS, Sorensen KE, Gooch VM, Spiegelhalter DJ, Miller OI, Sullivan ID, Lloyd JK, Deanfield JE. Non-invasive detection of endothelial dysfunction in children and adults at risk of atherosclerosis. Lancet. 1992; 340: 1111-1115.

Centers for Disease Control (CDC). Pneumocystis pneumonia - Los Angeles. MMWR Morb Mortal Wkly Rep. 1981a; 30(21):250-252.

Centers for Disease Control (CDC). Kaposi's sarcoma and Pneumocystis pneumonia among homosexual men--New York City and California. MMWR Morb Mortal Wkly Rep. 1981b; 30(25):305-308.

Centers for Disease Control and Prevention. HIV Surveillance Report, 2014; vol. 26. http://www.cdc.gov/hiv/library/reports/surveillance/. Published November 2015. [Accessed 06/03/2016].

Chambers SA, Rahman A, Isenberg DA. Treatment adherence and clinical outcome in systemic lupus erythematosus. Rheumatology (Oxford). 2007; 46: 895-898.

Chambless LE, Heiss G, Folsom AR, Rosamond W, Szklo M, Sharrett AR, Clegg LX. Association of coronary heart disease incidence with carotid arterial wall thickness and major risk factors: the Atherosclerosis Risk in Communities (ARIC) Study, 1987-1993. Am J Epidemiol. 1997; 146: 483-494.

Chan CF, Keenan N, Lightman S, Haskard D, Pennell DJ. Interferon-□ reduces early atherosclerosis in patients with Behcet's syndrome. doi:10.1136/heartjnl-2011-300920b.54.

Charakida M, Donald AE, Green H, Storry C, Clapson M, Caslake M, Dunn DT, Halcox JP, Gibb DM Klein NJ, Deanfield JE. Early structural and functional changes of the vasculature in

HIV-infected children: impact of disease and antiretroviral therapy. Circulation. 2005; 112: 103-109.

Cheng C, Tempel D, van Haperen R, van der Baan A, Grosveld F, Daemen MJAP, Krams R, de Crom R. Atherosclerotic lesion size and vulnerability are determined by patterns of fluid shear stress. Circulation. 2006; 113: 2744-2753.

Chin JH, Azhar S, Hoffman BB. Inactivation of endothelial derived relaxing factor by oxidized lipoproteins. J Clin Invest. 1992; 89: 10-18.

Chong Y, Ikematsu H, Kikuchi K, Yamamoto M, Murata M, Nishimura M, Nabeshima S, Kashiwagi S, Hayashi J. Selective CD27+ (memory) B cell reduction and characteristic B cell alteration in drug-naive and HAART-treated HIV type 1-infected patients. AIDS Res Hum Retroviruses. 2004; 20: 219-226.

Choudhury RP, Fuster V, Fayad ZA. Molecular, cellular and functional imaging of atherothrombosis. Nat Rev Drug Discov. 2004; 3: 913 -925.

Chow PC, Ho MH, Lee TL, Lau YL, Cheung YF. Relation of arterial stiffness to left ventricular structure and function in adolescents and young adults with pediatric-onset systemic lupus erythematosus. J Rheumatol. 2007; 34: 1345-1352.

Chu B, Kampschulte A, Ferguson MS, Kerwin WS, Yarnykh VL, O'Brien KD, Polissar NL, Hatsukami TS, Yuan C. Hemorrhage in the atherosclerotic carotid plaque: a high-resolution MRI study. Stroke. 2004; 35: 1079-1084.

Chung CP, Oeser A, Avalos I, Raggi P, Stein CM. Cardiovascular risk scores and the presence of subclinical coronary artery atherosclerosis in women with systemic lupus erythematosus. Lupus. 2006; 15: 562-569.

Chung DW, Chen J, Ling M, Fu X, Blevins T, Parsons S, Le J, Harris J, Martin TR, Konkle BA, Zheng Y, López JA. High-density lipoprotein modulates thrombosis by preventing von Willebrand factor self-association and subsequent platelet adhesion Blood. 2016;127: 637-645.

Cleeman JI, et al. Executive summary of the third report of the National Cholesterol Education Program (NCEP) expert panel on detection, evaluation, and treatment of high blood cholesterol in adults (ATPIII). JAMA. 2001; 285: 2486-2497.

Cohen AS, Reynolds WE, Franklin EC, Kulka JP, Ropes MW, Shulman LE, et al. Preliminary criteria for the classification of systemic lupus erythematosus. Bull Rheum Dis. 1971; 21: 643–648.

Cooney CM, Bruner GR, Aberle T, Namjou-Khales B, Myers LK, Feo L, Li S, D'Souza A, Ramirez A, Harley JB, Scofield RH. 46,X,del(X)(q13) Turner's Syndrome Female with Systemic Lupus Erythematosus in a Pedigree Multiplex for SLE. Genes Immun. 2009; 10: 478–481.

Cooper GS, Dooley MA, Treadwell EL, St Clair EW, Gilkeson GS.Risk factors for development of systemic lupus erythematosus: allergies, infections, and family history. J Clin Epidemiol. 2002; 55: 982-989.

Corti R, Fayad ZA, Fuster V, Worthley SG, Helft G, Chesebro J, Mercuri M, Badimon J. Effects of lipid-lowering by simvastatin on human atherosclerotic lesions: A longitudinal study by high-resolution, noninvasive magnetic resonance imaging. Circulation. 2001; 104: 249-252.

Corti R, Fuster V, Fayad ZA, Worthley SG, Helft G, Smith D, Weinberger J, Wentzel J, Mizsei G, Mercuri M, Badimon JJ. Lipid lowering by simvastatin induces regression of human atherosclerotic lesions: two years' follow-up by high-resolution noninvasive magnetic resonance imaging. Circulation. 2002; 106: 2884-2887.

Corti R, Fuster V, Fayad ZA, Worthley SG, Helft G, Chaplin WF, Muntwyler J, Viles-Gonzalez JF, Weinberger J, Smith DA, Mizsei G, Badimon JJ. Effects of aggressive versus conventional lipid-lowering therapy by simvastatin on human atherosclerotic lesions: a prospective, randomized, double-blind trial with high-resolution magnetic resonance imaging. J Am Coll Cardiol. 2005; 46: 106-112.

Corti R. Noninvasive imaging of atherosclerotic vessels by MRI for clinical assessment of the effectiveness of therapy. Pharmacol Ther. 2006; 110: 57-70.

Costedoat-Chalumeau N, Pouchot J, Guettrot-Imbert G, Le Guern V, Leroux G, Marra D, Morel N, Piette JC. Adherence to treatment in systemic lupus erythematosus patients. Best Pract Res Clin Rheumatol. 2013; 27: 329-340.

Costenbader KH, Kim DJ, Peerzada J, Lockman S, Nobles-Knight D, Petri M, Karlson EW. Cigarette smoking and the risk of systemic lupus erythematosus: a meta-analysis. Arthritis Rheum. 2004; 50: 849-857.

Costenbader KH, Feskanich D, Stampfer MJ, Karlson EW. Reproductive and menopausal factors and risk of systemic lupus erythematosus in women. Arthritis Rheum. 2007; 56: 1251-1262.

Croce K, Libby P. Intertwining of thrombosis and inflammation in atherosclerosis. Curr Opin Hematol. 2007; 14: 55-61.

Cromwell WC, Otvos JD, Keyes MJ, Pencina MJ, Sullivan L, Vasan RS, Wilson PWF, D'Agostino RB. LDL particle number and risk of future cardiovascular disease in the Framingham Offspring Study—implications for LDL management. J Clin Lipidol. 2007; 1: 583-592.

Crouse JR 3rd. Thematic review series: patient-oriented research. Imaging atherosclerosis: state of the art. J Lipid Res. 2006; 47: 1677-1699.

Culham JA, Vince DJ. Cardiac output by MR imaging: an experimental study comparing right ventricle and left ventricle with thermodilution. Can Assoc Radiol J. 1988; 39: 247-249.

D:A:D Study Group, Sabin CA, Worm SW, Weber R, Reiss P, El-Sadr W, Dabis F, De Wit S, Law M, D'Arminio Monforte A, Friis-Møller N, Kirk O, Pradier C, Weller I, Phillips AN, Lundgren JD. Use of nucleoside reverse transcriptase inhibitors and risk of myocardial infarction in HIV-infected patients enrolled in the D:A:D study: a multi-cohort collaboration. Lancet. 2008; 371: 1417-1426.

Dalager S, Paaske WP, Kristensen IB, Laurberg JM, Falk E. Artery-related differences in atherosclerosis expression: implications for atherogenesis and dynamics in intima-media thickness. Stroke. 2007; 38: 2698-2705.

Danchenko N, Satia JA, Anthony MS. Epidemiology of systemic lupus erythematosus: a comparison of worldwide disease burden. Lupus. 2006; 15: 308-318.

Danesh J, Collins R, Peto R: Lipoprotein(a) and coronary heart disease. Meta-analysis of prospective studies. Circulation. 2000; 102: 1082-1085.

D'Cruz DP, Khamashta MA, Hughes GRV. Systemic lupus erythematosus. Lancet. 2007; 369: 587-596.

Deapen D, Escalante A, Weinrib L, Horwitz D, Bachman B, Roy-Burman P, Walker A, Mack TM. A revised estimate of twin concordance in systemic lupus erythematosus. Arthritis Rheum. 1992; 35: 311-318.

De Caterina R, Libby P, Peng HB, Thannickal VJ, Rajavashisth TB, Gimbrone MA, Shin WS, Liao JK. Nitric oxide decreases cytokine-induced endothelial activation. Nitric oxide selectively reduces endothelial expression of adhesion molecules and proinflammatory cytokines. J Clin Invest. 1995; 96: 60-68.

De Caterina R, Liao JK, Libby P. Fatty acid modulation of endothelial activation. Am J Clin Nutr. 2000; 71(S1): 213S-223S.

de Graaf J, Hak-Lemmers HLM, Hectors MPC, Demacker PNM, Hendriks JCM, Stalenhoef AFH. Enhanced Susceptibility to In Vitro Oxidation of the Dense Low Density Lipoprotein Subfraction in Healthy Subjects. Arterioscler Thromb.1991; 11: 298-306.

Diffenderfer MR, Schaefer EJ. The composition and metabolism of large and small LDL. Curr Opin Lipidol. 2014; 25:221-226.

Dinoso JB, Kim SY, Siliciano RF, Blankson JN. A comparison of viral loads between HIV-1-infected elite suppressors and individuals who receive suppressive highly active antiretroviral therapy. Clin Infect Dis. 2008; 47: 102-104.

Doherty TM, Asotra K, Fitzpatrick LA, Qiao JH, Wilkin DJ, Detrano RC, Dunstan CR, Shah PK, Rajavashisth TB. Calcification in atherosclerosis: Bone biology and chronic inflammation at the arterial crossroads. Proc Natl Acad Sci USA. 2003; 100: 11201–11206.

Doria A, Shoenfeld Y, Wu R, Gambari PF, Puato M, Ghirardello A, Gilburd B, Corbanese S, Patnaik M, Zampieri S, Peter JB, Favaretto E, Iaccarino L, Sherer Y, Todesco S, Pauletto P. Risk factors for subclinical atherosclerosis in a prospective cohort of patients with systemic lupus erythematosus. Ann Rheum Dis. 2003; 62: 1071-1077.

Duivenvoorden R, Mani V, Woodward M, Kallend D, Suchankova G, Fuster V, Rudd JH, Tawakol A, Farkouh ME, Fayad ZA. Relationship of serum inflammatory biomarkers with plaque inflammation assessed by FDG PET/CT: the dal-PLAQUE study. JACC Cardiovasc Imaging. 2013; 6: 1087-1094.

Duprez DA, Neuhaus J, Kuller LH, Tracy R, Belloso W, De Wit S, Drummond F, Lane HC, Ledergerber B, Lundgren J, Nixon D, Paton NI, Prineas RJ, Neaton JD, Insight Smart Study Group. Inflammation, coagulation and cardiovascular disease in HIV-infected individuals. PLoS One 2012;7:e44454.

Eder L, Gladman DD, Ibañez D, Urowitz MB. The correlation between carotid artery atherosclerosis and clinical ischemic heart disease in lupus patients. Lupus. 2014; 23: 1142-1148.

Ehara S, Ueda M, Naruko T, Haze K, Itoh A, Otsuka M, Komatsu R, Matsuo T, Itabe H, Takano T, Tsukamoto Y, Yoshiyama M, Takeuchi K, Yoshikawa J, Becker AE. Elevated Levels of Oxidized Low Density Lipoprotein Show a Positive Relationship With the Severity of Acute Coronary Syndromes. Circulation. 2001; 103: 1955-1960.

Eldor R, Raz I. American Diabetes Association Indications for Statins in Diabetes Is there evidence? Diabetes Care. 2009; 32: S384-S391.

Ellsworth JL, Kraemer FB, Cooper AD. Transport of □-very low density lipoproteins and chylomicron remnants by macrophages is mediated by the low density lipoprotein receptor pathway. J Biol Chem. 1987; 262: 2316-2325.

El-Magadmi M, Bodill H, Ahmad Y, Durrington PN, Mackness M, Walker M, Bernstein RM, Bruce IN. Systemic lupus erythematosus: an independent risk factor for endothelial dysfunction in women. Circulation. 2004; 110: 399-404.

El-Sadr WM, Lundgren JD, Neaton JD, Gordin F, Abrams D, Arduino RC, Babiker A, Burman W, Clumeck N, Cohen CJ, Cohn D, Cooper D, Darbyshire J, Emery S, Fätkenheuer G,

Gazzard B, Grund B, Hoy J, Klingman K, Losso M, Markowitz N, Neuhaus J, Phillips A, Rappoport C. CD4+ Count–Guided Interruption of Antiretroviral. The Strategies for Management of Antiretroviral Therapy (SMART) Study Group Treatment. N Engl J Med. 2006; 355: 2283-2296.

Emerging Risk Factors Collaboration, Erqou S, Kaptoge S, Perry PL, Di Angelantonio E, Thompson A, White IR, Marcovina SM, Collins R, Thompson SG, Danesh J. Lipoprotein(a) concentration and the risk of coronary heart disease, stroke, and nonvascular mortality. JAMA. 2009; 302: 412-423.

Endo A. A historical perspective on the discovery of statins. Proc Jpn Acad Ser B Phys Biol Sci. 2010; 86: 484-493.

Esdaile JM, Abrahamowicz M, Grodzicky T, Li Y, Panaritis C, du Berger R, Côte R, Grover SA, Fortin PR, Clarke AE, Senécal JL. Traditional Framingham risk factors fail to fully account for accelerated atherosclerosis in systemic lupus erythematosus.
Arthritis Rheum. 2001; 44: 2331-2337.

European Centre for Disease Prevention and Control, WHO Regional Office for Europe. HIV/AIDS surveillance in Europe 2014. Stockholm: ECDC; 2015. [Accessed 06/03/2016].

Falk E, Shah PK, Fuster V. Coronary plaque disruption. Circulation. 1995; 92: 657-671.

Fang X, Weintraub NL, Rios CD, Chappell DA, Zwacka RM, Engelhardt JF, Oberley LW, Yan T, Heistad DD, Spector AA. Overexpression of human superoxide dismutase inhibits oxidation of low-density lipoprotein by endothelial cells. Circ Res. 1998; 82: 1289-1297.

Fayad ZA, Nahar T, Fallon JT, Goldman M, Aguinaldo JG, Badimon JJ, Shinnar M, Chesebro JH, Fuster V. In vivo magnetic resonance evaluation of atherosclerotic plaques in the human thoracic aorta: a comparison with transesophageal echocardiography. Circulation. 2000; 101: 2503-2509.

Ferreira GA, Navarro TP, Telles RW, Andrade LE, Sato EI. Atorvastatin therapy improves endothelial-dependent vasodilation in patients with systemic lupus erythematosus: an 8 weeks controlled trial. Rheumatology (Oxford). 2007; 46: 1560-1565.

Fessel WJ. Systemic lupus erythematosus in the community. Incidence, prevalence, outcome, and first symptoms; the high prevalence in black women. Arch Intern Med. 1974; 134: 1027–1035.

Finn AV, Nakano M, Narula J, Kolodgie FD, Virmani R. Concept of vulnerable/unstable plaque. Arterioscler Thromb Vasc Biol. 2010; 30: 1282-1292.

Fitch KV, Looby SE, Rope A, Eneh P, Hemphill L, Lee H, Grinspoon SK. Effects of aging and smoking on carotid intima-media thickness in HIV-infection. AIDS. 2013; 27: 49-57.

Flammer AJ, Anderson T, Celermajer DS, Creager MA, Deanfield J, Ganz P, Hamburg NM, Lüscher TF, Shechter M, Taddei S, Vita JA, Lerman A. The assessment of endothelial function: from research into clinical practice. Circulation. 2012; 126: 753-767.

Floris-Moore M, Fayad ZA, Berman JW, Mani V, Schoenbaum EE, Klein RS, Weinshelbaum KB, Fuster V, Howard AA, Lo Y, Schecter AD. Association of HIV viral load with monocyte chemoattractant protein-1 and atherosclerosis burden measured by magnetic resonance imaging. AIDS. 2009; 23: 941-949.

Ford ES, Ajani UA, Croft JB, Critchley JA, Labarthe DR, Kottke TE, Giles WH, Capewell S. Explaining the decrease in U.S. deaths from coronary disease, 1980-2000. N Engl J Med. 2007; 356: 2388-2398.

Frerix M, Stegbauer J, Kreuter A, Weiner SM. Atherosclerotic plaques occur in absence of intima-media thickening in both systemic sclerosis and systemic lupus erythematosus: a duplexsonography study of carotid and femoral arteries and follow-up for cardiovascular events. Arthritis Res Ther. 2014; 16: R54.

Friis-Møller N, Weber R, Reiss P, Thiébaut R, Kirk O, d'Arminio Monforte A, Pradier C, Morfeldt L, Mateu S, Law M, El-Sadr W, De Wit S, Sabin CA, Phillips AN, Lundgren JD; DAD study group. Cardiovascular disease risk factors in HIV patients – association with antiretroviral therapy. Results from the DAD study. AIDS. 2003; 17: 1179-1193.

Friis-Møller N, Reiss P, Sabin CA, Weber R, d'Arminio Monforte A, El-Sadr W, Thiébaut R, De Wit S, Kirk O, Fontas E, Law MG, Phillips A, Lundgren JD. Class of antiretroviral drugs and the risk of myocardial infarction. The DAD Study Group. N Engl J Med. 2007; 356: 1723-1735.

Friis-Møller N, Thiébaut R, Reiss P, Weber R, Monforte AD, De Wit S, El-Sadr W, Fontas E, Worm S, Kirk O, Phillips A, Sabin CA, Lundgren JD, Law MG; DAD study group. Predicting the risk of cardiovascular disease in HIV-infected patients: the data collection on adverse effects of anti-HIV drugs study. Eur J Cardiovasc Prev Rehabil. 2010; 17: 491-501.

Fuster V, Fayad ZA, Moreno PR, Poon M, Corti R, Badimon JJ. Atherothrombosis and high-risk plaque: Part II: approaches by noninvasive computed tomographic/magnetic resonance imaging. J Am Coll Cardiol. 2005; 46: 1209-1218.

Gaipl US, Kuenkele S, Voll RE, Beyer TD, Kolowos W, Heyder P, Kalden JR, Herrmann M. Complement binding is an early feature of necrotic and a rather late event during apoptotic cell death. Cell Death Differ. 2001; 8: 327-334.

Gao F, Bailes E, Robertson DL, Chen Y, Rodenburg CM, Michael SF, Cummins LB, Arthur LO, Peeters M, Shaw GM, Sharp PM, Hahn BH. Origin of HIV-1 in the chimpanzee Pan troglodytes troglodytes. Nature. 1999; 397: 436-441.

Genest JJ, Martin-Munley SS, Judith R. McNamara JR, Ordovas JM, Jenner J, Myers RH, Silberman SR, Wilson PWF, Salem DN, Ernst J. Schaefer EJ. Familial Lipoprotein Disorders in Patients With Premature Coronary Artery Disease. Circulation. 1992; 85: 2025-2033.

Ghodke-Puranik Y, Niewold TB. Immunogenetics of systemic lupus erythematosus: A comprehensive review. J Autoimmun. 2015; 64:125-136.

Gladman DD. Prognosis and treatment of systemic lupus erythematosus. Curr Opin Rheumatol. 1996a; 8: 430-437.

Gladman D, Ginzler E, Goldsmith C, Fortin P, Liang M, Urowitz M, Bacon P, Bombardieri S, Hanly J, Hay E, Isenberg D, Jones J, Kalunian K, Maddison P, Nived O, Petri M, Richter M, Sanchez-Guerrero J, Snaith M, Sturfelt G, Symmons D, Zoma A. The development and initial validation of the Systemic Lupus International Collaborating Clinics/American College of Rheumatology damage index for systemic lupus erythematosus. Arthritis Rheum. 1996b; 39: 363-369.

Glagov S, Weisenberg E, Zarins CK, Stankunavicius R, Kolettis GJ. Compensatory enlargement of human atherosclerotic coronary arteries. N Engl J Med. 1987; 316: 1371-1375.

Global Atlas on Cardiovascular Disease Prevention and Control. Mendis S, Puska P, Norrving B editors. World Health Organization, Geneva 2011.

Goldstein JL, Brown MS. The LDL receptor. Arterioscler Thromb Vasc Biol. 2009; 29: 431-438.

Golledge J, Greenhalgh RM, Davies AH. The symptomatic carotid plaque. Stroke. 2000; 31: 774-781.

Gotto AM, Moon JE. Recent clinical studies of the effects of lipid-modifying therapies Am J Cardiol. 2012; 110(1S): 15A-26A.

Granér M, Varpula M, Kahri J, Salonen RM, Nyyssönen K, Nieminen MS, Taskinen MR, Syvänne M. Association of carotid intima-media thickness with angiographic severity and extent of coronary artery disease. Am J Cardiol. 2006; 97: 624-629.

Grimaldi CM. Sex and systemic lupus erythematosus: the role of the sex hormones estrogen and prolactin on the regulation of autoreactive B cells. Curr Opin Rheumatol. 2006; 18: 456-461.

Grothues F, Smith GC, Moon JC, Bellenger NG, Collins P, Klein HU, Pennell DJ. Comparison of interstudy reproducibility of cardiovascular magnetic resonance with two-dimensional echocardiography in normal subjects and in patients with heart failure or left ventricular hypertrophy. Am J Cardiol. 2002; 90: 29-34.

Grothues F, Moon JC, Bellenger NG, Smith GS, Klein HU, Pennell DJ. Interstudy reproducibility of right ventricular volumes, function, and mass with cardiovascular magnetic resonance. Am Heart J. 2004; 147: 218-223.

Gudmundsson S, Steinsson K. Systemic lupus erythematosus in Iceland 1975 through 1984. A nationwide epidemiological study in an unselected population. J Rheumatol. 1990; 17: 1162-1167.

Gustafsson J, Gunnarsson I, Börjesson O, Pettersson S, Möller S, Fei GZ, Elvin K, Simard JF, Hansson LO, Lundberg IE, Larsson A, Svenungsson E.Predictors of the first cardiovascular event in patients with systemic lupus erythematosus - a prospective cohort study. Arthritis Res Ther. 2009; 11: R186.

Gustafsson JT, Simard JF, Gunnarsson I, Elvin K, Lundberg IE, Hansson LO, Larsson A, Svenungsson E. Risk factors for cardiovascular mortality in patients with systemic lupus erythematosus, a prospective cohort study. Arthritis Res Ther. 2012; 14: R46.

Gustafsson JT, Svenungsson E. Definitions of and contributions to cardiovascular disease in systemic lupus erythematosus. Autoimmunity. 2014; 47: 67-76.

Haley KJ, Lilly CM, Yang JH, Feng Y, Kennedy SP, Turi TG, Thompson JF, Sukhova GH, Libby P, Lee RT. Overexpression of eotaxin and the CCR3 receptor in human atherosclerosis: using genomic technology to identify a potential novel pathway of vascular inflammation. Circulation. 2000; 102: 2185-2189.

Hanna DB, Post WS, Deal JA, Hodis HN, Jacobson LP, Mack WJ, Anastos K, Gange SJ, Landay AL, Lazar JM, Palella FJ, Tien PC, Witt MD, Xue X, Young MA, Kaplan RC, Kingsley LA. HIV Infection Is Associated With Progression of Subclinical Carotid Atherosclerosis. Clin Infect Dis. 2015; 61: 640-650.

Hardin NJ, Minick CR, Murphy GE. Experimental induction of atheroarteriosclerosis by the synergy of allergic injury to arteries and lipid-rich diet. Am J Pathol. 1973; 73: 301-327.

Harker LA, Slichter SJ, Scott CR, Ross R. Homocystinemia Vascular injury and arterial thrombosis. N Engl J Med. 1974; 291: 537-543.

Hasegawa T, Shimada K (2015). Optical Coherence Tomography for the Assessment of Coronary Plaque Vulnerability, Coronary Artery Disease - Assessment, Surgery, Prevention, Prof. Kaan Kirali (Ed.), InTech, DOI: 10.5772/61615. Available from: http://www.intechopen.com/books/coronary-artery-disease-assessment-surgery-prevention/optical-coherence-tomography-for-the-assessment-of-coronary-plaque-vulnerability.

Hashimoto M, Akishita M, Eto M, Ishikawa M, Kozaki K, Toba K, Sagara Y, Taketani Y, Orimo H, Ouchi Y. Modulation of endothelium-dependent flow-mediated dilatation of the brachial artery by sex and menstrual cycle. Circulation. 1995; 92: 3431-3435.

Heart disease and stroke statistics – 2009 update: a report from the American Heart Association Statistics Committee and Stroke Statistics Subcommittee. Circulation. 2009; 119: e21-181.

Hel Z, Stringer E, Mestecky J. Sex steroid hormones, hormonal contraception, and the immunobiology of human immunodeficiency virus-1 infection. Endocr Rev. 2010; 31:79-97.

Helin P, Lorenzen I, Garbarich C, Matthienen ME. Repair in arterial tissue : morphological and biochemical changes in rabbit aorta after a single dilatation injury. Circ Res. 1971; 29: 542-554.

Hemelaar J, Gouws E, Ghys PD, Osmanov S; WHO-UNAIDS Network for HIV Isolation and Characterisation. Global trends in molecular epidemiology of HIV-1 during 2000-2007. AIDS. 2011; 25: 679-689.

Hemkens LG, Bucher HC. HIV infection and cardiovascular disease. Eur Heart J. 2014; 35: 1373–1381.

Hirsch VM, Olmsted RA, Murphey-Corb M, Purcell RH, Johnson PR. An African primate lentivirus (SIVsm) closely related to HIV-2. Nature. 1989; 339: 389-392.

Ho DD, Neumann AU, Perelson AS, Chen W, Leonard JM, Markowitz M. Rapid turnover of plasma virions and CD4 lymphocytes in HIV-1 infection. Nature. 1995; 373: 123-126.

Ho JE, Hsue P. Cardiovascular manifestations of HIV infection. Heart. 2009; 95: 1193-1202.

Hochberg MC. Updating the American College of Rheumatology revised criteria for the classification of systemic lupus erythematosus [Letter]. Arthritis Rheum. 1997; 40: 1725.

Hodis HN, Mack W, LaBree L, Selzer RH, Liu C, Liu C, Alaupovic P, Kwong-Fu H, Azen SP. Reduction in carotid arterial wall thickness using lovastatin and dietary therapy. A randomized, controlled clinical trial. Ann Intern Med. 1996; 124: 548-556.

Hodis HN, Mack WJ, Dunn M, Liu C, Liu C, Selzer RH, Krauss RM. Intermediate-density lipoproteins and progression of carotid arterial wall intima-media thickness. Circulation. 1997; 95: 2022-2026.

Hogan MC, Petersen SE, Hudsmith LE, Francis JM, Neubauer S, Robson MD. Effects of steady state free precession parameters on cardiac mass, function, and volumes. Int J Cardiovasc Imaging. 2007; 23: 583-589.

Holloway CJ, Ntusi N, Suttie J, Mahmod M, Wainwright E, Clutton G, Hancock G, Beak P, Tajar A, Piechnik SK, Schneider JE, Angus B, Clarke K, Dorrell L, Neubauer S. Comprehensive cardiac magnetic resonance imaging and spectroscopy reveal a high burden of myocardial disease in HIV patients. Circulation. 2013; 128: 814-822.

Holvoet P, Collen D. Oxidized lipoproteins in atherosclerosis and thrombosis. FASEB J. 1994; 8: 1279-1284.

Hsue PY, Lo JC, Franklin A, Bolger AF, Martin JN, Deeks SG, Waters DD. Progression of Atherosclerosis as Assessed by Carotid Intima-Media Thickness in Patients With HIV Infection. Circulation. 2004; 109: 1603-1608.

Hsue PY, Hunt PW, Schnell A, Kalapus SC, Hoh R, Ganz P, Martin JN, Deeks SG. Role of viral replication, antiretroviral therapy, and immunodeficiency in HIV-associated atherosclerosis. AIDS. 2009; 23: 1059-1067.

Hsue PY, Scherzer R, Hunt PW, Schnell A, Bolger AF, Kalapus SC, Maka K, Martin JN, Ganz P, Deeks SG. Carotid Intima-Media Thickness Progression in HIV-Infected Adults Occurs Preferentially at the Carotid Bifurcation and Is Predicted by Inflammation. J Am Heart Assoc. 2012;1: jah3-e000422 doi:10.1161/JAHA.111.000422. Epub 2012 Apr 24.

Hudsmith LE, Petersen SE, Tyler DJ, Francis JM, Cheng AS, Clarke K, Selvanayagam JB, Robson MD, Neubauer S. Determination of cardiac volumes and mass with FLASH and SSFP cine sequences at 1.5 vs. 3 Tesla: a validation study. J Magn Reson Imaging. 2006; 24: 312-318.

Hundley WG, Bluemke DA, Finn JP, Flamm SD, Fogel MA, Friedrich MG, Ho VB, Jerosch-Herold M, Kramer CM, Manning WJ, Patel M, Pohost GM, Stillman AE, White RD, Woodard

PK. American College of Cardiology Foundation Task Force on Expert Consensus Documents. ACCF/ACR/AHA/NASCI/SCMR 2010 expert consensus document on cardiovascular magnetic resonance: a report of the American College of Cardiology Foundation Task Force on Expert Consensus Documents. J Am Coll Cardiol. 2010; 55: 2614-2662.

Hunt PW. HIV and inflammation: mechanisms and consequences. Curr HIV/AIDS Rep. 2012; 9:139-147.

Hyafil F, Laissy JP, Mazighi M, Tchétché D, Louedec L, Adle-Biassette H, Chillon S, Henin D, Jacob MP, Letourneur D, Feldman LJ. Ferumoxtran-10-enhanced MRI of the hypercholesterolemic rabbit aorta: relationship between signal loss and macrophage infiltration. Arterioscler Thromb Vasc Biol. 2006; 26: 176-181.

Ibrahim T, Makowski MR, Jankauskas A, Maintz D, Karch M, Schachoff S, Manning WJ, Schömig A, Schwaiger M, Botnar RM. Serial contrast-enhanced cardiac magnetic resonance imaging demonstrates regression of hyperenhancement within the coronary artery wall in patients after acute myocardial infarction. JACC Cardiovasc Imaging. 2009; 2: 580-588.

Jaffer FA, O'Donnell CJ, Larson MG, Chan SK, Kissinger KV, Kupka MJ, Salton C, Botnar RM, Levy D, Manning WJ. Age and sex distribution of subclinical aortic atherosclerosis: a magnetic resonance imaging examination of the Framingham Heart Study. Arterioscler Thromb Vasc Biol. 2002; 22: 849-854.

James JA, Robertson JM. Lupus and Epstein-Barr. Curr Opin Rheumatol. 2012; 24: 383-388.

Jiménez S, Cervera R, Font J, Ingelmo M. The epidemiology of systemic lupus erythematosus. Clin Rev Allergy Immunol. 2003; 25: 3-12.

Jonasson L, Holm J, Skalli O, Bondjers G, Hansson GK. Regional accumulations of T cells, macrophages, and smooth muscle cells in the human atherosclerotic plaque. Arterioscler Thromb Vasc Biol. 1986; 6: 131-138.

Jones, PH, Davidson MH, Stein EA, Bays HE, McKenney JM, Miller E, Cain VA, Blasetto JW, for the STELLAR Study Group. Comparison of the Efficacy and Safety of Rosuvastatin Versus Atorvastatin, Simvastatin, and Pravastatin Across Doses (STELLAR* Trial). Am J Cardiol. 2003; 92:1 52-160.

Jongstra-Bilen J, Haidari M, Zhu SN, Chen M, Guha D, Cybulsky MI. Low-grade chronic inflammation in regions of the normal mouse arterial intima predisposed to atherosclerosis. J Exp Med. 2006; 203: 2073-2083.

Kang X, Polissar NL, Han C, Lin E, Yuan C. Analysis of the measurement precision of arterial lumen and wall areas using high-resolution MRI. Magn Reson Med. 2000; 44: 968-972.

Kannel WB. Contribution of the Framingham study to preventive cardiology. J Am Coll Cardiol. 1990; 15: 206-211.

Kannel WB, Vasan RS. Triglycerides as vascular risk factors: new epidemiologic insights. Curr Opin Cardiol. 2009; 24: 345-350.

Kao AH, Wasko MC, Krishnaswami S, Wagner J, Edmundowicz D, Shaw P, Cunningham AL, Danchenko N, Sutton-Tyrrell K, Tracy RP, Kuller LH, Manzi S. C-reactive protein and coronary artery calcium in asymptomatic women with systemic lupus erythematosus or rheumatoid arthritis. Am J Cardiol. 2008; 102: 755-760.

Kao AH, Lertratanakul A, Elliott JR, Sattar A, Santelices L, Shaw P, Birru M, Avram Z, Thompson T, Sutton-Tyrrell K, Ramsey-Goldman R, Manzi S. Relation of carotid intima-media thickness and plaque with incident cardiovascular events in women with systemic lupus erythematosus. Am J Cardiol. 2013; 112: 1025-1032.

Kaplan RC, Sinclair E, Landy AL, Lurain N, Sharrett AR, Gange SJ, Xue X, Hunt P, Karim R, Kern DM, Hodis HN, Deeks SG. T cell activation and senescence predict subclinical carotid artery disease in HIV-infected women. J Infect Dis. 2011; 203: 452–463.

Karim R, Mack WJ, Kono N, Tien PC, Anastos K, Lazar J, Young M, Cohen M, Golub E, Greenblatt RM, Kaplan RC, Hodis HN. Gonadotropin and sex steroid levels in HIV-infected premenopausal women and their association with subclinical atherosclerosis in HIV-infected and -uninfected women in the Women's Interagency HIV Study (WIHS). J Clin Endocrinol Metab. 2013; 98: E610-E618.

Karp I, Abrahamowicz M, Fortin PR, Pilote L, Neville C, Pineau CA, Esdaile JM. Recent corticosteroid use and recent disease activity: independent determinants of coronary heart disease risk factors in systemic lupus erythematosus? Arthritis Rheum. 2008; 59: 169-175.

Katz J, Milliken MC, Stray-Gundersen J, Buja LM, Parkey RW, Mitchell JH, Peshock RM. Estimation of human myocardial mass with MR imaging. Radiology. 1988; 169: 495-498.

Katz J, Whang J, Boxt LM, Barst RJ. Estimation of right ventricular mass in normal subjects and in patients with primary pulmonary hypertension by nuclear magnetic resonance imaging. J Am Coll Cardiol. 1993; 21: 1475-1481.

Keele BF, Van Heuverswyn F, Li Y, Bailes E, Takehisa J, Santiago ML, Bibollet-Ruche F, Chen Y, Wain LV, Liegeois F, Loul S, Ngole EM, Bienvenue Y, Delaporte E, Brookfield JF, Sharp PM, Shaw GM, Peeters M, Hahn BH. Chimpanzee reservoirs of pandemic and nonpandemic HIV-1. Science. 2006; 313: 523-526.

Keenan NG, Locca D, Varghese A, Roughton M, Gatehouse PD, Hooper J, Firmin DN, Pennell DJ. Magnetic resonance of carotid artery ageing in healthy subjects. Atherosclerosis. 2009a; 205: 168-173.

Keenan NG, Mason JC, Maceira A, Assomull R, O'Hanlon R, Chan C, Roughton M, Andrews J, Gatehouse PD, Firmin DN, Pennell DJ. Integrated cardiac and vascular assessment in Takayasu arteritis by cardiovascular magnetic resonance. Arthritis Rheum. 2009b; 60: 3501-3509.

Keenan NGJ. Cardiovascular magnetic resonance of the arterial wall. Unpublished MD dissertation, Imperial College London 2010.

Kenny JM, Cook A, Mirembe G, Masaku D, Wavamunno P, Odongo F, Rapala A, Deanfield J, Gibb DM, Klein NJ. Structural Cardiovascular Changes Are Reversible in HIV-Infected Children in Zambia and Uganda. Abstract Number: 37. Conference on retroviruses and infectious diseases: February 23-26, 2015, Seattle, Washington. Available at: http://www.croiconference.org/sessions/structural-cardiovascular-changes-are-reversible-hiv-infected-children-zambia-and-uganda. [Accessed: 20/06/2016].

Kerwin W, Hooker A, Spilker M, Vicini P, Ferguson M, Hatsukami T, Yuan C. Quantitative magnetic resonance imaging analysis of neovasculature volume in carotid atherosclerotic plaque. Circulation. 2003; 107: 851-856.

Kiani AN, Magder L, Petri M. Coronary calcium in systemic lupus erythematosus is associated with traditional cardiovascular risk factors, but not with disease activity. J Rheumatol. 2008; 35: 1300-1306.

Kim WY, Maintz D, Spuentrup E, Yeon SB, Manning WJ, Botnar RM. 2010. Atherosclerotic plaque imaging: coronaries. In: Manning WJ, Pennell DJ. Cardiovascular Magnetic Resonance, 2nd Edition. Saunders, Elsevier. p351-361.

Kontush A, Chantepie S, Chapman MJ. Small, dense HDL particles exert potent protection of atherogenic LDL against oxidative stress. Arterioscler Thromb Vasc Biol. 2003; 23: 1881-1888.

Kooi ME, Cappendijk VC, Cleutjens KB, Kessels AG, Kitslaar PJ, Borgers M, Frederik PM, Daemen MJ, van Engelshoven JM. Accumulation of ultrasmall superparamagnetic particles of iron oxide in human atherosclerotic plaques can be detected by in vivo magnetic resonance imaging. Circulation. 2003; 107: 2453-2458.

Kramer CM, Barkhausen J, Flamm SD, Kim RJ, Nagel E. Standardized cardiovascular magnetic resonance imaging (CMR) protocols, society for cardiovascular magnetic resonance: board of trustees task force on standardized protocols. J Cardiovasc Magn Reson. 2008; 10: 35.

Kugiyama K, Doi H, Motoyama T, Soejima H, Kenji Misumi K, Kawano H, Nakagawa O, Yoshimura M, Ogawa H, Matsumura T, Sugiyama S, Nakano T, Nakajima K, Yasue H. Association of remnant lipoprotein levels with impairment of endothelium-dependent vasomotor function in human coronary arteries. Circulation. 1998; 97: 2519-2526.

Kuller LH, Tracy R, Belloso W, De Wit S, Drummond F, Lane HC, Ledergerber B, Lundgren J, Neuhaus J, Nixon D, Paton NI, Neaton JD, Insight Smart Study Group. Inflammatory and coagulation biomarkers and mortality in patients with HIV infection. PLoS Med 2008; 5: e203.

Kyaw T, Tay C, Krishnamurthi S, Kanellakis P, Agrotis A, Tipping P, Bobik A, Toh BH. B1a B lymphocytes are atheroprotective by secreting natural IgM that increases IgM deposits and reduces necrotic cores in atherosclerotic lesions. Circ Res. 2011; 109: 830-840.

Lake JE, Wohl D, Scherzer R, Grunfeld C, Tien PC, Sidney S, Currier JS. Regional fat deposition and cardiovascular risk in HIV infection: the FRAM study. AIDS Care. 2011; 23: 929-938.

Lancelot E, Amirbekian V, Brigger I, Raynaud JS, Ballet S, David C, Rousseaux O, Le Greneur S, Port M, Lijnen HR, Bruneval P, Michel JB, Ouimet T, Roques B, Amirbekian S, Hyafil F, Vucic E, Aguinaldo JG, Corot C, Fayad ZA. Evaluation of matrix metalloproteinases in atherosclerosis using a novel noninvasive imaging approach. Arterioscler Thromb Vasc Biol. 2008; 28: 425-432.

Landry M. Phagocyte function and cell-mediated immunity in systemic lupus erythematosus. Arch Dermatol. 1977; 113: 147-154.

Laufs U, La Fata V, Plutzky J, Liao J. Upregulation of Endothelial Nitric Oxide Synthase by HMG CoA Reductase Inhibitors. Circulation. 1998; 97: 1129-1135.

Law MR, Wald NJ, Rudnicka AR. Quantifying effect of statins on low density lipoprotein cholesterol, ischaemic heart disease, and stroke: systematic review and meta-analysis. BMJ. 2003; 326: 1423-29.

Lee YW, Eum SY, Nath A, Toborek M. Estrogen-mediated protection against HIV Tat protein-induced inflammatory pathways in human vascular endothelial cells. Cardiovasc Res. 2004; 63: 139-148.

Lefer AM, Scalia R, Lefer DJ. Vascular effects of HMG CoA-reductase inhibitors (statins) unrelated to cholesterol lowering: new concepts for cardiovascular disease Cardiovasc Res. 2001; 49: 281-287.

Li AE, Kamel I, Rando F, Anderson M, Kumbasar B, Lima JA, Bluemke DA. Using MRI to assess aortic wall thickness in the multiethnic study of atherosclerosis: distribution by race, sex, and age. AJR Am J Roentgenol. 2004; 182: 593-597.

Libby P. Inflammation in atherosclerosis. Nature. 2002; 420: 868-874.

Libby P. Inflammation and cardiovascular disease mechanisms. Am J Clin Nutr. 2006; 83(S1): 456S-460S.

Libby P. Inflammation in atherosclerosis. Arterioscler Thromb Vasc Biol. 2012; 32: 2045-2051.

Ligabue G, Fiocchi F, Ferraresi S, Barbieri A, Rossi R, Modena MG, Romagnoli R, Torricelli P. 3-Tesla MRI for the evaluation of myocardial viability: a comparative study with 1.5-Tesla MRI. Radiol Med. 2008; 113: 347-362.

Lima DS, Sato EI, Lima VC, Miranda F Jr, Hatta FH. Brachial endothelial function is impaired in patients with systemic lupus erythematosus. J Rheumatol. 2002; 29: 292-297.

Lipshultz SE, Miller TL, Wilkinson JD, Scott GB, Somarriba G, Cochran TR, Fisher SD. Cardiac effects in perinatally HIV-infected and HIV-exposed but uninfected children and adolescents: a view from the United States of America. J Int AIDS Soc. 2013; 16: 18597.

Liu Z, Davidson A. Taming lupus-a new understanding of pathogenesis is leading to clinical advances. Nat Med. 2012; 18: 871-882.

Lloyd-Jones D, Adams R, Carnethon M, De Simone G, Ferguson TB, Flegal K, Ford E, Furie K, Go A, Greenlund K, Haase N, Hailpern S, Ho M, Howard V, Kissela B, Kittner S, Lackland D, Lisabeth L, Marelli A, McDermott M, Meigs J, Mozaffarian D, Nichol G, O'Donnell C, Roger V, Rosamon W, Sacco R, Sorlie P, Stafford R, Steinberger J, Thom T, Wasserthiel-Smoller S, Wong N, Wylie-Rosett J, Hong Y. Heart disease and stroke statistics – 2009 update: a report from the American Heart Association Statistics Committee and Stroke Statistics Subcommittee. Circulation. 2009; 119: e21-181.

Lo J, Plutzky J. The biology of atherosclerosis: General paradigms and distinct pathogenic mechanisms among HIV-infected patients. J Infect Dis. 2012; 205: S368–374.

Lohse N, Hansen AB, Pedersen G, Kronborg G, Gerstoft J, Sørensen HT, Vaeth M, Obel N. Survival of persons with and without HIV infection in Denmark, 1995-2005. Ann Intern Med. 2007; 146:87-95.

Longmore DB, Klipstein RH, Underwood SR, Firmin DN, Hounsfield GN, Watanabe M, Bland C, Fox K, Poole-Wilson PA, Rees RS, Denison D, McNeilly AM, Burman ED. Dimensional accuracy of magnetic resonance in studies of the heart. Lancet. 1985; 1: 1360-1362.

Lorenz MW, Markus HS, Bots ML, Rosvall M, Sitzer M. Prediction of clinical cardiovascular events with carotid intima-media thickness: a systematic review and meta-analysis. Circulation. 2007; 115: 459-467.

Lu Q, Wu A, Tesmer L, Ray D, Yousif N, Richardson B. Demethylation of CD40LG on the inactive X in T cells from women with lupus. J Immunol. 2007; 179: 6352-6358.

Lund-Katz S, Laplaud PM, Phillips MC, Chapman MJ. Apolipoprotein B-100 conformation and particle surface charge in human LDL subspecies: implication for LDL receptor interaction. Biochemistry. 1998; 37: 12867-12874.

Maartens G, Celum C, Lewin SR. HIV infection: epidemiology, pathogenesis, treatment, and prevention. Lancet. 2014; 384: 258–271.

Maceira AM, Prasad SK, Khan M, Pennell DJ. Normalized left ventricular systolic and diastolic function by steady state free precession cardiovascular magnetic resonance. J Cardiovasc Magn Reson. 2006a; 8: 417–426.

Maceira AM, Prasad SK, Khan M, Pennell DJ. Reference right ventricular systolic and diastolic function normalized to age, gender and body surface area from steady-state free precession cardiovascular magnetic resonance. Eur Heart J. 2006b; 27: 2879–2888.

Mach F, Sauty A, Iarossi AS, Sukhova GK, Neote K, Libby P, Luster AD. Differential expression of three T lymphocyte-activating CXC chemokines by human atheroma-associated cells. J Clin Invest. 1999; 104: 1041-1050.

Madec Y, Boufassa F, Avettand-Fenoel V, Hendou S, Melard A, Boucherit S, Surzyn J, Meyer L, Rouzioux C; ANRS SEROCO/HEMOCO Study Group. Early control of HIV-1 infection in long-term nonprogressors followed since diagnosis in the ANRS SEROCO/HEMOCO cohort. J Acquir Immune Defic Syndr. 2009; 50: 19-26.

Magder LS, Petri M. Incidence of and risk factors for adverse cardiovascular events among patients with systemic lupus erythematosus. Am J Epidemiol. 2012; 176: 708-719.

Maggi P, Serio G, Epifani G, Fiorentino G, Saracino A, Fico C, Perilli F, Lillo A, Ferraro S, Gargiulo M, Chirianni A, Angarano G, Regina G, Pastore G. Premature lesions of the carotid vessels in HIV-1-infected patients treated with protease inhibitors. AIDS. 2000; 14:123-128.

Magwenzi S, Woodward C, Wraith KS, Aburima A, Raslan Z, Jones H, McNeil C, Wheatcroft S, Yuldasheva N, Febbriao M, Kearney M, Naseem KM. Oxidized LDL activates blood platelets through CD36/NOX2–mediated inhibition of the cGMP/protein kinase G signaling cascade. Blood. 2015; 125: 2693–2703.

Maher BM,Ni Dhonnchu T, Burke JP, Soo A, Wood AE, Watson RWG. Statins alter neutrophil migration by modulating cellular Rho activity - a potential mechanism for statins-mediated pleotropic effects? J Leukoc Biol. 2009; 85: 186-193.

Malfitano AM, Marasco G, Proto MC, Laezza C, Gazzerro P, Bifulco M. Statins in neurological disorders: an overview and update. Pharmacol Res. 2014; 88: 74-83.

Mani V, Aguiar SH, Itskovich VV, Weinshelbaum KB, Postley JE, Wasenda EJ, Aguinaldo JGS, Samber DD, Fayad ZA. Carotid black blood MRI burden of atherosclerotic disease assessment correlates with ultrasound intima-media thickness. J Cardiovasc Magn Reson. 2006; 8: 529-534.

Maningat P, Gordon BR, Breslow JL. How do we improve patient compliance and adherence to long-term statin therapy? Curr Atheroscler Rep. 2013; 15: 291.

Manolio TA, Arnold AM, Post W, Bertoni AG, Schreiner PJ, Sacco RL, Saad MF, Detrano RL, Szklo M. Ethnic differences in the relationship of carotid atherosclerosis to coronary calcification: The Multi-Ethnic Study of Atherosclerosis. Atherosclerosis. 2008; 197: 132-138.

Manzi S, Meilahn EN, Rairie JE, Conte CG, Medsger TA Jr, Jansen-McWilliams L, D'Agostino RB, Kuller LH. Age-specific incidence rates of myocardial infarction and angina in women with systemic lupus erythematosus: comparison with the Framingham Study. Am J Epidemiol. 1997; 145: 408-415.

Manzi S, Selzer F, Sutton-Tyrrell K, Fitzgerald SG, Rairie JE, Tracy RP, Kuller LH. Prevalence and risk factors of carotid plaque in women with systemic lupus erythematosus. Arthritis Rheum. 1999; 42: 51-60.

Mason DP, Kenagy RD, Hasenstab D, Bowen-Pope DF, Seifert RA, Coats S, Hawkins SM, Clowes AW. Matrix metalloproteinase-9 overexpression enhances vascular smooth muscle cell migration and alters remodeling in the injured rat carotid artery. Circ Res. 1999; 85: 1179-1185.

Mason JC. Statins and their role in vascular protection. Clin Sci (Lond). 2003; 105: 251-266.

Mason JC, Libby P. Cardiovascular disease in patients with chronic inflammation: mechanisms underlying premature cardiovascular events in rheumatologic conditions. Eur Heart J. 2015; 36: 482-489.

Masuoka H, Kamei S, Wagayama H, Ozaki M, Kawasaki A, Tanaka T, Kitamura M, Katoh S, Shintani U, Misaki M, Sugawa M, Ito M, Nakano T. Association of remnant-like particle cholesterol with coronary artery disease in patients with normal total cholesterol levels. Am Heart J. 2000; 139: 305-310.

Mathew V, Cannan CR, Miller VM, Barber DA, Hasdai D, Schwartz RS, Holmes DR, Lerman A. Enhanced Endothelin-Mediated Coronary Vasoconstriction and Attenuated Basal Nitric Oxide Activity in Experimental Hypercholesterolemia. Circulation. 1997; 96: 1930-1936.

Mavrogeni S, Bratis K, Markussis V, Spargias C, Papadopoulou E, Papamentzelopoulos S, Constadoulakis P, Matsoukas E, Kyrou L, Kolovou G.
The diagnostic role of cardiac magnetic resonance imaging in detecting myocardial inflammation in systemic lupus erythematosus. Differentiation from viral myocarditis. Lupus. 2013; 22: 34-43.

Mavrogeni S, Smerla R, Grigoriadou G, Servos G, Koutsogeorgopoulou L, Karabela G, Stavropoulos E, Spiliotis G, Kolovou G, Papadopoulos G. Cardiovascular magnetic resonance evaluation of paediatric patients with systemic lupus erythematosus and cardiac symptoms. Lupus. 2016; 25: 289-295.

McCarey DW, McInnes IB, Madhok R, Hampson R, Scherbakov O, Ford I, Capell HA, Sattar N. Trial of Atorvastatin in Rheumatoid Arthritis (TARA): double-blind, randomised placebo-controlled trial. Lancet. 2004; 363: 2015-2021.

McComsey GA, O'Riordan MA, Hazen SL, El-Bejjani D, Bhatt S, Brennan ML, Storer N, Adell J, Nakamoto DA, Dogra V. Increased carotid intima media thickness and cardiac biomarkers in HIV infected children. AIDS. 2007; 21: 921-927.

McGrath KCY, Li XH, Puranik R, Liong EC, Tan JTM, Dy VM, DiBartolo BA, Barter PJ, Rye KA, Heather AK. Role of 3□-hydroxysteroid-□24 reductase in mediating antiinflammatory effects of high-density lipoproteins in endothelial cells. Arterioscler Thromb Vasc Biol. 2009; 29: 877- 882.

McKeown RE. The Epidemiologic Transition: Changing Patterns of Mortality and Population Dynamics. Am J Lifestyle Med. 2009; 3:19S–26S.

McMahon M, Grossman J, FitzGerald J, Dahlin-Lee E, Wallace DJ, Thong BY, Badsha H, Kalunian K, Charles C, Navab M, Fogelman AM, Hahn BH. Proinflammatory high-density lipoprotein as a biomarker for atherosclerosis in patients with systemic lupus erythematosus and rheumatoid arthritis. Arthritis Rheum. 2006; 54: 2541-2549.

McMahon M, Skaggs BJ, Grossman JM, Sahakian L, Fitzgerald J, Wong WK, Lourenco EV, Ragavendra N, Charles-Schoeman C, Gorn A, Karpouzas GA, Taylor MB, Watson KE, Weisman MH, Wallace DJ, Hahn BH.A panel of biomarkers is associated with increased risk of the presence and progression of atherosclerosis in women with systemic lupus erythematosus. Arthritis Rheumatol. 2014; 66: 130-139.

Meisinger C, Baumert J, Khuseyinova N, Loewel H, Koenig W. Plasma oxidized low-density lipoprotein, a strong predictor for acute coronary heart disease events in apparently healthy, middle-aged men from the general population. Circulation. 2005; 112: 651-657.

Mercie P, Thiébaut R, Lavignolle V, Pellegrin JL, Marie-Christine MC, Morlat P, Ragnaud JM, Dupon M, Malvy D, Bellet H, Lawson-Ayayi S, Roudaut R, Dabis F. Evaluation of cardiovascular risk factors in HIV-1 infected patients using carotid intima-media thickness measurement. Ann Med. 2002; 34:55-63.

Migrino RQ, Bowers M, Harmann L, Prost R, LaDisa JF. Carotid plaque regression following 6-month statin therapy assessed by 3T cardiovascular magnetic resonance: comparison with ultrasound intima media thickness. J Cardiovasc Magn Reson. 2011; 13: 37.

Mihos CG, Artola RT, Santana O. The pleiotropic effects of the hydroxy-methyl-glutaryl-CoA reductase inhibitors in rheumatologic disorders: a comprehensive review. Rheumatol Int. 2012; 32: 287–294.

Mikhail IJ, Purdy JB, Dimock DS, Thomas VM, Muldoon NA, Clauss SB, Cross RR, Pettigrew RI, Hazra R, Hadigan C, Gharib AM. High rate of coronary artery abnormalities in adolescents and young adults infected with human immunodeficiency virus early in life. Pediatr Infect Dis J. 2011; 30: 710–712.

Mooij CF, de Wit CJ, Graham DA, Powell AJ, Geva T. Reproducibility of MRI measurements of right ventricular size and function in patients with normal and dilated ventricles. J Magn Reson Imaging. 2008; 28: 67-73.

Moon JC, Lorenz CH, Francis JM, Smith GC, Pennell DJ. Breath-hold FLASH and FISP cardiovascular MR imaging: left ventricular volume differences and reproducibility. Radiology. 2002; 223: 789-797.

Morton G, Schuster A, Jogiya R, Kutty S, Beerbaum P, Nagel E. Inter-study reproducibility of cardiovascular magnetic resonance myocardial feature tracking. J Cardiovasc Magn Reson. 2012; 14: 43.

Moulis G, Béné J, Sommet A, Sailler L, Lapeyre-Mestre M, Montastruc JL; French Association of PharmacoVigilance Centres. Statin-induced lupus: a case/non-case study in a nationwide pharmacovigilance database. Lupus. 2012; 21: 885-889.

Mozaffarian D, Benjamin EJ, Go AS, Arnett DK, Blaha MJ, Cushman M, de Ferranti S, Després JP, Fullerton HJ, Howard VJ, Huffman MD, Judd SE, Kissela BM, Lackland DT, Lichtman JH, Lisabeth LD, Liu S, Mackey RH, Matchar DB, McGuire DK, Emile R. Mohler ER, Moy CS, Muntner P, Mussolino ME, Nasir K, Neumar RW, Nichol G, Palaniappan L, Pandey DK, Reeves MJ, Rodriguez CJ, Sorlie PD, Stein J, Towfighi A, Turan TN, Virani SS, Willey JZ, Woo D, Yeh RW, Turner MB, on behalf of the American Heart Association Statistics Committee and Stroke Statistics Subcommittee. Heart Disease and Stroke Statistics—2015 Update: A Report From the American Heart Association. Circulation. 2015; 131: e29-e322.

Müller C. Angina pectoris in hereditary xanthomatosis. Arch. Intern. Med.1939; 64: 675-700.

Munoz LE, Gaipl US, Franz S, Sheriff A, Voll RE, Kalden JR, Herrmann M. SLE - a disease of clearance deficiency? Rheumatology (Oxford). 2005; 44: 1101-1107.

Murray CJL, Lopez AD. Alternative projections of mortality and disability by cause 1990–2020:Global Burden of Disease Study. Lancet. 1997; 349: 1498–1504.

Naghavi M, Libby P, Falk E, Casscells SW, Litovsky S, Rumberger J, Badimon JJ, Stefanadis C, Moreno P, Pasterkamp G, Fayad Z, Stone PH, Waxman S, Raggi P, Madjid M, Zarrabi A, Burke A, Yuan C, Fitzgerald PJ, Siscovick DS, de Korte CL, Aikawa M, Juhani Airaksinen KE, Assmann G, Becker CR, Chesebro JH, Farb A, Galis ZS, Jackson C, Jang IK, Koenig W, Lodder RA, March K, Demirovic J, Navab M, Priori SG, Rekhter MD, Bahr R, Grundy SM, Mehran R, Colombo A, Boerwinkle E, Ballantyne C, Insull W Jr, Schwartz RS, Vogel R, Serruys PW, Hansson GK, Faxon DP, Kaul S, Drexler H, Greenland P, Muller JE, Virmani R, Ridker PM, Zipes DP, Shah PK, Willerson JT. From vulnerable plaque to vulnerable patient: a call for new definitions and risk assessment strategies: Part I. Circulation. 2003a; 108: 1664-1672.

Naghavi M, Libby P, Falk E, Casscells SW, Litovsky S, Rumberger J, Badimon JJ, Stefanadis C, Moreno P, Pasterkamp G, Fayad Z, Stone PH, Waxman S, Raggi P, Madjid M, Zarrabi A, Burke A, Yuan C, Fitzgerald PJ, Siscovick DS, de Korte CL, Aikawa M, Airaksinen KE, Assmann G, Becker CR, Chesebro JH, Farb A, Galis ZS, Jackson C, Jang IK, Koenig W, Lodder RA, March K, Demirovic J, Navab M, Priori SG, Rekhter MD, Bahr R, Grundy SM, Mehran R, Colombo A, Boerwinkle E, Ballantyne C, Insull W Jr, Schwartz RS, Vogel R, Serruys PW, Hansson GK, Faxon DP, Kaul S, Drexler H, Greenland P, Muller JE, Virmani R, Ridker PM, Zipes DP, Shah PK, Willerson JT. From vulnerable plaque to vulnerable patient: a call for new definitions and risk assessment strategies: Part II. Circulation. 2003b; 108: 1772-1778.

Nelson P, Rylance P, Roden D, Trela M, Tugnet N. Viruses as potential pathogenic agents in systemic lupus erythematosus. Lupus. 2014; 23: 596-605.

Neuhaus J, Jacobs DR, Baker JV, Calmy A, Duprez D, La Rosa A, Kuller LH, Pett SL, Ristola M, Ross MJ, Shlipak MG, Tracy R, Neaton JD. Markers of inflammation, coagulation, and renal function are elevated in adults with HIV infection. J Infect Dis. 2010; 201:1788-1795.

Nichols M, Townsend N, Scarborough P, Rayner M. Cardiovascular disease in Europe 2014: epidemiological update. Eur Heart J. 2014; 35: 2950-2959.

Nicholls SJ, Tuzcu EM, Wolski K, Sipahi I, Schoenhagen P, Crowe T, Kapadia SR, Hazen SL, Nissen SE. Coronary artery calcification and changes in atheroma burden in response to established medical therapies. J Am Coll Cardiol. 2007a; 49: 263-270.

Nicholls SJ, Tuzcu EM, Sipahi I, Grasso AW, Schoenhagen P, Hu T, Wolski K, Crowe T, Desai MY, Hazen SL, Kapadia SR, Nissen SE. Statins, high-density lipoprotein cholesterol, and regression of coronary atherosclerosis. JAMA. 2007b; 297: 499-508.

Nissen SE, Nicholls SJ, Sipahi I, Libby P, Raichlen JS, Ballantyne CM, Davignon J, Erbel R, Fruchart JC, Tardif JC, Schoenhagen P, Crowe T, Cain V, Wolski K, Goormastic M, Tuzcu EM; ASTEROID Investigators. Effect of very high-intensity statin therapy on regression of coronary atherosclerosis: the ASTEROID trial. JAMA. 2006; 295: 1556-1565.

Obel N, Thomsen HF, Kronborg G, Larsen CS, Hildebrandt PR, Sørensen HT, Gerstof J. Ischemic heart disease in HIV-infected and HIV-uninfected individuals: a population-based cohort study. Clin Infect Dis. 2007; 44: 1625-1631.

Ogden CA, Elkon KB. Single-dose therapy for lupus nephritis: C-reactive protein, nature's own dual scavenger and immunosuppressant. Arthritis Rheum. 2005; 52: 378-381.

O'Leary DH, Polak JF, Kronmal RA, Manolio TA, Burke GL, Wolfson SK Jr. Carotid-artery intima and media thickness as a risk factor for myocardial infarction and stroke in older adults. Cardiovascular Health Study Collaborative Research Group. N Engl J Med. 1999; 340: 14-22.

Olin-Lewis K, Krauss RM, La Belle M, Blanche PJ, Barrett PHR, Wight TN, Chait A
ApoC-III content of apoB-containing lipoproteins is associated with binding to the vascular proteoglycan biglycan. J. Lipid Res. 2002; 43: 1969-1977.

Olofsson SO, Borèn J. Apolipoprotein B: a clinically important apolipoprotein which assembles atherogenic lipoproteins and promotes the development of atherosclerosis. J Intern Med. 2005; 258: 395-410.

Otvos JD, Shalaurova I, Freedman DS, Rosenson RS. Effects of pravastatin treatment on lipoprotein subclass profiles and particle size in the PLAC-I trial. Atherosclerosis. 2002; 160: 41-48.

Pajkrt D, Lerch PG, van der Poll T, Levi M, Illi M, Doran JE, Arnet B, van den Ende A, ten Cate JW, van Deventer SJ. Differential effects of reconstituted high-density lipoprotein on coagulation, fibrinolysis and platelet activation during human endotoxemia. Thromb Haemost. 1997; 77: 303-307.

Palombo C, Kozakova M. Arterial stiffness, atherosclerosis and cardiovascular risk: Pathophysiologic mechanisms and emerging clinical indications. Vascul Pharmacol. 2016; 77: 1-7.

Panel on Antiretroviral Guidelines for Adults and Adolescents. Guidelines for the use of antiretroviral agents in HIV-1-infected adults and adolescents. Department of Health and Human Services Available at http://www.aidsinfo.nih.gov/ContentFiles/AdultandAdolescentGL.pdf. Accessed 15/05/2016.

Parish S, Offer A, Clarke R, Hopewell JC, Hill MR, Otvos JD, Armitage J, Collins R. Lipids and Lipoproteins and Risk of Different Vascular Events in the MRC/BHF Heart Protection Study. Circulation. 2012; 125: 2469-2478.

Parker B, Urowitz MB, Gladman DD, Lunt M, Bae SC, Sanchez-Guerrero J, Romero-Diaz J, Gordon C, Wallace DJ, Clarke AE, Bernatsky S, Ginzler EM, Isenberg DA, Rahman A, Merrill JT, Alarcón GS, Fessler BJ, Fortin PR, Hanly JG, Petri M, Steinsson K, Dooley MA, Manzi S, Khamashta MA, Ramsey-Goldman R, Zoma AA, Sturfelt GK, Nived O, Aranow C, Mackay M, Ramos-Casals M, van Vollenhoven RF, Kalunian KC, Ruiz-Irastorza G, Lim S, Kamen DL, Peschken CA, Inanc M, Bruce IN.Clinical associations of the metabolic syndrome in systemic lupus erythematosus: data from an international inception cohort. Ann Rheum Dis. 2013; 72: 1308-1314.

Parker B, Al-Husain A, Pemberton P, Yates AP, Ho P, Gorodkin R, Teh LS, Alexander MY, Bruce IN. Suppression of inflammation reduces endothelial microparticles in active systemic lupus erythematosus. Ann Rheum Dis. 2014; 73: 1144-1150.

Parks CG, Cooper GS.Occupational exposures and risk of systemic lupus erythematosus: a review of the evidence and exposure assessment methods in population- and clinic-based studies. Lupus. 2006; 15: 728-736.

Parks CG, De Roos AJ. Pesticides, chemical and industrial exposures in relation to systemic lupus erythematosus. Lupus. 2014; 23: 527-536.

Pedersen TR, Kjekshus J, Berg K, Haghfelt T, Faergeman O, Thorgeirsson G, Pyorala K, Miettinen T, Wilhelmsen L, Olsson AG, Wedel H. Randomised trial of cholesterol lowering in 4444 patients with coronary heart disease: the Scandinavian Simvastatin Survival Study (4S). Lancet. 1994; 344: 1383-1389.

Pereira Da Silva JA, Elkon KB, Hughes GR, Dyck RF, Pepys MB. C-reactive protein levels in systemic lupus erythematosus: a classification criterion? Arthritis Rheum. 1980; 23: 770-771.

Pereyra F, Palmer S, Miura T, Block BL, Wiegand A, Rothchild AC, Baker B, Rosenberg R, Cutrell E, Seaman MS, Coffin JM, Walker BD. Persistent low-level viremia in HIV-1 elite controllers and relationship to immunologic parameters. J Infect Dis. 2009; 200: 984-990.

Pereyra F, Lo J, Triant VA, Wei J, Buzon MJ, Fitch KV, Hwang J, Campbell JH, Burdo TH, Williams KC, Abbara S, Grinspoon SK. Increased coronary atherosclerosis and immune activation in HIV-1 elite controllers. AIDS. 2012; 26: 2409-2412.

Petri M, Perez-Gutthann S, Spence D, Hochberg MC. Risk factors for coronary artery disease in patients with systemic lupus erythematosus. Am J Med. 1992; 93: 513-519.

Petri M. Sex hormones and systemic lupus erythematosus. Lupus. 2008; 17: 412-415.

Petri M. Update on anti-phospholipid antibodies in SLE: the Hopkins' Lupus Cohort. Lupus. 2010; 19: 419-423.

Petri MA, Kiani AN, Post W, Christopher-Stine L, Magder LS. Lupus Atherosclerosis Prevention Study (LAPS). Ann Rheum Dis. 2011; 70: 760-765.

Petri M, Orbai AM, Alarcón GS, Gordon C, Merrill JT, Fortin PR, Bruce IN, Isenberg D, Wallace DJ, Nived O, Sturfelt G, Ramsey-Goldman R, Bae SC, Hanly JG, Sánchez-Guerrero J, Clarke A, Aranow C, Manzi S, Urowitz M, Gladman D, Kalunian K, Costner M, Werth VP,

Zoma A, Bernatsky S, Ruiz-Irastorza G, Khamashta MA, Jacobsen S, Buyon JP, Maddison P, Dooley MA, van Vollenhoven RF, Ginzler E, Stoll T, Peschken C, Jorizzo JL, Callen JP, Lim SS, Fessler BJ, Inanc M, Kamen DL, Rahman A, Steinsson K, Franks AG Jr, Sigler L, Hameed S, Fang H, Pham N, Brey R, Weisman MH, McGwin G Jr, Magder LS. Derivation and validation of the Systemic Lupus International Collaborating Clinics classification criteria for systemic lupus erythematosus. Arthritis Rheum. 2012; 64: 2677-2686.

Petri M, Bello KJ, Fang H, Magder LS. Vitamin D in systemic lupus erythematosus: modest association with disease activity and the urine protein-to-creatinine ratio. Arthritis Rheum. 2013; 65: 1865-1871.

Pieretti J, Roman MJ, Devereux RB, Lockshin MD, Crow MK, Paget SA, Schwartz JE, Sammaritano L, Levine DM, Salmon JE. Systemic lupus erythematosus predicts increased left ventricular mass. Circulation. 2007; 116: 419-426.

Pittilo RM. Cigarette smoking, endothelial injury and cardiovascular disease. Int J Exp Pathol. 2000; 81: 219-230.

Plantier JC, Leoz M, Dickerson JE, De Oliveira F, Cordonnier F, Lemée V, Damond F, Robertson DL, Simon F. A new human immunodeficiency virus derived from gorillas. Nat Med. 2009; 15: 871-872.

Pons-Estel GJ, Alarcón GS, Scofield L, Reinlib L, Cooper GS. Understanding the Epidemiology and Progression of Systemic Lupus Erythematosus. Semin Arthritis Rheum. 2010; 39: 257-268.

Pons-Estel GJ, Wojdyla D, McGwin G Jr, Magder LS, Petri MA, Pons-Estel BA; Grupo Latino Americano De Estudio del Lupus (GLADEL), Alarcón GS; LUMINA cohort. The American College of Rheumatology and the Systemic Lupus International Collaborating Clinics classification criteria for systemic lupus erythematosus in two multiethnic cohorts: a commentary. Lupus. 2014; 23: 3-9.

Poredos P. Intima-media thickness: indicator of cardiovascular risk and measure of the extent of atherosclerosis. Vasc Med 2004; 9: 46-54.

Prospective Studies Collaboration. Blood cholesterol and vascular mortality by age, sex, and blood pressure: a meta-analysis of individual data from 61 prospective studies with 55 000 vascular deaths. Lancet. 2007; 370:1829-1839.

Raza A, Kennedy S, Fan Y, Maher B, Codd M, Murphy T, Wood A, Watson W. Anti inflammatory effects of statins in cardiac surgery patients. World J Cardiovasc Surg. 2012; 2: 40-47.

Rees F, Doherty M Grainge M, Davenport G, Lanyon P, Zhang W. The incidence and prevalence of systemic lupus erythematosus in the UK, 1999–2012. Ann Rheum Dis. 2016; 75: 136-141.

Rehr RB, Malloy CR, Filipchuk NG, Peshock RM. Left ventricular volumes measured by MR imaging. Radiology. 1985; 156: 717-9.

Rezaie-Majd A, Prager GW, Bucek RA, Schernthaner GH, Maca T, Kress HG, Valent P, Binder BR, Minar E, Baghestanian M. Simvastatin reduces the expression of adhesion molecules in circulating monocytes from hypercholesterolemic patients Arterioscler Thromb Vasc Biol. 2003; 23: 397-403.

Rhoads MP, Smith CJ, Tudor-Williams G, Kyd P, Walters S, Sabin CA, Lyall EGH. Effects of highly active antiretroviral therapy on paediatric metabolite levels. HIV Med. 2006; 7: 16- 24.

Rhoads MP, Lanigan J, Smith CJ, Lyall EG. Effect of specific ART drugs on lipid changes and the need for lipid management in children with HIV. J Acquir Immune Defic Syndr. 2011; 57: 404-412.

Riddler SA, Smit E, Cole SR, Li R, Chmiel JS, Dobs A, Palella F, Visscher B, Evans R, Kingsley LA. Impact of HIV infection and HAART on serum lipids in men. JAMA. 2003; 289: 2978-2982.

Riddler SA, Li X, Otvos J, Post W, Palella F, Kingsley L, Visscher B, Jacobson LP, Sharrett AR; Multicenter AIDS Cohort Study. Antiretroviral therapy is associated with an atherogenic lipoprotein phenotype among HIV-1-infected men in the Multicenter AIDS Cohort Study. J Acquir Immune Defic Syndr. 2008; 48: 281-288.

Ridgway JP. Cardiovascular magnetic resonance physics for clinicians: part I. J Cardiovasc Magn Reson. 2010; 12: 71.

Ridker PM, Hennekens CH, Buring JE, Rifai N. C-reactive protein and other markers of inflammation in the prediction of cardiovascular disease in women. N Engl J Med. 2000; 342: 836-843.

Ridker PM. High-sensitivity C-reactive protein: potential adjunct for global risk assessment in the primary prevention of cardiovascular disease. Circulation. 2001; 103: 1813-1818.

Ridker PM, Bassuk SS, Toth PP. C-reactive protein and risk of cardiovascular disease: evidence and clinical application. Curr Atheroscler Rep. 2003; 5: 341-349.

Ridker PM, Danielson E, Fonseca FAH, Genest J, Gotto AM, Kastelein JJP, Koenig W, Libby P, Lorenzatti AJ, MacFadyen JG, Nordestgaard BG, Shepherd J, Willerson JT, and Glynn RJ, for the JUPITER Study Group. Rosuvastatin to Prevent Vascular Events in Men and Women with Elevated C-Reactive Protein. N Engl J Med. 2008; 359: 2195-2207.

Rizos EC, Agouridis AP, Elisaf MS. The effect of statin therapy on arterial stiffness by measuring pulse wave velocity: a systematic review. Curr Vasc Pharmacol. 2010; 8: 638-644.

Robertson J, Peters MJ, McInnes IB, Sattar N. Changes in lipid levels with inflammation and therapy in RA: a maturing paradigm. Nat Rev Rheumatol. 2013; 9: 513-523.

Rodriguez W, Mold C, Kataranovski M, Hutt J, Marnell LL, Du Clos TW. Reversal of ongoing proteinuria in autoimmune mice by treatment with C-reactive protein. Arthritis Rheum. 2005; 52: 642-650.

Roger VL, Go AS, Lloyd-Jones DM, Benjamin EJ, Berry JD, Borden WB, Bravata DM, Dai S, Ford ES, Fox CS, Fullerton HJ, Gillespie C, Hailpern SM, Heit JA, Howard VJ, Kissela BM, Kittner SJ, Lackland DT, Lichtman JH, Lisabeth LD, Makuc DM, Marcus GM, Marelli A, Matchar DB, Moy CS, Mozaffarian D, Mussolino ME, Nichol G, Paynter NP, Soliman EZ, Sorlie PD, Sotoodehnia N, Turan TN, Virani SS, Wong ND, Woo D, Turner MB; American Heart Association Statistics Committee and Stroke Statistics Subcommittee. Heart disease and stroke statistics-2012 update: a report from the American Heart Association. Circulation. 2012; 125(1): e2-e220.

Rohatgi A, Khera A, Berry JD, Givens EG, Ayers CR, Wedin KE, Neeland IJ, Yuhanna IS, Rader DR, de Lemos JA, Shaul PW. HDL Cholesterol Efflux Capacity and Incident Cardiovascular Events. N Engl J Med. 2014; 371: 2383-2393.

Roman MJ, Shanker BA, Davis A, Lockshin MD, Sammaritano L, Simantov R, Crow MK, Schwartz JE, Paget SA, Devereux RB, Salmon JE. Prevalence and correlates of accelerated atherosclerosis in systemic lupus erythematosus. N Engl J Med. 2003; 349: 2399-2406.

Roman MJ, Devereux RB, Schwartz JE, Lockshin MD, Paget SA, Davis A, Crow MK, Sammaritano L, Levine DM, Shankar BA, Moeller E, Salmon JE. Arterial stiffness in chronic inflammatory diseases. Hypertension. 2005; 46: 194-199.

Roman MJ, Naqvi TZ, Gardin JM, Gerhard-Herman M, Jaff M, Mohler E; American Society of Echocardiography; Society of Vascular Medicine and Biology. Clinical application of noninvasive vascular ultrasound in cardiovascular risk stratification: a report from the American Society of Echocardiography and the Society of Vascular Medicine and Biology. J Am Soc Echocardiogr. 2006; 19: 943-954.

Rose KA, Vera JH, Drivas P, Banya W, Keenan N, Pennell DJ, Winston A. Atherosclerosis is Evident in Treated HIV-Infected Subjects With Low Cardiovascular Risk by Carotid Cardiovascular Magnetic Resonance. J Acquir Immune Defic Syndr. 2016; 71: 514-521.

Rosenfeld ME, Campbell LA. Pathogens and atherosclerosis: Update on the potential contribution of multiple infectious organisms to the pathogenesis of atherosclerosis. Thromb Haemost. 2011; 106: 858-867.

Rosenson RS, Otvos JD, Hsia J. Effects of Rosuvastatin and Atorvastatin on LDL and HDL Particle Concentrations in Patients With Metabolic Syndrome. A randomized, double-blind, controlled study. Diabetes Care. 2009; 32:1087-1091.

Ross AC, Storer N, O'Riordan MA, Dogra V, McComsey GA.Longitudinal changes in carotid intima-media thickness and cardiovascular risk factors in human immunodeficiency virus-infected children and young adults compared with healthy controls. Pediatr Infect Dis J. 2010; 29: 634-638.

Ross R, Harker L. Hyperlipidemia and atherosclerosis. Science. 1976a; 193: 1094-1108.

Ross R, Glomset J. The pathogenesis of atherosclerosis (first of two parts). N Engl J Med. 1976b; 295: 369-377.

Ross R, Glomset J. The pathogenesis of atherosclerosis (second of two parts). N Engl J Med. 1976c; 295: 420-425.

Ross R. Atherosclerosis - an inflammatory disease. N Engl J Med. 1999; 340: 115-126.

Rothwell PM. The Interrelation between carotid, femoral and coronary artery disease. Eur Heart J. 2001; 22: 11-14.

Roubille C, Richer V, Starnino T, McCourt C, McFarlane A, Fleming P, Siu S, Kraft J, Lynde C, Pope J, Gulliver W, Keeling S, Dutz J, Bessette L, Bissonnette R, Haraoui B. The effects of tumour necrosis factor inhibitors, methotrexate, non-steroidal anti-inflammatory drugs and corticosteroids on cardiovascular events in rheumatoid arthritis, psoriasis and psoriatic arthritis: a systematic review and meta-analysis. Ann Rheum Dis. 2015; 74: 480-489.

Rullo OJ, Tsao BP. Recent insights into the genetic basis of systemic lupus erythematosus. Ann Rheum Dis. 2013; 72: ii56-61.

Saam T, Kerwin WS, Chu B, Cai J, Kampschulte A, Hatsukami TS, Zhao XQ, Polissar NL, Neradilek B, Yarnykh VL, Flemming K, Huston J 3rd, Insull W Jr, Morrisett JD, Rand SD, DeMarco KJ, Yuan C. Sample size calculation for clinical trials using magnetic resonance imaging for the quantitative assessment of carotid atherosclerosis. J Cardiovasc Magn Reson. 2005; 7: 799-808.

Sabio JM, Zamora-Pasadas M, Jiménez-Jáimez J, Albadalejo F, Vargas-Hitos J, Rodríguez del Aguila MD, Hidalgo-Tenorio C, Gonzalez-Gay MA, Jimenez-Alonso J.
Metabolic syndrome in patients with systemic lupus erythematosus from Southern Spain. Lupus. 2008; 17: 849-859.

Sackoff JE, Hanna DB, Pfeiffer MR, Torian LV. Causes of death among persons with AIDS in the era of highly active antiretroviral therapy: New York City. Ann Intern Med. 2006; 145:397-406.

Sacre K, Escoubet B, Pasquet B, Chauveheid MP, Zennaro MC, Tubach F, Papo T. Increased arterial stiffness in systemic lupus erythematosus (SLE) patients at low risk for cardiovascular disease: a cross-sectional controlled study. PLoS One. 2014 Apr 10; 9(4): e94511.

Samaras K, Gan SK, Peake PW, Carr A, Campbell LV. Proinflammatory markers, insulin sensitivity, and cardiometabolic risk factors in treated HIV infection. Obesity 2009; 17: 53-9.

Sanchez-Guerrero J, Karlson EW, Liang MH, Hunter DJ, Speizer FE, Colditz GA. Past use of oral contraceptives and the risk of developing systemic lupus erythematosus. Arthritis Rheum. 1997; 40: 804-808.

Saves M, Chene G, Ducimetiere P, Leport C, Le Moal G, Amouyel P, Arveiler D, Ruidavets JB, Reynes J, Bingham A, Raffi F, for the French WHO MONICA Project and the APROCO (ANRS EP11) Study Group. Risk factors for coronary heart disease in patients treated for human immunodeficiency virus infection compared with the general population. Clin Infect Dis. 2003; 37:292-298.

Scofield RH, Bruner GR, Namjou B, Kimberly RP, Ramsey-Goldman R, Petri M, Reveille JD, Alarcón GS, ViláLM, Reid J, Harris B, Li S, Kelly JA, Harley JB. Klinefelter's syndrome (47,XXY) in male systemic lupus erythematosus patients: support for the notion of a gene-dose effect from the X chromosome. Arthritis Rheum. 2008; 58: 2511-2517.

Sechtem U, Pflugfelder PW, Gould RG, Cassidy MM, Higgins CB. Measurement of right and left ventricular volumes in healthy individuals with cine MR imaging. Radiology. 1987; 163: 697-702.

Segrest JP. The Role of non-LDL:non-HDL Particles in Atherosclerosis. Curr Diab Rep. 2002; 2: 282-288.

Sella EM, Sato EI, Barbieri A. Coronary artery angiography in systemic lupus erythematosus patients with abnormal myocardial perfusion scintigraphy. Arthritis Rheum. 2003; 48: 3168-3175.

Seminari E, Pan A, Voltini G, Carnevale G, Maserati R, Minoli L, Meneghetti G, Tinelli C, Testa S. Assessment of atherosclerosis using carotid ultrasonography in a cohort of HIV-positive patients treated with protease inhibitors. Atherosclerosis. 2002; 162:433-438.

Seneviratne MG, Grieve SM, Figtree GA, Garsia R, Celermajer DS, Adelstein S, Puranik R. Prevalence, distribution and clinical correlates of myocardial fibrosis in systemic lupus erythematosus: a cardiac magnetic resonance study. Lupus. 2016; 25: 573-581.

Shang Q, Tam LS, Li EK, Yip GW, Yu CM. Increased arterial stiffness correlated with disease activity in systemic lupus erythematosus. Lupus. 2008; 17: 1096-1102.

Shepherd J, Cobbe SM, Ford I, Isles C, Lorimer AR, Macfarlane PW, McKillop JH, Packard CJ for the West of Scotland coronary prevention study group. Prevention of coronary heart disease with pravastatin in men with hypercholesterolaemia. N Engl J Med. 1995; 333: 1301-1307.

Shige H, Dart A, Nestel P. Simvastatin improves arterial compliance in the lower limb but not in the aorta. Atherosclerosis. 2001; 155: 245-250.

Shoenfeld Y, Gerli R, Doria A, Matsuura E, Cerinic MM, Ronda N, Jara LJ, Abu-Shakra M, Meroni PL, Sherer Y. Accelerated atherosclerosis in autoimmune rheumatic diseases. Circulation. 2005; 112: 3337–3347.

Siegel M, Holley HL, Lee SL. Epidemiologic studies on systemic lupus erythematosus. Comparative data for New York City and Jefferson County, Alabama, 1956–1965. Arthritis Rheum. 1970; 13: 802-811.

Siegel M, Lee SL. The epidemiology of systemic lupus erythematosus. Semin Arthritis Rheum. 1973; 3: 1-54.

Simes RJ, Tonkin A, et al. Prevention of cardiovascular events and death with pravastatin in patients with coronary heart disease and a broad range of initial cholesterol levels. The Long-Term Intervention with Pravastatin in Ischaemic Disease (LIPID) Study Group. N Engl J Med. 1998; 339:1349-1357.

Simó JM, Joven J, Vilella E, Ribas M, Pujana MA, Sundaram IM, Hammel JP, Hoover-Plow JL. Impact of Apolipoprotein(a) Isoform Size Heterogeneity on the Lysine Binding Function of Lipoprotein(a) in Early Onset Coronary Artery Disease. Thromb Haemost. 2001; 85: 412-417.

Simons PC, Algra A, Bots ML, Grobbee DE, van der Graaf Y. Common carotid intima-media thickness and arterial stiffness: indicators of cardiovascular risk in high-risk patients. The SMART Study (Second Manifestations of ARTerial disease). Circulation. 1999; 100: 951-957.

Sims A, Hadigan C. Cardiovascular complications in children with HIV infection.
Curr HIV/AIDS Rep. 2011; 8: 209-214.

Sirol M, Aguinaldo JG, Graham PB, Weisskoff R, Lauffer R, Mizsei G, Chereshnev I, Fallon JT, Reis E, Fuster V, Toussaint JF, Fayad ZA. Fibrin-targeted contrast agent for improvement of in vivo acute thrombus detection with magnetic resonance imaging. Atherosclerosis. 2005a; 182: 79-85.

Sirol M, Fuster V, Badimon JJ, Fallon JT, Moreno PR, Toussaint JF, Fayad ZA. Chronic thrombus detection with in vivo magnetic resonance imaging and a fibrin-targeted contrast agent. Circulation. 2005b; 112: 1594-1600.

Skaggs BJ, Hahn BH, McMahon M. Accelerated atherosclerosis in patients with SLE-mechanisms and management. Nat Rev Rheumatol. 2012; 8: 214-223.

Skingsley A, Yin Z, Kirwan P, Croxford S, Chau C, Conti S, Presanis A, Nardone A, Were J, Ogaz D, Furegato M, Hibbert M, Aghaizu A, Murphy G, Tosswill J, Hughes G, Anderson J, Gill ON, Delpech VC and contributors. HIV in the UK – Situation Report 2015: data to end 2014. November 2015. Public Health England, London.

Smilde TJ, Wissen S, Wollersheim H, Trip MD, Kastelein JJP, Stalenhoef AFH. Effect of aggressive versus conventional lipid lowering on atherosclerosis progression in familial hypercholesterolaemia (ASAP): a prospective, randomised, double-blind trial. Lancet. 2001; 357: 577-581.

Smith EB, Slater RS. Relationship between low-density lipoprotein in aortic intima and serum-lipid levels. Lancet. 1972; 1: 463-469.

So-Armah KA, Tate JP, Chang CH, Butt AA, Gerschenson M, Gibert CL, Leaf D, Rimland D, Rodriguez-Barradas MC, Budoff MJ, Samet JH, Kuller LH, Deeks SG, Crothers KA, Tracy RP, Crane HM, Sajadi MM, Tindle HA, Justice AC, Freiberg MS; The VACS Project Team. Do Biomarkers Of Inflammation, Monocyte Activation And Altered Coagulation Explain

Excess Mortality Between HIV Infected and Uninfected People? J Acquir Immune Defic Syndr. 2016; 72: 206-213.

Solomon DH, Reed GW, Kremer JM, Curtis JR, Farkouh ME, Harrold LR, Hochberg MC, Tsao P, Greenberg JD. Disease activity in rheumatoid arthritis and the risk of cardiovascular events. Arthritis Rheumatol. 2015; 67: 1449-1455.

Somers EC, Thomas SL, Smeeth L, Schoonen WM, Hall AJ. Incidence of systemic lupus erythematosus in the United Kingdom, 1990-1999. Arthritis Rheum. 2007; 57: 612-618.

Somers EC, Marder W, Cagnoli P, Lewis EE, Peter DeGuire P, Gordon C, Helmick CG, Wang L, Wing JJ, Dhar JP, Leisen J, Shaltis D, McCune WJ. Population-Based Incidence and Prevalence of Systemic Lupus Erythematosus: The Michigan Lupus Epidemiology and Surveillance Program. Arthritis Rheumatol. 2014; 66: 369-378.

Sorenson MB, Collins P, Ong PJL, Webb CM, Hayward CS, Asbury EA, Gatehouse PD, Elkington AG, Yang GZ, Kubba A, Pennell DJ. Long-term use of contraceptive depot medroxyprogesterone acetate in young women impairs arterial endothelial function assessed by cardiovascular magnetic resonance. Circulation. 2002; 106: 1646-1651.

Spyridopoulos I, Hoffmann J, Aicher A, Brümmendorf TH, Doerr HW, Zeiher AM, Dimmeler S. Accelerated telomere shortening in leukocyte subpopulations of patients with coronary heart disease: role of cytomegalovirus seropositivity. Circulation. 2009; 120: 1364-1372.

Ståhl-Hallengren C, Jönsen A, Nived O, Sturfelt G. Incidence studies of systemic lupus erythematosus in Southern Sweden: increasing age, decreasing frequency of renal manifestations and good prognosis. J Rheumatol. 2000; 27: 685-691.

Stanley TL, Grinspoon SK. Body composition and metabolic changes in HIV-infected patients. J Infect Dis. 2012; 205(S3):S383-390.

Stein JH. Carotid intima-media thickness progression and cardiovascular disease risk. J Am Coll Cardiol. 2011; 57: 2291.

Steven E Lipshultz, Tracie L Miller, James D Wilkinson, Gwendolyn B Scott, Gabriel Somarriba, Thomas R Cochran, Stacy D Fisher. Cardiac effects in perinatally HIV-infected

and HIV-exposed but uninfected children and adolescents: a view from the United States of America. J Int AIDS Soc. 2013, 16:18597.

Stojan G, Petri MJ. Atherosclerosis in systemic lupus erythematosus. J Cardiovasc Pharmacol. 2013; 62: 255-262.

Sturfelt G, Truedsson L. Complement and its breakdown products in SLE. Rheumatology (Oxford). 2005; 44: 1227-1232.

Subramanian S, Tawakol A, Burdo TH, Abbara S, Wei J, Vijayakumar J, Corsini E, Abdelbaky A, Zanni MV, Hoffmann U, Williams KC, Lo J, Grinspoon SK. Arterial inflammation in patients with HIV. JAMA. 2012; 308: 379-386.

Suwaidi JA, Hamasaki S, Higano ST, Nishimura RA, Holmes DR Jr, Lerman A. Long-term follow-up of patients with mild coronary artery disease and endothelial dysfunction. Circulation. 2000; 101: 948-954.

Svenungsson E, Jensen-Urstad K, Heimbürger M, Silveira A, Hamsten A, de Faire U, Witztum JL, Frostegård J. Risk factors for cardiovascular disease in systemic lupus erythematosus. Circulation. 2001; 104: 1887-1893.

Sztam KA, Jiang H, Jurgrau A, Deckelbaum RJ, Foca MD. Early increases in concentrations of total, LDL, and HDL cholesterol in HIV-infected children following new exposure to antiretroviral therapy. J Pediatr Gastroenterol Nutr. 2011; 52: 495-498.

Tabib A, Leroux C, Mornex JF, Loire R. Accelerated coronary atherosclerosis and arteriosclerosis in young human-immunodeficiency-virus-positive patients. Coron Artery Dis. 2000; 11:41-46.

Tahara N, Kai H, Ishibashi M, Nakaura H, Kaida H, Baba K, Hayabuchi N, Imaizumi T. Simvastatin attenuates plaque inflammation: evaluation by fluorodeoxyglucose positron emission tomography. J Am Coll Cardiol. 2006; 48: 1825-1831.

Takvorian SU, Merola JF, Costenbader KH. Cigarette smoking, alcohol consumption and risk of systemic lupus erythematosus. Lupus. 2014; 23: 537-544.

Taleb S, Romain M, Ramkhelawon B, Uyttenhove C, Pasterkamp G, Herbin O, Esposito B, Perez N, Yasukawa H, Van Snick J, Yoshimura A, Tedgui A, Mallat Z. Loss of SOCS3 expression in T cells reveals a regulatory role for interleukin-17 in atherosclerosis. J Exp Med. 2009; 206: 2067-2077.

Taleb S, Tedgui A, Mallat Z. Adaptive T cell immune responses and atherogenesis. Curr Opin Pharmacol. 2010; 10: 197–202.

Tan EM, Cohen AS, Fries JF, Masi AT, McShane DJ, Rothfield NF, Schaller JG, Talal N, Winchester RJ. The 1982 revised criteria for the classification of systemic lupus erythematosus. Arthritis Rheum. 1982; 25: 1271-1277.

Taniguchi H, Momiyama Y, Fayad ZA, Ohmori R, Ashida K, Kihara T, Hara A, Arakawa K, Kameyama A, Noya K, Nagata M, Nakamura H, Ohsuzu F. In vivo magnetic resonance evaluation of associations between aortic atherosclerosis and both risk factors and coronary artery disease in patients referred for coronary angiography. Am Heart J. 2004; 148: 137-143.

Tanner MA, Galanello R, Dessi C, Smith GC, Westwood MA, Agus A, Roughton M, Assomull R, Nair SV, Walker JM, Pennell DJ. A randomized, placebo-controlled, double-blind trial of the effect of combined therapy with deferoxamine and deferiprone on myocardial iron in thalassemia major using cardiovascular magnetic resonance. Circulation. 2007; 115: 1876-84.

Tavil Y, Kaya MG, Oktar SO, Sen N, Okyay K, Yazici HU, Cengel A. Uric acid level and its association with carotid intima-media thickness in patients with hypertension. Atherosclerosis. 2008; 197: 159-163.

Tawakol A, Fayad ZA, Mogg R, Alon A, Klimas MT, Dansky H, Subramanian SS, Abdelbaky A, Rudd JH, Farkouh ME, Nunes IO, Beals CR, Shankar SS. Intensification of statin therapy results in a rapid reduction in atherosclerotic inflammation: results of a multicenter fluorodeoxyglucose-positron emission tomography/computed tomography feasibility study. J Am Coll Cardiol. 2013; 62: 909-917.

Taylor PR, Carugati A, Fadok VA, Cook HT, Andrews M, Carroll MC, Savill JS, Henson PM, Botto M, Walport MJ. A hierarchical role for classical pathway complement proteins in the clearance of apoptotic cells in vivo. J Exp Med. 2000; 192: 359-366.

Thompson T, Sutton-Tyrrell K, Wildman RP, Kao A, Fitzgerald SG, Shook B, Tracy RP, Kuller LH, Brockwell S, Manzi S. Progression of carotid intima-media thickness and plaque in women with systemic lupus erythematosus. Arthritis Rheum. 2008; 58: 835-842.

Tien PC, Choi AI, Zolopa AR, Benson C, Tracy R, Scherzer R, Bacchetti P, Shlipak M, Grunfeld C. Inflammation and mortality in HIV-infected adults: Analysis of the FRAM study cohort. J Acquir Immune Defic Syndr. 2010; 55: 316-322.

Toussaint JF, LaMuraglia GM, Southern JF, Fuster V, Kantor HL. Magnetic resonance images lipid, fibrous, calcified, hemorrhagic, and thrombotic components of human atherosclerosis in vivo. Circulation. 1996; 94: 932-938.

Townsend N, Williams J, Bhatnagar P, Wickramasinghe K, Rayner M (2014). Cardiovascular disease statistics, 2014. British Heart Foundation: London.

Triant VA, Lee H, Hadigan C, Grinspoon SK. Increased acute myocardial infarction rates and cardiovascular risk factors among patients with human immunodeficiency virus disease. J Clin Endocrinol Metab. 2007; 92: 2506-2512.

Triant VA. HIV infection and coronary heart disease: an intersection of epidemics. J Infect Dis. 2012; 205: S355-361.

Triant VA. Cardiovascular disease and HIV infection. Curr HIV/AIDS Rep. 2013; 10: 199-206.

Trivedi RA, U-King-Im JM, Graves MJ, Cross JJ, Horsley J, Goddard MJ, Skepper JN, Quartey G, Warburton E, Joubert I, Wang L, Kirkpatrick PJ, Brown J, Gillard JH. In vivo detection of macrophages in human carotid atheroma: temporal dependence of ultrasmall superparamagnetic particles of iron oxide-enhanced MRI. Stroke. 2004; 35: 1631-1635.

Underhill HR, Kerwin WS, Hatsukami TS, Yuan C. Automated measurement of mean wall thickness in the common carotid artery by MRI: a comparison to intima-media thickness by B-mode ultrasound. J Magn Reson Imaging. 2006; 24: 379-387.

Underhill HR, Yuan C, Zhao XQ, Kraiss LW, Parker DL, Saam T, Chu B, Takaya N, Liu F, Polissar NL, Neradilek B, Raichlen JS, Cain VA, Waterton JC, Hamar W, Hatsukami TS. Effect of rosuvastatin therapy on carotid plaque morphology and composition in moderately

hypercholesterolemic patients: a high-resolution magnetic resonance imaging trial. Am Heart J. 2008; 155: 584.e1-8.

Uno K, Bayturan O, Lavoie A, Nicholls SJ. Rationale and approach to evaluation of the impact of medical therapies on progression of atherosclerosis with arterial wall imaging. Curr Med Res Opin. 2010; 26: 737-744.

Upala S, Sanguankeo A. Effects of statin therapy on arterial stiffness: a systematic review and meta-analysis of randomized controlled trial. J Am Coll Cardiol. 2016;67(13_S):2315-2315. doi:10.1016/S0735-1097(16)32316-6.

Uramoto KM, Michet CJ Jr, Thumboo J, Sunku J, O'Fallon WM, Gabriel SE. Trends in the incidence and mortality of systemic lupus erythematosus, 1950-1992. Arthritis Rheum. 1999; 42: 46-50.

Urbina EM, Srinivasan SR, Tang R, Bond MG, Kieltyka L, Berenson GS. Impact of multiple coronary risk factors on the intima-media thickness of different segments of carotid artery in healthy young adults (The Bogalusa Heart Study). Am J Cardiol. 2002; 90:953-958.

Urowitz MB, Bookman AAM, Koehler BE, Gordon DA, Smythe HA, Ogryzlo MA. The Bimodal Mortality Pattern of Systemic Lupus Erythematosus. Am J Med. 1976; 60: 221-225.

Urowitz MB, Gladman DD, Tom BD, Ibañez D, Farewell VT. Changing patterns in mortality and disease outcomes for patients with systemic lupus erythematosus. J Rheumatol. 2008; 35: 2152-2158.

Utz JA, Herfkens RJ, Heinsimer JA, Bashore T, Califf R, Glover G, Pelc N, Shimakawa A. Cine MR determination of left ventricular ejection fraction. AJR Am J Roentgenol. 1987; 148: 839-843.

van Popele NM, Grobbee DE, Bots ML, Asmar R, Topouchian J, Reneman RS, Hoeks AP, van der Kuip DA, Hofman A, Witteman JC. Association between arterial stiffness and atherosclerosis: the Rotterdam Study. Stroke. 2001; 32: 454-460.

van Wijk DF, Strang AC, Duivenvoorden R, Enklaar DJF, van der Geest RJ, Kastelein JJP, de Groot E, Stroes ESG, Nederveen AJ. Increasing spatial resolution of 3T MRI scanning

improves reproducibility of carotid arterial wall dimension measurements. Magn Reson Mater Phy. 2014; 27:219–226.

Varghese A, Crowe LA, Mohiaddin RH, Gatehouse PD, Yang GZ, Firmin DN, Pennell DJ. Interstudy reproducibility of 3D volume selective fast spin echo sequence for quantifying carotid artery wall volume in asymptomatic subjects. Atherosclerosis. 2005a; 183: 361-366.

Varghese A, Crowe LA, Mohiaddin RH, Gatehouse PD, Yang GZ, Nott DM, McCall JM, Firmin DN, Pennell DJ. Interstudy reproducibility of three-dimensional volume-selective fast spin echo magnetic resonance for quantifying carotid artery wall volume. J Magn Reson Imaging. 2005b; 21: 187-191.

Varghese A, Merrifield RD, Crowe LA, Collins SA, Keenan NGJ, Firmin DN, Yang GZ, Pennell DJ. Evaluation of carotid artery wall volume measurement using novel semiautomated analysis software. J Magn Reson Imaging. 2006; 24: 1401-1408.

Vera-Lastra O, Méndez-Flores S, Cruz-Dominguez MP, Medina G, Calderón-Aranda E, Jara LJ. Effect of ezetimibe plus pravastatin on endothelial dysfunction in patients with systemic lupus erythematosus. Lupus. 2016; 25: 741-748.

Virchow R. Lecture XVI, April 14 1858. A more precise account of fatty metamorphosis; Cellular Pathology as based upon physiological and pathological histology. John Churchill, London, 1960.

Virmani R, Ladich ER, Burke AP, Kolodgie FD. Histopathology of carotid atherosclerotic disease. Neurosurgery. 2006; 59(S3): 219-227.

Voss A, Green A, Junker P. Systemic lupus erythematosus in Denmark: clinical and epidemiological characterization of a county-based cohort. Scand J Rheumatol. 1998; 27: 98-105.

Wang DG, Tang XW, Fan Y, Leng RX, Ni J, Deng SM, Wang C, Cen H, Pan HF, Ye DQ. Decreased flow-mediated dilatation in patients with systemic lupus erythematosus: a meta-analysis. Inflammation. 2014; 37: 2067-2075.

Wang JC, Bennett M. Aging and atherosclerosis: mechanisms, functional consequences, and potential therapeutics for cellular senescence. Circ Res. 2012; 111: 245-259.

Watson DJ, Rhodes T, Guess HA. All-cause mortality and vascular events among patients with rheumatoid arthritis, osteoarthritis, or no arthritis in the UK General Practice Research Database. J Rheumatol. 2003; 30:1196-1202.

WHO Fact sheet on cardiovascular disease. Updated January 2015. http://www.who.int/cardiovascular_diseases/en/ Accessed 13/03/2016.

WHO Global Health Observatory Data Repository, Data on the size of the epidemic: Number of people (all ages) living with HIV. Accessed online 28/02/16.

Wiesmann F, Petersen SE, Leeson PM, Francis JM, Robson MD, Wang Q, Choudhury R, Channon KM, Neubauer S. Global impairment of brachial, carotid, and aortic vascular function in young smokers: direct quantification by high-resolution magnetic resonance imaging. J Am Coll Cardiol. 2004; 44: 2056-2064.

Winter PM, Morawski AM, Caruthers SD, Fuhrhop RW, Zhang H, Williams TA, Allen JS, Lacy EK, Robertson JD, Lanza GM, Wickline SA. Molecular imaging of angiogenesis in early-stage atherosclerosis with alpha(v)beta3-integrin-targeted nanoparticles. Circulation. 2003; 108: 2270-2274.

Worm SW, Kamara DA, Reiss P, Kirk O, El-Sadr W, Fux C, Fontas E, Phillips A, D'Arminio Monforte A, De Wit S, Petoumenos K, Friis-Mller N, Mercie P, Lundgren JD, Sabin C. Elevated triglycerides and risk of myocardial infarction in HIV-positive persons. AIDS. 2011; 25: 1497-1504.

Yap DY, Lai KN. The role of cytokines in the pathogenesis of systemic lupus erythematosus - from bench to bedside. Nephrology (Carlton). 2013; 18: 243-255.

Yarnykh VL, Terashima M, Hayes CE, Shimakawa A, Takaya N, Nguyen PK, Brittain JH, McConnell MV, Yuan C. Multicontrast black-blood MRI of carotid arteries: comparison between 1.5 and 3 tesla magnetic field strengths. J Magn Reson Imaging. 2006; 23: 691-698.

Yeon SB, Sabir A, Clouse M, Martinezclark PO, Peters DC, Hauser TH, Gibson CM, Nezafat R, Maintz D, Manning WJ, Botnar RM. Delayed-enhancement cardiovascular magnetic

resonance coronary artery wall imaging: comparison with multislice computed tomography and quantitative coronary angiography. J Am Coll Cardiol. 2007; 50: 441-7.

Yin Z, Brown AE, Hughes G, Nardone A, Gill ON, Delpech VC & contributors. HIV in the United Kingdom 2014 Report: data to end 2013. November 2014. Public Health England, London.

Yuan C, Beach KW, Smith LH Jr, Hatsukami TS. Measurement of atherosclerotic carotid plaque size in vivo using high resolution magnetic resonance imaging. Circulation. 1998; 98: 2666-2671.

Yuan C, Mitsumori LM, Ferguson MS, Polissar NL, Echelard D, Ortiz G, Small R, Davies JW, Kerwin WS, Hatsukami TS. In vivo accuracy of multispectral magnetic resonance imaging for identifying lipid-rich necrotic cores and intraplaque hemorrhage in advanced human carotid plaques. Circulation. 2001a; 104: 2051-2056.

Yuan C, Mitsumori LM, Beach KW, Maravilla KR. Carotid atherosclerotic plaque: noninvasive MR characterization and identification of vulnerable lesions. Radiology. 2001b; 221: 285-299.

Yuan C, Zhang SX, Polissar NL, Echelard D, Ortiz G, Davis JW, Ellington E, Ferguson MS, Hatsukami TS. Identification of fibrous cap rupture with magnetic resonance imaging is highly associated with recent transient ischemic attack or stroke. Circulation. 2002a; 105: 181-185.

Yuan C, Kerwin WS, Ferguson MS, Polissar N, Zhang S, Cai J, Hatsukami TS. Contrast-enhanced high resolution MRI for atherosclerotic carotid artery tissue characterization. J Magn Reson Imaging. 2002b; 15: 62-67.

Zevin AS, McKinnon L, Burgener A, Klatt NR. Microbial translocation and microbiome dysbiosis in HIV-associated immune activation. Curr Opin HIV AIDS. 2016; 11: 182-190.

Zimarino M, Prati F, Marano R, Angeramo F, Pescetelli I, Gatto L, Marco V, Bruno I, De Caterina R. The value of imaging in subclinical coronary artery disease. Vascul Pharmacol. 2016; 82: 20-29.

Appendix

Outputs arising from this thesis

Data contained in this thesis published in scientific journals or presented at scientific meetings are listed below.

Publications

Rose KA, Vera JH, Drivas P, Banya W, Keenan N, Pennell DJ, Winston A. Atherosclerosis is Evident in Treated HIV-Infected Subjects With Low Cardiovascular Risk by Carotid Cardiovascular Magnetic Resonance. J Acquir Immune Defic Syndr. 2016; 71: 514-521.

Publications in preparation

Rose KAM, Youngstein T, Munteanu I, Auger D, Chan C, Keenan N, Drivas P, Smith G, Wage R, Banya W, Penn H, Tench C, Mackworth-Young C, Mason JC, Pennell DJ.
Trial of rosuvastatin therapy for the prevention of atherosclerosis in normolipidaemic patients with systemic lupus erythematosus. [Manuscript complete ready for final author approval].

Rose KAM, Keenan NG, Mason JC, Maceira A, Assomull R, O'Hanlon R, Chan C, Banya W, Drivas P, Andrews J, Gatehouse PD, Firmin DN, Haskard DO, Pennell DJ.
Cardiovascular magnetic resonance for a comprehensive cardiovascular assessment in systemic lupus erythematosus. [Manuscript drafted].

Rose KAM, Rhoads M, Fiddler C, Foster S, Drivas P, Wage R, Pennell DJ, Tudor-Williams G. Carotid CMR in perinatally infected young adults with HIV. [Manuscript drafted].

Meetings

Poster presentations

Evidence of premature atherosclerosis in HIV-infected individuals with low cardiovascular disease risk factors. Vera JH, Rose K, Banya W, Drivas P, Keenan N, Pennell D, Winston A. 15th International Workshop on Co-morbidities and Adverse Drug Reactions in HIV, Brussels, 2013.

A randomised placebo controlled trial of rosuvastatin in SLE. Kathleen Rose, Justin Mason, Dorian Haskard, Colin Tench, Andrew Russell, Charles Mackworth-Young, Dudley J Pennell. 1st Annual NOCRI Cardiovascular Workshop, Barts and The London Cardiovascular Biomedical Research Unit, July 2010.

Presentations

Invited lectures: CMR of the Vessel Wall. Cardiovascular Magnetic Resonance Unit, Royal Brompton Hospital, London, CMR Course, May 2010, October 2010.

Abbreviations

ACR	American College of Rheumatology
AEs	Adverse events
AIDS	Acquired immunodeficiency syndrome
ANA	Antinuclear antibody
anti-dsDNA	Anti-double stranded DNA
anti-nRNP	Anti-nuclear ribonucleoprotein
aPL	Antiphospholipid antibody
BAR	Brachial artery reactivity
BLys	B-lymphocyte stimulators
BMI	Body mass index
BSA	Body surface area
CAD	Coronary artery disease
cART	Combination anti-retroviral treatment
CHD	Coronary heart disease
C-IMT	Carotid intima media thickness
CMR	Cardiovascular magnetic resonance
CoV	Coefficients of variation
CSF	Cerebrospinal fluid
CV	Cardiovascular
CVD	Cardiovascular disease
DHEA	Dehydroepiandrosterone
EBCT	Electron beam-CT
ECG	Electrocardiogram
EF	Ejection fraction
eGFR	Estimated glomerular filtration rate
eNOS	Endothelial-derived nitric oxide
ESR	Erythrocyte sedimentation rate
FDG	Fluorodeoxyglucose
FMD	Flow-mediated dilatation
FOV	Field of view
FSE	Fast spin echo
GE	Gradient echo
GTN	Glyceryl trinitrate
^{1}H	Single nuclear proton

HAART Highly active antiretroviral therapy

HASTE Half-Fourier acquisition turbo spin-echo

HDL High-density lipoprotein

HIV Human Immunodeficiency Virus

HMGCoA 3-hydroxy-3-methylglutaryl coenzyme A

hsCRP High sensitivity C reactive protein

ICA Internal carotid artery

ICAM-1 Intercellular adhesion molecule 1

ICCs Intraclass correlation coefficients

IDL Intermediate density lipoprotein

IFN-□ Interferon-□

IL Interleukin

INF- γ Interferon-γ

IVUS Intravascular ultrasound

LDL Low-density lipoprotein

TH17 17-producing T-helper lineage

LGE Late gadolinium enhancement

Lp(a) Lipoprotein (a)

LPS Lipopolysaccharide

LTNPs Long-term non-progressors

MCP-1 Monocyte chemoattractant protein-1

M-CSF Macrophage colony-stimulating factor

MHC-II Major histocompatibility complex

MI Myocardial infarction

MMPs Matrix metalloproteinases

MRI Magnetic resonance imaging

MSCT Multislice computed tomography

MSM Men who have sex with men

NCEP National Cholesterol Education Program

NIRS Near Infrared Spectroscopy

NMR Nuclear magnetic resonance

NNRTIs Non-nucleoside reverse transcriptase inhibitors

NO Nitric oxide

NRTIs Nucleoside reverse transcriptase inhibitors

OCT Optical coherence tomography

PDGF Platelet-derived growth factor

PDW Proton-density-weighted

PET Positron emission tomography

PIs Protease inhibitors

PWV Pulse wave velocity

RCT Randomised controlled trial

RF Radiofrequency

ROS Reactive oxygen species

SAEs Serious adverse events

SE Spin echo

SIV Simian immunodeficiency virus

SLE Systemic lupus erythematosus

SLEDAI Systemic Lupus Erythematosus Disease Activity Index SELENA Modification

SLICC Systemic Lupus International Collaborating Clinics

SMCs Smooth muscle cells

SNR Signal to noise ratio

SPECT Single photon-emission computed tomography

SSFP Steady state free precession

SV Stroke volume

T1w T1-weighted

T2w T2-weighted

T Tesla

TE Time to echo

TGF-β Transforming growth factor-β

TGs Triglycerides

TNF-α Tumour necrosis factor-α

TOF Time of flight

TR Repetition time

USPIOs Ultrasmall paramagnetic particles of iron oxide

VCAM-1 Vascular adhesion molecule 1

VLDL Very low-density lipoprotein

W/OW Wall/outer wall ratio

Supplemental Data

Table(a). Coefficients of variation of cardiac and carotid parameters measured for the two observers.

Variable	Year	Observer 1	Observer 2
LVEF	0	0.08	0.08
	1	0.08	0.09
	2	0.09	0.09
RVEF	0	0.08	0.08
	1	0.08	0.09
	2	0.08	0.09
LVEDV Index	0	0.16	0.18
	1	0.17	0.17
	2	0.18	0.17
LVESV Index	0	0.29	0.33
	1	0.31	0.35
	2	0.35	0.35
LV Mass Index	0	0.14	0.21
	1	0.16	0.18
	2	0.14	0.18
RVEDV Index	0	0.16	0.17
	1	0.18	0.16
	2	0.17	0.16
RVESV Index	0	0.32	0.32
	1	0.32	0.33
	2	0.32	0.28
Total Wall Volume	0	0.18	0.21
	1	0.19	0.19
	2	0.15	0.18
Total Lumen Volume	0	0.21	0.22
	1	0.23	0.22
	2	0.20	0.22
Total Vessel Volume	0	0.20	0.20
	1	0.21	0.20
	2	0.18	0.19
W/OW	0	0.07	0.10
	1	0.07	0.10
	2	0.08	0.10
Distensibility	0	0.32	0.32
	1	0.18	0.32
	2	0.39	0.27

Table(b). Intraclass correlation coefficients for carotid and cardiac parameters between observer 1 and 2, at baseline, year-1 and year-2.

Parameter	Baseline ICC (95%CI)	Year 1 ICC (95%CI)	Year 2 ICC (95%CI)
Carotid			
Total Lumen Volume	0.92 (0.83, 0.96)	0.96 (0.92, 0.98)	0.97 (0.93, 0.99)
Total Wall Volume	0.82 (0.64, 0.91)	0.80 (0.61, 0.90)	0.73 (0.49, 0.87)
Total Vessel Volume	0.94 (0.86, 0.97)	0.98 (0.96, 0.99)	0.98 (0.96, 0.99)
W/OW ratio	0.43 (0.08, 0.69)	0.37 (0.002, 0.65)	0.18 (0.004, 0.66)
Distensibility	0.28 (-0.1, 0.59)	0.64 (0.37, 0.82)	0.26 (-0.13, 0.59)
Cardiac			
LVEF	0.76 (0.54, 0.88)	0.78 (0.58, 0.89)	0.87 (0.73, 0.94)
LVEDV Indexed	0.85 (0.70. 0.93)	0.93 (0.86, 0.97)	0.92 (0.84, 0.86)
LVESV Indexed	0.76 (0.55, 0.88)	0.87 (0.73, 0.94)	0.94 (0.87, 0.97)
LV Mass Indexed	0.65 (0.36, 0.82)	0.73 (0.49, 0.87)	0.66 (0.38, 0.83)
RVEF	0.86 (0.72, 0.93)	0.74 (0.51, 0.87)	0.57 (0.25, 0.78)
RVEDV Indexed	0.86 (0.71, 0.93)	0.84 (0.69, 0.92)	0.60 (0.28, 0.79)
RVESV Indexed	0.88 (0.76, 0.94)	0.84 (0.68, 0.92)	0.94 (0.87, 0.97)